Fucoidans from South African brown seaweeds – establishing the link between their structure and biological properties

(anti-diabetic and anti-cancer activities)

A thesis submitted in fulfilment of the requirements for the degree of

DOCTOR OF PHILOSOPHY

On the subject of

BIOCHEMISTRY

at

RHODES UNIVERSITY

by

BLESSING MABATE

ORCID ID: 0000-0002-3584-5703

Supervisor: Prof. Brett I. Pletschke

Co-supervisor: Prof. Adrienne L. Edkins

February 2022

ABSTRACT

Type 2 diabetes mellitus (T2DM) and cancer are major non-communicable diseases causing a heavy morbidity-mortality and economic burden globally. The therapeutic efforts in managing these diseases are primarily chemotherapeutic and are associated with demerits, including side effects and toxicity, limiting the prescribed amounts. These dosage limits may cause drug resistance, another major challenge in maintaining quality global health. The pursuit of novel natural bioproducts is a reasonable strategy to add to the arsenal against T2DM and cancer. Fucoidans, sulphated fucose polysaccharides abundant in brown seaweeds, have recently become popular for their biological activities, including anti-diabetic and anti-cancer properties. However, endemic South African brown seaweeds have not been adequately explored. Therefore, this study sought to characterise fucoidans extracted from South African brown seaweeds and elucidate their structure to their biological activities. Also, this study highlighted carbohydrate and glucose metabolism as major target processes in the control efforts of T2DM and cancer using fucoidans.

Harvested brown seaweeds were identified as *Ecklonia radiata* and *Sargassum elegans. E. maxima* was kindly donated by KelpX. The fucoidans were then extracted using hot water, EDTA assisted, and acid extraction protocols. The integrity of the extracted fucoidan was confirmed through structural analysis using FTIR, NMR and TGA. The fucoidan extracts were then chemically characterised to determine their carbohydrate and monosaccharide composition and sulphate content. The characterised fucoidans were profiled for inhibiting the major amylolytic enzymes, namely α-amylase and α-glucosidase. The mode of inhibition by fucoidans and synergy experiments with the commercial anti-diabetic drug acarbose were also investigated.

Furthermore, the fucoidans were screened for potential anti-cancer activities on the human colorectal HCT116 cancer cell line. The cytotoxicity of fucoidans was quantified using the resazurin assay. The effect of fucoidan on HCT116 cell adhesion on the tissue culture plastic was also investigated using the crystal violet-based cell adhesion assay. In addition, cancer antimigration properties of fucoidans were also investigated using 2D wound healing and 3D spheroid-based assays. Furthermore, the long-term

survival of HCT116 cells was investigated through the clonogenic assay after treatment with fucoidans. Lastly, glucose uptake and lactate export assays revealed the influence of fucoidan on glucose uptake and the glycolytic flux of HCT116 cells.

Fucoidans were successfully extracted with a yield between 2.2% and 14.2% on a dry weight basis. EDTA extracts produced the highest yields than the water and the acid extracts. *Ecklonia* spp. fucoidans displayed the highest total carbohydrate content, with glucose and galactose being the major monosaccharides. *S. elegans* and commercial *Fucus vesiculosus* had lower carbohydrate contents but contained more sulphates than the *Ecklonia* spp. fucoidans. Furthermore, the extracted fucoidan contained little to no contaminants, including proteins, phenolics and uronic acids. In addition, the extracted fucoidans were determined to be >100 kDa through ultracentrifugation. Mass spectrometry also detected the most abundant peak for all fucoidans to be around 700 Da (m/z). Extracted fucoidans inhibited the activity of α-glucosidase more strongly than the commercial anti-diabetic agent acarbose but were inactive on α-amylase. Fucoidans were also shown to be mixed inhibitors of α-glucosidase. Compellingly, fucoidans synergistically inhibited α-glucosidase in combination with the anti-diabetic agent acarbose, highlighting prospects for combination therapy.

Finally, fucoidans demonstrated some anti-proliferative characteristics on HCT116 cancer cells by inhibiting their ability to adhere to the tissue culture plate matrix. Furthermore, some fucoidan extracts inhibited the migration of HCT116 cancer cells from 3D spheroids. Some of our fucoidan extracts also inhibited HCT116 colony formation, demonstrating inhibition of long-term cell survival. The *E. maxima* water extract also inhibited glucose uptake by HCT116 cells, thereby influencing the glycolytic flux.

In conclusion, biologically active fucoidans were successfully extracted from South African brown seaweeds. These fucoidans demonstrated anti-diabetic and anti-cancer properties, revealing their relevance as potential drugs for these diseases.

Keywords: cancer; fucoidan; Type 2 diabetes mellitus

PLAGIARISM DECLARATION

I, Blessing Mabate, declare that this thesis submitted for a Doctor of Philosophy in Science degree at Rhodes University has not been submitted for a degree at this University or any other university. The work entailed in the document is my own in design and execution. Also, all the reference material in this thesis has been duly acknowledged.

Signature: 

Date: 08 February 2022

DEDICATION

This thesis is lovingly dedicated to God almighty, my family, friends and everyone who has contributed to this journey!

PREFACE

This thesis is presented in six chapters, as outlined below, based on the various thematic areas covered within the study. Some aspects of the thesis have been published in peer-reviewed articles and a topical paper. Manuscripts in preparation are also listed (see list of outputs, page xvi). The thesis chapters are outlined as follows:

- **Chapter 1:** The general introduction and literature review describes the scope of this study and the relevance of fucoidan as a therapeutic agent. The background, including relevant literature, is discussed here to cover the broad aim of the study

- **Chapter 2:** The problem statement and rationale of the study are indicated. The hypothesis and the study objectives have also been stated here.

- **Chapter 3:** This chapter characterises the extracted fucoidan using colourimetric and structural methods. The composition of fucoidans is compared, noting trends that may be essential for their biological activities.

- **Chapter 4:** The relevance of fucoidans as antidiabetic therapeutic agents is elucidated in this chapter. The prospects of combination therapy using fucoidans and acarbose (a commercial anti-diabetic drug) are highlighted.

- **Chapter 5:** This chapter demonstrates the anti-cancer activities of fucoidan on human colorectal cancer cells (HCT116).

- **Chapter 6:** This chapter includes the general discussion, future perspectives and concluding remarks.

ACKNOWLEDGEMENTS

A journey of a thousand miles is said to begin with a single step, and I believe its completion significantly depends on the guidance and support given, among other things. Having been blessed with so much support, I would like to acknowledge the following for the success of this work;

My supervisor, Prof. B. I Pletschke and co-supervisor Prof. A. L Edkins for their guidance, mentorship, and encouragement. Their support has made it possible to see this work to completion. Dr. S Malgas who has been an excellent mentor, patiently editing my work and always keen to share ideas. Also, I would like to thank Dr. X. S Noundou, Mr Justin Safari for helping with the chemistry aspects of this work.

The Enzyme Science Programme (ESP)-Bioproducts research group with special thanks to Ms Chantal Daub and Dr. L Mkabayi for their undying support. The Biomedical Biotechnology Research Unit (BIOBRU) for giving so much technical support and inducting me into cell culture techniques. Special thanks within this group would go to Ms Kelly Schwarz, Dr. A. Chakraborty and Ms B. Sibiya for their patience in mentoring me through certain experimental techniques.

My family, especially my mother (Mrs P. Mabate) who has always been a pillar of strength throughout this journey. Also, my sister Ms T. P Mabate for her encouragement and taking time to proofread part of my work. I would like to acknowledge my friends with a special mention of Ms ST. Mnciva, Dr. T. C Madzivanzira, Dr. L Mathomu, Mr S. Dube and Mr S. Karambwe for moral support and proofreading some sections of my thesis.

The German Academic Exchange Service (DAAD) In-Region Scholarship (grant no. 57408782) for the funding and support through workshops which was pivotal in the completion of this work. I would also like to acknowledge KelpX for funding this work in part.

Space would not permit the listing of everyone who partook in this journey, but I appreciate all who did. Most importantly, I greatly thank God almighty for being with me throughout this journey. His favours and grace have taken me this far

Table of Contents

List of Figures

List of Tables

List of Abbreviations

Symbols and interpretation of units

°C	Degree Celsius
µg	Microgram
µg/ml	Microgram per millilitre
µM	Micromolar
µmol	Micromole
BSA	Bovine serum albumin
DNS	3,5-Dinitrosalicylic acid
D_2O	Deuterium Oxide
FTIR	Fourier-transform infrared spectroscopy
g	Gram
HCl	Hydrochloric acid
K	Kilo
kDa	Kilo Dalton
K_M	Michaelis constant
mg	Milligram
Mg/ml	Milligram per millilitre
MHz	Megahertz
ml	Millilitre
min	Minute
Mw	Molecular weight
NaOH	Sodium hydroxide
nm	Nanometer
NMR	Nuclear magnetic resonance
pNPG	*p*-nitrophenol-α-D-glucopyranoside
T2DM	Type 2 diabetes mellitus
V_{max}	Maximum velocity
v/v	Volume per volume
w/v	Weight per volume
w/w	Weight per weight
× *g*	Relative centrifugal field

List of Outputs

a. Publications in peer reviewed journals:

1. Daub, C.D., Mabate, B., Malgas, S., Pletschke, B.I. (2020). Fucoidan from *Ecklonia maxima* is a powerful inhibitor of the diabetes-related enzyme, α-glucosidase. *International Journal of Biological Macromolecules* 151, 412 -420, https://doi.org/10.1016/j.ijbiomac.2020.02.161.

2. Mabate, B.; Daub, C.D.; Malgas, S.; Edkins, A.L. Pletschke, B.I. (2021). Fucoidan Structure and Its Impact on Glucose Metabolism: Implications for Diabetes and Cancer Therapy. *Marine Drugs*, 19, 30, https://doi.org/10.3390/md19010030

3. Mabate, B., Daub, C.D., Malgas, S., Edkins, A.L., Pletschke, B.I. (2021). A combination approach in inhibiting type 2 diabetes-related enzymes using *Ecklonia radiata* fucoidan and acarbose. *Pharmaceutics* (Special Issue)*,* 13(11),1979, https://doi.org/10.3390/pharmaceutics13111979

b. Topical paper

4. Mabate, B., Daub, C.D., Malgas, S. and Pletschke, B.I. (2020). Kelp extracts and their pharmaceutical properties. Atlas of Science (https://atlasofscience.org/kelpextracts-and-their-pharmaceutical properties/#more-30415).

c. Manuscripts in preparation

5. Mabate, B.; Daub, C.D. Pletschke, B.I., Edkins, A.L. (2022). Fucoidans from endemic South African seaweed exhibit anti-cancer activity towards human colorectal cancer cells (HCT116). In prep.

6. Mabate, B., Noundou,X. S., Malgas, S., Edkins, A.L, Pletschke, B.I. (2022). The significance of fucoidan extraction methods; A link between their structure and biological activity. In prep.

d. Oral presentations

1. **Mabate, B.,** Daub, C.D., Malgas, S., Edkins, A. L and Pletschke, B. I. Relevance of brown seaweed fucoidans as therapeutics for Type 2 diabetes mellitus (T2DM) and cancer progression. The South African Society of Biochemistry and Molecular Biology conference (SASBMB) (Online). University of Pretoria. 23-26 January 2022. Awarded first prize for best overall PhD oral presentation.

2. **Mabate B.,** Edkins, A. L., Pletschke, B. I. Breaking the walls of diseases using seaweeds. National 3-minute thesis competition (Online). University of the Free State 13 November 2020. Joint winner of this national competition.

3. **Mabate B** and Pletschke B. I. Fucoidan from *E. maxima* inhibit α-glucosidase a type 2 diabetes related enzyme. 9th DAAD South Africa Conference (Johannesburg). 5-8 September 2019.

CHAPTER 1: REVIEW OF FUCOIDAN AS A RELEVANT POTENTIAL DRUG FOR DIABETES AND CANCER THERAPEUTIC EFFORTS

1.1 Introduction

Diabetes and cancer are noncommunicable diseases with high mortality and economic burden, diminishing lifespan and overall quality of life. Amid the advancement of chemotherapeutic efforts to combat these diseases, there is still a need for innovative strategies to alleviate the strain caused by these diseases on human life and overall health. The mechanisms by which the diseases progress, will be elucidated in this chapter and hence flagged as targets for potential drugs. In addition, most chemotherapeutic efforts in controlling cancer and Type 2 diabetes mellitus (T2DM) have been implicated with toxicity/side effects that limit the amount used to achieve high efficacy (He et al., 2014). This chapter also describes a marine source of natural bioproducts abundant in brown seaweeds, namely fucoidan. Fucoidans have received much attention in the past decade with their promising biological activities. Some of the fucoidans' biological activities include anti-diabetic and anti-cancer properties. Furthermore, marine bioproducts are deemed a sustainable source with a limited risk of endangering species than terrestrial medicinal plants. Brown seaweeds were characterised to show their abundance and underutilisation as a resource in South Africa.

1.2 Background on seaweeds

Seaweeds are multicellular, macroscopic, marine algae that utilise sunlight as an energy source to convert carbon dioxide and water into carbohydrates (Gao & McKinley, 1994). Their classification is based on morphology, ecology, habitat, size, pigments, and polysaccharide composition. The seaweeds are further grouped into three categories: red seaweed (Rhodophyta) with 6500 known species, brown seaweed (Phaeophyta) with 1800 known species and green seaweed (Chlorophyta) with approximately 1500 known species (Ahmad, 2015). Seaweeds are more abundant in cold waters, but limited diversity exists compared to that found in tropical regions. They can grow underwater to the depths

of around 30-50 meters, but they are primarily present in the oceans' intertidal and upper sublittoral zones. Seaweeds generally absorb green light of medium wavelengths for photosynthesis. With a very high productivity rate, they naturally grow on coastlands. It has been estimated that the productivity of the non-cultivated brown algae can reach the range between 3.3 – 11.3 kg dry weight m^{-2} $year^{-1}$ (Gao & McKinley 1994).

South Africa has a large area with coastlands where seaweeds naturally grow (Fig. 1.1). The country has had a seaweed industry for over 60 years. The commercial exploitation of seaweeds in South Africa is mainly based on beach-cast collecting and cutting of kelp. Commercial exploitation only began in the early 1950s (McHugh, 1987), followed by hand-picking of *Gelidium* sp. in the Eastern Cape since 1957. Most of this harvest was shipped to Europe, North America, and Asia for alginate extraction (Rothman et al., 2020).

Figure 1.1:Map of South Africa showing the seaweed rich coastline.
The numbers indicate positions of the coastal sections for which species of seaweeds have been identified (Adapted from Bolton & Stegenga, 2002).

Since commercial seaweed exploitation began in South Africa in the 1950s, only six seaweed genera (*Ecklonia, Laminaria, Gracilaria, Gelidium, Gigartina,* and *Porphyra*) have been harvested, with most of this material being exported for use in the phycocolloid

industry. The known seaweed diversity of South Africa has increased from 547 species in 1984 to around 900 species in 2012, making the region one of the richest with marine floras in the world, with a high level of endemism (Ale & Meyer, 2013), although inadequately profiled for significant biological activities. Moreover, seaweeds are easily renewable, and some are grown on a large scale in aquaculture operations to meet seaweed food demands in Asia. Seaweed aquaculture in South Africa could be introduced, which could be a source of job creation.

Seaweeds are often exposed to adverse environmental conditions, including high oxygen concentrations and ultraviolet light, which may lead to the formation of free radicals. However, seaweeds do not show severe photodynamic damage *in vivo* regardless of exposure to unfriendly conditions (Maina, 2014). These seaweeds are deemed to possess the ability to produce compounds with antioxidative properties to protect them from harsh environmental conditions. Several seaweeds contain macromolecules, including polysaccharides and other secondary metabolites with therapeutic and medicinal properties (Lakshmanasenthil et al., 2013).

1.2.1 Medicinal uses of seaweeds

Seaweeds have various therapeutic applications. Their utilisation in medicine dates back to the 4th and 6th century BC in Asia, specifically in Japan and China (Liu et al., 2012). In China, some seaweeds have treated goitre and phlegm accumulation in the respiratory tract since ancient times. The use of seaweeds as traditional medicine in the Western world arrived later. The earliest documentation dates to the Greek and Roman empires, where a gelatinous substance (mucilage) was employed to treat burns and rashes (Karleskint et al., 2010). In Europe, seaweed use in medicine began at sea, where it was used to treat scurvy ailments (Karleskint et al., 2010). They have found various applications, such as synthesising pharmaceutical compounds (Michanek, 2013). For instance, *Digenea* spp. (Rhodophyta) produce an effective vermifuge (kainic acid) (Smit, 2004). *Laminaria* and *Sargassum* species have been used to treat cancer (Khan & Satam, 2003). Antiviral compounds discovered in *Undaria spp.* have been used to inhibit the

Herpes simplex virus (Thompson & Dragar, 2004). Brown seaweeds, among others, are an important source of valuable techno-functional and potentially bioactive polysaccharides such as fucoidans. Even though seaweeds have a profound history of application in medicine, they also exhibit nutritional properties.

1.2.2 Nutritive utilisation of seaweeds

Edible seaweeds are rich in dietary fibre, minerals, and proteins. The consumption of seaweeds was dated from ancient times, mainly in Asia (Chapman & Chapman, 1980; Indergaard & Minsaas, 1991), although their use has spread to other places. Unprocessed seaweed consumption provides several healing benefits (Jiménez-Escrig & Sánchez-Muniz, 2000). The use of seaweeds as nutritive sources is gaining increasing attention as the world is gaining some awareness about the importance of these marine products in diet and health. Several marine products have been marketed, and these have been shown to possess health benefits such as decreasing the risk of diseases (Annunziata & Vecchio, 2011). In recent years, some marine foods have been added to various food products such as meat, dairy, and vegetable-based products to add to their functionality in nutrition. Furthermore, some seaweeds are deemed to increase certain food products' shelf life and quality (Roohinejad et al., 2017). However, their health benefits and potential risks should be further investigated for better comprehension.

1.2.3 Potential risks and health benefits of seaweeds

A concern has been raised that seaweeds could harbour pathogenic microorganisms. Such a concern is deemed highly likely since the surfaces of seaweeds pose a favourable environment for the growth of microbes. Most studies regarding microbial concerns have been limited to ecological focus, describing the numbers and diversity of microbes on the seaweed surfaces. Literature has reported that the possible survival of some pathogenic bacteria is an issue that has remained unresolved as seaweeds are usually eaten raw (Løvdal et al., 2021). Despite the potential risks of seaweeds, several studies have shown a complementary role of seaweeds as therapeutic medicines. For example, brown and

some red seaweeds have been reported to possess therapeutic properties such as anticancer activity (Jin et al., 2021). Seaweeds have been reported to have anti-inflammatory properties (Takahashi et al., 2018), anticoagulant characteristics (Castro et al., 2015), immunomodulatory effects (Peng et al., 2019), neuroprotective and anti-Alzheimer properties (Wei et al., 2017), in addition to their other various health benefits.

In general, seaweeds as a food source have been reported to have direct health benefits. For instance, it was reported that the incorporation of *A. nodosum* in bread reduced the carbohydrate intake by 16.4% in the test subjects without significant effects of hunger or fullness being noted (Hall et al., 2012). In a separate study, freshwater algae reduced body weight and blood glucose levels in test subject populations. Thus, it was concluded that water algae as a food source could modify cardiovascular risk factors, including glucose levels, hence reducing obesity (Oben et al., 2007). The use of seaweeds has also been implicated in reducing hypertension occurrence. Bread enriched with renin inhibitory *Palmaria palmata*, a protein hydrolysate, showed a significant decrease in hypertension in test subjects who consumed the bread compared to the control population (Fitzgerald, 2014).

Furthermore, the potential benefits of seaweeds extend to their therapeutic significance in the alleviation of Type 2 diabetes mellitus (T2DM). T2DM, incorrect dietary habits, and lack of physical exercise are lifestyle-related diseases, among others (Garcimartín et al., 2015). Garcimartín and colleagues (2015) reported that *Undaria pinnatifida* (Wakame) and *Halomonas elongata* (sea spaghetti) displayed antidiabetic properties where one had an inhibitory effect on α-glucosidase activity, while the other was a glucose diffusion reducer. In an independent study, *Lonicera japonica* fermented with a Korean tea (Makgeolli) displayed significantly high antidiabetic activity without the seaweed taste spoiling the flavour (Choi et al., 2014). In this regard, seaweed-derived bio-actives, including fucoidans, have more health benefits than the potential risks associated with their consumption.

1.3 Fucoidan

Fucoidan is a fucose-rich, sulphated polysaccharide, usually composed of a backbone of α-linked L-fucose residues with various substitutions. Fucoidan polysaccharides are mainly found in brown seaweeds. However, they differ in structure among brown seaweed species. Fucoidans are generally negatively charged, with a highly hygroscopic and mucilaginous nature. A high fucoidan content is found in the blades of brown seaweeds, including *Laminaria digitata*, *Ascophyllum nodosum*, *Macrocystis pyrifera* and *Fucus vesiculosus*. Fucoidans are soluble in water and acid solutions (Nagaoka et al., 2000). Chemically, fucoidans cover several different structural entities that designate a family of fucose-containing sulphated polysaccharides (FCSPs) (Ale et al., 2011). There are various marine sources of fucoidans. Fucoidans bioactivities are related to their structural makeup, monosaccharide composition, sulphate content, the position of sulphate ester groups, and molecular weight.

1.3.1 Sources of fucoidans

Sulphated polysaccharides are found among marine organisms such as sea cucumbers (Eluvakkal et al., 2010), urchins or brown algae. Over the years, several algae and different invertebrates have been identified for their fucoidan contents, including *F. vesiculosus*, *Sargassum stenophyllum*, *Chorda filum*, *Ascophyllum nodosum* *Cladosiphon okamuranus*, *Dictyota menstrualis*, *Fucus evanescens*, *Fucus serratus*, *Fucus distichus*, *Caulerpa racemosa*, *Hizikia fusiforme*, *Padina gymnospora*, *Kjellmaniella crassifolia*, *Analipus japonicus* (Li et al., 2008) and *Laminaria hyperborea* (Black, 1954). All these various seaweeds, shown in Figure 1.2, contain diverse types of fucoidans, the structures of which are crucial for our understanding of these polysaccharides.

Figure 1.2: Examples of common brown seaweeds in the literature
The numbers correspond to the seaweed species stated. 1: *Fucus vesiculosus*, 2*: Laminaria digitata,* 3: *Fucus evanescens*, 4: *Fucus serratus*, 5: *Ascophyllum nodosum*, 6: *Pelvetia canaliculata*, 7: *Cladosiphon okamuranus*, 8: *Hizikia fusiforme,* 9: *Laminaria japonica*, 10: *Sargassum horneri*, 11: *Nemacystus decipiens*, 12: *Padina gymnospora*, and 13: *Laminaria hyperborean*. Adapted from Luthuli et al. (2019).

1.3.2 Structure of fucoidan

The structures of fucoidans extracted from various brown seaweeds differ within different seaweed species, but intraspecies variation is also common. The main determinants of these structural differences are the fucoidan backbone, monosaccharide composition, sulphate content and molecular weight.

1.3.2.1 Fucoidan backbone & monosaccharide composition

Fucoidans from brown seaweeds generally consist of a backbone of α(1→3)-L-fucopyranose residues or alternating α(1→3) and α(1→4)-linked L-fucopyranosyls. These fucoidan structures (in either case) may be substituted with

sulphate (Fig. 1.3), acetate or have side branches containing fucopyranoses or other glycosyl units, e.g., glucuronic acid (Ale et al., 2011).

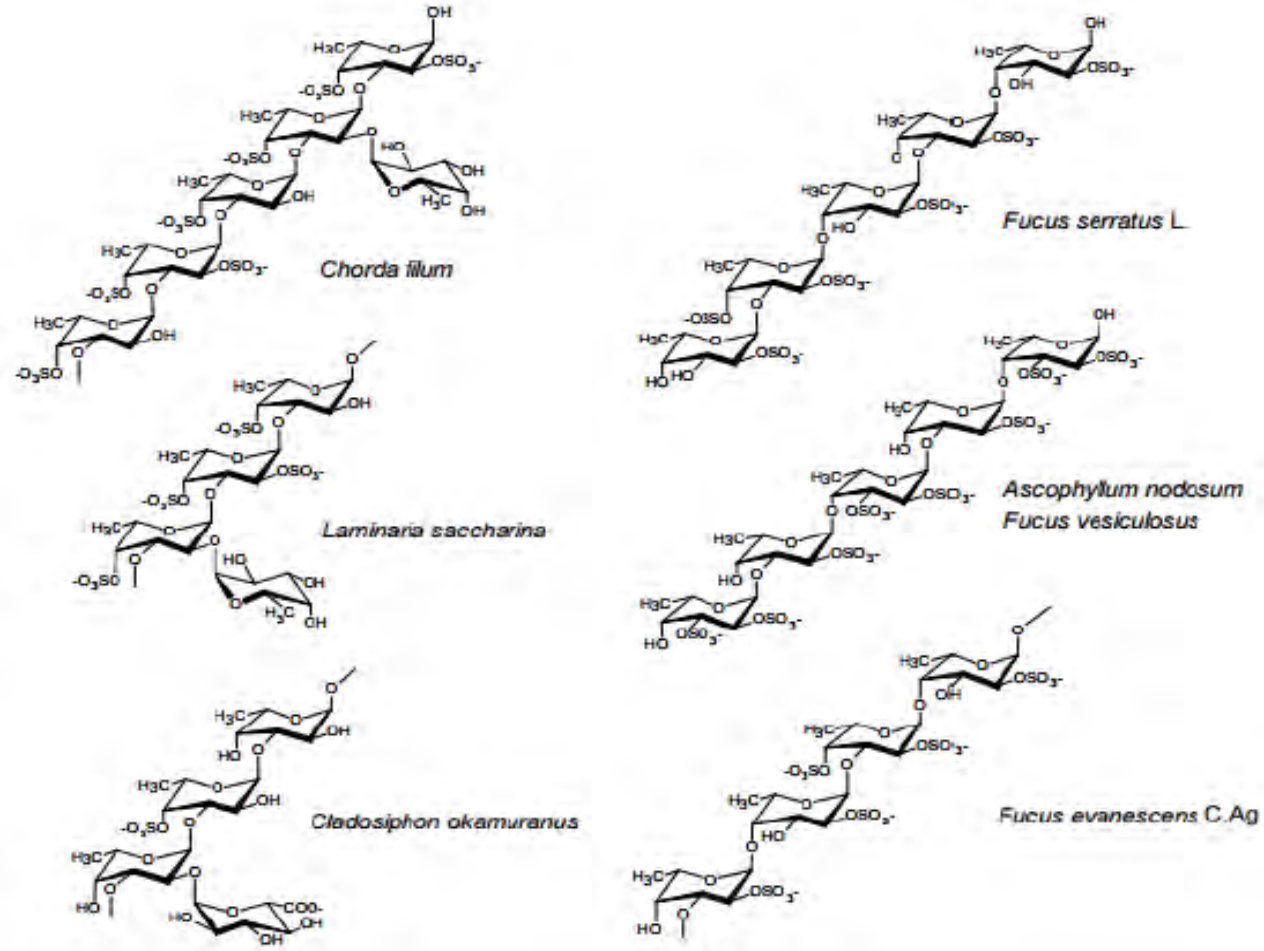

Figure 1.3:Structural features of fucoidan.
The structural motifs of fucose-containing sulphated polysaccharides obtained from various sources of brown algae. Adapted from Ahmad (2015).

Several fucoidan structures reported in the literature contain small amounts of various other monosaccharides, e.g., glucose, galactose, xylose, or mannose. These monosaccharides may represent contamination with other polysaccharides or maybe genuine substitutions on the fucoidan molecular entities. The fucoidans in different brown seaweeds have variable ratios of α(1→3) and α(1→4)-linked L-fucopyranose residues, which may be substituted with sulphate (SO_4) on C-2 and C-4 (Badrinathan et al., 2012).

Table 1.1 summarises the monosaccharide compositions of some of the characterised fucoidans from brown seaweeds**.**

Table 1.1: Chemical composition of known brown seaweeds

Brown seaweed	Chemical composition
Adenocytis utricularis	Fucose, galactose, mannose, sulphates
Ascophyllum nodosum	Fucose, xylose, glucuronic acid, sulphates
Bifurcaria bifurcate	Fucose, xylose, glucuronic acid, sulphates
Dictyota menstrualis	Fucose, xylose, uronic acid, galactose, sulphates
Ecklonia kurome	Fucose, galactose, mannose, xylose, glucuronic acid, sulphates
F. distichus	Fucose, sulphates
F. evanescens	Fucose, sulphates
F. serratus L.	Fucose, sulphates
F. vesiculosus	Fucose, sulphates
Hizikia fusiforme	Fucose, galactose, mannose, xylose, glucuronic acid, sulphates
Laminaria angustata	Fucose, galactose, sulphates
Lessonia vadosa	Fucose, sulphates
Macrocytis pyrifera	Fucose, galactose, sulphates
Padina pavonia	Fucose, xylose, mannose, glucose, galactose, sulphates
Pelvetia wrightii	Fucose, galactose, sulphates
Sargassum stenophyllum	Fucose, galactose, mannose, sulphates

(Adapted from Maina, 2014)

The variations in the reported structural properties of fucoidans from different brown seaweed species confirm that fucoidans are diverse and complex. It also seems clear that fucoidans extracted from brown seaweeds under the same seaweed classification (i.e., order) have a different composition. In turn, structural traits cannot be categorised or predicted according to algal order (Ale & Meyer, 2013). Due to their potential for inhibiting cancer cell growth, antidiabetic and anti-obesity activity, antioxidant activity, anticoagulant activity, anti-inflammatory, and antiviral activity, it was of interest to extract fucoidans from brown seaweeds with high bioactivity. Seaweed species, geographic location, harvest season, and especially the extraction and purification methods used (Ale & Meyer, 2013; Mak et al., 2013), are all related to fucoidan's biological activity.

1.3.2.2 Position of sulphate on the fucoidan structure

The sulphate positioning in characterised fucoidan varies and can be seen from the different attachment patterns of sulphate groups and glycosidic linkages (Fig. 1.3). The sulphate groups may occur at carbon positions 2,3, and 4, and the monosaccharides are linked with α (1→2), α (1→3) and α (1→4) glycosidic bonds (Badrinathan et al., 2012). The positioning of sulphate groups is crucial to the biological activities of sulphated polysaccharides (Maina, 2014). Several methods can be utilised to investigate the position of sulphates in fucoidans which include infrared spectroscopy (IR), ion chromatography (IC), desulphation, methylation analysis, mass spectroscopy (MS) and nuclear magnetic resonance (NMR). Grachev and colleagues (2006) reported that, when using NMR, there is some influence from sulphate groups at C-2 and C-3 on the conformational behaviour of fucoidan fragments with a homo-(1→3)-linked backbone. In addition, MS is advantageous over other techniques since it can differentiate between positional isomers based on their fragmentation patterns (Fletcher et al., 2017). Another important characteristic component implicated in fucoidan bioactivity is their molecular weight.

1.3.2.3 Molecular weight

The molecular weights of fucoidans have been one of the major factors affecting their functional properties. Fucoidans vary in size from 10 kDa to about 10 000 kDa, and the average fucoidan size is approximately 20 kDa (Wang et al., 2019). However, their source influences their size. The considerable variation in the size of fucoidans has led to the categorisation of fucoidans; low molecular weight fucoidans (LMWF) with <10 kDa in size, medium molecular weight fucoidans (MMWF) if between 10 and 10 000 kDa and high molecular weight fucoidans (HMWF) with >10 000 kDa in size (Senthilkumar et al., 2013). Native fucoidans usually have high molecular weights, resulting in low cell membrane permeability and low bioavailability. Due to their high molecular weights, the lack of fucoidans' bioaccessibility may reduce their efficiency in potential clinical applications (Suprunchuk, 2019). Recently, depolymerisation of fucoidan into oligomeric subunits has

gained attention as it is a plausible method to deal with the problems of high molecular weight native fucoidan (Suprunchuk, 2019).

1.4 Effect of geographic location and seasonality on fucoidan dry weight

The structure and content of fucoidan have been previously reported to vary according to species, seasonality, geographic location and maturity of the seaweed. However, there is currently little published data available to support these claims. Understanding the seasonal variation in fucoidan content is of paramount importance to optimise harvesting times and ensure consistent fucoidan composition for research and industrial purposes (Fletcher et al., 2017).

Previously, the amounts of bioactive polysaccharides (fucoidan) of *Saccharina longicruris* were determined to increase by about 1.6% from March to May but decrease by about 7.2% between November and June the following year (Rioux et al., 2007). In another similar but independent study, it was reported that the fucoidan content of *U. pinnatifida* almost quadrupled between July and September (3.6-13.7 %) (Mak et al., 2013). Recently, fucoidan yields from *Fucus serratus*, *Fucus vesiculosus* and *Ascophyllum nodosum* were highest between September and March (Fletcher et al., 2017). The general trend was that lower levels of fucoidan are found during spring, rising to a maximum in autumn, which would suggest that the best harvest time will be late autumn or early winter. It was also reported that intertidal zones affect fucoidan content. In addition, it has been suggested that sugar content gradually increases when algae are exposed to higher amounts of sunlight – the UV light, which might be destructive to algal cell constituents (Honya et al., 1999). Therefore, it is important to know the time-dependent distribution of fucoidan (i.e. over various seasons) so that the maximum yield of fucoidan may be extracted from harvests.

1.5 Extraction technology of fucoidan

Due to the importance of isolating good quality fucoidan, several extraction methods have been used to try and preserve high-quality fucoidan. The extracted crude fucoidans can be purified through ethanol precipitation, gel percolation and ion-exchange chromatography (Eluvakkal et al., 2010). Fucoidans are usually extracted from seaweed using acidic or alkali solvents (Yang et al., 2008). However, acid and alkali extraction methods have been associated with residual components affecting the quality of the fucoidan. Therefore, hot water has become popular as an extracting solvent to preserve molecular weight stability, net charge, and natural bioactivity of the fucoidan; however, the yield is largely reduced (Peasura et al., 2015) when compared to acid and alkali extraction.

Several studies have reported using acid extraction in the isolation of fucoidan as it gives a higher yield (Yang et al., 2008; Zhao et al., 2018). However, the technology produces undesirable by-products such as alginic acids and metals that may cause degradation of the fucose chains (Ale et al., 2011). Nevertheless there is an invariably effective method for removing insoluble components formed through acid extraction; by salt solutions like calcium chloride ($CaCl_2$), the purity and yield of fucoidan is significantly reduced (Imbs et al., 2015). The extraction of fucoidans was started in the early 19^{th} century using acetic acid, and the techniques were improved to three rounds of extraction with dilute HCl acid followed by ethanol precipitation. This method is still currently used commercially by Sigma Aldrich (Ermakova et al., 2011). In addition, a microwave-assisted approach has also been used to extract fucoidan. It displays a high fucoidan yield after a shorter extraction time (Zhao et al., 2018). To date, little is known on the effects of microwave-assisted extraction on the structural and bioactive integrity of fucoidan (Zhao et al., 2018). A biological catalyst approach was also developed, employing enzyme-assisted fucoidan extraction. It was reported that this method extracted fucoidans from *F. vesiculosus* with preserved biological activity (Heo et al., 2005). However, the enzymatic approach has met a significant obstacle: seaweed's chemically and structurally heterogeneous cell wall character. A well-defined enzyme cocktail to break the cell wall is quite challenging to acquire (Ale & Meyer, 2013).

After any method of fucoidan extraction is employed, the efficacy of the extraction parameters and purification process must be evaluated by determining the number of impurities, including proteins, phenolics and uronic acids. Different extraction parameters and purification treatments of fucoidans have generated diverse compositional results and structural suggestions for fucoidan polysaccharides. These variations caused by different extraction methods significantly impact the evaluation of fucoidan polysaccharide products for biological activity. It is imperative for scientists in this field to benchmark extraction procedures that will advance the comprehension of these intriguing fucose-rich seaweed substances that exhibit unique biological activities (Ale & Meyer, 2013).

1.6 The biological activities of fucoidans

Fucoidans have gained much attention because of the bioactivities they possess. It has been established in several studies that fucoidans and their oligosaccharides are non-toxic and non-allergenic. They have no adverse effects on the human system after consumption (Løvdal et al., 2021). Chung and colleagues conducted an *in vivo* study that reported no toxicological effects on rodents after feeding them with about 1000 mg/kg fucoidan per day for 28 days. However, a slight increase in the plasma alanine transaminase (ALT) level, a biomarker of liver injury, was noted when the amount of fucoidan was doubled (Chung et al., 2010). Nevertheless, fucoidan has been linked to improved liver function with liver fibrosis, where ALT levels significantly decreased with an increased dosage of fucoidan in mice (Li et al., 2016). Thus, in the past decade, fucoidans have attracted scientists into determining their potential biological functions, such as their effect on hepatic disorders (Hakayawa & Nagamine, 2009), antitumor activity (Lin et al., 2020), antioxidant activity (Hifney et al., 2016), immunomodulatory effects (Li et al., 2011), antiviral (Rabanal et al., 2014), and antidiabetic activity (Daub et al., 2020).

1.7 Diabetes mellitus

Diabetes is generally a metabolic disorder characterised by high glucose levels in the plasma. It is classified into four distinct types: type I, II, III, and IV. The major types of diabetes are Type I and II. Type I (T1DM) is known as insulin-dependent diabetes because the defective pancreas fails to secrete enough or no insulin at all (Kim et al., 2014). On the other hand, type II diabetes mellitus (T2DM) is characterised by hyperglycaemia (elevated levels of blood glucose) caused by a deficiency in the secretion of the hormone insulin, its impaired functionality or an imbalance between blood sugar absorption and insulin secretion (Shan et al., 2016). As the most prevalent of all types, T2DM accounts for over 90 % of diabetes cases worldwide (WHO, 2020). It has received more attention in research due to its prevalence and yet preventable (Kim et al., 2014), aetiology.

The aetiology of diabetes mellitus is linked to various factors, including sedentary lifestyle, obesity, age, diet, and lack of physical exercise. T2DM remains one of the significant emerging chronic diseases in humans, with about 400 million people living with diabetes worldwide (WHO, 2020). T2DM burdens the world in mortality, morbidity and disability-adjusted life years (DALYs), which significantly steers economic pressure in medium or low-income countries to a greater extent than in developed nations (WHO, 2020). T2DM is characterised by hyperglycaemia, leading to considerable damage to organs and the nervous and cardiovascular systems (Galicia-Garcia et al., 2020). Diabetes is projected to be the seventh-highest global cause of death by 2030 (Moini, 2019), due to elevated blood glucose levels.

It has been established that the primary source of blood glucose levels is carbohydrate (starch) hydrolysis by catabolic enzymes in the alimentary canal, including amylases, maltases and glucosidases. Therefore, delaying carbohydrate digestion or preventing glucose absorption is considered a promising approach to treating diabetes and its complications (Lakshmanasenthil et al., 2013). Moreover, understanding the pathophysiology and physiology of carbohydrate metabolism can help elucidate target pathways and mechanisms in chemotherapy.

1.7.1 Physiology of carbohydrate metabolism

The metabolism of carbohydrates in the human system involves starch (a polysaccharide), mainly as a source of blood glucose, compared to other macromolecules (lipids and proteins). In the human system, glucose is the primary molecule in energy production, and hence it is implicated in all forms of diabetes mellitus. The amount of glucose available in the bloodstream is influenced by three processes, namely, digestion (e.g. of starch to glucose), hormonal regulation (secretion of insulin, glucagon, amylin etc.) and transportation mechanisms of glucose via glucose transporter molecules (Aronoff et al., 2004).

1.7.2 Carbohydrate digestion and absorption

Carbohydrates including starches, sucrose and lactose are the main suppliers of glucose in the human body. They are digested within the intestinal tract to yield glucose, the major energy source within the human body (Aronoff et al., 2004). The digestion of carbohydrates depends on enzymes, including amylases, oligosaccharidases; glucosidases, lactases and sucrases (Molnar & Gair, 2019).

The digestion process begins in the mouth with salivary amylase breaking down starches into maltose, a disaccharide. This step is followed by carbohydrate digestion occurring in the duodenum, where pancreatic amylases break down carbohydrates into disaccharides. The salivary and pancreatic amylases are endosaccharides only specific to α-1,4 glycosidic bonds (Devlin, 2006). The respective oligosaccharides are broken down in the duodenum by oligosaccharidases into monosaccharides (mainly glucose) (Molnar & Gair, 2019). Subsequently, glucose becomes available for harnessing energy during metabolism. The monosaccharides, including glucose from the breakdown by amylases and brush border enzymes in the small intestines, are absorbed through the enterocytes. This process of the digestion of carbohydrates and their absorption is shown illustratively in Figure 1.4.

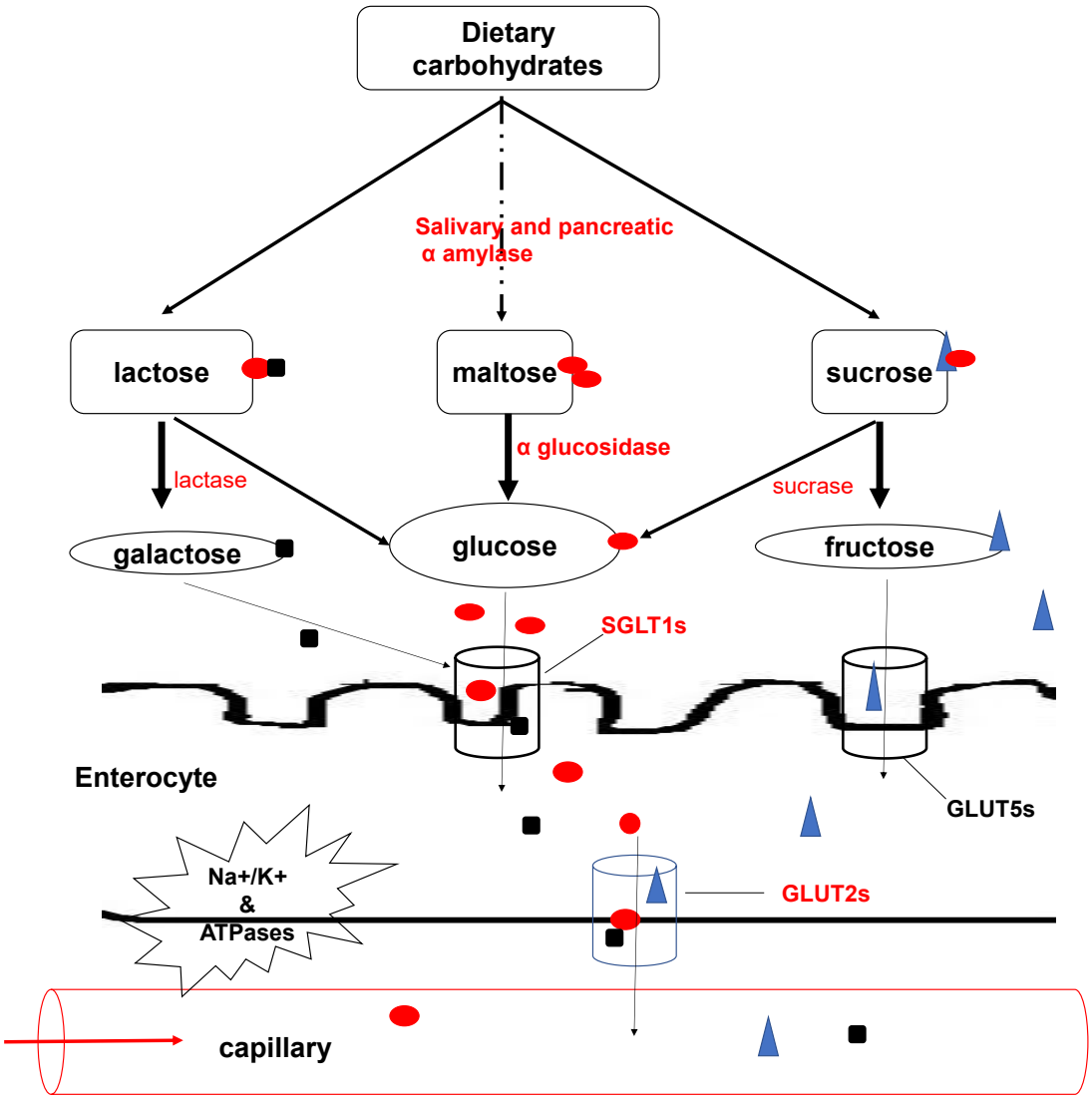

Figure 1.4: Carbohydrate digestion, absorption, and assimilation.
The diagram summarises the simplified route involved in carbohydrate digestion to monosaccharide assimilation. Different shapes show the respective monosaccharides; squares represent galactose, circles glucose and triangles fructose. The steps of carbohydrate digestion are shown with corresponding hydrolytic enzymes (shown in red). Also, the monosaccharide transporter molecules are shown as cylindrical shapes. Of note, the highlighted steps can be therapeutic targets for fucoidan. Adapted from (Goodman, 2010) and reviewed in Mabate et al. (2021).

The absorption process of the monosaccharides occurs through selective active transport of D-isomers (mostly D-glucose and D-galactose) *via* the sodium (Na)-coupled secondary active transport symporter known as the Na-glucose transporter 1 (SGLT1) (Goodman,

2010). This transport mechanism is vital to ensure a one-directional flow of glucose from the gut to the epithelial cells regardless of the glucose gradient (Fig. 1.4).

The SGLT1 is a Na-glucose transporter with a binding affinity directly influenced by a 2:1 stoichiometric ratio for Na^+ and D-glucose, respectively (Chen et al., 2016). On the outer surface of the enterocyte, the binding of Na^+ allows for a conformational change on the SGLT1, enabling the D-glucose to bind with higher affinity. Within the enterocyte cytoplasm, the Na^+ dissociates from its binding site causing a decreased transporter affinity for D-glucose, which causes its release. Besides, the SGLT1 completes its cycle in a slow transition to reorient its binding site to the extracellular process (Longpré & Lapointe, 2011). The active movement conferred by Na^+, K^+ and ATPases in bringing in D-glucose through the SGLT1 creates a steep glucose concentration gradient across the luminal membrane (Aronson et al., 2003). Afterwards, glucose leaves the basolateral side of the cell by facilitated diffusion through glucose transporters (GLUT2s) (Fig. 1.4) to the extracellular medium near blood capillaries (Röder et al., 2014). The absorbed glucose within the capillaries is then transported via mesenteric circulation to target cells for use and regulation.

1.7.3 Regulation of glucose homeostasis

The amount of glucose within the bloodstream should be maintained at a steady level as hypoglycaemia or hyperglycaemia may be fatal. Therefore, blood glucose levels in humans are maintained at a stringent level of approximately 90 mg/dL (Sharabi et al., 2015). Glucose homeostasis is regulated by nutritional and hormonal signals, thus maintaining a balance between the appearance and disappearance of glucose in the bloodstream. Thus, processes like carbohydrate digestion and gastric emptying, which directly influence the influx of glucose into the bloodstream, are worth examining. Also, to better comprehend glucose homeostasis, it is essential to consider and appreciate the contribution of individual tissues involved in glucose (Baron et al., 1988; Kelley et al., 1988). Under glucose post absorption scenarios, the brain disposes about 23% of the glucose, and about 29% is utilised by splanchnic tissues (liver and gut). The other 25%

of glucose disappearance is due to insulin-dependent skeletal tissues, and the rest is utilised by other tissues such as the heart, adipose tissue and the kidney (Aronoff et al., 2004). Therefore, it is important to understand the key players (enzymes and hormones) involved in glucose metabolism homeostasis.

There are several hormones produced by the pancreas and the small intestine involved in glucose homeostasis. These hormones include insulin and amylin produced by the β-cells of the pancreas, which activate glucose uptake on the target sites, including muscle and adipose tissue (Wilcox, 2005). Insulin's roles include promoting glucose uptake by cells and stimulating protein and fat synthesis (Wilcox, 2005). Additionally, insulin suppresses postprandial glucagon secretion. The other β-cell produced hormone, amylin, suppresses glucagon and slows down gastric emptying (Aronoff et al., 2004). Thus, hormones of the pancreas play an important role in glucose regulation in addition to those produced by the small intestine.

Moreover, the predominant intestinal *L*-cell lining produced hormones, glucose-dependent insulinotropic polypeptide (GIP) and glucagon-like peptide-1 (GLP-1), are also responsible for glucose disappearance in the blood capillaries (Nauck & Meier, 2016; Nauck & Meier, 2019). They mediate glucose disappearance by slowing down gastric emptying, suppressing postprandial glucagon secretion and enhancing glucose-dependent insulin secretion (Aronoff et al., 2004). The GLP-1 and GIP hormones have stimulatory effects on insulin but not glucagon (Aronoff et al., 2004). Another hormone, glucagon, produced by pancreatic α-cells, is responsible for glucose appearance during hypoglycaemic situations (Jiang & Zhang, 2003). The principal roles of glucagon include the breakdown of stored liver glycogen and stimulation of gluconeogenesis and ketogenesis (Aronoff et al., 2004). Hence, glucose metabolism is dependent on both the pancreas and small intestine hormonal balance.

1.7.4 Glucose metabolism in cells

After absorption from the gut, glucose is transported by the circulatory system to target cells, where insulin-mediated/independent glucose uptake occurs (Wilcox, 2005). Glucose uptake in the muscles is mediated by a glucose transporter 4 (GLUT4), accounting for approximately 70% of insulin-dependent glucose uptake (Smith, 2002). Also, GLUT4 facilitates a further 10% of insulin-mediated intracellular glucose into adipocytes. Notably, glucose uptake by the liver accounts for about 30% of the whole body's insulin-mediated glucose disposal; however, it is insulin-independent. Insulin stimulates glycogen production and inhibits gluconeogenesis and ketone body production through intracellular signalling (Smith, 2002). The physiological cellular regulation of glucose uptake is complex; it relies on several factors, including the delivery of glucose to the cells, transport of glucose into cells by glucose transporters like GLUT4 and processes of glycolysis which are dependent on several enzymatic reactions (Wasserman et al., 2011). Apart from GLUT 4, there are other glucose transporters, and their distribution in specialised tissues is shown in Table 1.2.

Table 1.2: The main glucose transporters

Transporter	Tissue distribution	Properties	Reference
GLUT 1	Most cells	Basal glucose uptake	Gould et al., 1991
GLUT 2	Liver, β-cells, hypothalamus and the basal lateral membrane in the small intestine	Carrier for glucose and fructose in liver and intestine	Gould et al., 1991
GLUT 3	Neurons, placenta, testes and brain	Basal glucose uptake	Gould et al., 1991
GLUT 4	Skeletal, cardiac and adipose muscle	Activity increased by insulin	James et al., 1989
GLUT 5	Mucosal membrane in small intestines	Involved in fructose transport	Davidson et al., 1992

GLUT4 translocation pathways can be studied to gain a deeper knowledge of glucose transport. Natural compounds deemed to have hypoglycaemic properties like fucoidans can also be studied to investigate how they affect these pathways.

1.7.5 Glycolytic flux

Glycolysis is the primary metabolic pathway that provides energy and various intermediates vital for metabolism in humans (Tanner et al., 2018). These intermediates of the glycolytic pathway are essential sources of precursors for biomass production. The established ten glycolysis steps are known to yield 2ATP molecules per glucose molecule. These glycolytic steps preceded by glucose uptake via transporters, followed by lactate export through monocarboxylate transporters (MCTs) constitute the phenomenon known as the glycolytic flux (Tanner et al., 2018). One of the central processes which influence the glycolytic flux is hepatic glucose production, as it significantly contributes to blood hyperglycaemia (Sharabi et al., 2015). Moreover, the regulation of hepatic glucose is dependent on the glycolytic/gluconeogenic flux.

There are ten reactions in glycolysis. Seven of these can be used for both glycolysis and gluconeogenesis. The other three reactions, which include the conversion of glucose- 6- phosphate (G6P) to glucose, fructose-1,6-bisphosphate (F-1,6-biP) to fructose-6-phosphate (F6P) and the conversion of pyruvate to phosphoenolpyruvate (PEP), are unique to gluconeogenesis (Melkonian et al., 2020; Sharabi et al., 2015). The glycolytic metabolite flux in muscles, adipose tissues and hepatic glucose production is regulated by several vital enzymes affected by the relative presence of insulin or glucagon. The regulation and balance of reactions contributing to the glycolytic flux are critical for mammalian physiology as they contribute to glucose homeostasis (Buck et al., 2017). Importantly, glucose metabolism dysregulation is a hallmark of diseases, including diabetes and cancer (Tanner et al., 2018).

1.7.6 Antidiabetic relevance of fucoidan

It has been demonstrated that the most effective way of tackling disorders caused by hyperglycemia is by targeting one of the physiological aspects of carbohydrate metabolism. The most targeted step is carbohydrate digestion, as it is the primary source of blood glucose. The enzymes responsible for carbohydrate digestion, i.e. α-amylases, α-glucosidases, maltases and sucrases, are inhibited to avoid postprandial hyperglycaemia by retarding glucose absorption (Attjioui et al., 2021). A common inhibitor of these enzymes is acarbose; however, it has been associated with side effects like abdominal discomfort, flatulence and diarrhoea. These adverse effects could be caused by excessive inhibition of the colon's pancreatic α-amylase and bacterial fermentation. Therefore, it will be advantageous to use an inhibitor with mild inhibition of α-amylase but more pronounced inhibition of α-glucosidase and α-glucoamylase (Cho et al., 2011).

Another leading antidiabetic drug is metformin, a plant derivative, which increases insulin sensitivity, thus reducing hyperglycaemia (Rena et al., 2017). In addition, miglitol, which slows down the breakdown of starches into glucose (Felman, 2020), is also used. However, these compounds have been associated with side effects, including flatulence, diarrhoea, and abdominal discomfort (He et al., 2014). Moreover, recently, the Food and Drug Administration (FDA) recalled metformin with issues surrounding excessive limits of nitrosamine impurity associated with its formulation (FDA , 2020). These factors, including an increasing disease burden, cytotoxicity and low therapeutic drug availability, necessitate the search for natural, readily abundant remedies such as fucoidan. In the past decade, the antidiabetic potential of fucoidan has gained momentum as a novel bio-compound with its therapeutic effects reported at the various levels of glucose metabolism.

The antidiabetic nature of reviewed fucoidans has been observed to differ among brown seaweed species, fucoidan structure, and chemical composition (especially the number of sulphates residues). Fucoidans with higher sulphate compositions have been reported to have higher α-amylase and α-glucosidase inhibition potential (Lakshmanasenthil et al., 2013). A few studies have reported the inhibition patterns of some fucoidans on the

enzymes responsible for carbohydrate metabolism, namely α-amylase and α-glucosidase. Low-molecular-weight fucoidans have been reported to improve endoplasmic reticulum stress-reduced insulin sensitivity through adenosine monophosphate (AMP)-activated protein kinase activation in L6 myotubes. Also, they can restore lipid homeostasis in a mouse model of type II diabetes (Jeong et al., 2013). Slowing down or regulating the activity of these enzymes will thus directly influence the amount of monosaccharides, especially glucose, available for absorption (Fig. 1.4).

Furthermore, fucoidan extracted from *Cucumaria frondosa* has been reported to activate the PI3K/PKB pathway, regulating insulin production (Wang et al., 2016). Also, the fucoidan triggered translocation *via* GLUT4. Another fucoidan from *U. pinnatifida* reduced blood glucose levels, improved insulin sensitivity in mice, and decreased basal lipolysis in 3T3-L1 adipocytes. This may reduce hyperglycaemia by glucose uptake (Sim et al., 2019). Interestingly, *Acaudina molpadioides* was reported to inhibit glucose metabolism enzymes, including hexokinase and pyruvate kinase (Hu et al., 2014), major players implicated in the glycolytic flux. In summary, some of the fucoidans which showed therapeutic character against T2DM are listed in Table 1.3.

Table 1.3 Selected fucoidan extracts with antidiabetic properties

Fucoidan source	Harvest location	MW (kDa)	Sulphate w/w (%)	α-amylase (IC_{50})	α-glucosidase (IC_{50})	Other	Test system	Reference
Turbinaria ornata	India	ND	33 ±. 0.42	36.6 µg/ml	ND	Not cytotoxic to normal cells	*In vitro*	(Lakshmanasenthil et al., 2013)
Ascophyllum nodosum	Canada	420	ND	120 - 464 µg/ml	13 – 47 µg/ml		*In vitro*	(Kim et al., 2014; Foley et al., 2011)
Fucus vesiculosus	Canada	98	23.7 ± 0.04	No activity	49 µg/ml		*In vitro*	(Kim et al., 2014; Zayed et al., 2016; Oliveira et al., 2018)
Sargassum wightii	India	637	36 ± 0.60%	ND	139 µg/ml		*In vitro*	(Vinoth et al., 2015)
Cucumaria frondosa	China	ND	ND	ND	ND	-Activates the PI3K/PKB pathway, which regulates insulin production -Activates GLUT4 translocation	*In vivo*	(Wang et al., 2016)
Algal extract mixture (*F. vesiculosus* & *A. nodosum*)	Commercial (Italy)	ND	ND	1.49 ± 0.32 µg/ml	0.604 ± 0.004 µg/ml	- Significantly reduced postprandial glucose - Implicated in preventing progression of non-alcoholic steatohepatitis to T2DM	*Invitro & in vivo*	(Gabbia et al., 2017)

Fucoidan source	Harvest location	MW (kDa)	Sulphate w/w (%)	α-amylase (IC_{50})	α-glucosidase (IC_{50})	Other	Test system	Reference
Undaria pinnatifida	Commercial (Sigma Aldrich)			ND	ND	- Reduced blood glucose levels and improve insulin sensitivity in mice - Reduction of basal lipolysis in 3T3-L1 adipocytes	*In vivo*	(Sim et al., 2019)
	New Zealand	ND	15.02	190 ± 5 µg/ml	137 ± 1.2 µg/ml	- Non-competitive inhibitor of α amylase -Competitive inhibitor of α glucosidase	*In vitro*	(Koh et al., 2020; Zhao et al., 2018)
Acaudina molpadioides	China	1614.1	26.3 ± 2.7	ND	ND	-Acutely reduced blood glucose levels and improves insulin resistance -Inhibition of glucose metabolism-related enzyme (hexokinase, pyruvate kinase) activities and up-regulation of the PKB/GLUT4 pathway.	*In vivo*	(Hu et al., 2014)
Ecklonia maxima	South Africa	470	6.01 ± 0.97	No activity	290 µg/ml	Mixed inhibitor of α glucosidase	*In vitro*	(January et al., 2019; Daub et al., 2020)
Ecklonia radiata	South Africa		8.8 ± 1.4	No activity	19 µg/ml	-Mixed inhibitor of α glucosidase -Synergistically inhibits α glucosidase with acarbose	*In vitro*	(Mabate et al., 2021)

Modified from the review by Mabate et al. (2021)

1.8 Cancer

Cancer is a term that encompasses a diverse class of diseases characterised by the uncontrolled, abnormal growth of cells. Primary cancers can invade surrounding tissues and spread to other tissues and organs through metastasis using the circulatory or the lymphatic system (Marudhupandia et al., 2015). Sometimes these tumours are benign and are not invasive to other tissues; thus, they are localised. However, benign tumours may be large and sometimes life-threatening, especially if they grow in sensitive areas like the brain (NIH, 2021). However, most deaths from cancer occur due to metastases (NIH, 2021).

Cancer imposes a considerable burden (morbidity, mortality and economic) on society and has been identified as one of the leading causes of death in developed and developing countries. However, the latter is more significant (Torre et al., 2015). There are treatment options available for several cancers, including radiotherapy, chemotherapy, and surgery. The common chemotherapeutic drugs used to date include Taxol, irinotecan, oxaliplatin, capecitabine and 5-fluorouracil (Hsu & Hwang, 2019). Although there have been advancements in therapeutic strategies against cancers, including immunotherapy, there is currently no standardized treatment effective in preventing metastasis, and many cancers have high recurrence rates (Ustyuzhanina et al., 2014). These challenges demand innovativeness, development, and the search for additional strategies with minimal toxicity and side effects. Such chemoprotective strategies include the use of natural bioactive compounds. The use of natural compounds, including fucoidan, has gained much attention in the past decade as these compounds demonstrate anticancer properties with low toxicity (Hsu & Hwang, 2019). The following sections will highlight the established and proposed anticancer mechanisms of fucoidan.

1.8.1 Anticancer activity of fucoidan

The anticancer properties of fucoidan have been demonstrated *in vivo* and *in vitro* in diverse cancers. Fucoidan mediates its activity through mechanisms such as the induction of cell cycle arrest, apoptosis, anti-angiogenesis, inhibition of cellular migration, and activation of the immune system by enhancement of the activity of

natural killer (NK) cells. Additional activities of fucoidan have been reported that may be linked to observed anticancer properties. These include inducing inflammation through the immune system, reducing oxidative stress and stem cell mobilisation (Kwak, 2014).

1.8.2 Molecular mechanisms of anticancer effects of fucoidan

Cancer proliferation depends on various mechanisms which are of interest to drug discovery research. A better understanding of these mechanisms gives researchers in the drug discovery niche opportunity to design, discover and apply novel compounds like fucoidans to inhibit, block or manipulate the control points, which may prove helpful in disrupting the proliferation of cancer cells. The subsections below describe the effects of compounds on well-established cancer cell proliferation mechanisms.

1.8.2.1 Effects on growth signalling molecules

Several seaweed compounds possess chemopreventive and chemotherapeutic properties as they inhibit the phosphorylation of some membrane receptors involved in mitosis and the regulation of cell growth and proliferation. Some of the membrane receptors include members of the receptor tyrosine kinase (RTK) family like EGFR and platelet-derived growth factor receptor (PDGFR) (Senthilkumar et al., 2013).

Some marine compounds have been reported to disrupt growth factor-stimulated cell signalling pathways, often constitutively active in cancers due to mutations. Two of the main mitogenic pathways downstream of RTKs and deregulated in cancer are the mitogen-activated protein kinase (MAPK) cascade, particularly via Ras and Raf, and the PI3K-Akt pathway (Fig. 1.5). MAPK and PI3K pathways also modulate cell cycle arrest apoptosis and metastasis (Wada & Penninger, 2004), and activation increases the invasive behaviour of tumour cells. An unspecified fucoidan from Sigma Aldrich was reported to have an antimetastatic effect by inactivating the ERK pathway by inhibiting ERK1/2 phosphorylation in A549 human lung cancer cells (Senthilkumar et al., 2013). The PI3K-Akt pathway was implicated in regulating the invasion of non-small-cell lung cancer (NSCLC), developing and proliferating the tumour cells (Liao et al., 2006).

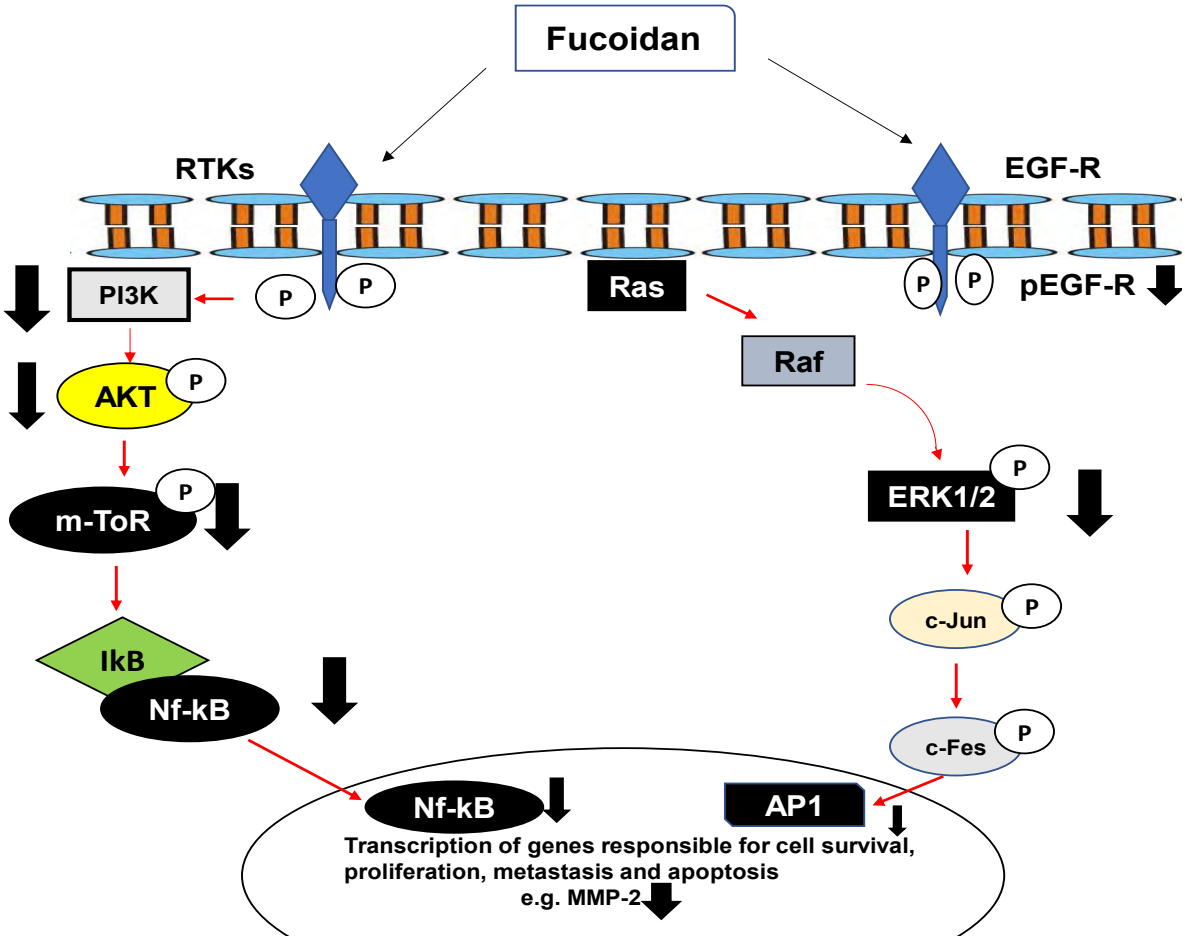

Figure 1.5:Schematic diagram showing some growth signalling molecules targeted by fucoidan.
The PI3/Akt mediated pathway and MAPK pathways are illustrated as they play major roles in cancer development. Fucoidans inhibit the signalling molecules as depicted by the downward facing black arrows. Generally, these signalling molecules regulate cell survival, proliferation, and apoptosis. Modified from Senthilkumar et al. (2013).

Some pathways, including the PI3/Akt/mTOR/p70S6K1 pathway, can regulate the apoptosis pathway and suppress metastasis. The mammalian target of rapamycin (mTOR) is a serine/threonine kinase also involved in cell growth and proliferation, cell survival, protein synthesis and cell motility. PI3K and Akt are upstream regulators of mTOR, while p70S6K1 is the downstream target of mTOR (Han et al., 2015a). Fucoidan has been reported to effectively downregulate the expression of MMP-2 through the suppression of the PI3K–Akt–mTOR and ERK signalling pathway in A549 human lung cancer cells. According to Lee et al. (2012), fucoidan also significantly inhibited p70S6K and 4EBP1, the downstream targets of mTOR, at a maximum inhibitory concentration of 200 µg/ml. NF-kB and AP-1 (shown in Figure 1.5) are

transcription factors that regulate genes associated with several pathological processes, including cancer. The inhibition of NF-kB and AP-1 results in suppressing tumour formation and subsequent metastasis (Wu et al., 2008). Figure 1.5 summarises two main signalling pathways associated with cancer cell proliferation.

1.8.2.2 Induction of cell cycle arrest

The cell cycle is a high energy process that enables cells to divide and systematically ascertain the proper duplication and separation of the genome (Senthilkumar et al., 2013). It is composed of two major stages, mitosis and interphase. Mitosis, which precedes cytokinesis, is the cell cycle process when daughter chromosomes separate. Mitosis (represented as M in Fig. 1.6) and cytokinesis last for a minimal time. Thus, most of the time is spent in the interphase, a stage where the cell grows steadily and duplicates genetic material. The interphase stage is divided into three stages: the G1 phase, S phase, and G2 phase (see Fig. 1.6). During the G1 stage, the metabolically active cell grows continuously but does not duplicate its DNA. The following S phase is characterised by DNA replication. In the G2 phase, the cell grows, and specific proteins are synthesised in preparation for mitosis (Nelson et al., 2002).

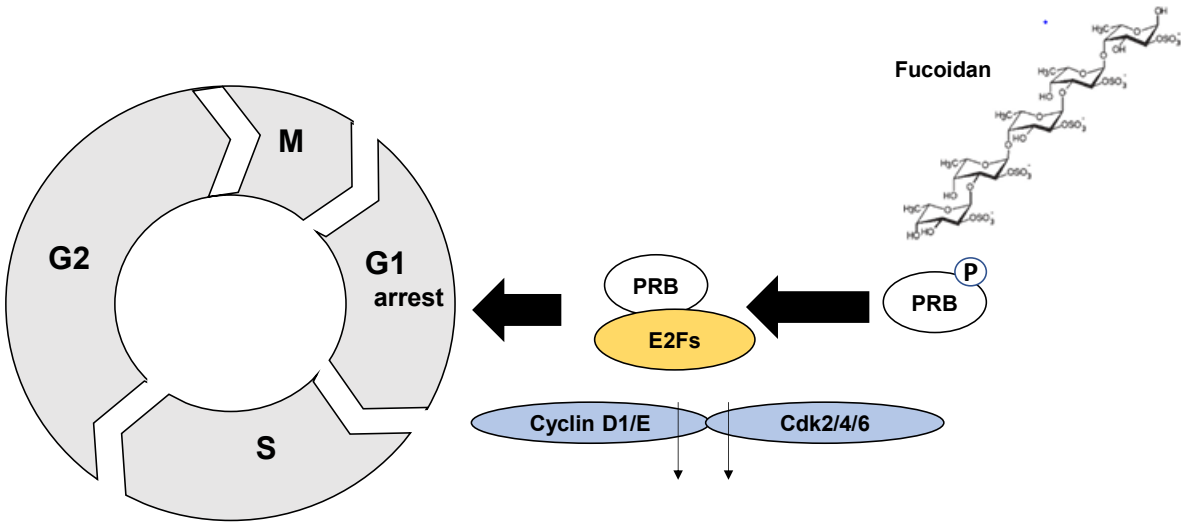

Figure 1.6: Fucoidan targets within the cell cycle.
M represents the mitosis phase, G1, the first growth phase, S, the DNA synthesis stage, and G2 represents the second growth stage in preparation for mitosis. Fucoidan targets the G1 phase of the cell cycle.

The proper function of the cell cycle is regulated by cyclins and cyclin-dependent kinases (CDKs). Cyclins are proteins associated with the cell division deemed to initiate mitosis (Sherr, 1996). Cyclins and CDK inhibitors regulate the activity of CDKs. The G1 phase is the most common target for anticancer therapeutics, as this stage of the cell cycle depends on mitogens and antiproliferative cytokines (Park et al., 2014). The process of transition from the G1 phase to the S phase is controlled via the formation of cyclin complexes. The p21 and p27 proteins are cyclin inhibitors known to be key participants in the G1 transition process. Cyclin inhibitors suppress the CDKs by combining them with the cyclin/CDK complexes (Park et al., 2014). The transcription factors, E2F-1 and E2F-4 are important for the G1-S phase transition. Fucoidan was reported to downregulate cyclin D1, cyclin E and CDKs but did not affect the CDK inhibitors. Also, fucoidan promoted the dephosphorylation of retinoblastoma protein (pRB) thus enhancing the binding of pRB and transcription factors (Fig. 1.6) (Park et al., 2015).

1.8.2.3 Induction of apoptosis

Apoptosis is a necessary physiological process characterised by programmed cell death. It is crucial in homeostasis and embryological development but may also participate in pathological processes, including cancer (Burz et al., 2009). Apoptosis is characterised by morphological changes in cells, including membrane blebbing, chromatin condensation, and cell shrinkage. Research on apoptosis mechanisms has enabled some of its stages to be targeted for chemotherapy. Some significant proteins, among others in the procession of apoptosis, have been reported. These include Bcl-2 family proteins and caspase proteins (cysteine proteases including multiple isoforms like caspase-3, caspase-8 and caspase-9), Bid and Bax (Park et al., 2011). Literature has also reported that several fucoidans induce apoptosis via various mechanisms (Fig. 1.7).

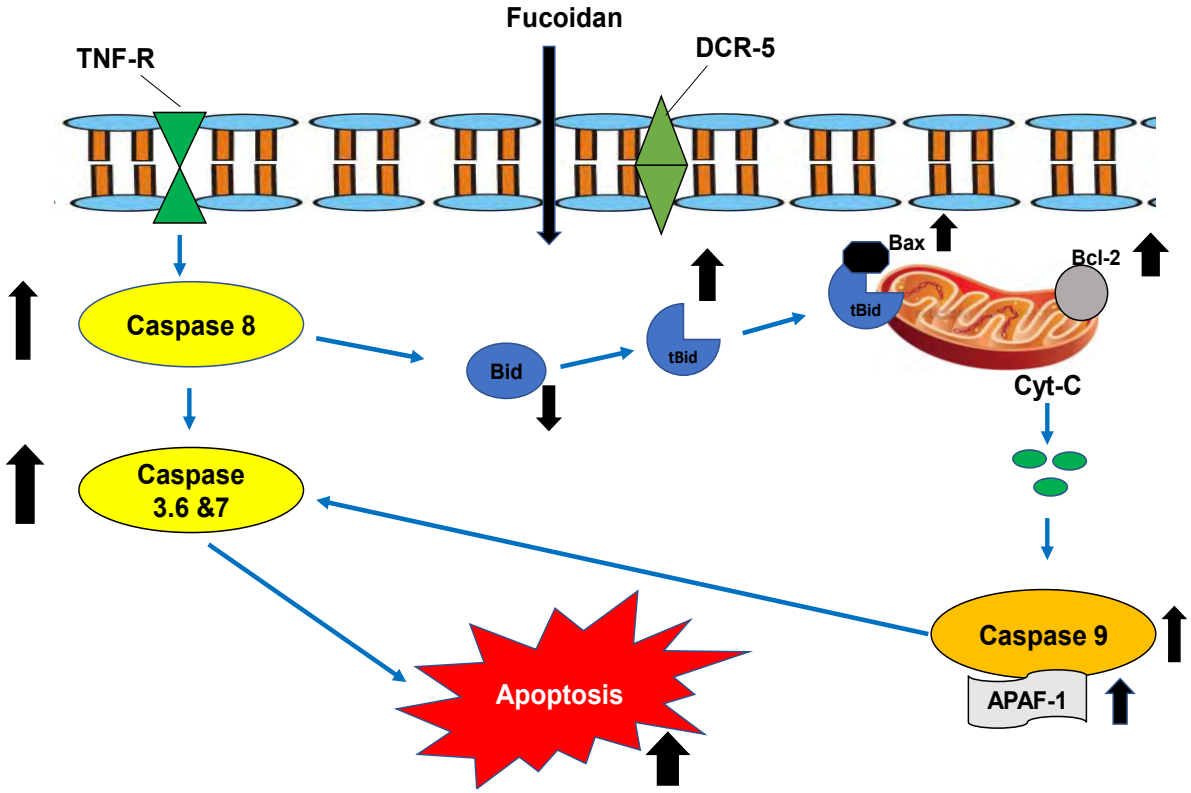

Figure 1.7:Apoptotic pathway induced by fucoidan.
The fucoidan mainly induces mainly the mitochondrial (intrinsic) pathway, although the extrinsic pathway can also be activated. Modified from Senthilkumar et al. (2013).

Fucoidan isolated from *Cladosiphon navae-caledoniae* suppressed the expression of Bcl-xL and Mcl-1. However, *C. navae-caledoniae* fucoidan upregulated the expression of Bax and the production of ROS in human breast cancer cell lines MCF-7 and MDA-MB-231 *in vitro* (Zhang et al., 2013). Fucoidan from *C. okamuranus* was deemed to induce apoptosis through pathways that result in the downregulation of the expression of survivin and cyclin D2, leading to the activation of the caspase-3,8,9 in human T cell leukaemia (Haneji et al., 2005).

Furthermore, fucoidan obtained from *F. vesiculosus* was reported to induce apoptosis by increasing the levels of caspase-3 in human colon carcinoma HT-29 tissue and melanoma cells using Western blotting *in vitro* and immunohistochemical staining of tissues *ex vivo* (Han et al., 2015). However, crude fucoidan from *F. vesiculosus* significantly reduced the expression of Bcl-2, survivin and morphological changes using the mouse breast cancer cell line 4T1 by flow cytometry, Western blotting and fluorescence microscopy *in vivo* (Xue et al., 2012). In addition, fucoidan from *Sargassum henslowianum* induced melanoma cell apoptosis by stimulating the

caspase-3 pathway as detected by flow cytometry and spectrophotometric detection of *p*-nitroaniline (*p*NA) *in vitro* (Ale et al., 2011). Fucoidan extracted from *U. pinnatifida* induced apoptosis in the human hepatocellular carcinoma cell line SMMC-7721 by ROS mediated mitochondrial pathway, activating the caspase pathways (Yang et al., 2013). Boo and colleagues (2013) also reported that fucoidan from *U. pinnatifida* induced apoptosis in the human prostate cancer cell line PC-3. Its mechanism of action involves activating the ERK1/2 pathway while inactivating the PIK3/Akt pathway and thus down-regulating the Wnt/β pathway *in vitro*. Furthermore, fucoidan from *U. pinnatifida* could induce apoptosis on the human lung carcinoma cell line A549. Apoptosis occurred through the regulation of the Bcl-2 protein family, activating ERK1/2 and thereby downregulating the PIK3/Akt pathway (Boo et al., 2011).

Apoptosis has been the process most targeted by researchers investigating the anticancer effects of fucoidan. However, it has been challenging to draw conclusions, as different brown seaweed species, different cell lines, and different objectives have been used or pursued in these studies. Nevertheless, the apoptotic effects of fucoidans thus far reviewed, have focused mainly on the caspase-dependent pathways linked to the Bcl-2 family of proteins, PIK3/Akt pathway and Wnt/β pathway (Wu et al., 2016).

1.8.2.4 Anti-angiogenesis

Angiogenesis is the process of new blood vessel formation in physiological and pathological conditions. It is vital for tumour growth and metastasis (Liu et al., 2012). Moreover, angiogenesis is vital for wound healing and embryonic development processes. However, if it continues uncontrolled, it can cause pathological states, including tumour growth. Tumour growth is dependent on angiogenesis for the supply of nutrients and oxygen. Thus, angiogenesis inhibition can reduce or stop tumour proliferation, making the process a logical target for cancer therapy (Nelson, 1998).

Pro-angiogenic molecules, including the family of vascular endothelial growth factors (VEGFs), play a significant role in angiogenesis. This family is a rate-limiting factor in the process (Ferrara et al., 2003). VEGF-A is a survival factor of endothelial cell lines (EC), which contributes significantly to the proliferation and migration of the EC cell

line. It is worth noting that the VEGF expression is regulated by HIF-1α (Lunt et al., 2009).

Several researchers have reported the influence of fucoidans from different brown seaweeds on angiogenesis. A purified commercial fucoidan from *F. vesiculosus* significantly suppressed VEGF expression in mouse breast cancer 4T1 cells by Western blotting *in vitro* (Xue et al., 2012). In another study, Han et al. (2015b) determined that the expression of VEGF and CD31 on the human colon cancer cell line HT-29 was significantly reduced by fucoidan obtained from *F. vesiculosus* by immunofluorescence staining *in vivo*. Fucoidan obtained from *S. hemiphyllum* of about 760 Da significantly suppressed angiogenesis in bladder cancer cells under hypoxia, by inhibiting the VEGF through suppression of HIF-1α expression using Western blotting *in vitro* (Chen et al., 2015). In addition, fucoidan isolated from *U. pinnatifida* was reported to inhibit the expression of VEGF-A by downregulating angiogenesis in human umbilical vein endothelial cells (HUVEC) through phase-contrast microscopy, Western blot and RT-PCR *in vitro* (Liu et al., 2012). Limited literature generally exists that focuses on the effect of fucoidan on angiogenesis. However, Wu et al. (2016) highlighted that fucoidans of different sources and molecular weight could significantly affect the anti-angiogenesis effect.

1.8.2.5 Suppression of cellular migration

The tumour microenvironment is characterised by hypoxia, low pH and insufficient glucose supply. These conditions are essential in tumour metastasis (Lunt et al., 2009). Tumour metastasis occurs in processes involving cancer cells detaching from the primary tumour, invading surrounding tissues, intravasating into the circulatory system or lymphatic, and ultimately developing a secondary tumour in target organs. A group of matrix metalloproteinases (MMPs) are vital in the process of tumour metastasis. The involvement of MMPs is inevitable in the degradation of the extracellular matrix (ECM), allowing epithelial cells to migrate to other regions (Lunt et al., 2009). It is worth noting that the expression of MMPs is regulated by NF-kB, AP-1, MAPK and PI3K/Akt pathways. In addition, CXCL12 may also induce the secretion of MMPs (Schneider et al., 2015).

Some studies on the inhibition of the cellular migration of tumour cells have been reported. Fucoidan isolated from *F. vesiculosus* significantly inhibited the migration of the human colon cancer cell line HT-29 by suppressing PI3/Akt/mTOR/p70S6K1, which, in turn, inhibited the expression of MMP-2 *in vitro* (Han et al., 2015a). In addition, the fucoidan also inhibited the migration and invasion of human lung carcinoma *in vitro* (Lee et al., 2012). An *in vivo* study performed by Xue et al. (2012) also suggested that purified fucoidan from *F. vesiculosus* could inhibit the metastasis of mouse breast cancer 4T1 cells significantly by enumerating metastatic lung nodules.

Furthermore, fucoidan from *S. hemiphyllum* inhibited the invasion of a hepatocellular carcinoma cell line HCC, by invoking pathways that inhibit the degradation of the ECM and thus decreasing the MMP expression levels as observed through RT-PCR, Western blot, and the luciferase reporter assay (Yan et al., 2015). In addition, a purified fucoidan from *S. latissima* was deemed to suppress the migration of Burkitt's lymphoma cells by inhibiting the expression of MMP-9 through an ELISA technique, flow cytometry and gelatin-based zymography *in vitro* (Schneider et al., 2015). It is therefore clear that metastasis is critical for the invasiveness of tumours. The inhibition of the migration of tumour cells by fucoidan may contribute to the therapeutic efforts against different cancers.

1.8.3 Relevance of glucose metabolism and fucoidan to cancer therapeutic efforts

Glucose metabolism within cancerous cells is essential for the survival of these cells, as it is vital for supporting the cells' rapid growth necessary for their invasion. Therefore, understanding the dynamics of glucose metabolism in cancerous cells is important in searching for and discovering novel natural product-based drugs.

1.8.3.1 Tumour glucose metabolism

Cancerous cells reprogramme glucose metabolism to ensure their survival and progression (Heiden et al., 2009). Cancer progression relies on uncontrolled proliferation accompanied by amplified energy production and circumvention of

metabolic stresses. Cancer cells preferably switch to glycolysis which produces only 2 ATP molecules per glucose instead of the normal oxidative phosphorylation (OXID- P) route (Yu et al., 2017). In typical normoxic conditions, pyruvate from glycolysis is converted to acetyl coenzyme A (acetyl CoA) through a decarboxylation reaction to produce carbon dioxide and water via the Krebs cycle. However, pyruvate is converted to lactate through the anaerobic glycolytic pathway (Yu et al., 2017). Therefore, cancerous cells preferably use the latter process, characterised by elevated glycolysis rates even under normoxic conditions (Gottschalk et al., 2004; Nolop et al., 1987). This phenomenon seen in tumour cells is commonly described as the Warburg effect (Warburg et al., 1924).

Notably, an energy metabolism shift (distinguished by an increased glycolytic flux in cancer cells) does not imply a defective OXID-P process, as most tumour cells possess functional mitochondria (Zhang & Yang, 2013). Moreover, literature has shown a metabolism shift from converting phosphoenolpyruvate to pyruvate, catalysed by the enzyme pyruvate kinase M2 (PKM2), often overexpressed in cancerous cells. (Cortés-Cros et al., 2013). The resulting pyruvate from this unique pathway is converted to lactate by lactate-dehydrogenase (LDH), accompanied by ATP production. Also, acetyl-CoA is preferably produced, entering the Krebs cycle (Akins et al., 2018).

Because of the Warburg effect, cancer cells need to increase glucose uptake to adapt to the associated high energy demands since glycolysis has low energy yields. This characteristic of cancer cells has been exploited clinically in cancer diagnosis using a radiolabelled glucose analogue (Bomanji et al., 2001; Weiler-Sagie et al., 2010). Aerobic tumour glycolysis has been demonstrated as a promising target for cancer therapeutic efforts. Therefore, the inhibition of mitochondrial OXID-P has been proven to suppress hepatocellular tumour proliferation (Zhou et al., 2014). In addition, it has also been shown that inhibition of OXID-P reduced the multidrug resistance of melanoma cells (Roesch et al., 2013).

1.8.3.2 Metabolic phenotypes of tumour cells

Cancer cells have two metabolic phenotypes: the glycolytic phenotype, which follows the Warburg glucose metabolism, and the non-glycolytic oxidative phenotype (Abdel-

Wahab et al., 2019). These cells can switch between the two phenotypes, and the switching mechanism is not yet fully understood. However, the most common among tumour cells is the glycolytic phenotype. Interestingly, the glycolytic phenotype usually shows a non-glycolytic characteristics under acidic conditions caused by lactate accumulation. The process of lactate acidosis is a recurrent consequence of the Warburg effect in solid tumours (Gatenby & Gillies, 2004; Jiang, 2017). The low pH caused by lactate accumulation inhibits the glycolytic enzymes, which reduces the glycolytic flux and is detrimental to cancer cells' proliferation. Therefore, under lactate acidosis, the glycolytic tumour cells can switch from the glycolytic phenotype to the non-glycolytic oxidative phenotype, which slowly metabolises glucose to ensure cell survival (Hu et al., 2017).

Also, in hypoxic conditions, or even mitochondrial dysfunction, cancer cells switch from oxidative glucose metabolism to Warburg metabolism to sustain cell growth (Lu et al., 2012). This metabolic shift is used by breast cancer cells to resist radiation (Lu et al., 2015). Furthermore, hybrid metabolism is common in aggressive tumour cell lines, including SiHa and HeLa cell lines, due to the robust activation of hypoxia-inducible factor-1 (HIF-1) due to lactate accumulation (De Saedeleer et al., 2012). Also, the hybrid phenotype of tumours helps them adapt to oxygen shock when they invade oxygen-rich tissues by switching from the glycolytic phenotype to the non-glycolytic oxidative phenotype (Jia et al., 2018). The metabolic plasticity of tumour cells is supported by the hybrid Warburg/OXID-P phenotype switching, promoting cancer invasion, metastasis, and chemotherapy resistance (Maiuri & Kroemer, 2015). Therefore, targeting the hybrid metabolic state is a sound therapeutic strategy to reduce the burden of tumour metabolic plasticity (Abdel-Wahab et al., 2019).

1.8.3.3 Glycolytic flux targets for therapeutic efforts

Glycolysis relies on the import of glucose by glucose-transporters (GLUTs). Notably, the primary glucose transporters in tumour cells are GLUT3 and GLUT5, which are usually overexpressed (Tanner et al., 2018). Inhibitors impeding glucose transport have been reported, including phloretin and ritonavir combined with metformin, and have entered the clinical trial stage (Dalva-Aydemir et al., 2015; Lin et al., 2016). The potential targets within the glycolytic flux pathway are shown in Figure 1.8.

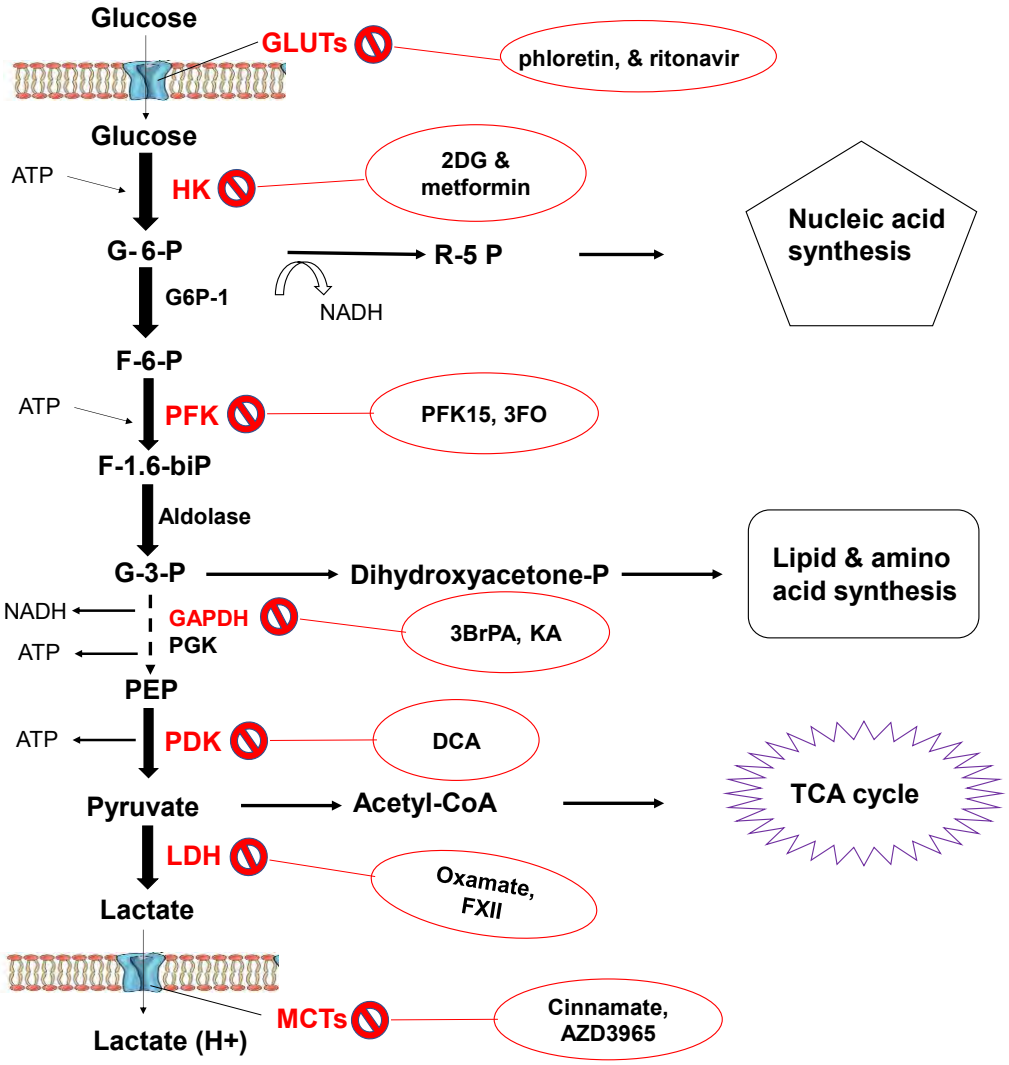

Figure 1.8:The glycolytic flux pathway and potential targets for novel drugs.
The glycolysis pathway with its metabolic intermediates is illustrated. The known glycolytic enzyme inhibitors are presented in red circles and their target enzymes in red. Glucose transporters (GLUTs) and lactate monocarboxylate transporters (MCTs) are shown as transmembrane proteins in blue. The enzymes and transporters highlighted are appropriate targets for fucoidan. Adapted from Abdel-Wahab et al. (2019) & reviewed in Mabate et al. (2021).

Soon after glucose enters the cell through transporters, it is immediately phosphorylated by hexokinase (HK). This is a rate-limiting step designed to conserve energy in the cell (Mathupala et al., 2009). Metformin, a plant-derived bio-compound that partially impairs glucose metabolism, can inhibit hexokinase activity and thus suppresses tumour growth in breast cancer (Marini et al., 2013). An analogue of glucose, 2-deoxy-D-glucose (2DG), can mimic the hexokinase substrate (glucose),

thus inhibiting the enzyme function (Raez et al., 2013). Usually, after HK facilitated phosphorylation, glucose-6-phosphate is isomerised by glucose-6-phosphate isomerase. The resulting fructose-6-phosphate is subsequently phosphorylated by different isoforms of phosphofructokinases (PFK-1 & PFK-2) into fructose-1.6-biphosphate and fructose-2.6-biphosphate, respectively (Fig. 1.8).

Typically, PFK1 is vital in regulating glycolysis as high intracellular amounts of ATP inhibit the enzyme. However, PFK2 is overexpressed in cancer cells to produce excess fructose-2.6-biphosphate, thereby activating PFK1 to maintain a high glycolytic rate independent of ATP levels (Colombo et al., 2010). Another isoform of PFKs, PFKFB3, also overexpressed in cancer cells, has been targeted therapeutically using PFK15 (1-(4-pyridinyl)-3-(2-quinolinyl)-2-propen-1-one) (Zhu et al., 2016). Tanner and colleagues suggested by systematic enzyme overexpression that the enzymes acting on the upper glycolytic reactions mediate the control of the glycolytic flux (Tanner et al., 2018).

However, some enzymes in lower glycolysis, including aldolase (ALDOA), glyceraldehyde-3-phosphate dehydrogenase (GAPDH), phosphoglycerate kinase (PGK), pyruvate kinases (PKM1 and PKM2), and lactate dehydrogenase (LDH), have been reported to have a significant effect on the Warburg process (Rahier et al., 2015). Remarkably, the enzyme GAPDH has been strategically targeted by several compounds, including koningic acid (KO) and iodoacetate (IO), which are in the preclinical stages (Ganapathy-Kanniappan, 2018; Rahier et al., 2015) . Also, pyruvate dehydrogenase kinase (PDK) is inhibited by dichloroacetate (DCA), which is in the first phase of clinical trials (Dunbar et al., 2014), while oxamate is in the preclinical trial phase for regulating lactate dehydrogenase A (LDHA) (Le et al., 2010). Finally, some of the essential membrane proteins, monocarboxylate transporters (MCTs), are also targeted by cinnamate and AZD3965 which are in the preclinical and phase 1 stages, respectively (Halestrap, 2012; Marchiq & Pouyssegur, 2016).

Even though glycolysis yields about 18 times less ATP than mitochondrial OXID-P, the accelerated rate of glycolysis can achieve 100 times more ATP production than OXID-P (Locasale & Cantley, 2010). In addition, cancer cells benefit from metabolic intermediates such as lipids, nucleotides, and amino acids, on top of ATP, which are essential in the biosynthesis of macromolecules required during cell proliferation

(Deberardinis et al., 2008). The Warburg effect in cancer cells produces considerable amounts of NADPH and NADH that act as redox buffers to avoid the free radical effect of chemotherapeutics on the cell (Zhu et al., 2018). Additionally, lactate influx and efflux by cancerous cells are essential for their survival. The metabolic symbiosis of glycolytic and non-glycolytic cells, or switching into the hybrid phenotype, creates favourable conditions for survival in solid tumours (Abdel-Wahab et al., 2019). The lactate produced within the system is released outside the cell mainly by MCT4 (Pinheiro et al., 2012). These lactate transporters may also be targeted in therapeutic efforts to combat cancer cell progression.

Cancer cells organise their glycolytic phenotypes to achieve maximal energy production for their proliferation and survival. Thus, it is essential to invest in research in prospective pharmacological products such as fucoidan, which may be potential therapeutics that target one or more stages in the glucose metabolism pathways unique to cancer cells.

1.9 Conclusion

Diabetes and cancer, among other diseases, are a burden to society as they reduce lifespan by direct mortality and health complications. There are therapeutic strategies in place, but they have drawbacks, including severe side effects, toxicity limitations, and cost. However, seaweeds, regarded as bio-waste, harbour bioactive compounds such as fucoidan, which is of interest to this study. Although fucoidans are promising natural therapeutics for various ailments, challenges limiting their utilisation in clinical trials include the complex heterogeneous structure of fucoidan, highly variable doses, different administration routes and possible negative interactions with other established drugs (Atashrazm et al., 2015). Due to the wide variability in fucoidan structure, the current study will investigate critical factors affecting bioactivities such as fucoidan content, sulphate content, monosaccharide constitution and molecular weight. The proposed main target for our fucoidans, as illustrated in this chapter, is carbohydrate and glucose metabolism, although other mechanisms are also discussed.

CHAPTER 2: PROBLEM STATEMENT, STUDY RATIONALE, AIMS AND OBJECTIVES

2.1 Problem statement

Persistent (chronic) diseases, including type 2 diabetes mellitus (T2DM) and cancer, are examples of non-communicable diseases that kill about 41 million people annually, contributing to about 71% of overall deaths globally (WHO, 2021). Cancer-related mortality is at about 10 million annually and diabetes at about 2 million (WHO, 2021), and together, they account for about 29% of the non-communicable disease deaths. In addition, the World Health Organisation has also stated a key fact that 77% of these non-communicable disease deaths occur in low- and medium-income countries.

More than 100 000 people are diagnosed with cancer annually in South Africa, which is likely to keep increasing because of environmental and lifestyle factors. Such factors include smoking, diet, and lack of exercise (National Cancer Registry, 2017). Cancer incidence is inevitably increasing, and from a global point of view. The increase in new cancer cases is expected to rise to approximately 22 million by the year 2030. Cancer is a considerable global burden, with a high mortality rate (60%). It has been estimated that there will be an increase in cancer incidence in South Africa by about 75% by the year 2030 (Ferlay et al., 2015). Diabetes, another persistent disease, has a high occurrence worldwide, with over 425 million people living with the disease and 16 million of these people residing in the African continent. This number (16 million) is expected to increase to about 41 million by 2030. In South Africa, about 2 million diabetes cases were reported in 2017 (International Diabetes Federation, 2018).

In addition, the Disability-Adjusted Life Years (DALYs) are reported to be shifting from communicable infectious diseases like TB and HIV to non-communicable diseases in Sub-Saharan Africa (Gouda et al., 2019). These authors also highlighted that diabetes and cancers are the major contributors to the increase of DALYs in sub-Saharan Africa.

There is no doubt that South Africa (among other countries) is heavily burdened by both cancer and diabetes. Currently, there are treatment regimens for these persistent

diseases, and these are primarily chemotherapeutic. However, most of these cause severe side effects in patients. The toxicities limit the dose of the drugs administered, which, in turn, lowers the efficacy of the treatment (Atashrazm et al., 2015). Furthermore, the emergence of acquired resistance to chemotherapeutic agents has resulted in a need for other interventions (like using natural products) to alleviate the burden caused by these diseases. Such natural compounds include fucoidan, with limited cytotoxicity but with therapeutic properties (Isnansetyo et al., 2017).

2.2 Study rationale

Chemotherapeutic drugs are the most widely used remedies for diseases, including cancer and diabetes. Most of these drugs target primary regulatory functions necessary for the manifestations of these diseases (Atashrazm et al., 2015). Despite the success of chemotherapeutic drugs, side effects associated with toxicity often surface, limiting the dosage usable to achieve a desirable therapeutic effect. Therefore, there is a need to develop better-tolerated treatment remedies with improved therapeutic properties. Chemotherapeutic resistance in cancer also results in patients' therapeutic failure and eventually death. Resistance to chemotherapy might be due to the use of limited concentrations of drugs to avoid toxicity to the host.

Natural products have been known to have therapeutic advantages in history. Their importance in alleviating ailments caused by diseases cannot be ignored. Marine products have been implicated to have therapeutic and nutritional benefits (Yuan et al., 2016). Recently, the focus has diverted from terrestrial resources (medicinal plants), which are easily endangered, towards the study of marine natural resources. Furthermore, seaweeds (among other marine organisms at ocean edges) have attracted scientists to explore their potential therapeutic applications (Ahmad, 2015). In the current study, natural compounds (fucoidans) extracted from brown seaweeds are of interest as they are reported to possess potential therapeutic properties. These properties include anti-diabetic, anti-cancer, anti-inflammatory and anticoagulant effects. Fucoidans are a significant family of sulphated fucose abundant polysaccharides. Literature has reported that fucoidan's distinct structural features, for example, 1,3-linked α-L-Fuc*p*-4-*O*SO_3^- repeating units, obtained from different brown

seaweeds, may be necessary for bioactivity potential (Ale & Meyer, 2013; Anastyuk et al., 2017)

Different and specific structures of fucoidans may be obtained through different extraction conditions (Hahn et al., 2012; Li et al., 2008). Furthermore, the heterogeneity in the structural makeup of seaweed interspecies and intraspecies may lead to various products being extracted. Understanding the structural features of fucoidans and their potential bioactivities are exasperated by the many extraction methods that exist (Ale & Meyer, 2013). Thus, the current study sought to design a novel standard, environmentally friendly extraction method that will effectively preserve the fucoidan's structural features.

Moreover, cancer and diabetes remain a severe burden in South Africa (Gouda et al., 2019), and fucoidans have been shown to have therapeutic properties. Most studies involving the therapeutic characteristics of marine resources have been performed in other countries - mainly in China and Japan. However, limited literature on this topic exists in South Africa, a country with a wide range of marine resources. Therefore, this study will identify different South African brown seaweeds, isolate their fucoidans, characterise these natural products and screen the bio-actives for their anti-cancer and anti-diabetic potential.

2.3 Research hypothesis

Fucoidan extracted from South African seaweeds display anti-diabetic and anti-cancer activities.

2.4 Aim

To establish the relationship between extracted fucoidan structures and their biological activity (anti-diabetic and anti-cancer activities)

2.5 Objectives

- To extract fucoidans from a variety of South African brown seaweeds;
- To characterise extracted fucoidan through structural analysis and chemical profiling;
- To determine the anti-diabetic activity of extracted fucoidan (via α-amylase and α-glucosidase inhibition assays);
- To investigate the anti-cancer properties of the extracted fucoidans on HCT116 colorectal human cells; and
- To elucidate the link between fucoidan structures and their biological activity (anti-diabetic and anti-cancer properties).

CHAPTER 3: CHARACTERISATION OF FUCOIDANS EXTRACTED FROM SOUTH AFRICAN BROWN SEAWEEDS

3.1 Introduction

Fucoidan, a sulphated polysaccharide found within the mucilage of brown seaweeds, has become an important biological compound with various pharmacological applications (January et al., 2019). One of the most exciting questions in fucoidan-related literature is the relationship between the structural make-up of extracted fucoidans and their biological functions. It has been established that the yields, chemical properties, and structural diversity of fucoidans vary between genera of brown seaweeds, although compositional variations within the same species are also common (Ale & Meyer, 2013). Seasonal variation in seaweed harvests and geographical location also affect fucoidan's structural composition and yield from seaweeds (Rani et al., 2017). Fucoidan contents within brown seaweeds range from 2-6%. Fucoidans are generally heterofucans with a sulphated fucose backbone and varying proportions of monosaccharides, including glucose, galactose, xylose and mannose (Maina, 2014).

Over the past few decades, fucoidan and other polysaccharides have been extracted from brown seaweeds using several extraction techniques. Fucoidan extraction technologies have influenced the yield, structural composition, molecular weight, and chemical composition of the resulting fucoidan (Ale et al., 2011). Some of the commonly used technologies in the extraction of fucoidans are hot water, dilute acid, enzyme-assisted, alkali extraction and microwave-assisted extraction (Ponce & Stortz, 2020). The challenges associated with producing fucoidan are its yield, biological activity and the chemical waste associated with some of its extraction methods, including alkali extraction (Xing et al., 2013). With these challenges, there is a need to scrutinise and improve the existing production methods to produce better yields and maintain the biological activities of the extracted fucoidan. This chapter investigated the effect of the different extraction methods (hot water, EDTA, and acid) on the yields and chemical and structural compositions of the fucoidans obtained.

3.1.1 Objectives

The objectives of this chapter were to:

- Extract fucoidan from harvested South African brown seaweeds using three extraction technologies (hot water, EDTA and acid).
- Chemically and structurally characterise the extracted fucoidan.

3.2. Materials and methods

Fucus vesiculosus fucoidan (Cat. No. F5631) was purchased from Sigma-Aldrich (St. Louis, MO, USA). The analytical kits used in this study were purchased from Megazyme™ (Bray, WC, Ireland). The rest of the reagents used in this study were purchased from Sigma-Aldrich, MERCK, Flucka Saarchem (Darmstadt, HE, Germany), and Celtic Diagnostic and Life Technologies (Cape Town, South Africa) (Table A1; Appendix A).

3.2.1 Sampling and seaweed processing

The brown seaweeds, *Ecklonia radiata* and *Sargassum elegans* utilised in this study were harvested from Kelly's beach in Port Alfred with coordinates (33° 36' 36.8424" S; 26° 53' 23.4996" E) in the Eastern Cape province, South Africa (Fig. 3.1).

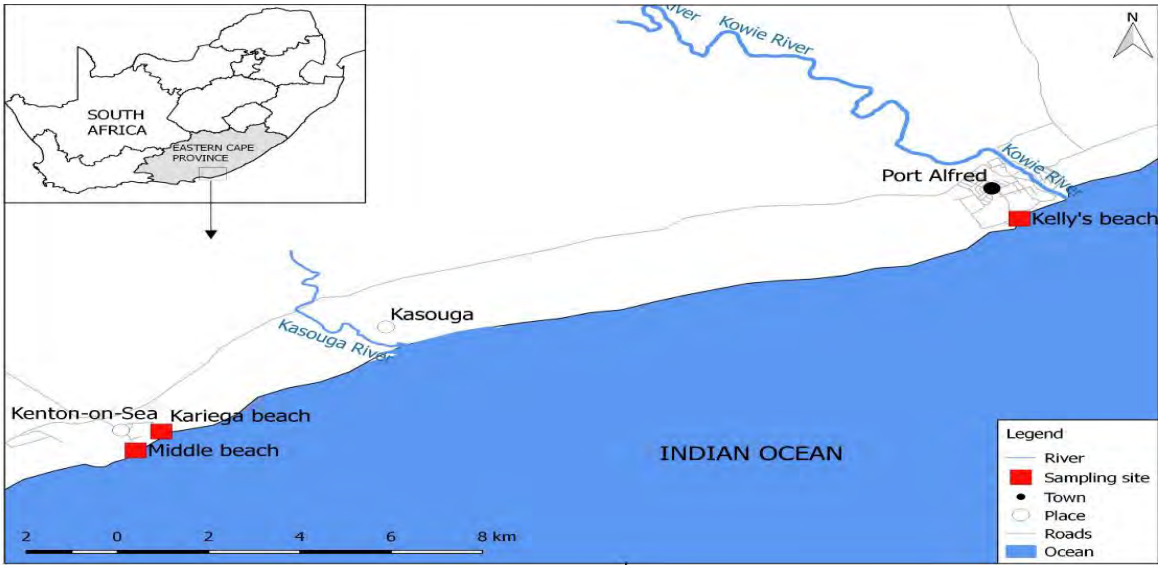

Figure 3.1: Map showing the seaweed sampling sites within the Eastern Cape province, South Africa.

Ecklonia maxima seaweed was kindly donated by the HIK-Abalone Farm located in Hermanus, Western Cape province, South Africa. Most of *E. radiata* seaweed was collected as beach cast. However, some were harvested together with the *S. elegans* from rock pools. The beach cast and rockpool collected *E. radiata* was mixed and processed as a single batch. These seaweeds were harvested between February and March 2019. The pictures of the harvested seaweeds are shown in Figure 3.2 and these were identified based on their morphological characteristics.

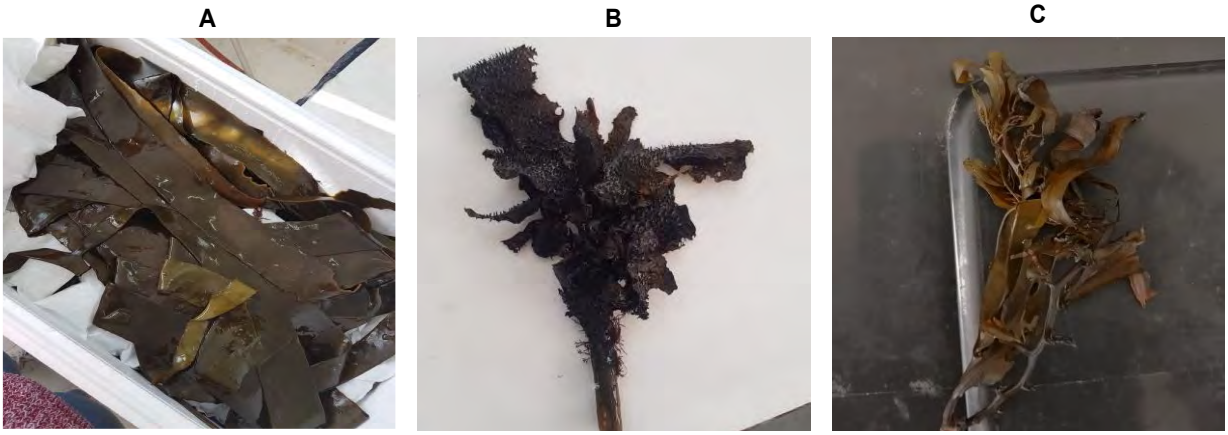

Figure 3.2: Visual illustration of harvested seaweeds.
Seaweeds identified as **A:** *E. maxima*, **B**: *E. radiata*, **C:** *S. elegans.*

The harvested seaweeds were stored on ice during transportation to the laboratory. Upon arrival at the laboratory, the seaweed was washed 3x with distilled water, cut into smaller pieces and oven-dried at 40 °C for 72 hours. The remainder of the seaweed was stored at -20 °C. The dried seaweed was pulverised using a coffee grinder, and the resulting powder was stored at room temperature until use.

3.2.2 Extraction of fucoidan

Three extraction protocols were utilised to extract fucoidans: hot water extraction, EDTA-Na assisted extraction, and dilute acid extraction. The seaweed was defatted by extracting lipids and pigments using a high methanol percentage mixture; with a solvent ratio of 4: 2: 1 for MeOH: $CHCl_3$: H_2O (Suresh et al., 2013; Yuan & Macquarrie, 2015). In short, approximately 80 g of pulverised seaweed was dissolved in 800 ml of the methanol solution and heated at 70 ^oC with agitation for ~2 hours. After filtration,

the resulting residue was dried at 40 °C and stored at room temperature until further use.

3.2.2.1 Hot water extraction

Fucoidan was extracted from *E. maxima*, *E. radiata* and *S. elegans* as described by Lee and co-workers using the hot water extraction method with minor modifications (Lee et al., 2012). Briefly, 15 g of dry, defatted seaweed powder was dissolved in 450 ml of distilled water in a 1:30 (w/v) ratio. The mixture was heated at 70 °C with agitation overnight. The extracted solution was centrifuged at 5000 *g* for 20 minutes at 4 °C. The supernatant was incubated in 1% $CaCl_2$ (w/v) overnight at 4 °C to precipitate the alginate. The mixture was centrifuged at a speed of 5000 *g* for 10 minutes at 4 °C, and 20% (v/v) absolute ethanol was added as another step to remove the remaining alginate. Centrifugation then followed as described previously, and fucoidan was precipitated by adding 80% (v/v) absolute ethanol and incubation at 4 °C overnight. The fucoidan precipitate was collected through centrifugation at 8000 *g* for 10 minutes at 4 °C. The fucoidan was then oven-dried until a constant mass was obtained. After the drying process, fucoidan was placed in a desiccator for about 4 hours and finally stored in a cool, dry place.

3.2.2.2 EDTA-Na assisted extraction

An optimised method described by Zhao et al. (2018) was used with minor modifications to investigate the effects of EDTA-Na on the yield of extracted fucoidan from seaweed. An amount of 15 g of defatted seaweed powder was dissolved in 450 ml of 0.5% EDTA-Na (w/v), and the mixture was heated at 70 °C with agitation for 3 hours. The mixture was centrifuged at 5000 *g* for 20 minutes at 4 °C. The supernatant was neutralised by adding 0.1 M NaOH and adjusting the pH to 7. The extracts were centrifuged, treated with $CaCl_2$, and the fucoidan ethanol precipitated as described in section 3.2.2.1.

3.2.2.3 Acid assisted extraction

An amount of 15 g of defatted seaweed powder was dissolved in 450 ml of 0.15 M HCl in a 1:30 (w/v) ratio and heated at 70 ºC with stirring. Centrifugation of the mixture at 5000 *g* for 20 minutes at 4 ºC was then performed. The supernatant was then neutralised with 2 M NaOH. Thereafter, the extracts were also $CaCl_2$ treated, and the fucoidans were ethanol precipitated as described in section 3.3.2.1.

3.2.2.4. Fucoidan yield

The dry weight yield of fucoidan upon extraction from the seaweed was calculated according to the formula below:

$$\%\ yield = \frac{mass\ of\ crude\ fucoidan}{mass\ of\ defatted\ seaweed} \times 100$$

3.2.3 Chemical characterisation of fucoidan

3.2.3.1 Total sugar determination

The total sugar content was analysed using the phenol-sulfuric acid method, using L-fucose as a standard (Dubois et al., 1956). Briefly, 300 µl of concentrated sulfuric acid (95-97%) was added to 100 µl of 1 mg/ml fucoidan. Subsequently, 50 µl of 5% (w/v) phenol was added, and the mixture was vortexed and then heated at 90 °C for 10 minutes. After cooling to room temperature, total sugars were quantified by reading the absorbance at 490 nm using a Hidex microplate reader (Bio-Tek instruments with KC Junior software®). The total sugar content was interpolated using an *L*-fucose standard curve (Appendix B1).

3.2.3.2 Total protein determination

Protein content was measured using bovine serum albumin (BSA) as a standard (Bradford, 1976). Briefly, 10 µl of fucoidan samples and BSA standards were mixed with 230 µl of Bradford's reagent. The mixture was incubated at room temperature for

10 minutes. The absorbance values of the samples were read at 595 nm, and the protein concentrations were interpolated using the BSA standard curve (Appendix B2).

3.2.3.3 Acid hydrolysis of fucoidan for chemical characterisation

About 20 mg of fucoidan extracts were hydrolysed in 2 M trifluoroacetic acid (TFA) at 100 ^{o}C for 4 hours in safe lock Eppendorf tubes. The hydrolysed samples were then dried in a Centrivap (Vacutec) at 80 ^{o}C for 6 hours. After this, the hydrolysed fucoidan was reconstituted to a 20 mg/ml concentration using ddH2O.

3.2.3.4 Total reducing sugar assay

The total reducing sugar content in fucoidan were investigated using the dinitrosalicylic acid (DNS) assay (Miller, 1959). Briefly, 300 µl of DNS solution (1% (w/v) NaOH; 1% (w/v) dinitrosalicylic acid; 20% (w/v) sodium potassium tartrate; 0.2% (w/v) phenol and 0.05% (w/v) sodium metabisulphite) was added to 150 µl of hydrolysed (1 mg/ml) fucoidan stock. The reaction was heated at 100 °C for 6 minutes on a digital dry bath (Labnet AccuBlock^{TM}), then cooled on ice for 6 minutes. After cooling, the samples were loaded onto a 96 clear bottom microplate, and the optical density was read at 540 nm using a Hidex microplate reader (Bio-Tek instruments with KC Junior software®). The amount of reducing sugars within the fucoidan was quantified by interpolation using a D-glucose standard curve (Appendix B3).

3.2.3.5 Monosaccharide and uronic acid determination

The quantitative analysis of L-fucose, D-fructose, D-galactose, D-xylose, L-arabinose, D mannose in the extracted fucoidan was investigated using a Shimadzu HPLC (RID) instrument (Table B1; Appendix B). All samples and standards were filtered through a 0.22 µm PES membrane and diluted before injection in the HPLC run. The HPLC analysis of the sugars was performed using a Fortis Amino column using a slight modification of the recommended method from the supplier (Fortis Technologies Ltd, Cheshire, UK). The method outline is summarised below:

Analytical Column:	Fortis Amino (150 mm x 4.6 mm)
Product number:	FNH-050703
Mobile phase:	Acetonitrile: H_2O (Milli-Q), in a ratio of 3:1
Flow rate:	0.8 ml/min
Column temperature:	30 ºC
Injection volume:	20 µl
Detector:	Refractive index detector (RID)

Standard curves were constructed for each sugar to interpolate the amount of respective sugars in the fucoidan samples. The assays were performed in technical and experimental triplicates to ensure validity and reproducibility in the method. The uronic acid content within the extracts was determined calorimetrically according to a microplate Megazyme assay kit (K-URONIC).

3.2.3.6 Sulphates determination

The sulphate content in the fucoidans was measured using a barium chloride–gelatin method as described previously (Dodgson & Price, 1962), which was downscaled to microtitre volumes. Briefly, the test samples were hydrolysed in 1 M HCl at 110 °C for 3 hours using sodium sulphate as standard. A volume of 380 µl of 4% trichloroacetic acid (TCA) was added to a 20 µl fucoidan sample, then 100 µl of $BaCl_2$ reagent was added, and the reaction was mixed. The reaction was incubated at room temperature for 20 minutes, after which the optical density was read at 360 nm. The sulphate composition was quantified using the sodium sulphate standard curve (Appendix B4).

3.2.3.7 Estimation of total polyphenols

The total polyphenols were determined using a modified Folin–Ciocalteu method (Huang et al., 2005). Briefly, a mixture of 30 µl of 1 mg/ml fucoidan, 540 µl of ddH_20 and 60 µl of the Folin-Ciocalteu reagent was incubated at room temperature in a low light environment for 10 minutes. An aliquot of 50 µl 2 M sodium carbonate was then

added, and the reaction mixture was incubated for a further 30 minutes at 37 °C. Absorbance was then measured at 765 nm, with the amount of total polyphenols determined from a gallic acid standard curve (Appendix B5).

3.2.3.8 Quantification of EDTA-Na

The amount of EDTA within the fucoidan extracts was quantified using a spectrophotometric method through ferroin formation using sodium sulphite as the reducing agent as described by Wang et al. (2013) with minor modifications. Briefly, 20 µl of ferric chloride (3.6 mM) was added, followed by 20 µl EDTA of the desired concentrations (0 - 3.6 mM). After mixing, 20 µl of Na_2SO_3 solution (1.8 mM) was added to each reaction. Thereafter, 40 µl of 1,10-phenanthroline monohydrate (PTM) solution (7.6 mM) and 100 µl of 1M NaAc buffer was added. Lastly, 820 µl of dH_20 was added to make up a total reaction of 1 ml. The reactions were left at room temperature for 10 min, and OD was then read at 510 nm, with the amount of EDTA determined from an EDTA-Na standard curve (Appendix B6).

3.2.3.9 Determination of fucoidan kinematic viscosities

The kinematic viscosities of 1 mg/ml solutions of the fucoidans were measured using a glass capillary viscometer (Cannon-Manning (State College, PA, USA) semi-micro glass viscometer of capillary diameter size 50) at 37°C. Samples were prepared in dH_2O and equilibrated to the required temperature for 30 minutes before taking measurements. The averages of no fewer than three readings were taken using two separately prepared replicates of the various fucoidan samples. Distilled water was used as a control and reference for the experiment. To obtain kinematic viscosity in mm^2 /s (cSt), the efflux time in seconds was multiplied by the viscometer constant (K= 0.003992) using the following equation:

$$Viscocity = viscometer\ constant\ (K) x\ time\ (t)$$

3.2.4 Structural characterisation

3.2.4.1 Molecular weight estimation

Analytical ultracentrifugation was performed in triplicate to determine the molecular weight of the fucoidan from *E. maxima, E. radiata and S. elegans*. A 15 ml fucoidan stock (0.5 mg/ml) was prepared in distilled water and filtered through ddH_2O pre-washed 100K, 50K, 30K and 10K Amicon® Ultracentrifugation filters (Merck Millipore, Tullagreen, Carrigtwohill, Ireland). The supernatants were obtained by centrifuging the filters at 4 000 g for 20 minutes. The sample fractions were analysed for fucoidan in triplicate according to the phenol-sulfuric acid assay described in section 3.2.3.1.

3.2.4.2 FTIR analysis

An amount of 100 mg of ground fucoidan was scanned using Fourier-transform infrared spectroscopy (FTIR) using a 100 FT-IR spectrometer system (Perkin Elmer, Wellesley, MA, USA). The signals were automatically recorded by averaging 4 scans over the range of 4000–650 cm^{-1}. The baseline and ATR corrections for penetration depth and frequency variations were performed using Spectrum One software (version 1.2.1) system (Perkin Elmer, Wellesley, MA, USA).

3.2.4.3 NMR spectroscopy analysis

Fucoidan samples (each 10 mg) were dissolved in 1 ml of D_2O, centrifuged at 13 000 g for 2 minutes and the supernatant filtered through 0.45-*μ*m filters to remove any insoluble material. The deuterium-exchanged samples were subjected to ^{1}H-NMR analysis, and spectra were recorded at 23 °C using a Bruker, Switzerland 400 MHz spectrometer, with Topspin 3.5 software. The chemical shifts were expressed in ppm.

3.2.4.4 Thermogravimetric analysis

Thermogravimetric analysis of fucoidan extracts was conducted on a thermogravimetric analyser (*PerkinElmer*®, Pyris Diamond model). Approximately 4 mg of each fucoidan sample was placed in an aluminium crucible for analysis. Pure nitrogen (purity of 99.99%), with a flow rate of 20 ml/min, was used as the carrier gas

during all the experiments to extinguish the mass transfer effect to a minimum level. The fucoidan was heated from 30 °C to 900 °C at a heating rate of 30 °C/min. A separate blank run was conducted for baseline correction in each test, using an empty pan. Lastly, the mass loss relative to the temperature increment was automatically recorded, and the derivative thermogram (DTG) was then plotted using GraphPad Prism v 6.

3.2.4.5 Scanning Electron Microscopy

The morphology of the various fucoidan extracts was captured using the VEGA TESCAN Scanning Electron Microscope (SEM) device (Wirsam Scientific and Precision Equipment, (PTY) LTD, Johannesburg, South Africa). The fucoidan extracts were gold-coated using a quorum (Q150RS) metal coater (Advanced Laboratory Solutions, Randburg, South Africa). The SEM pictures were scanned at various magnifications, from 100x to 5000x magnification.

3.2.4.6 High-performance liquid chromatography-mass spectrometry

The Ultra-High-Performance Liquid Chromatography- High Resolution-Mass Spectrometry (UHPLC-HRLC-MS) analyses of the samples were performed at Rhodes University Mass Spectrometry Centre using a Thermo Scientific Ultimate 3000 Dionex UHPLC (Thermo Fisher Scientific, Sunnyvale, CA, USA) equipped with a Fortis C18 column (3.0 × 100 mm, 3 µm; Fortis Technologies Ltd, Cheshire, UK) at 25 °C. A guard column (5 mm × 2.1 mm, 3 µm) containing the same packing material was placed before the column. The flow rate was set at 0.2 ml/min. The mobile phase consisted of a mixture of water solvent (A) and acetonitrile (ACN, solvent B), both adjusted with 0.1% formic acid (FA). The isocratic mobile phase consisted of 90% A and 10% B and was operated for 5 min. The thermostat of the RS Auto-Sampler WPS-3000 was set at 40 °C, while the injection volume was set at 5 µl for a final concentration of 10 µg/ml prepared for each sample. An HPG-3400 RS pump and a DAD-3000 RS detector were coupled to the UHPLC system. The HR-LC-MS acquisitions were performed on a Bruker Compact quadrupole time of flight (QToF) mass spectrometer using an electrospray ionization probe in positive mode (ESI^+) (Bruker, Bremen, Germany). A mass range of 100–3000 m/z was set up for the

acquisition of the HR-LC-MS spectra. The ESI^+ source parameters were set as follows: Endplate offset: 500 V, Nebulizer: 3.0 Bar, Dry gas: 9.0 L/min, Dry temperature 220 °C; Capillary voltage 4.5 KV. Nitrogen was used as a nebulizer and dry gas.

3.3 Results

3.3.1 Fucoidan yield

Three methodologies were used to extract fucoidan from South African brown seaweed: hot water, EDTA-Na assisted, and acid assisted extractions. The dry weight % fucoidan yield from dried seaweed biomass was determined (Fig. 3.3).

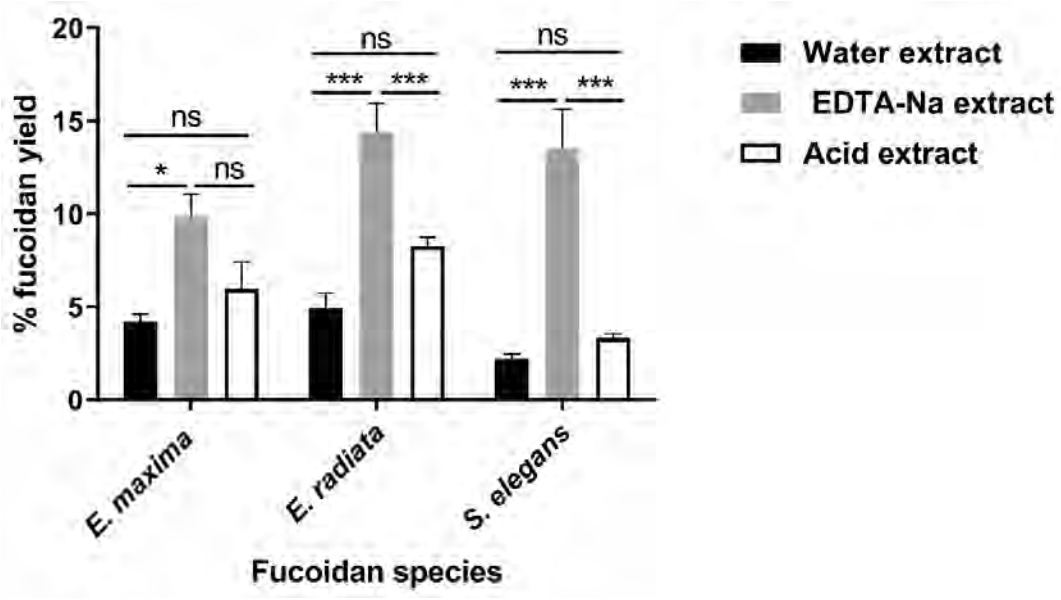

Figure 3.3: Yield of extracted fucoidan from dry weight seaweed biomass.
The bars represent the fucoidan yield in terms of means ± SD from 3 biological replicates (n=3). Two-way ANOVA analysis of fucoidan extracts, the (*) represents the strength of significance where the p value in the range $0.001 < p < 0.05$, (***) represents a p value < 0.001 and (ns) represents data that is not significantly different at a 95% confidence interval.

There was a clear trend in the extraction protocol employed and fucoidan yield. The EDTA extraction method yielded more fucoidan among all the seaweed extraction procedures studied (Fig. 3.3). *E. maxima* seaweed produced a 9.9% (w/w) fucoidan yield, *E. radiata* about 14.2%, and *S. elegans* displayed about a 12.5% yield using the EDTA extraction method. Also, acid extracts produced slightly higher yields than the

water extracts, although this difference was not statistically significant (Fig. 3.3). The water extraction method yielded 4.3%, 4.9% and 2.2% fucoidan for *E. maxima, E. radiata* and *S. elegans,* respectively – while the acid extraction method produced 6%, 8.3% and 3.3% fucoidan yields for *E. maxima*, *E. radiata* and *S. elegans*, respectively. The extracted fucoidans were then chemically characterised to determine their composition.

3.3.2 Chemical characterisation of extracted fucoidan extracts

The fucoidan extracts were tested for total carbohydrate content using the phenol-sulphuric acid method described in section 3.2.4.1 The *Ecklonia* spp. (*E. maxima* and *E. radiata*) extracts contained the highest levels of total carbohydrates, with the acid extracts containing almost 90% carbohydrate content (Table 3.1). *S. elegans* had relatively lower total carbohydrates compared to the *Ecklonia* spp. extracted fucoidan. Also, the commercial *F. vesiculosus* fucoidan total sugars were quantified, and they were comparable to the *S. elegans* fucoidan with approximately 40% (w/w) total carbohydrates (Table 3.1). A notable difference was observed among the different extraction methodologies, with the EDTA extracted fucoidan having significantly lower amounts of total carbohydrates across all the seaweed species studied.

To further determine the composition of the fucoidan extracts, the compounds were partially hydrolysed in 2 M TFA and then assayed for the presence of several monosaccharides using HPLC and Megazyme kits. The HPLC method was optimised to ensure validity and reproducibility. The detection and separation profile of the sugar standards is demonstrated in Appendix B7. The monosaccharide profiles of the fucoidans are shown below in Table 3.1. The monosaccharides which were detected in most extracts were fucose, glucose, galactose, xylose and mannose. Glucose and galactose were the predominant monosaccharides in the *Ecklonia* spp. However, *S. elegans* and the commercial *F. vesiculosus* derived fucoidans contained relatively higher fucose levels than the other extracts. *S. elegans* fucoidan displayed a notably higher mannose content than the other fucoidan extracts (Table 3.1). The sizes of the fucoidan extracts were determined through ultrafiltration, and all the extracts were greater than 100 kDa in size.

Table 3.1: Quantified monosaccharides % (w/w) in the fucoidan structure

Fucoidan extracts from various seaweeds	Total carbohydrate ± SD	*L*-fucose ± SD	*D*-glucose ± SD	*D*-galactose ± SD	*D*-fructose ± SD	*L*-arabinose ± SD	*D*-mannose± SD	*D*-xylose± SD	Estimated size in kDa
***E. maxima* (water extract)**	72.8 ± 5.2	4.56 ± 0.84	8.1 ± 3.4	4.8 ± 0.1	ND	3.2 ± 1.34	3.00 ± 0.45	4.5 ± 0.7	>100
EDTA-Na extract	47.9 ± 4.7	3.5 ± 0.95	7.9 ± 3.9	7.3 ± 2.4	ND	ND	4.35 ± 1.45	2.4 ± 0.9	>100
Acid extract	86 ± 10.6	2.67 ± 0.32	9.0 ± 4.7	ND	3.1 ± 1.2	5.35 ± 2.1	3.76 ± 1.1	3.9 ± 1.2	100>f<50
***E. radiata* (water extract)**	88.1 ± 7.4	3.73 ± 0.13	7.1 ± 2.3	4.9 ± 1.2	ND	ND	4.23 ± 0.22	4.7 ± 1.2	>100
EDTA-Na extract	34 ± 4.7	3.7 ± 0.68	7.2 ± 2.7	9.23 ± 1.21	ND	3.51 ± 1.02	2.99 ± 0.33	2.05 ± 0.9	>100
Acid extract	91.1 ± 8.8	2.72± 0.26	9.4 ± 4.8	ND	ND	5.02 ± 2.03	ND	2.0 ± 0.7	>100
***S. elegans* (water extract)**	44.4 ± 6.2	4.88 ± 0.99	5.7 ± 1.7	5.68 ± 0.1	2.2 ± 0.87	ND	7.14 ± 1.78	5 ± 1.9	>100
EDTA-Na extract	27.9 ± 7.9	2.44 ± 0.18	7.0 ± 3.3	ND	ND	ND	4.34 ± 0.85	2.4 ± 0.7	>100
Acid extract	46.8 ± 6.7	2.35 ± 0.40	5.7 ± 2.1	5.4 ± 0.46	ND	ND	3.73 ± 0.43	4.2 ± 1.6	>100
***F. vesiculosus* (commercial standard)**	41.3 ± 9.8	8.15± 0.41	5.1 ± 2.1	7.1 ± 0.83	2.2 ± 1.08	ND	4.48 ± 0.72	1.6 ± 0.6	>100

The values are represented as means ± SD (n=3). ND: Not detected

In addition, the total sulphate, phenolics and protein content of the fucoidan extracts were quantified. Commercial *F. vesiculosus* had the highest sulphate content, which was about 15%. *S. elegans* fucoidan had the highest quantity of sulphate (9.7%) among our “in-house” extracts (Table 3.2). The sulphate content seemed to be dependent on the extraction method. The water extracted fucoidans from all the seaweed species displayed the highest sulphate contents, followed by the EDTA extracts and lastly, the acid extracts (Table 3.2). There was little protein detected within all extracts, with quantities being lower than 4.64%. There were also minimal amounts of phenolics detected within the extracts, and in some extracts, no phenolics were detected.

Total uronic acid monosaccharide content (glucuronic acid) was also quantified, as these sugars are usually associated with alginate contamination in fucoidan extracts. All the extracts contained low amounts of uronic acids, with *S. elegans* having the highest amount (4.8%) (Table 3.2). *Ecklonia* sp. fucoidans contained lower amounts of uronic acids at approximately 2%. Moreover, the ash content of the fucoidan extracts was profiled using TGA, and most extracts had approximately 20% ash, with the highest observed for *S. elegans* fucoidan (24%) (Table 3.2). The kinetic viscosity of the fucoidans was measured, and the results revealed that the extracts had a similar viscosity (Table 3.2) to water, which had a kinematic viscosity of about 1.06 cSt. However, the water extracted fucoidan across all seaweed species were relatively the most vicious, and the EDTA extracted fucoidans were the least viscous compared to the water standard (Table 3.2). It should be noted that the amount of trace EDTA was investigated in the EDTA extracted fucoidan, and no EDTA was detected in any of these extracts.

Table 3.2: Total phenolics, protein and uronic acids quantities % (w/w) in fucoidans

Fucoidan extracts from various seaweeds	Sulphate ± SD	Protein content ± SD	Total phenolics ± SD	Total uronic acid ± SD	Total ash content ± SD	EDTA-Na content ± SD	Viscosity mm^2/s^2 (cSt/s) ± SD
E. maxima (water extract)	7.2 ± 1.2	2.1 ± 0.67	1.90 ± 0.6	2.6 ± 1.2	20 ± 2.6	ND	1.12 ± 0.02
EDTA-Na extract	4.7± 0.87	1.27 ± 0.11	0.88± 0.5	2.4 ± 0.8	22 ± 3.8	0	1.08 ± 0.01
Acid extract	2.0± 0.4	1.63 ± 0.31	1.70± 0.9	2.0 ± 0.9	19 ± 2.9	ND	1.1 ± 0.01
E. radiata (water extract)	8.8± 1.4	2.36 ± 0.89	1.90± 0.4	2.2 ± 0.7	16 ± 3.8	ND	1.12 ± 0.01
EDTA-Na extract	1.5 ± 0.22	2.05 ± 0. 65	0.47 ± 0.12	2.2 ± 0.8	18 ± 2.1	0	1.08 ± 0.002
Acid extract	1.3 ± 0.51	3.24 ± 1.11	0.89 ± 0.21	2.6 ± 0.5	12 ± 3.6	ND	1.12 ± 0.01
S. elegans (water extract)	9.7 ± 1.8	4.64 ± 2.45	2.83 ± 0.86	4.8 ± 0.6	24 ± 3.1	ND	1.12 ± 0.005
EDTA-Na extract	3.4 ± 0.7	1.96 ± 0.59	1.08 ± 0.75	2.9 ± 0.7	19 ± 3.2	0	1.06 ± 0.01
Acid extract	2.3± 0.69	2.2 ± 0.77	1.50± 0.69	4.4 ± 0.7	24 ± 2.8	ND	1.07 ± 0.01
F. vesiculosus (commercial standard)	14.7 ± 2.3	1.96 ± 0.60	0 ± 0.043	2.2 ± 0.8	ND	ND	1.11 ± 0.004

The values represented are means ± SD of biological replicates (n=3). ND: Not determined

3.3.3 Structural analysis of fucoidan

3.3.3.1 FTIR analysis

Fucoidan extracts were also structurally analysed by Fourier-transform infrared spectroscopy (FTIR). All the fucoidan extracts showed a spectral band between 3500 cm^{-1} and 3200 cm^{-1}, characteristic of polysaccharides. This peak is associated with the stretching vibrations of the OH groups within the carbohydrate. This peak seemed to be more pronounced in the water extracted *E. maxima* and *E. radiata* fucoidan than in the EDTA and acid extracted fucoidan (Fig. 3.4).

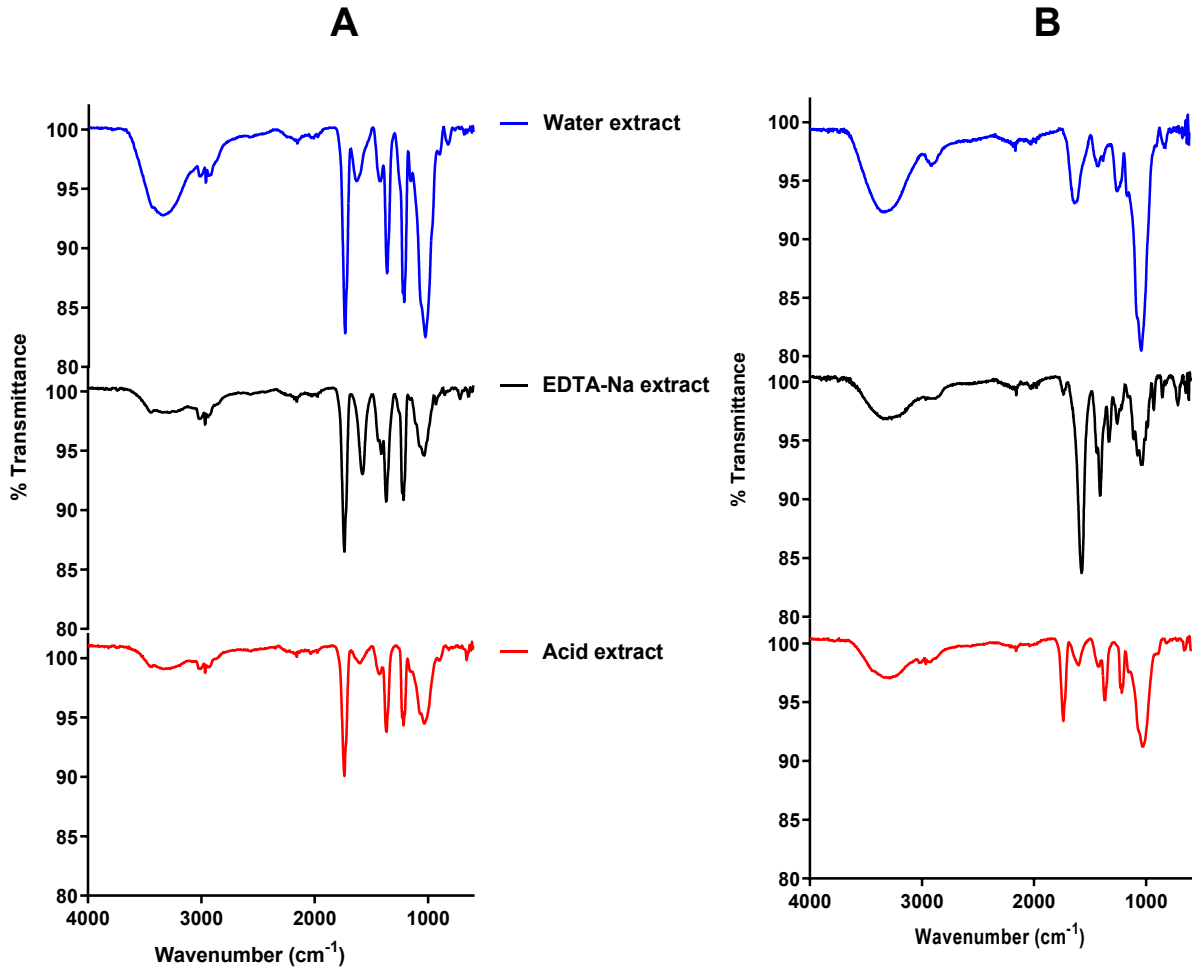

Figure 3.4: FTIR spectra overlays of *Ecklonia* sp fucoidan extracts
A; *E. maxima* fucoidan extracts and **B**; *E. radiata* fucoidan extracts.

Smaller bands were observed in the 2900 to 3000 cm^{-1} region, usually assigned to the CH stretching in the pyranose ring and methyl groups associated with fucose (Zhao et al., 2018). The peaks observed around 1650 cm^{-1} represents the carbonyl groups and stretching of *0*-acetyl groups (Sanjeewa et al., 2017). This peak is more pronounced in *E. maxima* extracts than in *E. radiata* extracts. The *E. radiata* EDTA extract had an extended peak in this region. The dips around 1200 cm^{-1} were prominent in the water extracts in both *Ecklonia* spp. However, the bands were smaller within the EDTA and acid extracts. The peaks between 1210 cm^{-1} and 1270 cm^{-1} are associated with stretching of the S═O bond linked with sulphate groups, a characteristic of fucoidans. Stretching vibrations of the glycosidic C─O bonds are represented in the peak around 1100 cm^{-1} (Vinoth Kumar et al., 2015). All samples analysed exhibited a broad band at around 1220–1260 cm^{-1} (Pereira et al., 2013).

The *Ecklonia* extracts also displayed very small peaks around 850 cm^{-1}. The peaks at approximately 850 represent sulphate groups attached to the carbonyl groups of sidechains such as galactose (Sanjeewa et al., 2017). An additional sulphate absorption band around 845 cm^{-1}, which is linked to the C–O–S 'the secondary axial sulphate', might indicate that the sulphate group is located at C-4 of the fucopyranosyl residue. In contrast, absorptions around 820– 825 cm^{-1} could be associated with low substitution amounts at the equatorial C-2 and C-3 positions, confirming that most of the sulphate groups in fucoidans are on the C-4 of fucose (Wang et al., 2010).

The peak at around 3200 to 3550 cm^{-1} seemed to disappear in the acid extracted *S. elegans* fucoidan (Fig. 3.4A), just as in the *Ecklonia* sp. acid extracted fucoidans (Fig. 3.4). Also, the bands around 1370 to 1250 cm^{-1}, associated with sulphate residues, seemed to vary. This peak was much more pronounced in the water extracts than the EDTA extracts, and almost vanished in the acidic extract. Furthermore, the IR spectra of the water extracted fucoidan were overlaid with that of the commercial *F. vesiculosus* sample to compare the distribution of the functional groups (Fig. 3.5B). The commercial *F. vesiculosus* standard profile had less peak distribution (around 1650 cm^{-1}), which depicts the occurrence of carbonyl groups associated with carbohydrates. This was also true for the *S. elegans* fucoidan (Fig. 3.5B). However, more prominent peaks were observed in the 850 to the 830 cm^{-1} region, which is linked to the sulphate in the fucoidan structure.

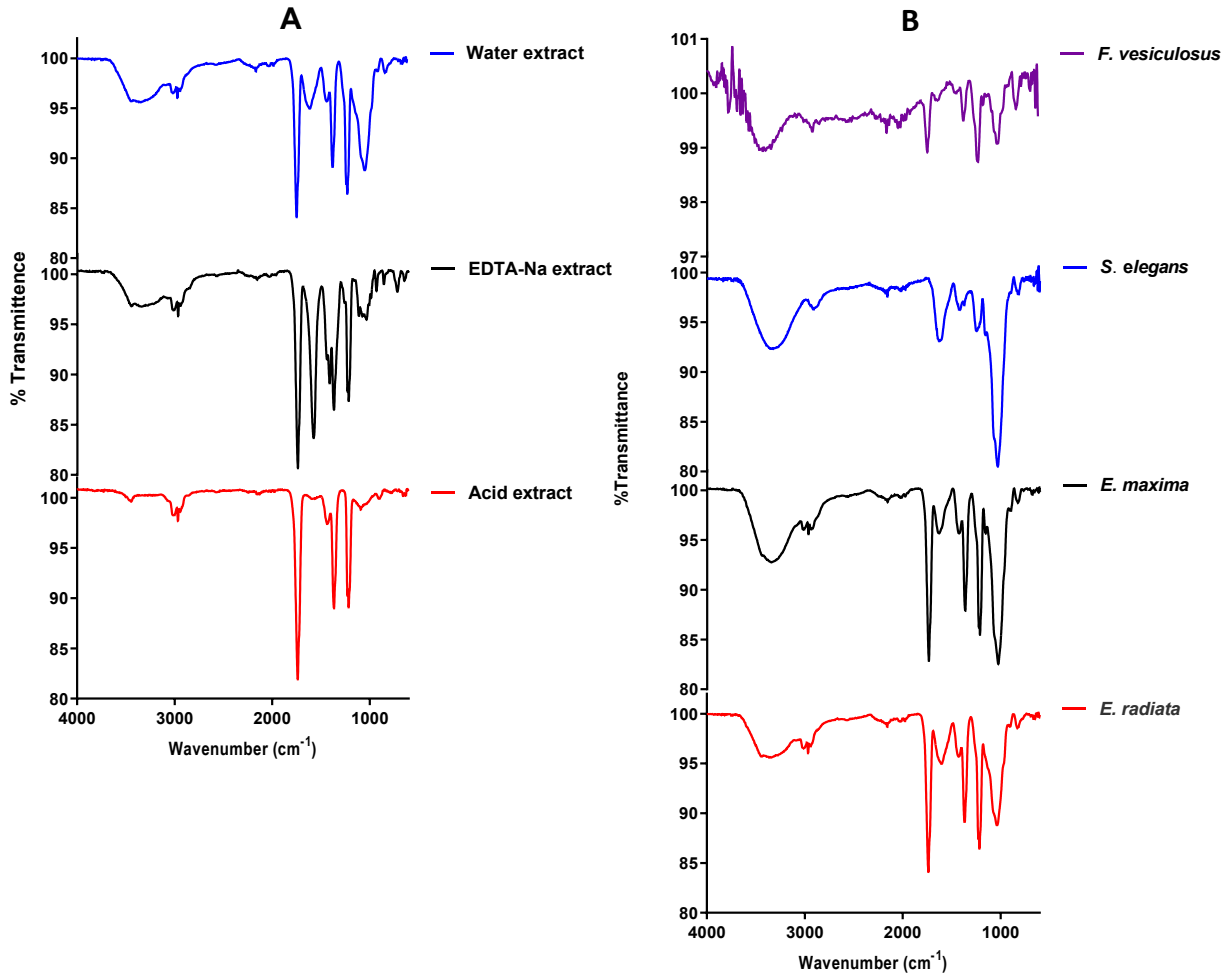

Figure 3.5: FTIR spectra for extracted fucoidan.
A; shows the overlaid spectra for the *S. elegans* extracts and **B**; shows the overlaid spectra obtained with the various water extracts and the commercial *F. vesiculosus* fucoidan.

3.3.3.2 Proton NMR analysis of extracted fucoidans

To further elucidate the structural composition of the extracted fucoidan, proton NMR was conducted. Generally, chemical shifts in all extracts showing as peaks at 1.28 ppm and 1.45 ppm suggest the presence of alternating α (1-3) and α (1-4) linkages of fucose residues (α-L-Fuc, α-L-Fuc (2-SO_3^-) and α-L-Fuc (2,3-diSO_3^-) (Shan et al., 2016). Also, the peaks at 1.45 ppm are assigned to symmetric CH_3 deformations emanating from methyl proton on C6 of fucose (Kopplin et al., 2018). The peak at 2.1 ppm is assigned to the H-6 methylated protons of L-fucopyranosides (Alwarsamy et al., 2016). The peaks in the range 3.5-4.5 ppm are characteristic of the (H2 to H5) ring protons of L-fucopyranosides. The exhibited peaks in the ring proton region also suggest variable fucosal sulphates are located at variable glycosidic linkages with

varying monosaccharide patterns. These are consistent with previously characterised fucoidans (Alwarsamy et al., 2016). Definitive peaks at 3.3 ppm and 3.7 ppm in all extracts suggest the presence of hexoses, including glucose, galactose and mannose (Alwarsamy et al., 2016). Furthermore, chemical shifts in the region around 5.8 ppm are characteristic of uronic acids and alginate impurities (Nguyen et al., 2020).

The proton NMR spectra of the hot water *E. maxima* fucoidan extracts revealed peaks in the 1.1 to 5.25 ppm range, with the EDTA-Na fucoidan extract showing peaks between 1 and 4.75 ppm and the acid extract in the 1.05 to 5.3 ppm range (Fig. 3.6).

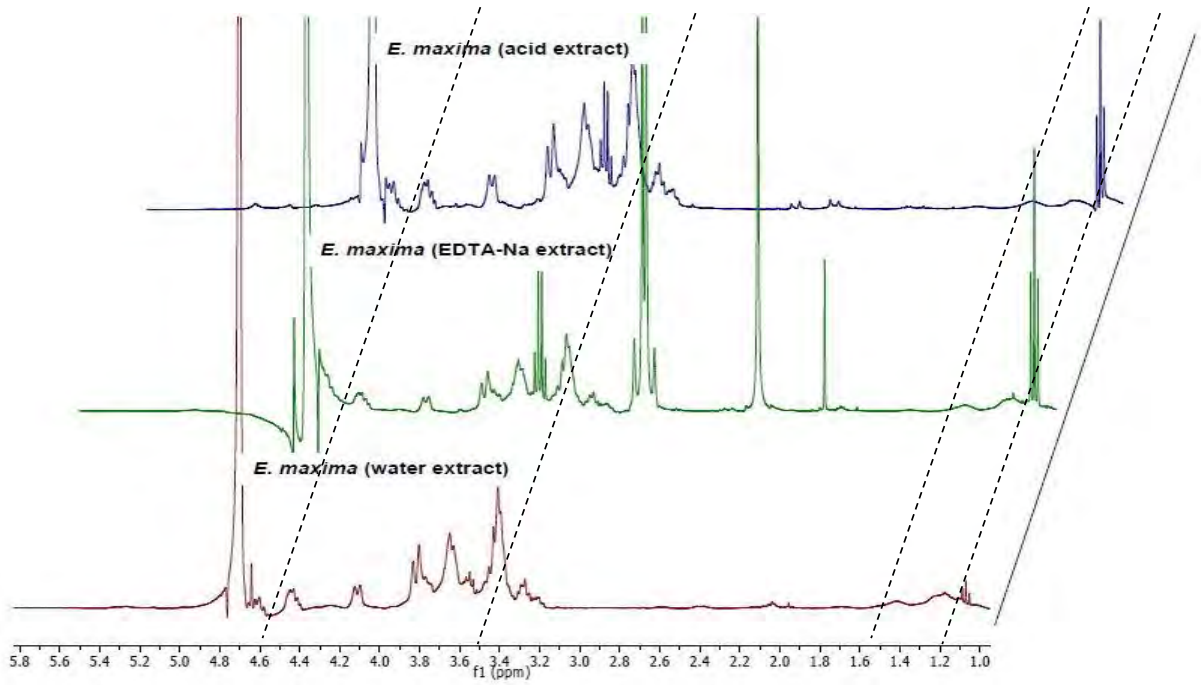

Figure 3.6: ^{1}H NMR spectra of overlaid *E. maxima* fucoidan extracts.

The major NMR spectral regions linked to the fucoidan structure are guided by the lines shown in Figure 3.6. The general structure profiled by NMR was consistent in all the *E. maxima* extracts, although the EDTA-Na extracts showed some additional peaks around 2.2 and 2.8 ppm (Fig. 3.6). Of note, the 3.5 to 4.5 ppm peaks characteristic of (H2 to H5) ring protons of *L*-fucopyranosides were less pronounced in the EDTA extracts than in the water and acid extracts.

The *E. radiata* fucoidan extracts also showed a similar profile regardless of the extraction method which was used. All extracts had a distinct region of alternating

fucose residues (1.28 – 1.45 ppm), and peaks in the region 3.5 -4.5 ppm, characteristic of protons in L-fucopryanose rings and monosaccharides (Fig. 3.7). The 3.5 – 4.5 range peaks were diminished in the *E. radiata* EDTA extracted fucoidan (Fig. 3.7). Also, peaks around 1.5 ppm present in both *Ecklonia* sp. EDTA and acid extracted fucoidans were diminished within the water extracts (Fig. 3.6 & 3.7).

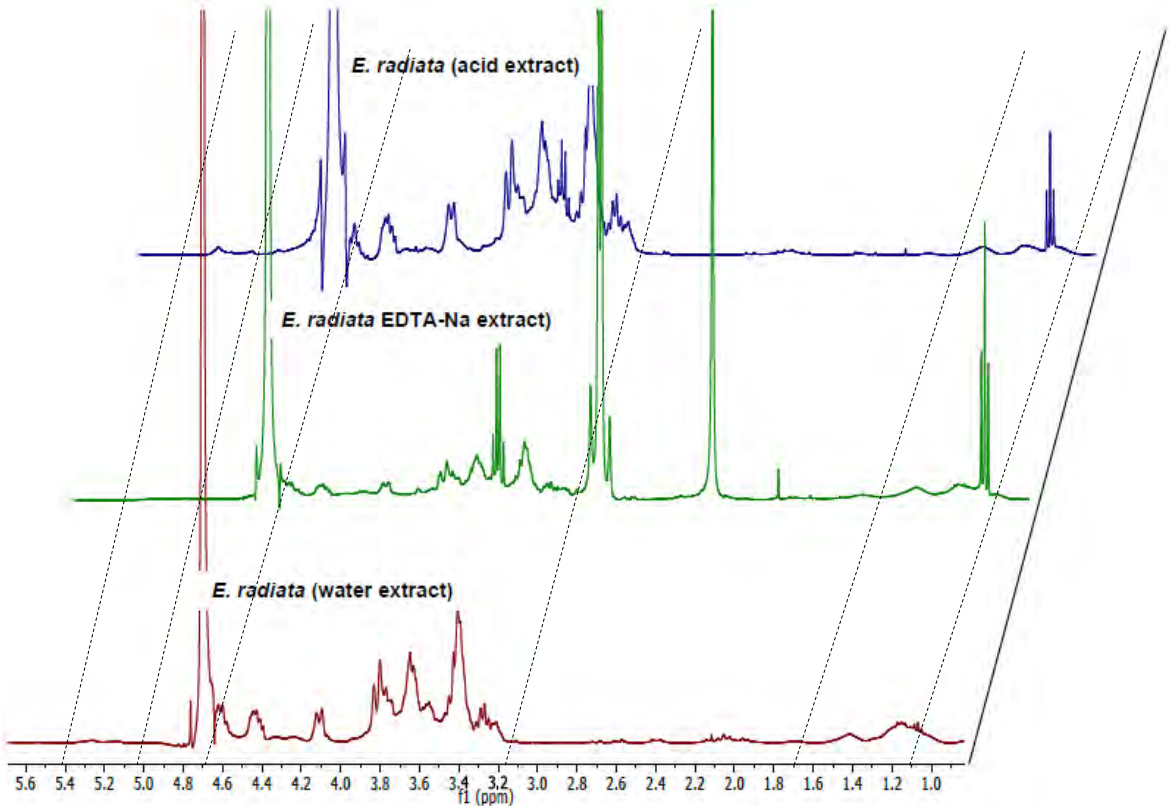

Figure 3.7: 1H NMR for overlaid *E. radiata* extracts.

S. elegans fucoidan extracts were also subjected to proton NMR analysis. All the compounds showed a characteristic fucoidan structure consistent with the *Ecklonia* sp. fucoidans shown in Figures 3.5 and 3.6. However, the *S. elegans* water extracted fucoidan showed peaks associated with anomeric proton resonances with chemical shifts ranging from 5 ppm to 5.4 ppm; these were absent in the EDTA and acid extracts. Also, the peaks at 3.5 – 4.5 ppm from the *S. elegans* EDTA extracts were drastically reduced (Fig. 3.8), as in the case of the other previously described fucoidans extracted from *Ecklonia* sp extracts. Additionally, two chemical shifts at 2.2 ppm and 2.8 ppm were observed only in the EDTA extract (Fig. 3.8). The chemical shift around 2 ppm could be EDTA-Na ions. Our deduction is supported by the findings of Mónico and colleagues, who reported similar proton NMR spectra for EDTA (Mónico

et al., 2017). Also, the peaks at approximately 1.1 ppm could be due to ethanol as it was used for precipitating the fucoidans.

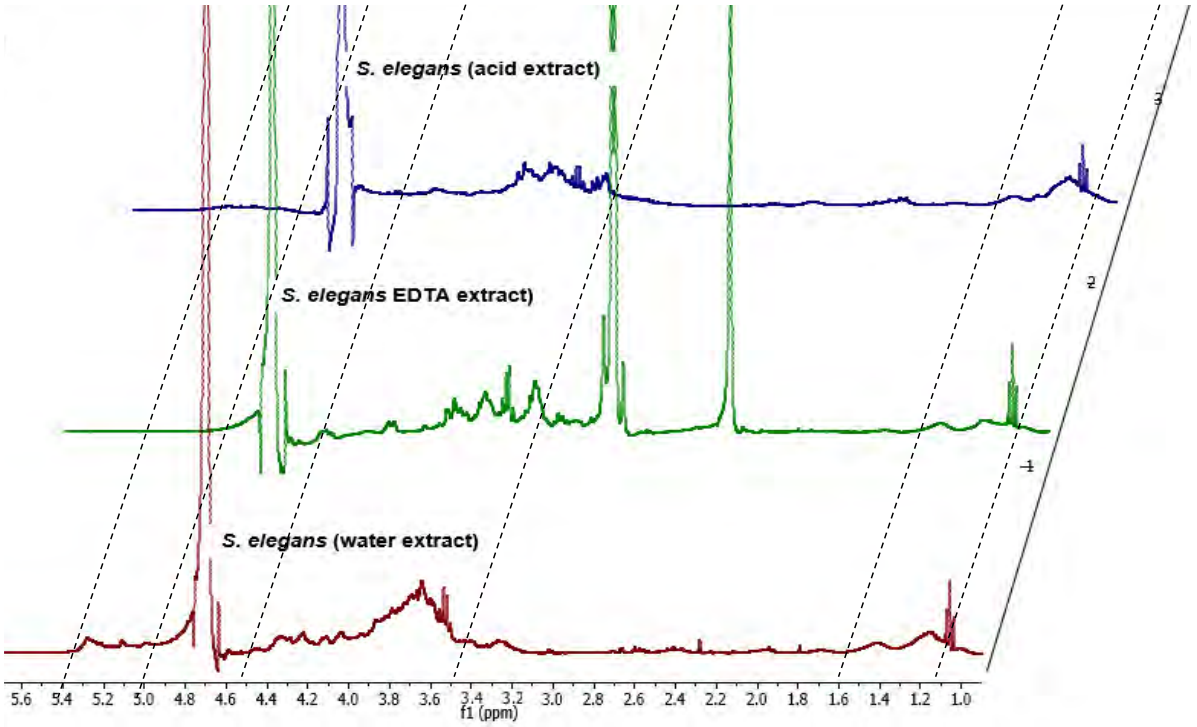

Figure 3.8: ^{1}H NMR for overlaid *S. elegans* extracts.

Finally, the water extracted fucoidan from the various species were overlaid with the commercial *F. vesiculosus* fucoidan (Fig. 3.9). The chemical shifts were different between the distinct species, although all the shifts were within the categorised ppm ranges characteristic of fucoidan. Compared to any of our extracted fucoidan samples, the chemical shifts (1.2 – 1.45 ppm) were relatively large and obvious for *F. vesiculosus* fucoidan (Fig. 3.9). Also, the chemical shifts (3.5 – 4.5 ppm) were less prominent for the *F. vesiculosus* and *S. elegans* than the *Ecklonia* sp. fucoidans, which exhibited a similar profile. Finally, the *F. vesiculosus* and *S. elegans* samples exhibited chemical shifts denoting the anomeric protons absent in the *Ecklonia* sp. fucoidan (Fig. 3.9).

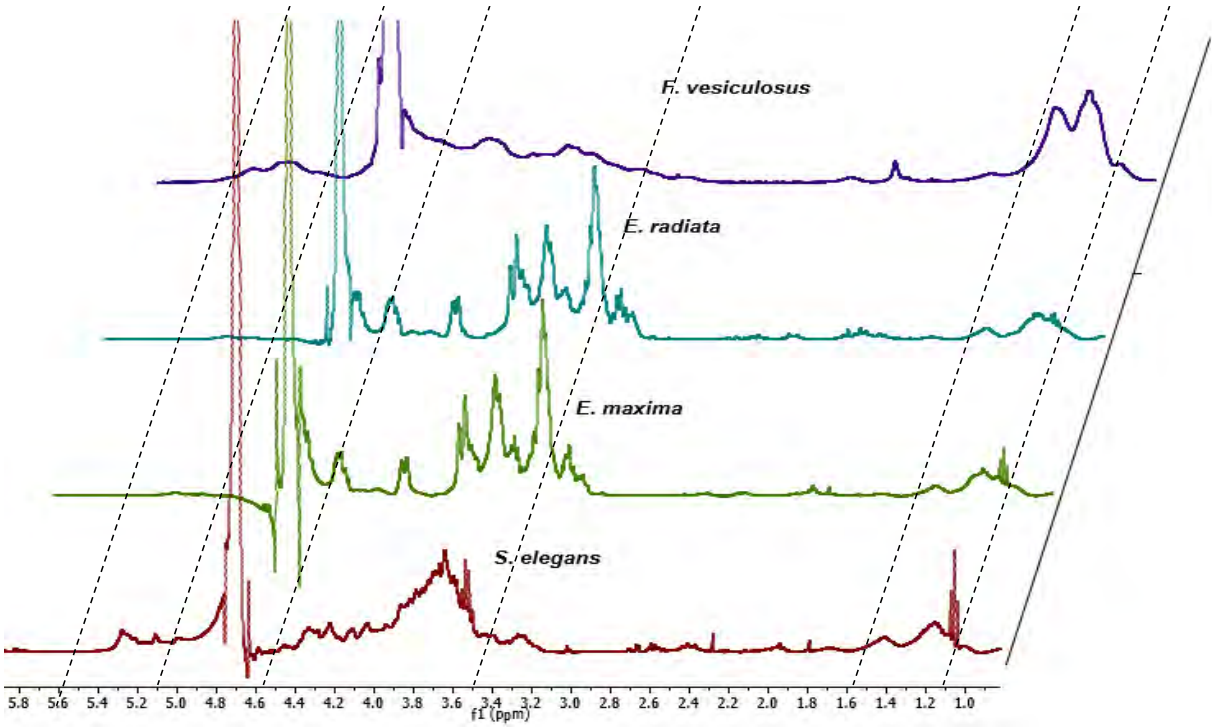

Figure 3.9: ^{1}H NMR for the different seaweed fucoidans.

3.3.3.3 SEM of extracted fucoidan

The morphology of extracted fucoidan samples was analysed by SEM after the compounds were gold coated. The results showed that the extraction methodology influenced the morphological characteristics of fucoidan. The water extracted fucoidans of all seaweed species studied displayed a somewhat compacted morphology, characterised by close packing. In contrast, the EDTA extracted fucoidans generally still showed some intact packing, but the surface appeared flocculent and porous, with a fluffy morphological character. However, the *S. elegans* EDTA extract showed a more disintegrated morphology compared to the other EDTA extracts. The acid extracted fucoidan displayed a disintegrated morphology compared to the water extracts. In addition, the different seaweed extracts also differed in their respective morphologies (Fig. 3.10)

	Water extract	EDTA extract	Acid extract
E. maxima	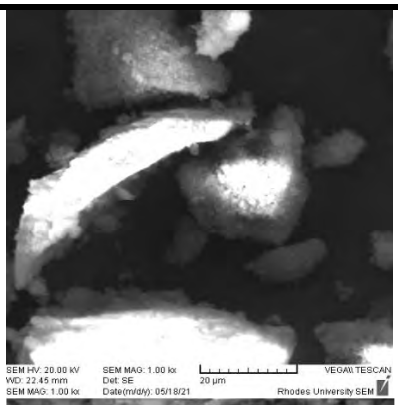	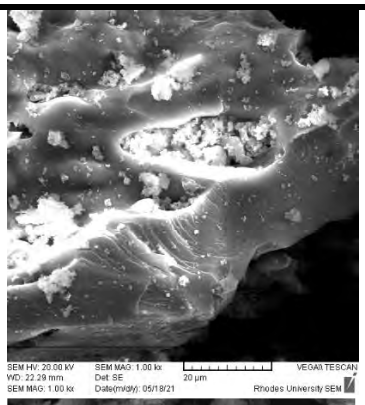	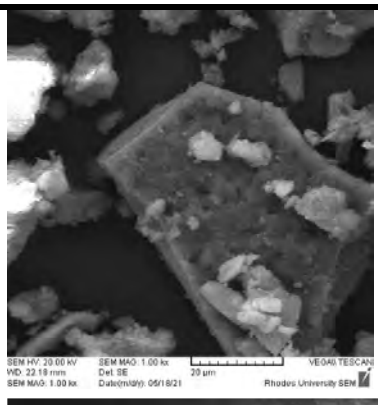
E. radiata	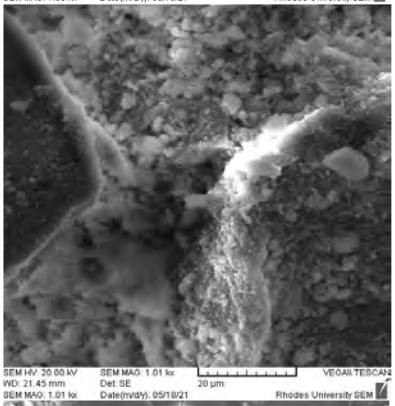	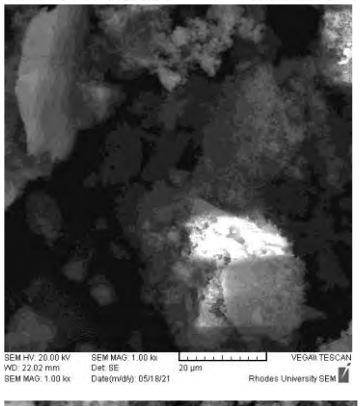	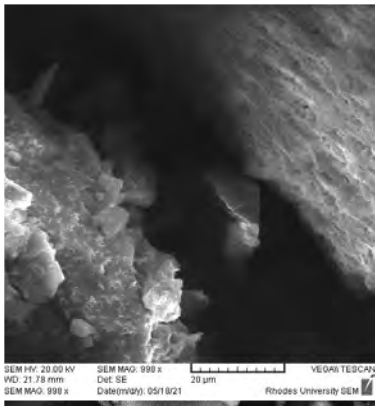
S. elegans	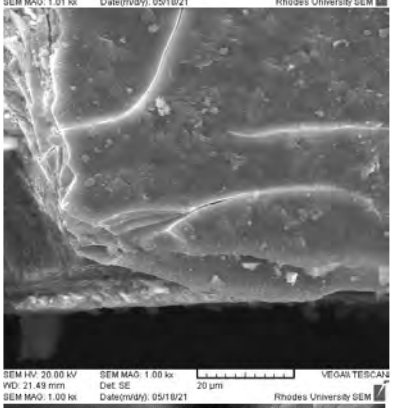	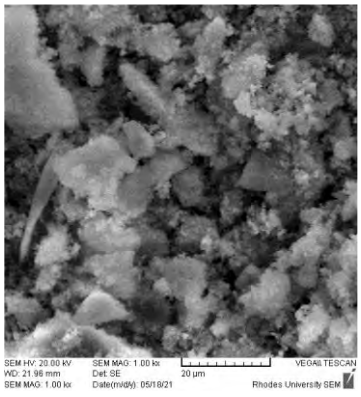	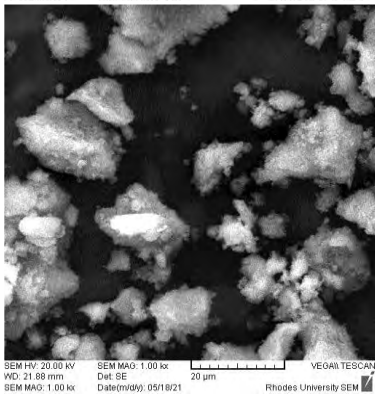
F. vesiculosus	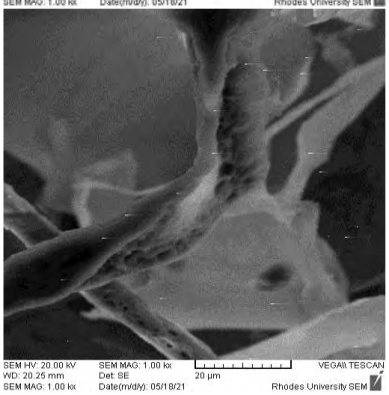		

Figure 3.10: SEM analyses of the various fucoidan extracts. Magnification was set at 1000x. The morphological characteristics of fucoidan were affected by the various extraction methodologies used.

3.3.3.4 Thermogravimetric analysis of fucoidan extracts

Thermal gravimetric analysis of the fucoidan extracts was conducted primarily to determine the ash content of the compounds. There were three distinct mass degradation stages observed during the heating of the fucoidan samples. The first mass degradation stages are associated with the loss of readily volatile substances; the second decrease may be due to polymer degradation, the third may be due to carbon black and lastly, ash content. These characteristic mass degradations were observed in the thermograms of all our fucoidan extracts (Fig. 3.11).

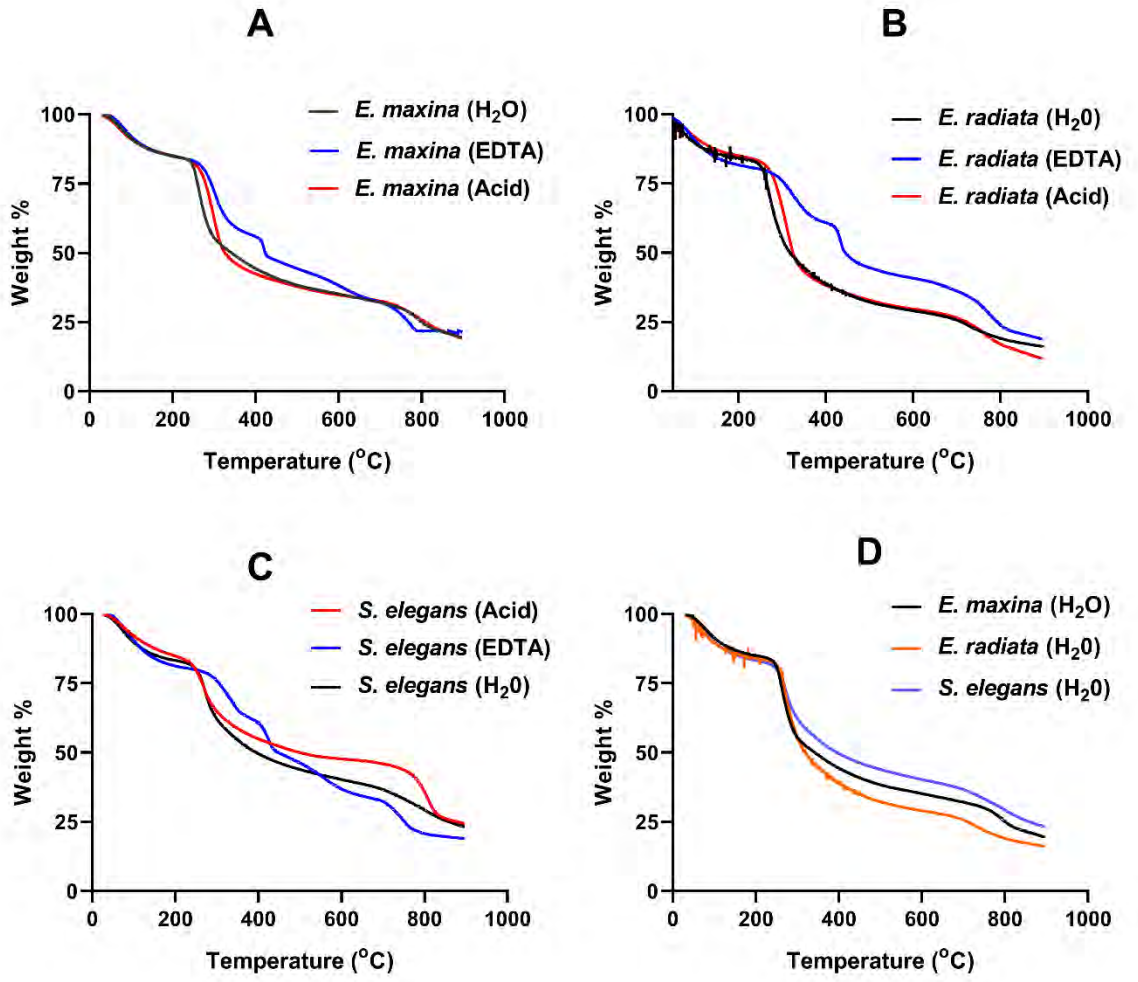

Figure 3. 11: Thermal gravimetric analysis (TGA) analysis of fucoidan extracts.
A; thermograms for *E. maxima* fucoidan extracts. **B;** thermograms for *E. radiata* fucoidan extracts. **C;** thermograms for *S. elegans* fucoidan extracts and **D;** Superimposed thermograms for all the water extracted fucoidans in the study.

The TGA thermograms for all the fucoidans extracts exhibited similar moisture contents (~ 20%), as could be seen with the TGA thermograms in the first stage of the downward slope between 0 and 240 °C. The major mass loss in weight (~ 45%) was between ~240 °C and ~ 420 °C, where most of the depolymerisation and decomposition of organic constituents, including polysaccharides, occurred. However, it can be noted that all the EDTA extracted fucoidans degraded much slower than the water and the acid extracts (Fig. 3.11). In addition, the ash contents of all these fucoidans (which were extracted differently) were between 12 and 24%. The amount of ash between the different extracts was minimal, although the *E. radiata* fucoidan contained less ash than the others (Table 3.2).

3.3.3.5 High-performance liquid chromatography-mass spectrometry (HPLC-MS)

The structural differences between the extracted fucoidans were investigated using ultra-high-performance liquid chromatography-high resolution mass spectrometry UHPLC-HR-MS). The fucoidan extraction methods inherently generated structurally different end products. The *E. maxima* water and acid extracts showed a similar LC-MS profile, where the peak distribution formed a positive skew shape with more fragments to the right side of the prominent peak, which was at 125.9 Da. Of note, there were more peaks with a higher abundance within the water extracts than the acid extracts (Fig. 3.12). Also, the *E. maxima* EDTA extract had a relatively different profile from the water and acid extracts. The EDTA extract had the prominent peak 293 Da showing a less abundant fragmentation pattern. In addition, all the *E. maxima* fucoidan extracts had a long tail of high molecular weight peaks (Fig. 3.12)

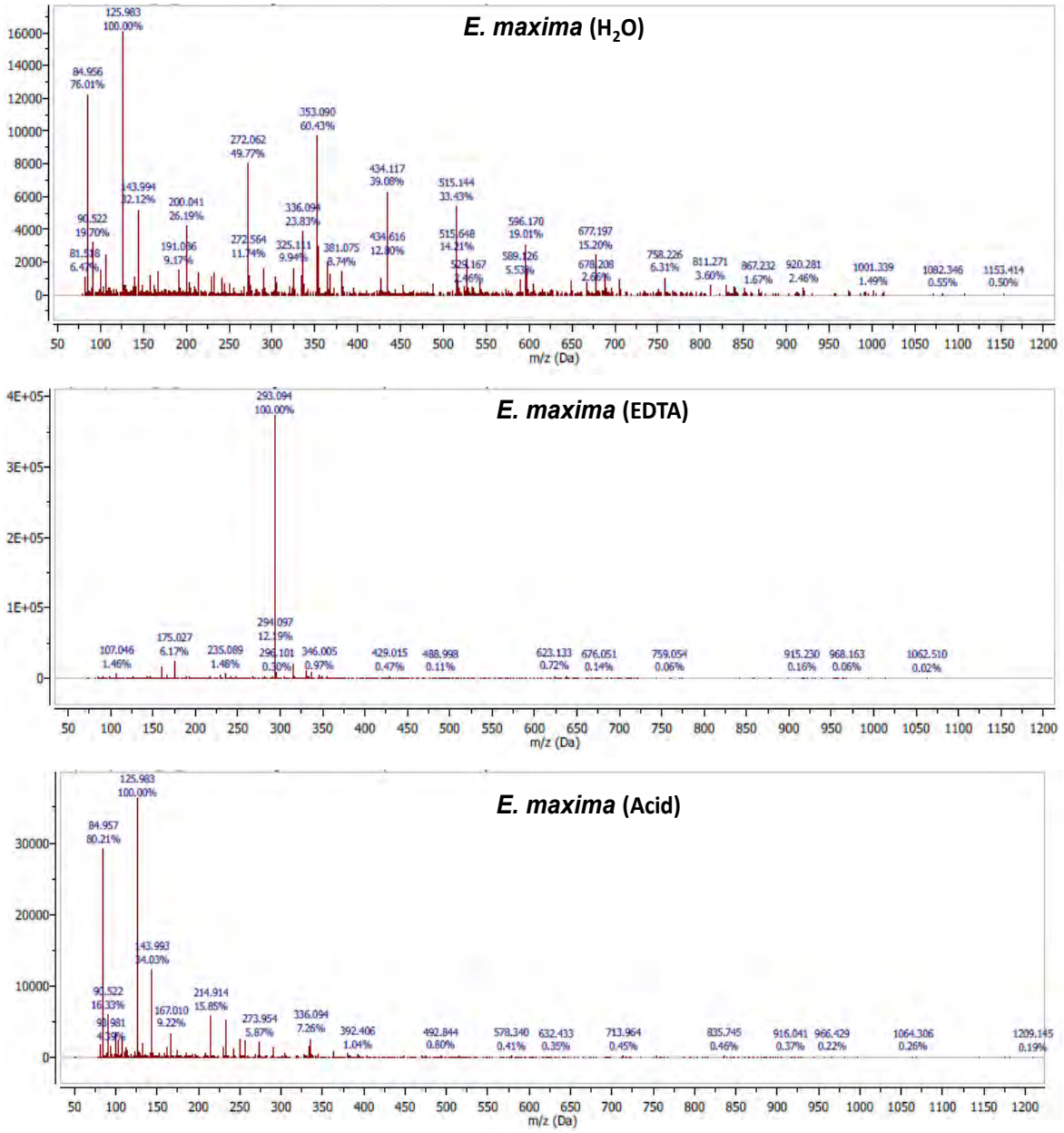

Figure 3.12: LC-MS fragment profiles for the *E. maxima* fucoidan extracts.
The extraction methodology affects the structural nature of the fucoidan product. The acid extraction method produced a lower fragment distribution compared to the water method. The EDTA extraction, in turn, produced a unique fragmentation pattern.

The LC-MS fragmentation patterns for the *E. radiata* fucoidan extracts (showed a similar pattern to fragmentation patterns of the *E. maxima* fucoidans. The *E. radiata* fucoidan water and acid extracts showed a slight positive skew around the most prominent peak with a mass of 125.9 Da (Fig. 3.13). The water and the acid extracted fucoidans had common fragments with 84.9, 125.9, 143 and 336 Da masses. These

fragments were more abundant within the water extracts. Nevertheless, the EDTA extracted *E. radiata* fucoidan had a distinctive parent peak with a mass of 293 Da and displayed fewer fragments than the water and acid extracted fucoidans (Fig. 3.13).

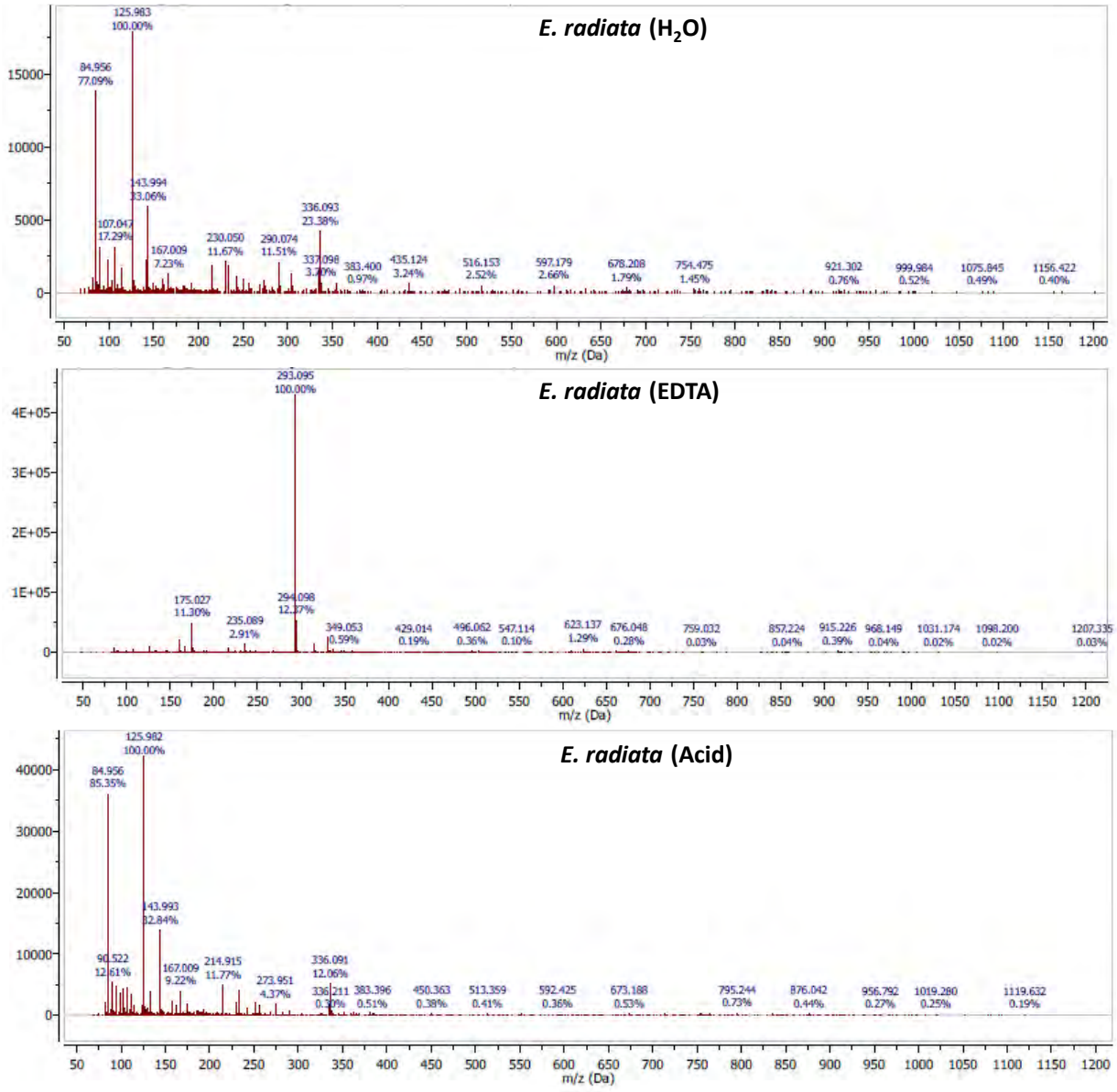

Figure 3.13: LC-MS fragment profiles for the *E. radiata* fucoidan extracts.

The water extraction protocol preserved some functional groups in the product (*E. radiata* fucoidan), which disappeared or diminished within the acid extracts. The EDTA extracts, in turn, displayed a different fragmentation pattern.

The *S. elegans* extracts also showed that the extraction method affected the nature of the product fucoidans. Similar to the *Ecklonia* sp. fucoidan extracts described before, *S. elegans* water and acid extracts exhibited related fragmentation patterns (Fig. 3.14).

These shared a parent fragment with a mass of 125 Da. The other common fragments observed had masses of 84.9, 143, 214 and 336 Da. The EDTA extract displayed the most stable fragment with a mass of 293 Da. Distinctive fragments with masses of 175, 235 and 349 Da were also observed (Fig. 3.14).

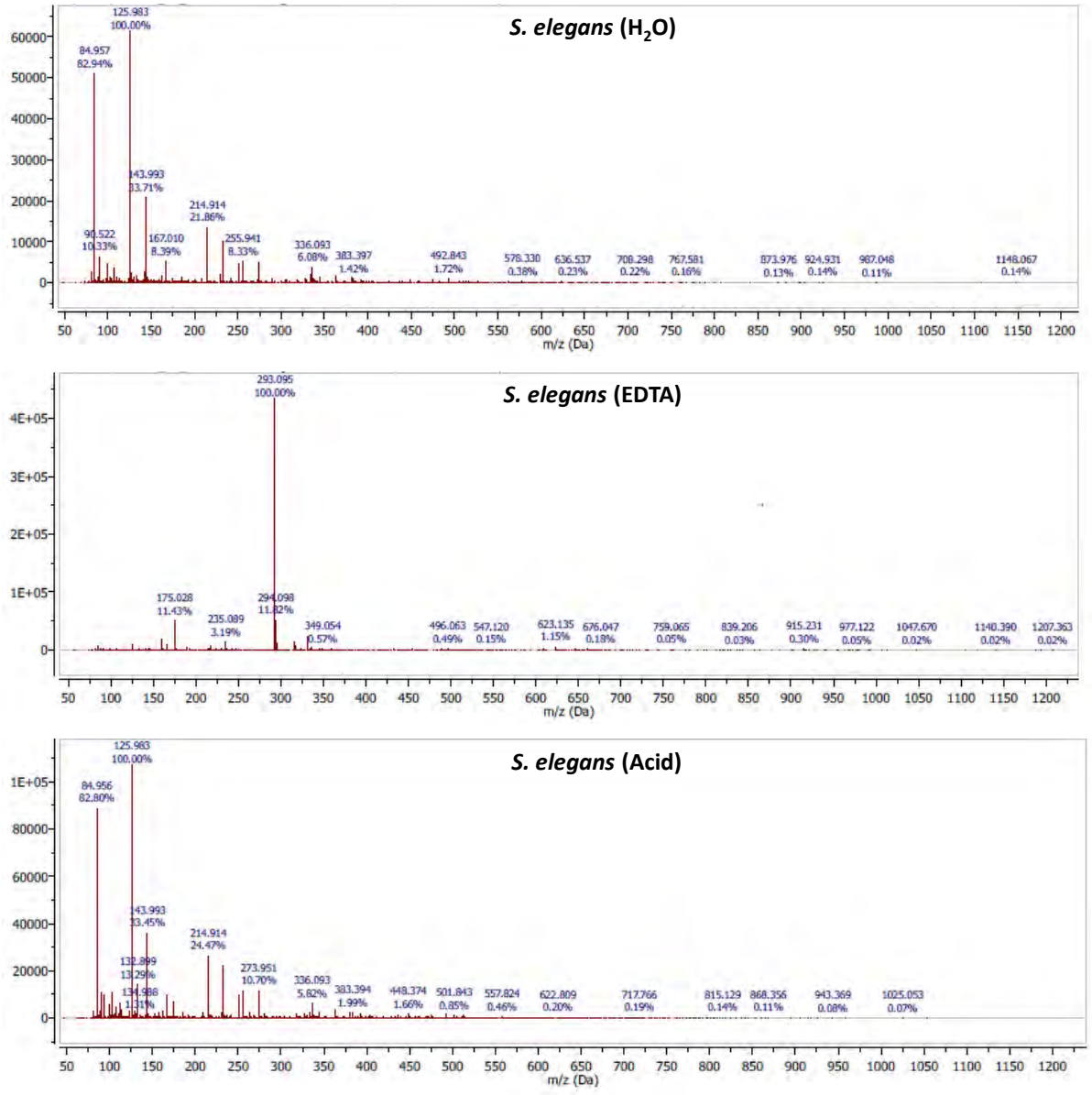

Figure 3.14: LC-MS fragment profiles for the *S. elegans* fucoidan extracts.
The water extracted *S. elegans* fucoidan displayed the most diverse fragmentation pattern, followed by the acid extracted fucoidan, and finally, the EDTA extracted fucoidan the least.

The LC-MS profiles of the water extracted fucoidans were overlaid with the commercial *F. vesiculosus* fucoidan to investigate how structural compositions vary in fucoidans extracted from different seaweeds (Fig. 3.15).

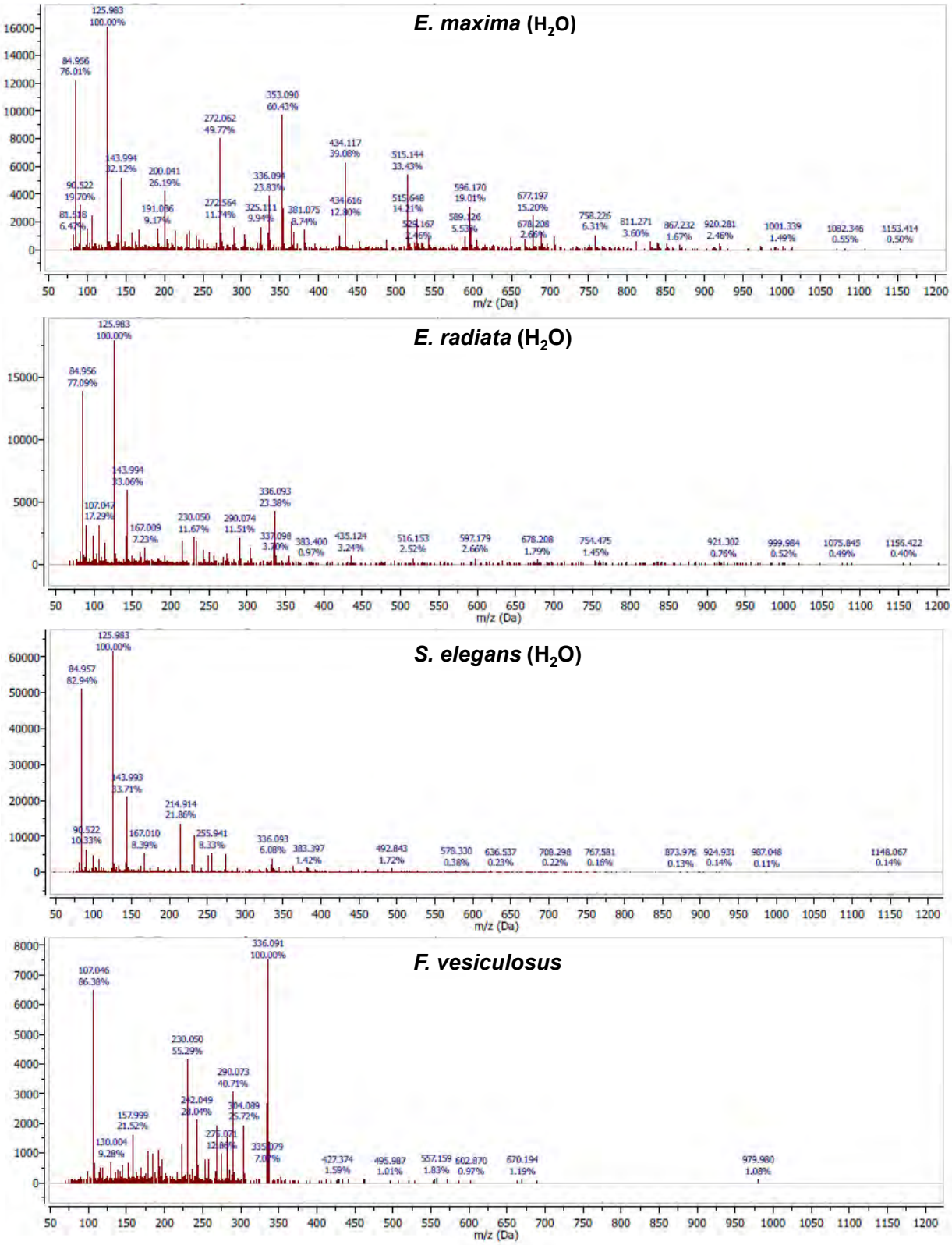

Figure 3.15: LC-MS fragment profiles of the water extracted fucoidans overlaid with the commercial *F. vesiculosus* fucoidan.

Overlaying all the extracts with the commercial *F. vesiculosus* fucoidan showed that the *E. maxima* water extracted fucoidan displayed the most complex fragmentation pattern (Fig. 3.15). Also, all the extracts had the same prominent parent peak with 125. 9 Da mass (Table 3.3).

Table 3.3: Main fucoidan fragments after HPLC/MS analysis

Fucoidan extracts	Main fragments (Da)
E. maxima (H_2O)	84.9, 125.9, 353
E. maxima (EDTA)	175, 293
E. maxima (Acid)	84.9, 125.9, 143.9
E. radiata (H_2O)	84.9, 125.9, 143.9
E. radiata (EDTA)	175, 293
E. radiata (Acid)	84.9, 125.9, 143.9
S. elegans (H_2O)	84.9, 125.9, 143.9
S. elegans (EDTA)	175, 293
S. elegans (H_2O)	84.9, 125.9, 143.9
F. vesiculosus	107, 230, 336

Other common fragments displayed masses of 84.9, 143.9 and 336 Da. However, the *F. vesiculosus* fucoidan showed a unique fragmentation pattern, characterised by the parent fragment of mass 336 Da (Fig. 3.15). The 336 Da fragment was present in all the extracts, although in relatively lower abundance than in the *F. vesiculosus* fucoidan. Also, the fragmentation pattern of *F. vesiculosus* is negatively skewed as most of the fragments occur on the left of the parent peak. The fragment of 336 Da consistently present within our analysed fucoidans could be $[Fuc_4(SO_3Na)_5 - 3Na]^{3-}$ as proposed by Thanh and colleagues (Thanh et al., 2013). Also, another fragment with mass 230 from our extracts may correspond to $[Fuc_3(SO_3)_2]^{2-}$ as proposed by Ermakova and colleagues (Ermakova et al., 2016). Of note, the fragment of 293 Da was consistent with the EDTA extracted compounds and could be trace EDTA within the fucoidans (Table 3.3). These common fragments confirm the integrity of our extracted fucoidans. Moreover, our data show that a variation in seaweed species determines the structural nature of the extracted fucoidan.

3.4 Discussion

The fucoidan yield depended on the extraction technology employed, with the EDTA extraction method consistently yielded the highest amount of fucoidan (regardless of the seaweed species studied). This was followed by the acid extraction method, with the second-highest yield, and the hot water extraction method which produced the lowest yields (Fig. 3.4). The high yield associated with the EDTA extraction agrees with the findings of Zhao et al. (2018), who showed that EDTA produced a better yield than the acid extraction, which is routinely used. Furthermore, the EDTA method eliminates the depigmentation step as the EDTA managed to depigment seaweed biomass in solution in a single step. This method is more efficient as it saves time and limits the use of organic solvents associated with the depigmentation process. The method is environmentally friendly and could be techno-economically feasible if used on an industrial scale.

Chemical analysis of the extracted fucoidan showed that the fucoidans extracted from *Ecklonia* spp. had a higher carbohydrate content than that of *S. elegans* and commercial *F. vesiculosus*-derived fucoidan (Table 3.1). Also, the *Ecklonia* spp. fucoidan had a relatively high monosaccharide content, with glucose, galactose and mannose being the most prominent sugars (Table 3.1). These findings are consistent with the findings of January and colleagues (January et al., 2019). These authors also detected considerable amounts of glucose, galactose and mannose in their fucoidan extracts from *E. maxima* (harvested in South Africa) (January et al., 2019). Also, our extracted fucoidan had relatively low to no contaminants, including proteins, phenolics and uronic acids.

The sulphate content of the extracted fucoidan appeared to be linked to the extraction method employed (Table 3.3). The water extracted fucoidan had the highest sulphate content, followed by the EDTA and acidic extracts. This trend was also reported by January et al. (2019), who found a significantly reduced sulphate content in acid extracted fucoidan – compared to that in the water extracts. *S. elegans* and *F. vesiculosus* fucoidans had higher sulphate contents compared to the *Ecklonia* spp.-derived fucoidan. All the fucoidans had ash contents between 19 and 24%, consistent with those in characterised fucoidans (Catarino et al., 2018; Li et al., 2008).

The extracted fucoidan extracts from the three seaweed species were examined structurally using FTIR. It was evident that the extraction technologies employed to extract fucoidans impacted their structure (Figs 3.3 & 3.4). The observed trend is that some functional groups on the extracted fucoidans were diminished or lost as the extraction solutions varied. Water extracted fucoidans in all the studied seaweed species exhibited the most functional groups, followed by EDTA extracted fucoidans, and finally, the acidic extracted fucoidans (Figures 3.4 & 3.5). However, the peak associated with carbohydrate content (1650 cm^{-1}) did not appear to change among the different extraction methods (Figs 3.4 & Fig. 3.5). The *F. vesiculosus* and *S. elegans* fucoidans displayed a less prominent peak around 1650 cm^{-1}, agreeing with the low total carbohydrate contents detected in these fucoidan samples (Table 3.1). However, these fucoidan samples had more pronounced peaks around 840 cm^{-1}, which explained their higher sulphate contents compared to the *Ecklonia* spp. fucoidans (Table 3.1). All the extracts exhibited spectra characteristic to previously characterised fucoidans (Kopplin et al., 2018; Zhao et al., 2018), which confirmed the integrity of these extracts. The integrity of the extracted fucoidans was also confirmed by the peaks observed in the commercial *F. vesiculosus* fucoidan, which was overlaid with the extracted fucoidans (Fig. 3.5B).

The fucoidan extracts were also profiled structurally using ^{1}H NMR. All the extracted fucoidans conformed to the structures of previously described fucoidans in the literature (Alwarsamy et al., 2016; Kopplin et al., 2018; Shan et al., 2016). Our results also showed that the different extraction methods affected the structure of the fucoidans (Figs 3.6-.3.8). NMR results indicated that *F. vesiculosus* and *S. elegans* had relatively higher sulphate contents compared to *Ecklonia* sp. derived fucoidans. In addition, the NMR spectra suggested the presence of higher amounts of carbohydrate in the *Ecklonia* sp. fucoidans compared to the fucoidans of *F. vesiculosus* and *S. elegans* (Fig 3.9). These observations were reconciled with the data from chemical composition experiments (Table 3.1 & Table 3.3).

SEM analyses of fucoidan extracts revealed that the extraction method affected the morphology of the compounds. The water extracts exhibited a more compact morphology than the EDTA and acidic extracts (Fig. 3.10). Limited literature is available regarding SEM studies that are related to fucoidan structure. However, the

morphological traits shown by our extracts do agree with the SEM analysis of fucoidan characterised by Saravanaa and colleagues (2018). These researchers described the water extracted native fucoidan structure as amorphous - however, with a solid matrix-like material, their treated fucoidan appeared as small broken fragments (Saravanaa et al., 2018).

Thermal gravimetric analysis of the fucoidan extracts was performed primarily to further elucidate their composition and, ultimately, their ash content. The fucoidan extract TGA decomposition profiles validated fucoidans as polysaccharides, as their decomposition started just above 200 ^{o}C (Fig. 3.11.), characteristic of organic polymers (Liu & Yu, 2006). The TGA plots of all the fucoidan extracts showed about 20% loss in mass at a temperature of 240 ^{o}C, associated with the loss in moisture content through evaporation (White et al., 2011) and some volatile matter (Chen et al., 2015). The major loss of mass (~45%) occurred between 240 ^{o}C and 413 ^{o}C, which accounted for the arbitrary depolymerisation and decomposition of organic constituents such as carbohydrates. Above 420 ^{o}C, combustion of carbon black occurred. After the compounds were heated to about 900 ^{o}C, the remaining residual mass accounted for the ash content, usually containing sulphates, phosphates, and carbonates (Carpio et al., 2019). The profiles that our extracts showed were characteristic of previously profiled fucoidan extracts in the literature (Morimoto et al., 2014; Saravanaa et al., 2018).

LC-MS was also used to characterise the fucoidans extracted from various seaweeds using different protocols. LC-MS data showed that the extracted fucoidans were relatively pure, as single defined peaks were observed with reverse phase HPLC (Appendix B8). In addition, the extraction protocols impacted the fucoidan structures, with the water extraction method preserving some functional groups, compared to the EDTA and acid extraction approach (Figs. 3.11- 3.13). However, our fucoidans showed similar fragmentation patterns to a few other fucoidans characterised in literature (Ermakova et al., 2016; Fletcher et al., 2017).

In summary, this chapter confirmed that different extraction technologies affect the yield and structural and chemical characteristics of the resulting fucoidans in various ways. Most significantly, the new EDTA-assisted technology significantly increased the yield of fucoidan. Furthermore, these differences are also attributed to the varying

species of seaweed. Lastly, the observed structural differences in the extracted bioproducts may have implications with respect to the biological activities of the fucoidans.

The fucoidan extracts isolated from the South African brown seaweeds were shown to exhibit different structural and chemical profiles. These varying profiles may influence their biological potency as anti-diabetic compounds.

CHAPTER 4: EVALUATION OF FUCOIDANS AS INHIBITORS OF TYPE 2 DIABETES RELATED ENZYMES

4.1 Introduction

Diabetes is a chronic condition that is caused by abnormal glucose metabolism, which leads to hyperglycaemia. Prolonged hyperglycaemia causes detrimental damage to blood vessels, nerves and organs like the heart and kidneys (WHO, 2020). The most common type is type 2 diabetes mellitus (T2DM), accounting for about 90 % of all diabetes cases. Type 1 diabetes, on the other hand, occurs when the pancreas does not produce insulin or produces insufficient quantities (Saeedi et al., 2019). The burden of diabetes has increased over the past few decades, and access to affordable treatment, especially in low-to-medium income countries, is critical for the survival of patients. There is a global consensus acknowledging that diabetes is a threat, and that the rise of this disease should be halted by 2025 (WHO, 2020).

The human body uses glucose for energy generation predominantly through metabolism. Hence, the homeostatic imbalance of glucose metabolism directly affects metabolic complications leading to type 2 diabetes (Shan et al., 2016). The manipulation of amylolytic enzymes, namely α-amylase and α-glucosidase (linked to blood glucose levels), serve as therapeutic targets for the control of hyperglycaemia (Mabate et al., 2021). Alpha-amylase breaks down carbohydrates, mostly starch, into oligosaccharides, while α-glucosidase breaks down the oligosaccharides into glucose (Picot et al., 2014). There are currently synthetic drugs, such as acarbose and miglitol, that partially inhibit these amylolytic enzymes, but these drugs have side effects, such as flatulence and diarrhoea (DiNicolantonio et al., 2015).

Besides regulating postprandial glucose levels by inhibiting amylolytic enzymes, hormonal control by insulin plays a central part in the homeostasis of glucose (Aronoff et al., 2004). Insulin has an integral role in the disposal of excess glucose in muscle, hepatic and adipose cells (Kalekar et al., 2013). People with diabetes produce little or no insulin, inferring partial to no blood glucose regulation, leading to hyperglycemia. In addition to insulin therapy, severe T2DM patients rely on oral drugs that mimic insulin, including compounds such as biguanides, glitazones and sulfonylurea (Kushwaha et al., 2013). These drugs have been associated with side effects,

including hepatic impairment, renal complications, mild anaemia, oedema, anorexia and heart complications (Kushwaha et al., 2013).

Current diabetes control measures are primarily synthetic chemotherapeutic drugs targeting various glucose homeostasis components in the human body. These drugs are expensive, and some have severe side effects due to their synthetic nature (Cho et al., 2011). Novel therapeutic efforts which are cheaper and less toxic are necessary. Fucoidan, a natural bioproduct extracted from brown seaweeds, has shown remarkable anti-diabetic properties, especially in inhibiting the activity of carbohydrate digesting enzymes (Kim et al., 2014). To date, there has been little-to-no literature investigating the anti-diabetic potential of fucoidans extracted from seaweeds endemic to South African coastlines (Daub et al., 2019; January et al., 2019). In addition, the mode of action of fucoidan amongst the processes involved in glucose homeostasis is generally poorly understood or is unexplored.

Most characterised fucoidans are more effective in inhibiting α-glucosidase and ineffective towards α-amylase (Mabate et al., 2021). On the contrary, acarbose is a more potent inhibitor of α-amylase than α-glucosidase (Daub et al., 2019; Kim et al., 2014). Therefore, fucoidans and acarbose have complimentary potencies and were deemed as perfect candidates for a potentially synergistic therapeutic effect on the activity of these two enzymes. Combining multiple drugs is a popular approach in the biomedical field and pharmaceutical sciences (Morán-Santibañez et al., 2016). The rationale behind drug combinations with non-overlapping side effects is to obtain regimens with lowered adverse effects and possibly attain direct empirical synergy of the compounds against a targeted biological process (Greco et al., 1996). In this case, the activity of α-glucosidase was of interest. The definition of synergy is diverse and usually conflicting. However, in this context, it is defined as a combined practical effect that is more significant than the additive effect of the individual compounds acting separately (Chou, 2020).

In summary, this chapter investigated the anti-diabetic effect of fucoidan extracted from South African seaweeds. To achieve this, the following objectives were set:

4.1.1 Objectives

The objectives of this chapter were to:

- Determine the inhibition potential of fucoidan extracts on the activity of the major carbohydrate digestion enzymes (α-amylase and α-glucosidase);
- Investigate the potential mode of inhibition of the enzymes by fucoidans;
- Explore the fucoidan-to-enzyme interactions during inhibition; and
- Examine the potential synergistic effect of fucoidan with acarbose with regards to α-glucosidase activity.

4.2 Materials and methods

Materials

The fucoidan extracts from harvested seaweed species, namely *E. maxima*, *E. radiata* and *S. elegans*, characterised in Chapter 3, were used in this investigation. The fucoidan obtained from *F. vesiculosus* (Cat. No. F5631) and acarbose (Cat No. LRAA9057) were purchased from Sigma Aldrich (St. Louis, USA). The two carbohydrate digesting enzymes, porcine pancreatic α-amylase (Cat. No. E-PANAA-9G) and *Saccharomyces cerevisiae* α-glucosidase (Cat. No.029M4179V), were purchased from Megazyme™ (Bray, Ireland) and Sigma Aldrich, respectively. The remainder of the reagents and kits utilised in these experiments were of analytical grade and were purchased from Sigma-Aldrich, MERCK (Darmstadt, Germany) and Megazyme™.

4.2.1 α-amylase activity assay

The inhibition potential of all the extracted fucoidans (*E. maxima*, *E. radiata* and *S. elegans*) (using different extraction methods) and the controls (*F. vesiculosus* fucoidan, acarbose) were investigated using the α-amylase activity assay. In brief, 2% (w/v) potato starch dissolved in 0.05 M sodium phosphate buffer (pH~7.0) was mixed with various concentrations of potential inhibitors ranging from 0.01-1 mg/ml. The reaction was started by adding 0.1 mg/ml (10 U/ml) α-amylase to give a total reaction

volume of 400 µl. The reaction mixture was incubated at 37 °C for 20 minutes and then terminated by centrifugation. The amount of reducing sugars (RS) produced was measured according to the DNS method (Miller, 1959). A control reaction was prepared using the same procedure, replacing the inhibitor with distilled water. Absorbance values were extrapolated against a standard calibration curve using glucose as a standard (Appendix B3). The inhibitory effects of fucoidan against α-amylase were expressed as a relative percentage of the control according to the following formula:

$$Enzyme\ inhibition\ \% = \frac{(RS\ released\ by\ control - RS\ released\ by\ test\ reaction)}{RS\ released\ by\ control} \times 100$$

The inhibitor concentration resulting in 50% inhibition of α-amylase activity (IC_{50}) was determined graphically using GraphPad Prism Software version 6.0 (GraphPad Inc.).

4.2.1.1 Pyrolysis of acarbose and fucoidans during the DNS assay

The thermal stability of acarbose, fucoidans and starch during the assay was investigated following the protocol suggested by Singla et al. (2016) with minor alterations. Briefly, varying concentrations (ranging from 0 to 0 to 1 mg/ml) of acarbose, starch, fucoidan and a fixed concentration of 10 U/ml α-amylase in each reaction were incubated at 37 °C for 20 minutes. Reducing sugars were quantified by the DNS reaction at 95 °C for 5 minutes (Miller, 1959). Reducing sugars were extrapolated from a glucose standard curve (Appendix Fig B3).

4.2.1.2 Investigating acarbose as a substrate for porcine α-amylase

Acarbose (1 mg/ml) and 2% (w/v) potato starch were incubated with α-amylase (0.1 mg/ml) for 30 minutes. The presence of glucose was detected by the glucose oxidase/peroxidase (GOPOD) method (Megazyme™), following the manufacturer's instructions. Thin-layer chromatography (TLC) analysis was also used to profile other potential products. Briefly, 5 µl of each reaction mixture was spotted onto a labelled silica gel 60 F_{254} plate (Merck, Darmstadt, Germany). The plate was developed twice using a mobile phase consisting of 1-butanol, acetic acid and water in a 2:1:1 ratio. The plate was then sprayed with the Molisch's reagent (0.3% (w/v) naphthol dissolved

in methanol and sulphuric acid in a 95:5 ratio (v/v)). The spots were visualised by oven heating the plate at 110 °C for 10 minutes.

4.2.2 α-glucosidase activity assay

The ability of all the extracted fucoidans to inhibit the activity of α-glucosidase was investigated using α-glucosidase activity assay. The substrate, 10 mM *p*NPG, was dissolved in 0.05 M sodium phosphate buffer (pH 7.0) with various concentrations (0.01 -2 mg/ml) of potential inhibitors also added to the reaction. The reaction was initiated by adding 0.1 U/ml α-glucosidase to make up a total reaction volume of 400 µl. The reaction mixture was incubated at 37 °C for 20 minutes and terminated by adding 400 µl of 2 M Na_2CO_3. An inhibition negative control was included, replacing the inhibitors with an equal volume of water. The absorbance of the released *p*-nitrophenol was measured at 405 nm (Hidex microplate reader from Bio-Tek with KC Junior software®). The amount of *p*-nitrophenol produced (*p*NP) was extrapolated from a *p*-nitrophenol standard curve (Appendix B9).

The *α*-glucosidase % inhibition was calculated as:

$$Enzyme\ inhibition\ \% = \frac{(p\mathrm{NP}\ released\ by\ control - pNP\ \ released\ by\ test\ reaction)}{p\mathrm{NP}\ released\ by\ control} \times 100$$

The inhibitor concentration resulting in 50 % inhibition of enzyme activity (IC_{50}) was determined graphically using GraphPad Prism Software version 6.0 (GraphPad Inc.).

4.2.3 Mode of *α*-glucosidase inhibition

The α-glucosidase activity was assayed in the presence of water extracted fucoidans at fixed concentrations of; 0, 0.1, 0.5 and 1 mg/ml with various concentrations of *p*NPG (0.25 to 6.25 mM), according to the protocol previously described (Section 4.2.2). The enzymatic reaction rates (v) were calculated using the released *p*-nitrophenol, obtained from a calibration curve constructed using *p*-nitrophenol (Appendix B9). The Michaelis-Menten curve was constructed, and the K_M and V_{max} values were determined using GraphPad Prism 6.0 software (GraphPad Inc). The reaction velocity

data were used to construct a Lineweaver-Burk plot to identify the type of inhibition observed.

4.2.4 Deactivation of α-glucosidase

The deactivation of α-glucosidase to further elucidate the type of enzyme inhibition was performed. Briefly, 0 mg/ml α-glucosidase enzyme was preincubated with the deactivator/ inhibitor (using a range of 0.01 to 1 mg/ml) at 37°C for 30 minutes. After pre-incubation, *p*NPG was added to a final concentration of 10 mM, and the reaction proceeded as previously described (Section 4.2.2). A control reaction was set up by replacing the inhibitor with distilled water. This control reaction was used as a reference for calculating the loss of α-glucosidase activity in the presence of water extracted fucoidans.

4.2.5 Interaction between fucoidan and α-glucosidase

4.2.5.1 Investigation of the fucoidan-induced conformational changes of α-glucosidase using tryptophan fluorescence-based analysis

The α-glucosidase-fucoidan interaction was analysed through intrinsic tryptophan fluorescence (Zininga et al., 2016). Briefly, samples composed of α-glucosidase (20 µg/ml and water extracted fucoidans (0.0625-0.5 mg/ml) in 0.05 M sodium phosphate buffer (pH 7.4) were incubated for 20 minutes at 37 °C. After incubation, fluorescence was measured between 320 and 500 nm, in 5 nm increments, after initial excitation at 295 nm using a SpectraMax M3 (Separations, Molecular Devices, USA) microplate reader at 25°C using standard 96-well black microplates. Relative fluorescence was calculated as the average value obtained from at least 4 spectrum scans less the baseline (buffer with or without inhibitors in the absence of enzyme) reading.

4.2.5.2 Circular Dichroism (CD) analysis of secondary structural changes of α-glucosidase upon interaction with fucoidan

The secondary structural conformation of α-glucosidase was analysed using Far-UV circular dichroism (CD) as previously described (Zininga et al., 2015). Briefly, 0.2 µM

α-glucosidase was suspended in 0.05 M phosphate buffer, pH 7.0. The analysis was conducted using a Chirascan v.4.4.1 Build spectrometer (Applied Photophysics Ltd, London, UK) equipped with a Peltier temperature controller at 19 ºC, using a 0.1 cm path-length quartz cuvette (Hellma). The data were analysed and de-convoluted to α-helix, β-sheet, β-turns and unordered regions using the CONTIN program of the Dichroweb online server (Whitmore & Wallace, 2008). The procedure was repeated on α-glucosidase, which was incubated with varying concentrations of the water extracted fucoidans.

4.2.6 Investigating the synergistic potential of extracted fucoidan with acarbose

The α-glucosidase assay was performed (as described in section 4.2.2), with varying concentrations of inhibitor (0 to 2 mg/ml) in the reactions. The combination (acarbose: fucoidan) was maintained at a constant ratio. The % inhibition was represented as normalised enzyme inhibition using GraphPad Prism v 6. The IC_{25}, IC_{50} and IC_{75} values were also determined for each inhibitor. The synergy of these combinations (IC_{25}, IC_{50} and IC_{75}) of inhibitors were investigated using the α-glucosidase assay protocol. The synergistic effects of the inhibitors were calculated using a combination index (CI) described previously by Chou and colleagues and CompuSyn software (Chou, 2020).

The median-effect equation is stated below:

$$\log\left(\frac{fa}{fu}\right) = mlogD - mlogD_m$$

Where *fa* is the fraction affected by dose *D*, *fu* is the unaffected fraction (*fu* = 1 − *fa*), *m* is the coefficient signifying the shape of the dose-effect curve, *D* is the inhibitor, and D_m is the median-effect dose (IC_{50} in this case).

The *CI* was determined through the equation below:

$$CI = \frac{D_1}{(D_x)_1} + \frac{D_2}{(D_x)_2}$$

Where D_1 and D_2 are the doses of inhibitors that produce a certain level of inhibition in the combination system, and $(D_x)_1$ and $(D_x)_2$ are the doses of inhibitors added alone that lead to the same level of inhibition. CI was calculated from the data as a measure of the interaction among drugs. *CI* values lower than 1 indicate synergy, *CI* values equal to 1 indicate an additive effect and *CI* values higher than 1 indicate antagonism.

4.2.7 Statistical analysis

All the experiments were repeated at least in triplicate, and the data were expressed as means ± standard deviations (SD) were applicable. Significant differences ($p < 0.05$) between the activities of the enzymes in the absence and presence of inhibitors were determined by one-way analysis of variance (ANOVA). The ANOVA test was performed using the data analysis feature in GraphPad Prism software version 6 (GraphPad Inc).

4.3 Results

4.3.1 Extracted fucoidan did not inhibit the activity of α-amylase

The activity of porcine α-amylase in the presence of inhibitors was investigated through the α-amylase activity assay using potato starch as its substrate to measure the amount of reducing sugars produced (Miller, 1959). The fucoidans, from *E. maxima*, *E. radiata* and *S. elegans*, extracted using different methods, were used in this experiment. Acarbose (a positive commercial control), and a commercial standard fucoidan from *F. vesiculosus*, were used as standards. Generally, the fucoidans evaluated did not inhibit the activity of α-amylase (Fig. 4.1). However, high amounts (0.8- 1 mg/ml) of *E. maxima* and *E. radiata* fucoidan showed between 10 to 15% α-amylase inhibition (Fig. 4.1). In addition, the fucoidan extracts obtained using different methods (hot water, EDTA and acid) did not display any inhibitory effects on the activity of α-amylase (Appendix B10).

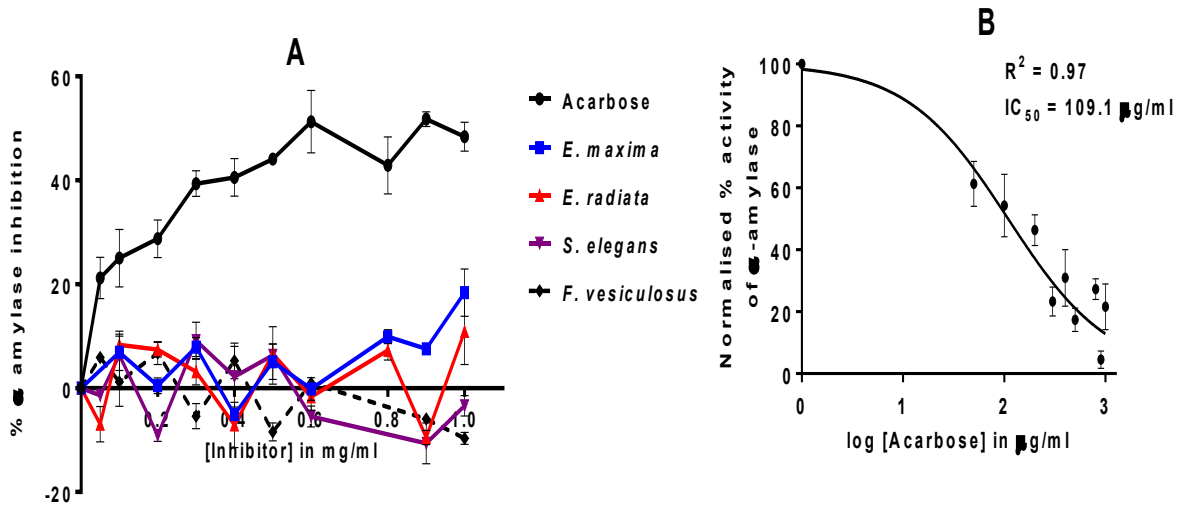

Figure 4.1: Inhibition of porcine α-amylase by extracted fucoidans.
A: The graphical figure of the α-amylase inhibition by potential inhibitors. **B**: The IC_{50} curve for the acarbose positive control. The data values are represented as means ± standard deviation (n ≥3) where n was the number of independent assays.

The *F. vesiculosus* fucoidan did not display inhibitory effects on α-amylase activity. In contrast, acarbose inhibited α-amylase activity *in vitro* in a dose-dependent fashion. However, the percentage inhibition began to drop at high acarbose concentrations (> 600 µg/ml), which was unexpected. However, this unexpected anomaly was explained by acarbose pyrolysis studies (Section 4.3.1.1), which showed that acarbose decomposed at elevated temperatures during the DNS protocol. The potency (IC_{50}) of acarbose as an inhibitory agent for α-amylase activity was determined graphically using GraphPad Prism software and was determined as 109 µg/ml ($p < 0.05$).

4.3.1.1 Acarbose thermally decomposes at 95 °C

The unusual (and unexpected) decrease in inhibition of α-amylase activity in the presence of higher concentrations of acarbose was concerning. This anomaly led to an investigation of the thermal stabilities of acarbose, fucoidans, starch and the enzyme. During the DNS assay, acarbose decomposes at elevated temperatures, more precisely at 95 °C (Fig. 4.2). However, starch did not degrade under elevated temperatures. The enzyme and fucoidan, in turn, also did not decompose to produce any additional reducing sugars.

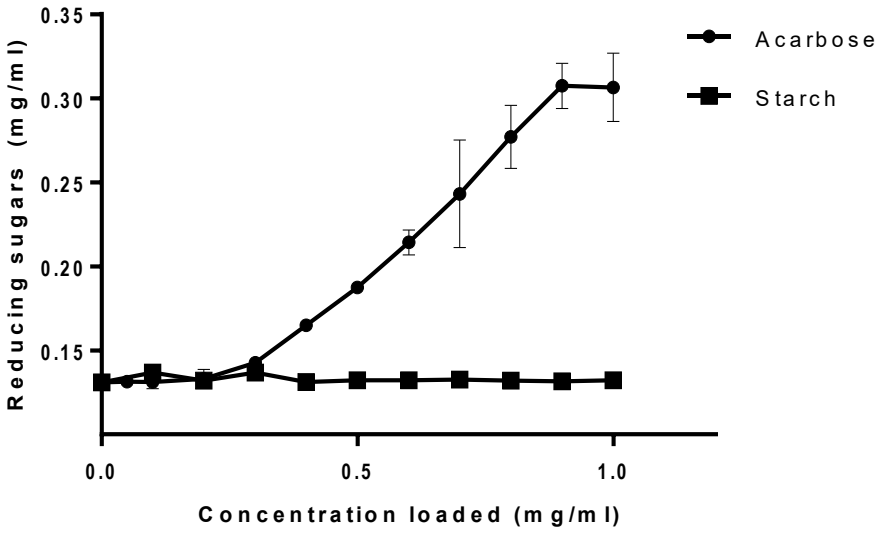

Figure 4.2: Thermal decomposition of acarbose at 95 ^{O}C.
The data values are represented as means ± standard deviation (n ≥3) where n was the number of independent assays.

4.3.1.2 Acarbose is not hydrolysed by porcine α-amylase

Acarbose and potato starch were incubated separately with α-amylase (0.1 mg/ml) for 30 minutes to investigate if the enzyme will act on acarbose to produce reducing sugars. The GOPOD assay was used to investigate the release of D-glucose from the inhibitor (i.e. the acarbose) by the enzyme. Furthermore, TLC was used to analyse the sugar profiles of other reducing sugars released from acarbose by the enzyme. However, no detectable glucose was formed from acarbose in the α-amylase reaction. However, a small amount of glucose (~0.05 mg/ml) was detected by the GOPOD assay (Fig. 4.3A). TLC indicated the presence of two oligosaccharides, assumed to be maltose and maltotriose in the α-amylase reaction with starch (Fig. 4.3B). The glucose formed from the α-amylase and starch reaction could not be detected on the TLC plate (but was quantified using the GOPOD test) (Fig. 4.3B).

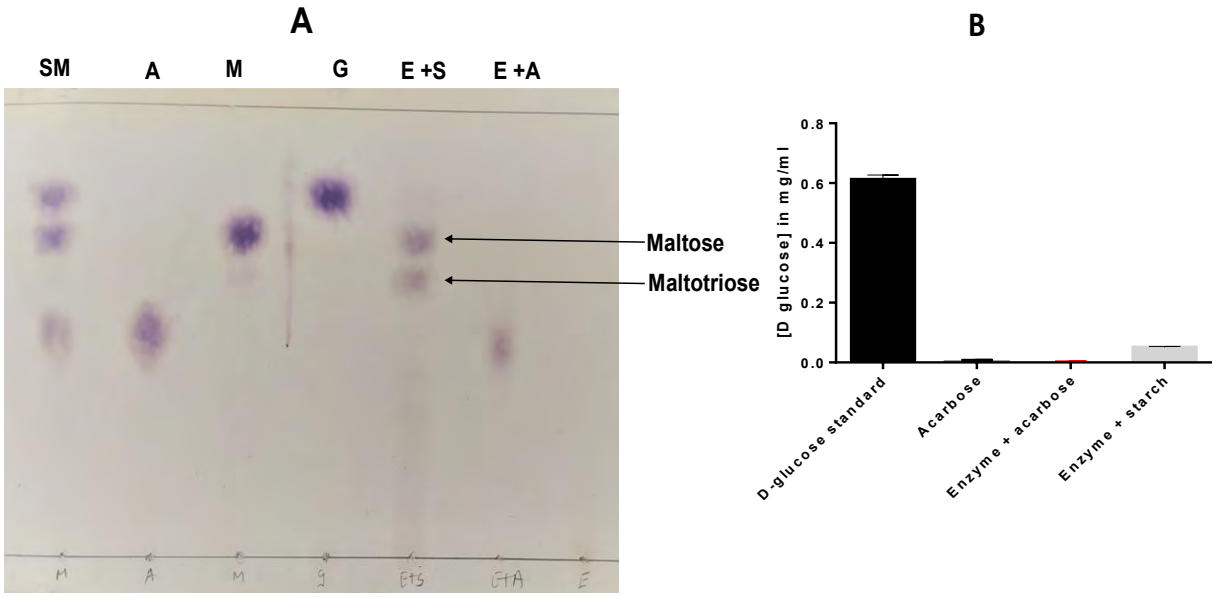

Figure 4.3: Acarbose and starch digestion by porcine α-amylase resolved by TLC and D-glucose formation and detection in the GOPOD test.
A: TLC plate of the products of acarbose and starch digestion. Acarbose was not digested to any detectable glucose product **B**: Glucose as determined by the GOPOD assay. On the TLC plate SM- represents standards mixture (acarbose, maltose and glucose), A- acarbose only, M - maltose only, G - glucose only, E + S- enzyme & starch reaction and E + A- enzyme & acarbose reaction.

4.3.2 Fucoidan exhibits powerful inhibitory effects on α-glucosidase activity

The potential of fucoidans (from the different seaweed species) to inhibit the activity of α-glucosidase, an enzyme necessary for breaking down oligosaccharides (mainly maltose) produced during starch digestion by α amylase, was investigated (Section 4.2.2). All the fucoidan water extracts inhibited the activity of α-glucosidase (Fig. 4.4). Interestingly, all the fucoidan extracts were better inhibitors of the α-glucosidase enzyme than the commercial acarbose control. The inhibition potential of the extracts was of the following order: *F. vesiculosus* ≈ *E. radiata* ≈ *S. elegans* > *E. maxima.* The positive control fucoidan from *F. vesiculosus* displayed the best enzyme inhibition of all the extracted fucoidans.

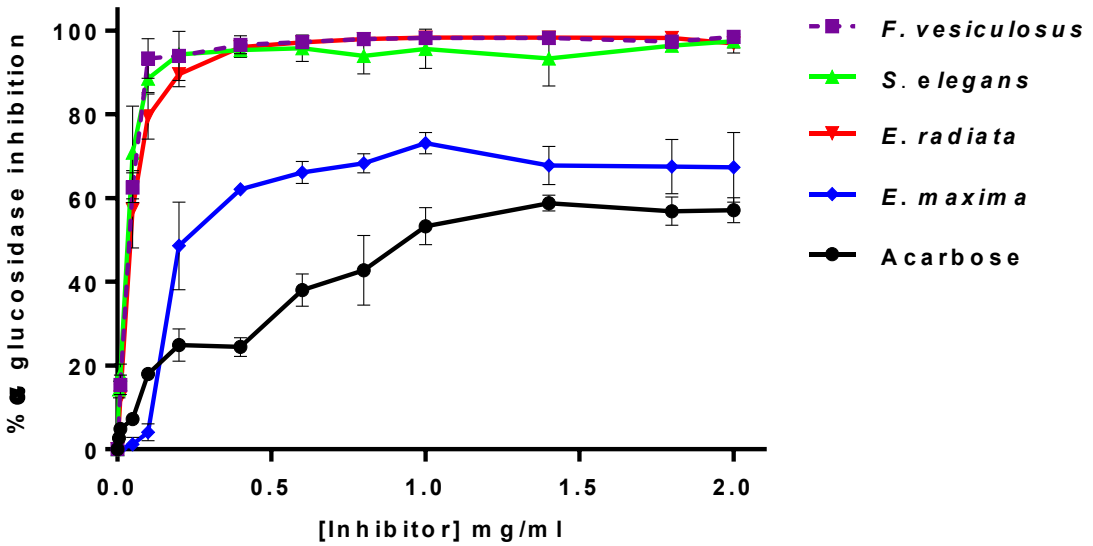

Figure 4.4: Inhibition of α-glucosidase activity by water-extracted fucoidans obtained from various seaweeds in the study.
The data values are represented as means ± standard deviation (n ≥3) where n was the number of independent assays.

4.3.2.1 Effect of extraction methods on the inhibition potential of α-glucosidase by fucoidans

Fucoidans were extracted from the seaweeds using various protocols, namely hot water- EDTA-Na- and acid assisted-methods. These individual extracts were used to investigate their ability to inhibit α-glucosidase. All the water extracted fucoidans displayed significantly higher α-glucosidase inhibition, followed by the EDTA-Na extracted fucoidans and, lastly, the acid extracted fucoidans (Fig. 4.5). The acid extracted fucoidans from *E. maxima* showed some limited inhibitory activity on α-glucosidase. (Fig. 4.5A). There was no inhibitory activity exhibited by the *E. radiata* acid extracted fucoidan. The *S. elegans* acid extract showed some limited inhibition potential, which was not considered significant, as this inhibition did not follow a dose-dependent response (Fig. 4.5C). All three EDTA-Na extracted fucoidans elicited some impressive inhibitory activity towards α-glucosidase, but, ultimately, the water extracted-fucoidans were shown to be the most potent inhibitors of α-glucosidase activity.

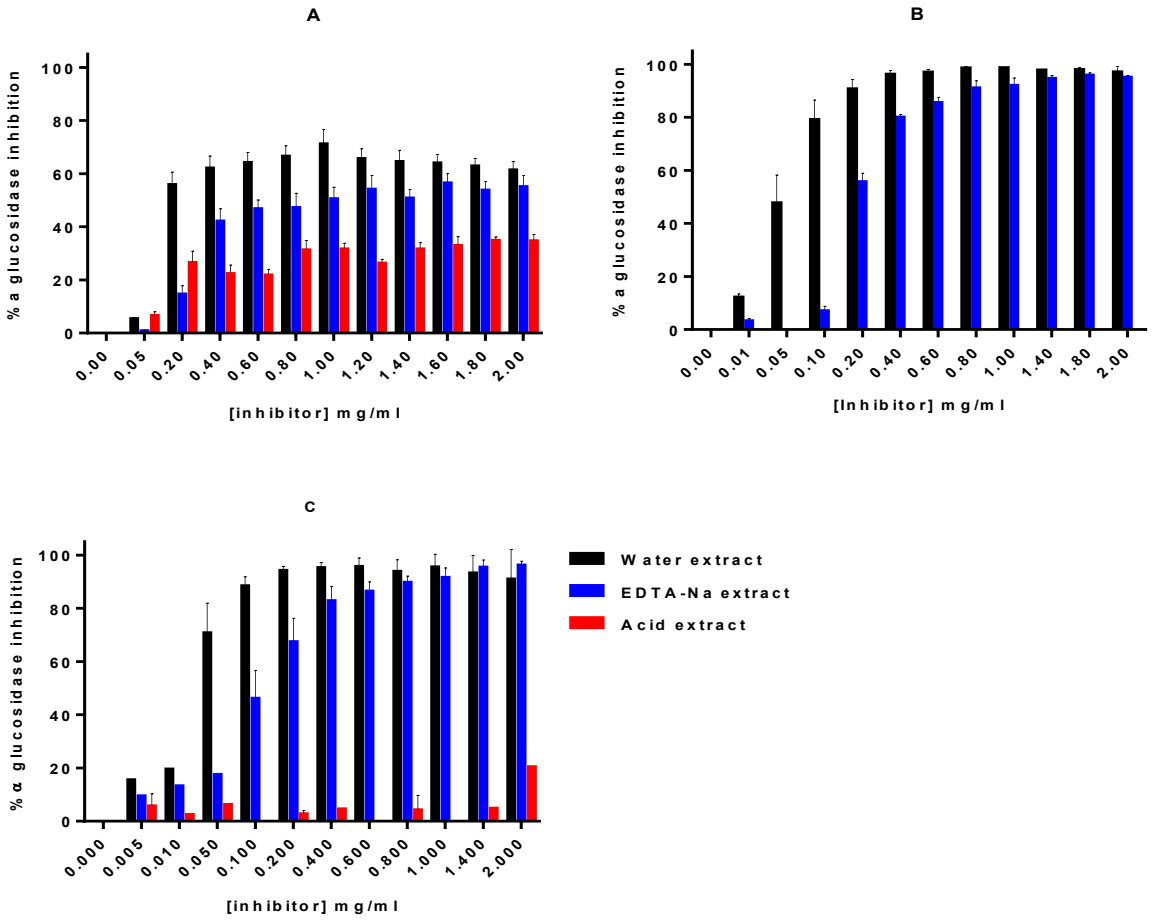

Figure 4.5: Inhibition potential of individual seaweed fucoidan extracts.
A: Fucoidan extracts from *E. maxima,* **B**: Fucoidan extracts from *E. radiata*, and **C**: Fucoidan extracts from *S. elegans.*The water extracted fucoidans from the various seaweeds demonstrated the highest degree of inhibition against the α-glucosidase enzyme. The data values are represented as means ± standard deviation (n ≥3) where n is the number of independent assays

4.3.2.2 Potency of fucoidan extracts as inhibitors of α-glucosidase

The half-maximal inhibitory concentrations (IC_{50}) for the inhibitors were determined to measure the efficacies of the fucoidan extracts in inhibiting α-glucosidase. The water extracted fucoidans displayed the lowest IC_{50} values, followed by the EDTA-Na extracts and, lastly, the acid extracts (Table 4.1). The efficacies of these extracts were compared against the commercial standard α-glucosidase inhibitor acarbose and the commercially available *F. vesiculosus* fucoidan.

Table 4.1: IC_{50} µg/ml of selected seaweeds for the α-glucosidase enzyme

	IC_{50} in µg/ml		
Fucoidan/Inhibitor	**Water extract**	**EDTA-Na extract**	**Acid extract**
E. maxima	189 ***/*	206.6 ***/**	296***/***
E. radiata	39.66 ***/ns	193.3***/ *	-
S. elegans	36.81***/ns	159.9***/*	-
F. vesiculosus	18.16		
Acarbose control	435		

The results are presented as means ± standard deviation from triplicates of three independent experiments. The statistical significance of the results was tested using ANOVA employing the Tukey-Kramer's test between the control and different groups and between groups. The results were considered significant at (*) P<0.05, (**) P<0.01, (***) P<0.001 and (ns) when not significant. The "/" separates significant differences between the groups and acarbose and significant differences between groups and *F. vesiculosus* fucoidan.

The *E. maxima* fucoidan extracts were more powerful inhibitors of α-glucosidase than acarbose; however, they were less potent than the *F. vesiculosus* fucoidan. Also, the IC_{50} values of the *E. maxima* fucoidan extracts were significantly different from each other, with the water extract being most active and the acid extract least active (Table 4.1) (Appendix B11; Table B2). The *E. radiata* water and EDTA extracts showed more substantial inhibitory potential compared to acarbose. In addition, the *S. elegans* water and EDTA fucoidan extracts displayed significantly lower IC_{50} values than acarbose (Table 4.1). The *E. radiata* and *S. elegans* water-extracted fucoidans, therefore, appeared to be especially attractive as inhibitors, as they displayed relatively low IC_{50} values (Table 4.1). However, their acid extracts did not show any inhibitory effects on the α-glucosidase enzyme.

4.3.2.3 Mode of α-glucosidase inhibition by fucoidan

The kinetic parameters (K_M, V_{max} (converted to k_{cat}) of α-glucosidase in the presence of fucoidans were determined by non-linear regression fit of Michaelis-Menten plots, using GraphPad statistical software (GraphPad Prism v 6, GraphPad Inc). Of note, only the water extracted fucoidans were used in this experiment as they were the most potent among the fucoidan extracts. The α-glucosidase showed a dose-dependent response to all the inhibitors (extracted fucoidan and acarbose) (Fig. 4.6). The derived

kinetic parameters of the enzyme reaction are shown in the table included in Figure 4.6.

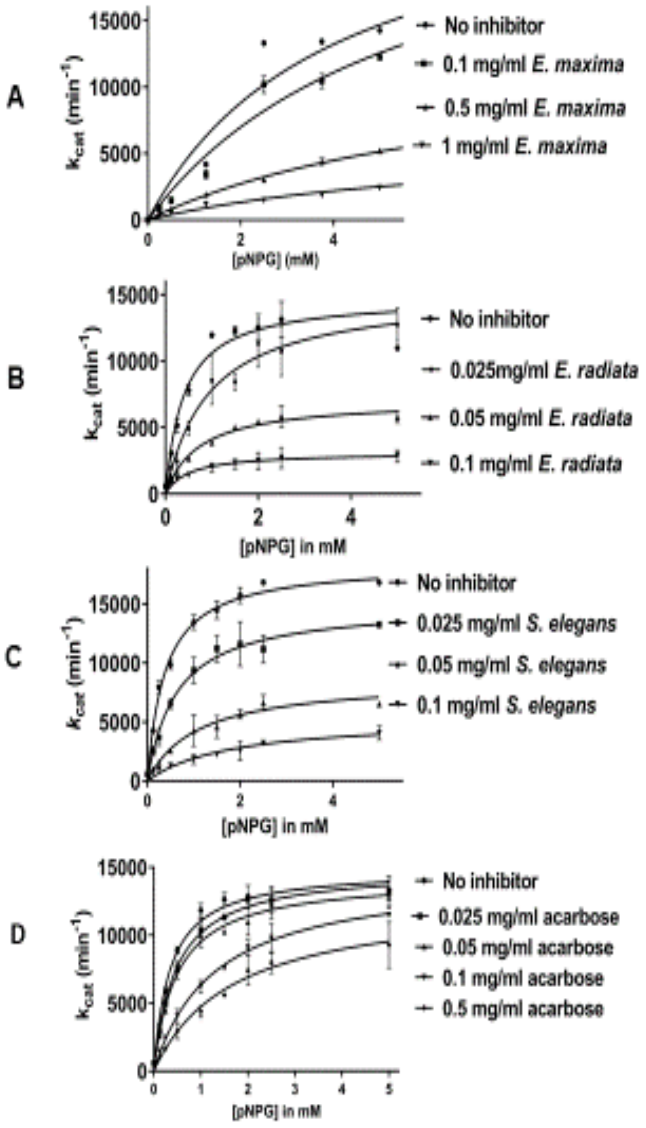

Experiment		K_M (mM)	k_{cat} (min)$^{-1}$
No inhibitor		0.4	14 812
[*E. maxima*]	0.1 mg/ml	0.58	13 134
	0.5 mg/ml	0.79	10 706
	1 mg/ml	1.48	8 400
[*E. radiata*]	0.05 mg/ml	0.72	7 099
	0.1 mg/ml	0.94	3 113
	0.5 mg/ml	1.65	1 121
[*S. elegans*]	0.05 mg/ml	0.63	10 956
	0.1 mg/ml	1.08	4 618
	0.5 mg/ml	1.77	1 321
[Acarbose]	0.05 mg/ml	0.43	14 367
	0.1 mg/ml	1.2	14 557
	0.5 mg/ml	1.9	14 747

Figure 4.6: Michaelis-Menten curves and the derived kinetic parameters of α-glucosidase in the presence of inhibitors.
A: Michaelis-Menten curves for the enzyme in the presence of varying concentrations of *E. maxima* fucoidan, **B:** α-glucosidase enzyme reaction curves in the presence of varying concentrations of *E. radiata* fucoidan, **C;** enzyme reaction curves of α-glucosidase enzyme in the presence of varying concentrations of *S. elegans* fucoidan, and **D**; α-glucosidase enzyme reactions in the presence of varying concentrations of acarbose. The error bars represent the standard deviations from the mean of at least 3 independent assays

The Michaelis-Menten non-linear regression analyses showed a dose-dependent increase in the K_M and decrease in V_{max}, as fucoidan concentration was increased for all fucoidan extracts (Fig. 4.6). This observation suggested that fucoidan may be a mixed inhibitor of α-glucosidase. In contrast, the K_M of the enzyme increased with the acarbose dose while the V_{max} remained relatively unchanged (Fig. 4.6). This α-glucosidase response to acarbose suggested that the drug is a competitive inhibitor. Lineweaver- Burk plots were also constructed through linear regression analysis and suggested that all the fucoidans displayed a mixed-type inhibition (Appendix B14).

4.3.2.4 Deactivation of α-glucosidase by inhibitors

Deactivation studies are characterised by preincubating the enzymes with inhibitors before the substrate is introduced. This allows the enzymes to interact with inhibitors before introducing the substrate. Thus, different types of inhibitors would display distinct reaction responses. In our study, the α-glucosidase was pre-incubated for 30 minutes at 37 ^{o}C with the water extracted fucoidans or acarbose, before the substrate was added, to investigate whether the inhibitors could directly interact with the enzyme before forming the enzyme-substrate complex. All the inhibitors (fucoidans and acarbose) partially deactivated the enzyme's activity (Fig 4.7).

The deactivation reactions improved the efficacy of the inhibitors. This improvement was more noticeable in the case of the weaker inhibitors, i.e. acarbose and *E. maxima* fucoidan, as a higher degree of inhibition was observed in their respective deactivation reactions (Fig. 4.7 A, E). Preincubation with a competitive inhibitor would change the dynamics and improve the inhibition potency of a compound as the inhibitor competes for the active site with the substrate. Thus, deactivation from a non-competitive inhibitor would be relatively lower. In our case, the degree of inhibition is improved more significantly within the acarbose reaction, where acarbose behaved as a competitive inhibitor (Fig. 4.7 E). The water extracted fucoidans were mixed inhibitors of α-glucosidase (Fig. 4.6); thus, the impact of deactivation was not as pronounced, except for *E. maxima* fucoidan (Fig. 4.7).

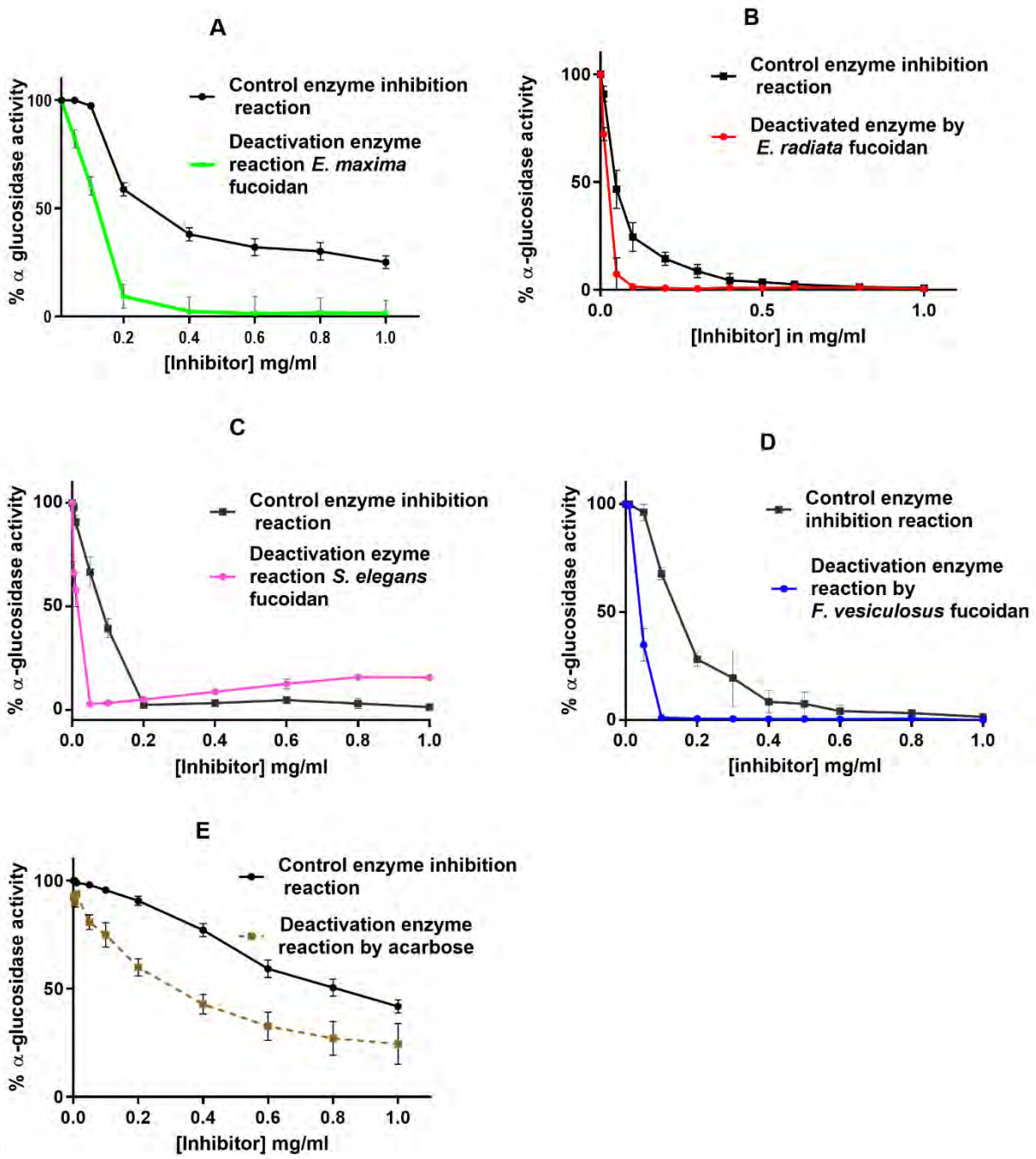

Figure 4.7: Deactivation of α-glucosidase by pre-incubation with various inhibitors. The letters **A-E** represent the enzyme deactivation reactions by fucoidans extracted *from E. maxima*, *E. radiata* and *S. elegans*, commercial *F. vesiculosus* fucoidan and the acarbose control, respectively. The error bars on the data represent the standard deviations from the mean of at least 3 independent assays

4.3.3 Fucoidan interactions with α-glucosidase

Fucoidans, as inhibitors, directly interacted with the α-glucosidase enzyme (Fig. 4.7). To further prove this hypothesis, the conformational changes of this enzyme in the absence and presence of fucoidan was investigated using an intrinsic fluorescence assay and circular dichroism (CD) spectroscopy.

4.3.3.1 Fucoidan perturbs the tertiary structural conformation of α glucosidase

The tertiary structural conformational changes of α-glucosidase in the presence of inhibitors were evaluated by intrinsic tryptophan fluorescence. The spectra reduced in intensity as the fucoidan concentrations increased in a dose-dependent fashion (Fig. 4.8).

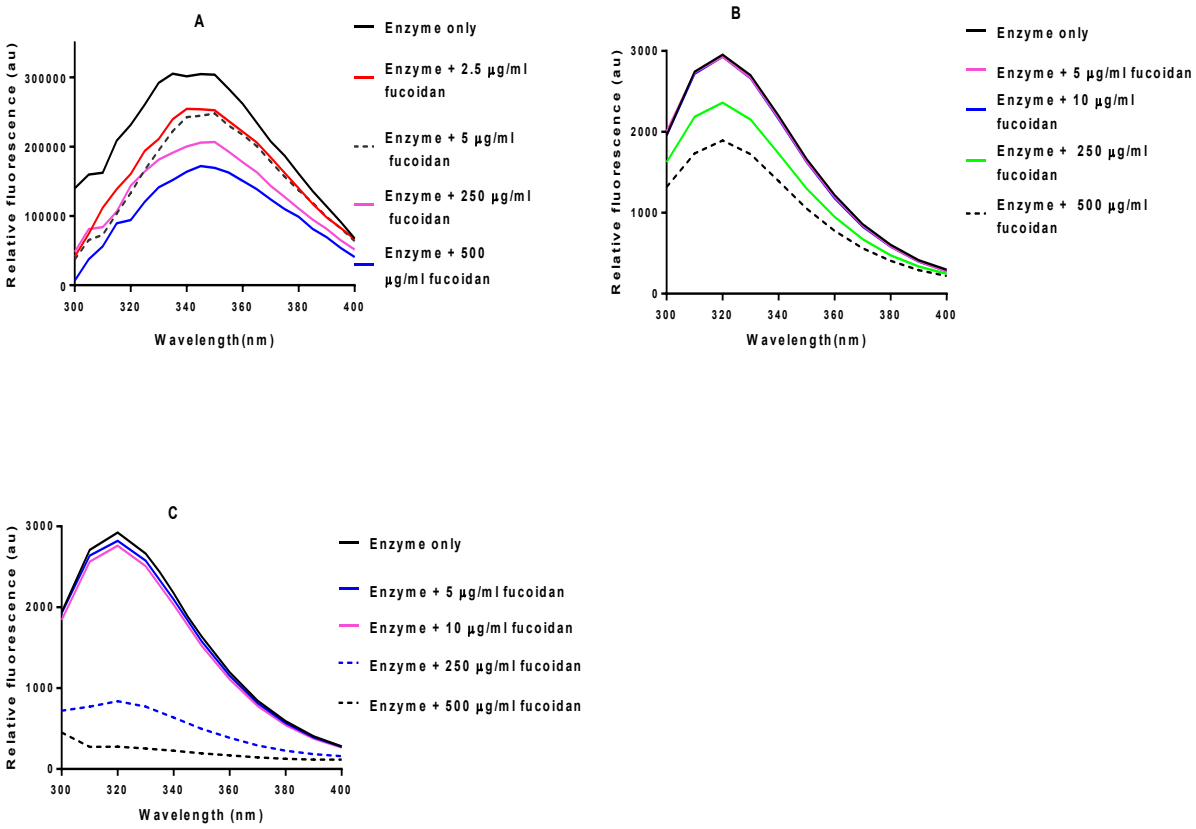

Figure 4.8: Analysis of the tertiary structural conformational changes in α-glucosidase in the presence of fucoidan by intrinsic tryptophan fluorescence.
A represents the interactions of *E. maxima* fucoidan with the enzyme, **B** interactions of *E. radiata* fucoidan with the enzyme, and **C**, interactions of *S. elegans* fucoidan with the α-glucosidase.

The maximum relative fluorescence was observed at about 340 nm. All the fucoidans from the different seaweeds showed a similar pattern. This observation suggested that the enzyme's structure undergoes conformational shifts in its tertiary structure, concealing the tryptophan residues, which translates to the reduced relative fluorescence with increasing inhibitor strength. In addition, the *E. maxima* fucoidan induced a red shift in the fluorescence of the treated reaction (Fig. 4.8A). In contrast, the *E. radiata* fucoidan did not induce any shifts (Fig. 4.8B), while *S. elegans* fucoidan resulted in a blue shift (Fig. 4.8C). These shifts may be caused by solvent accessibility in the inhibitor enzyme mixture, affecting the observed relative fluorescence.

4.3.3.2 Fucoidan interacts with α-glucosidase, changing the enzyme's secondary structure conformation

CD spectroscopy is considered a reliable and sensitive method for monitoring changes in macromolecules at a secondary structural level, including proteins. Therefore, the secondary structural changes of α-glucosidase, in the absence and presence of fucoidan, was investigated by CD spectroscopy. The experimentally recorded signals between 190 and 240 nm were superimposed on the predicted signals using the DICHROWEB database. The correlation of the signals resolved with the CONTIN method gave normalised root mean squared deviation (NRMSD) values of less than 0.1, depicting a good correlation. The fucoidan and α-glucosidase interactions showed a dose-dependent red shift towards the higher wavelength horizontal axis (Fig 4.9).

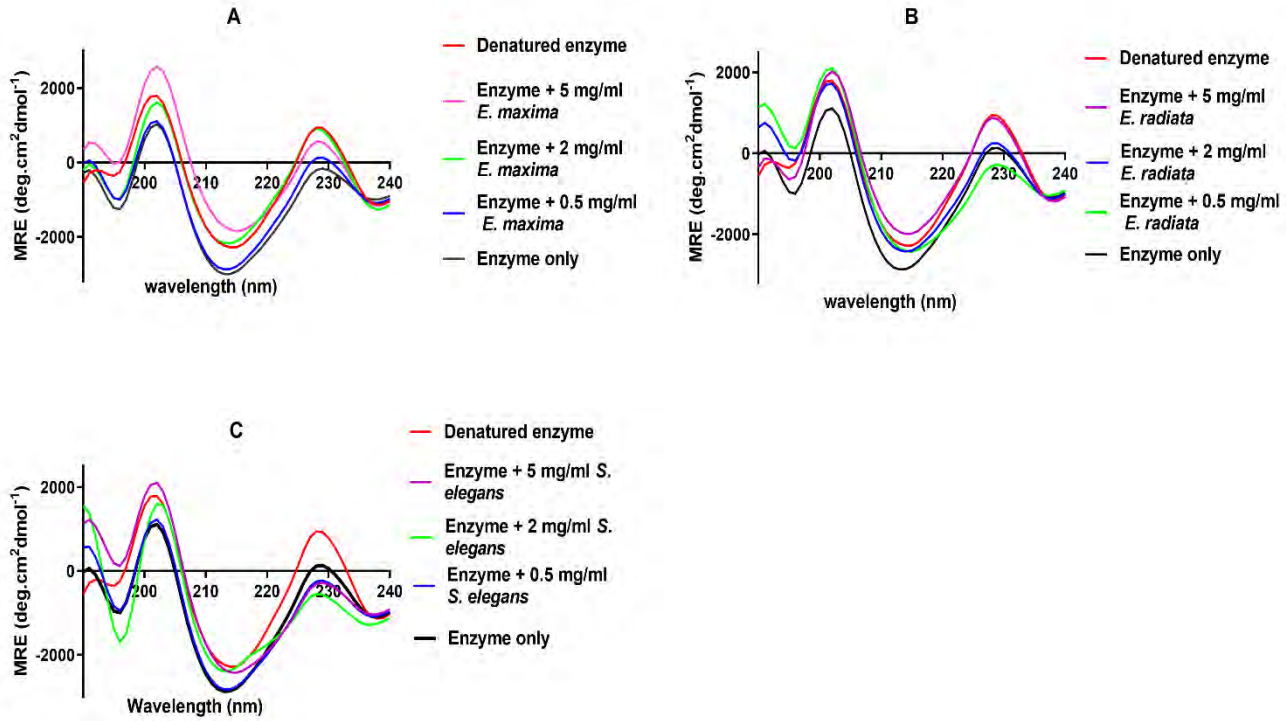

Figure 4.9: Circular dichroism de-convoluted spectral shifts in the secondary structure of α-glucosidase in the absence and presence of fucoidan.
The CD spectrum for α-glucosidase was presented as molar residue ellipticity (deg.cm^2.dmol^{-1}). **A**: represents interactions of *E. maxima* fucoidan, **B**: interactions of *E. radiata* fucoidan and **C** represents interactions of *S. elegans* fucoidan, with α glucosidase.

The α-glucosidase deconvolution data revealed that the enzyme's secondary structure is mainly composed of the β-conformation. This finding was expected as α-glucosidase has a TIM barrel active site topology. About 39.6% β-strands constitute the enzyme's secondary structure, while there are 18.9% β-turns, 37.9% unordered regions and 3.6% α-helices. These proportions of the secondary structural elements changed within the enzyme upon pre-incubation with various amounts of the fucoidans (Table 4.2). These findings further confirm that the fucoidans interact directly with the enzyme.

Table 4.2: Effect of fucoidans on the secondary conformation of α-glucosidase

Fractions of de-convoluted secondary structure	α-helix	β-strands	β-turns	Unordered
α-glucosidase	0.036	0.396	0.189	0.379
boiled enzyme	0.026	0.425	0.204	0.344
0.5 mg/ml *E. maxima*	0.033	0.384	0.182	0.400
2 mg/ml *E. maxima*	0.026	0.416	0.194	0.364
5 mg/ml *E. maxima*	0.031	0.408	0.194	0.367
0.5 mg/ml *E. radiata*	0.024	0.413	0.201	0.362
2 mg/ml *E. radiata*	0.033	0.392	0.190	0.380
5 mg/ml *E. radiata*	0.039	0.403	0.177	0.381
0.5 mg/ml *S. elegans*	0.033	0.397	0.190	0.380
2 mg/ml *S. elegans*	0.035	0.392	0.183	0.388
5 mg/ml *S elegans*	0.037	0.43	0.213	0.319

4.3.4 The synergistic inhibitory effects of fucoidan extracts and acarbose on the activity of α-glucosidase

The inhibition potential of individual compounds and acarbose-fucoidan extract combinations (in constant ratios) on α-glucosidase was investigated – to investigate their ability to be used in combination to inhibit the enzyme's activity. It is evident from Figure 4.10 that all fucoidan extracts displayed better inhibition of α-glucosidase compared to acarbose (Fig. 4.10), especially the commercial fucoidan (*F. vesiculosus*) and *E. radiata* fucoidan (Fig. 4.10 B & D).

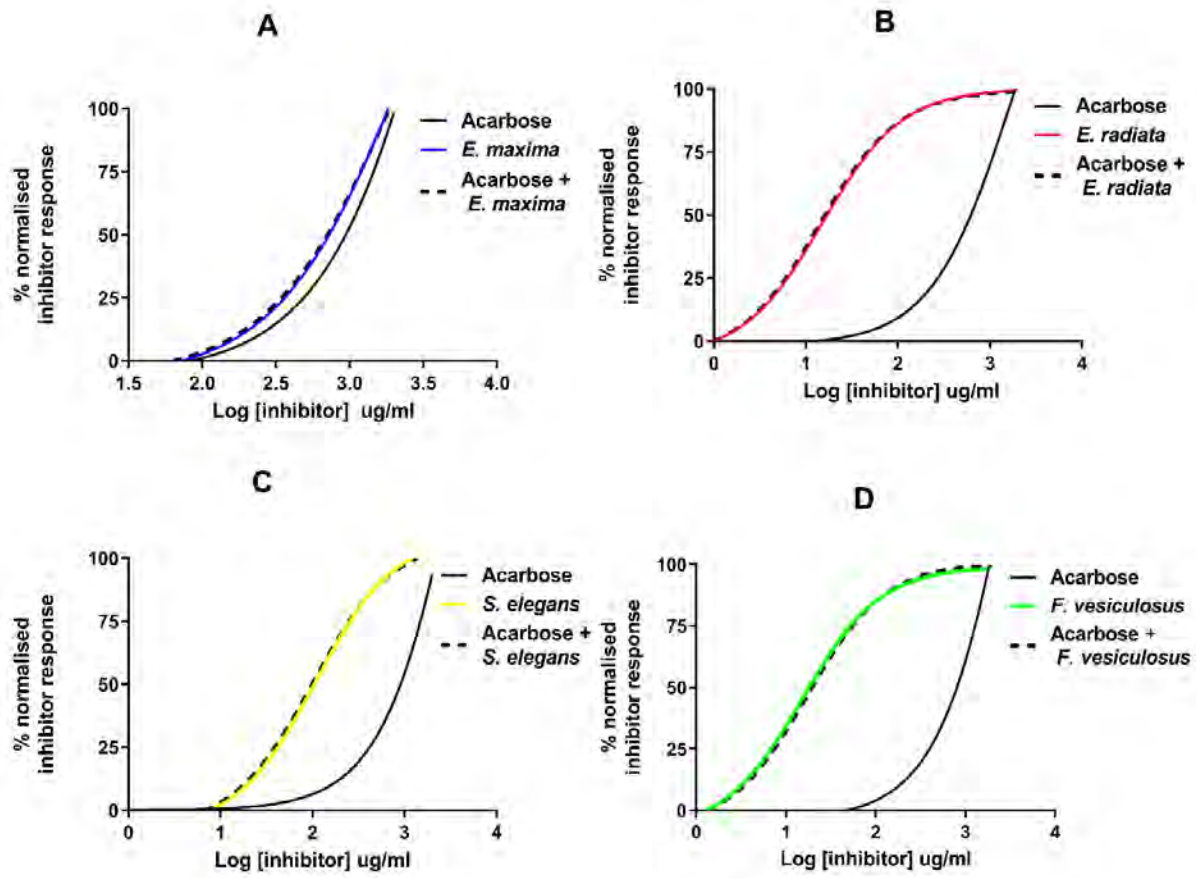

Figure 4.10: Dose-response curves of the inhibition potential of compounds with α-glucosidase.
A: Acarbose and *E. maxima* fucoidan combinations, **B**: Acarbose and *E. radiata* fucoidan combinations, **C**: Acarbose and *S. elegans* fucoidan combinations, **D**: Acarbose and *F. vesiculosus* fucoidan combinations.

The combinations shifted the curves slightly to the left to become more sigmoidal at some compound concentrations compared to when the compounds acted alone, signifying some synergism. The constant ratio experimental data was analysed according to the methods of Chou-Talalay to determine the combination indexes (CI) and 'enzyme inhibition' or fraction affected (fa) at each point (Fig. 4.11). The table excerpts shown in Figure 4.11 were obtained from the Compusyn analysis report and show the Total Dose (= total respective half doses of compounds used), Fa (the amount of enzyme inhibited), and CI value.

A

CI values for actual experimental points:

Total Dose	Fa	CI Value
10.0	0.0020	12.5194
200.0	0.024	8.79754
400.0	0.28	0.81960
800.0	0.41	0.95291
1200.0	0.51	0.99620
1600.0	0.63	0.86853
2000.0	0.66	0.97185
4000.0	0.79	1.12527

B

CI values for actual experimental points:

Total Dose	Fa	CI Value
10.0	0.1	1.96224
20.0	0.38	0.91240
100.0	0.81	0.87001
200.0	0.92	0.74537
400.0	0.98	0.43212
800.0	0.99	0.47391
1200.0	0.99	0.71087
1600.0	0.99	0.94782
2000.0	0.99	1.18478
3000.0	0.99	1.77717
4000.0	0.99	2.36956

C

CI values for actual experimental points:

Total Dose	Fa	CI Value
10.0	0.0050	12.9218
20.0	0.08	1.76726
40.0	0.13	2.12368
80.0	0.5	0.71004
200.0	0.79	0.51026
400.0	0.89	0.49644
800.0	0.96	0.35691
1200.0	0.94	0.79975
1600.0	0.98	0.36468
2000.0	0.92	1.78300
4000.0	0.98	0.91170

D

CI values for actual experimental points:

Total Dose	Fa	CI Value
10.0	0.13	6.79589
20.0	0.28	3.68471
40.0	0.64	0.92769
80.0	0.89	0.23586
200.0	0.94	0.24036
400.0	0.95	0.37004
800.0	0.93	1.20247
1200.0	0.95	1.11012
1600.0	0.95	1.48017
2000.0	0.95	1.85021
4000.0	0.95	3.70041

Figure 4.11: CI values of the actual experimental points.
A; The combination of acarbose and *E. maxima* fucoidan. **B**; The combination of acarbose and *E. radiata* fucoidan. **C;** The combination of acarbose and *S. elegans* fucoidan and **D;** represents the combination of acarbose and *F. vesiculosus* fucoidan.

It can generally be noted from all the fucoidan-acarbose combinations that fucoidan extracts have a synergistic co-operation or additive effect with acarbose in the inhibition of α- glucosidase, as most combinations had a CI value less than 1 or close to 1 (Fig. 4.11). The data also showed that at low inhibitor concentrations or remarkably high inhibitor concentrations, an antagonistic pattern was shown in the inhibition of α- glucosidase. However, this pattern was more pronounced at low inhibitor concentrations. The synergistic or additive profile modelled by the Compusyn software was consistent with the logarithmic dose-response curves (Fig. 4.10) independently constructed using GraphPad Prism.

Furthermore, several concentrations (i.e. in variable and non-constant ratios) of inhibitors (representing their IC_{75}, IC_{50} and IC_{25} values obtained through GraphPad Prism 6) were combined to investigate their synergistic potential in inhibiting the activity of α-glucosidase. The experimental data (Appendix B15) for the α-glucosidase assay were quantified using the Compusyn software, and the results are shown in Table 4.3 below.

Table 4.3: Synergistic effects of acarbose and fucoidan extracts in inhibiting α-glucosidase activity

Points on isobologram	Compounds combinations	Compound concentration (μg/ml) Acarbose: *E. max*		% α-glucosidase activity ± SD	CI	Description
1	IC_{75}-IC_{75}	2223	816	47.4 ± 3.4	0.80	Synergistic
2	IC_{75}-IC_{50}	2223	432	55.5 ± 7.7	0.86	Synergistic
3	IC_{75}-IC_{25}	2223	228	60.0 ± 7.3	0.86	Synergistic
4	IC_{50}-IC_{75}	922	816	57.8 ± 7.4	1.03	Additive
5	IC_{50}-IC_{50}	922	432	57.4 ± 5.8	0.62	Synergistic
6	IC_{50}-IC_{25}	922	228	68.0 ± 6.4	0.76	Synergistic
7	IC_{25}-IC_{75}	382	816	53.6 ± 3.0	0.72	Synergistic
8	IC_{25}-IC_{50}	382	432	59.3 ± 5.9	0.55	Synergistic
9	IC_{25}-IC_{25}	382	228	70.3 ± 1.3	0.62	Synergistic
Points on isobologram	**Compounds combinations**	**Compound concentration (μg/ml) Acarbose: *E. rad***		**% α - glucosidase activity ± SD**	**CI**	**Description**
1	IC_{75}-IC_{75}	2223	35.2	18.1 ± 2.35	0.63	Synergistic
2	IC_{75}-IC_{50}	2223	18.6	26.1 ± 3.64	0.68	Synergistic
3	IC_{75}-IC_{25}	2223	9.9	39.8 ± 2.96	0.98	Synergistic
4	IC_{50}-IC_{75}	922	35.2	20.1 ± 2.56	0.58	Synergistic
5	IC_{50}-IC_{50}	922	18.6	26.8 ± 3.4	0.51	Synergistic
6	IC_{50}-IC_{25}	922	9.9	47.7 ± 6.39	0.83	Synergistic
7	IC_{25}-IC_{75}	382	35.2	20.6 3.41	0.52	Synergistic
8	IC_{25}-IC_{50}	382	18.6	29.6 ± 3.72	0.49	Synergistic
9	IC_{25}-IC_{25}	382	9.9	51.4 ± 7.2	0.68	Synergistic
Points on isobologram	**Compounds combinations**	**Compound concentration (μg/ml) Acarbose: *S. ele***		**% α-glucosidase activity ± SD**	**CI**	**Description**
1	IC_{75}-IC_{75}	2223	69	35.4 ± 5.4	1.6	Antagonistic
2	IC_{75}-IC_{50}	2223	44	39.4 ± 4.4	1.5	Antagonistic
3	IC_{75}-IC_{25}	2223	27.8	48.7 ± 4.7	1.34	Antagonistic
4	IC_{50}-IC_{75}	922	69	37.6 ± 5.5	1.23	Antagonistic
5	IC_{50}-IC_{50}	922	44	45.9 ± 4.4	1.17	Antagonistic
6	IC_{50}-IC_{25}	922	27.8	51.3 ± 6.3	1.14	Antagonistic

7	IC_{25}-IC_{75}	382	69	35.1 ± 4.6	0.95	Synergistic
8	IC_{25}-IC_{50}	382	44	44.1 ± 3.5	0.92	Synergistic
9	IC_{25}-IC_{25}	382	27.8	58.7 ± 5.7	1.1	Antagonistic
Points on isobologram	**Compounds combinations**	**Compound concentration (μg/ml) Acarbose: *F. vesi***		**% α-glucosidase activity ± SD**	**CI**	**Description**
1	IC_{75}-IC_{75}	2223	16.1	24.6 ± 3.2	1.14	Antagonistic
2	IC_{75}-IC_{50}	2223	10.3	31.6 ± 3.5	1.18	Antagonistic
3	IC_{75}-IC_{25}	2223	6.7	41.5 ± 2.38	1.5	Antagonistic
4	IC_{50}-IC_{75}	922	16.1	29.6 ± 3.3	1.17	Antagonistic
5	IC_{50}-IC_{50}	922	10.3	36 ± 4.5	1.06	Antagonistic
6	IC_{50}-IC_{25}	922	6.7	51 ± 5.5	1.37	Antagonistic
7	IC_{25}-IC_{75}	382	16.1	30 ± 3.3	1.07	Antagonistic
8	IC_{25}-IC_{50}	382	10.3	38 ± 4.1	1.00	Additive
9	IC_{25}-IC_{25}	382	6.7	58 ± 5.6	1.47	Antagonistic

CI = the combination index quantifying the degree of inhibitor interactions. E. max within the table represents *E. maxima* fucoidan, E. rad represents *E. radiata* fucoidan and F. vesi represents *F. vesiculosus* fucoidan

The α-glucosidase activity was expressed relative to the uninhibited reaction. The best synergistic combination was observed at IC_{25}:IC_{50} acarbose to *E. maxima* fucoidan, represented by the low combination index (Table 4.3). The best synergistic combinations for acarbose and *E. radiata* fucoidan were at IC_{25}:IC_{50}, IC_{50}:IC_{50} and IC_{25}:IC_{75} in descending order with compound inhibitions of 70.4%, 74% and 79.4%, respectively. As for the acarbose-*S. elegans* fucoidan combinations, most combinations were antagonistic, and only the IC_{25}:IC_{50} and IC_{25}:IC_{75} were synergistic. The commercial *F. vesiculosus* fucoidan and acarbose combinations were also mainly antagonistic.

Also, normalised isobolograms were generated using Compusyn software according to Chou-Talalay methods (Chou, 2010). The isobolograms visually illustrate synergistic combinations as represented below (Fig. 4.11). All the points below the hypotenuse show synergistic points (Fig. 4.11); those on the line illustrate additivity, and antagonistic combinations are plotted above the line (Fig. 4.11). The further the points are from the line, the stronger the effect, whether synergy or antagonism. Furthermore, the points on the key in the figure correspond to the points in Table 4.3

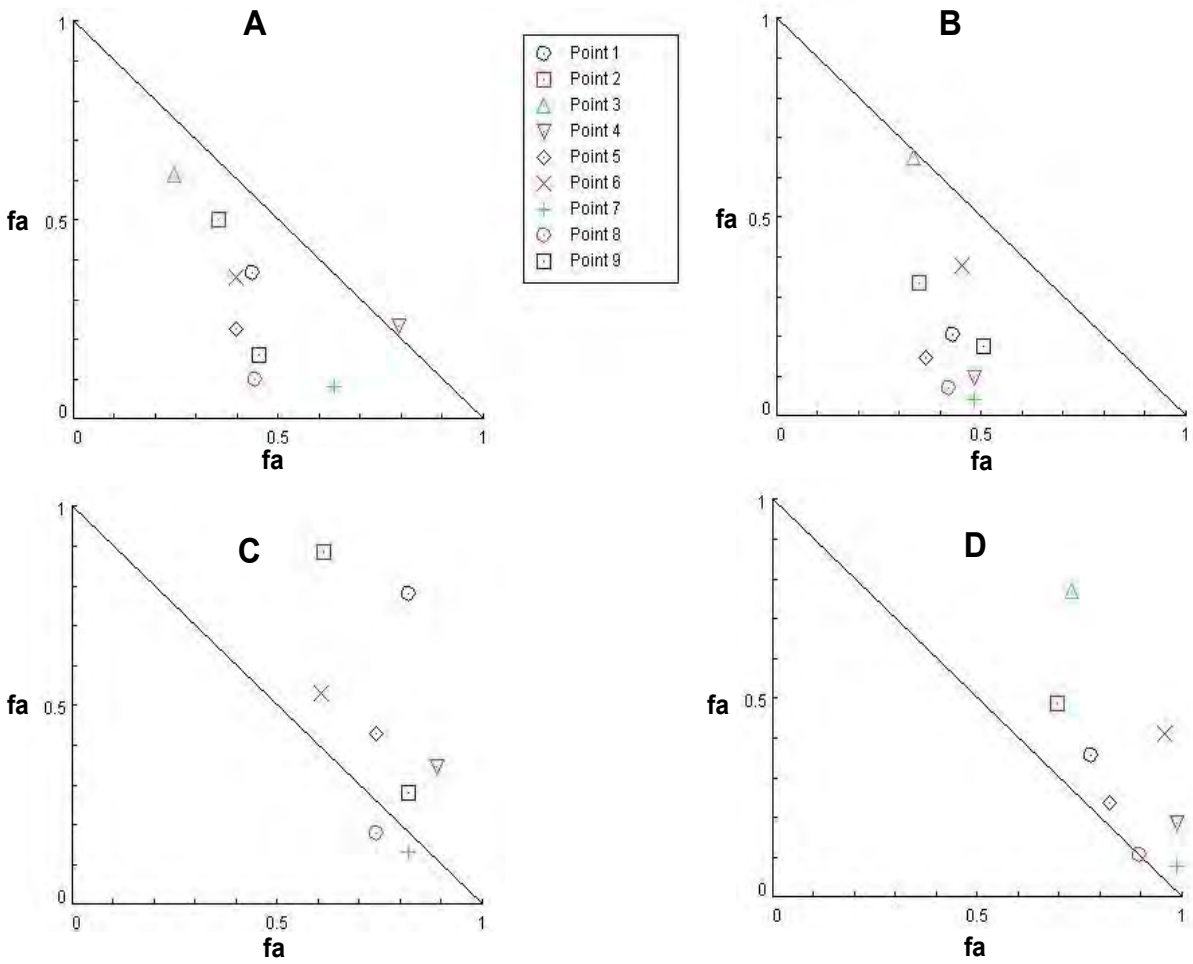

Figure 4.12: Normalised isobologram analysis of acarbose and fucoidan combinations. Fa in the figures represents the affected fraction (inhibited enzyme). **A:** Acarbose and *E. maxima* fucoidan combinations, **B**: Acarbose and *E. radiata* combinations, **C**: Acarbose and *S. elegans* combinations, **D**: Acarbose and *F. vesiculosus* combinations. Various combinations of acarbose and fucoidan based on IC_{75}, IC_{50} and IC_{25} values were tested by the Compusyn software and the combination indexes were determined. CI values represented by points below the hypotenuse line of the triangles indicate synergy as a particular effect. Points on the line represent additivity, and those above the line represent antagonism.

4.4 Discussion

In this chapter, fucoidans were investigated as potential inhibitors of the amylolytic enzymes α-amylase and α-glucosidase as part of the drive of drug discovery in the fight against diabetes. The manipulation of the activities of these enzymes could significantly impact the amount of blood glucose levels that may be necessary for the control of type 2 diabetes. The crude water extracted fucoidans from *E. maxima*, *E. radiata*, *S. elegans,* and commercial *F. vesiculosus* did not inhibit the activity of porcine α-amylase to any significant extent (Fig. 4.1A). The fucoidans extracted by the other methods (EDTA-Na and acid) also failed to inhibit the enzyme's activity (Appendix

B10). These observations were expected for *F vesiculosus,* as Kim et al. (2014) demonstrated that the seaweed extracted fucoidans did not possess inhibitory characteristics towards α- amylase. *Ecklonia* spp. and *S. elegans* seaweed fucoidan activity on porcine α- amylase have also not been reported in the literature (to the best of our knowledge). However, the acarbose control did inhibit α-amylase activity more significantly and displayed an IC_{50} of 109.1 µg/ml (Fig. 4.1B).

Interestingly, acarbose inhibited the enzyme's activity in a dose-dependent manner up to about 0.5 mg/ml (Fig. 4.1). Above 0.5 mg/ml, the activity of α-amylase appeared to increase, although this was due to acarbose degradation in the reaction during the DNS heating stage. Our observations agreed with one study which reported that acarbose thermally decomposes during the DNS protocol, which requires heating at about 95 ^{o}C, and further suggested that acarbose may be a substrate for α- amylase (Singla et al., 2016).

Our findings concurred with Singla et al. (2016) regarding the degradation of acarbose during heating to produce reducing sugars (Fig. 4.2). However, our findings could not confirm acarbose as a substrate for porcine α-amylase, as this enzyme could not cleave acarbose to produce any detectable reducing sugars or smaller oligosaccharides (Fig. 4.3). Moreover, the methodology involved in quantifying the reducing sugars by Singla and colleagues also involved the DNS protocol, which again brings the factor of acarbose pyrolysis into consideration. In this current study, acarbose digestion by amylase was analysed by the GOPOD assay and TLC. No evidence could be found to indicate that acarbose was a substrate for α-amylase. Nevertheless, Singla et al. (2016) suggested that acarbose attaches to the enzyme's active site more firmly than starch, making it a perfect inhibitor for starch hydrolysis. This hypothesis by Singla and colleagues is reasonable, as the present study (Fig. 4.6) and literature have both established that acarbose is a competitive inhibitor.

The extracted fucoidans all inhibited *Saccharomyces* α-glucosidase to a greater extent than acarbose (Fig. 4.4). Acarbose is currently used as a medication for type 2 diabetes, has well-known side effects, including flatulence, meteorism, abdominal distension and even diarrhoea (Kotowaroo et al., 2006). Therefore, the extracted fucoidans may potentially be potent inhibitors of α-glucosidase, which may present fewer side effects as they are natural bioproducts. The fucoidan extracted by the

EDTA-Na method also showed significantly higher inhibition potential than the acarbose control, lower inhibition than the water-extracted fucoidan (Fig. 4.5). This observation shows that EDTA-Na extraction produced biologically active fucoidan.

The pharmacological potencies of the fucoidan extracts were represented as IC_{50} values. All the extracted fucoidans (water and EDTA-Na assisted) were shown to be better inhibitors of α-glucosidase than acarbose (Table 4.1). The water extracted fucoidans from *E. radiata* and *S. elegans* compared exceedingly well with the commercial *F. vesiculosus* fucoidan standard. Compared to most fucoidans inhibiting α-glucosidase, the extracted fucoidans outcompeted acarbose, displaying IC_{50} values in an approximate range of 280 – 415 µg/ml (Shan et al., 2016). However, the extracted fucoidans have IC_{50} values close to those of the most potent known fucoidans, including *Ascophyllus nodusum* with an IC_{50} of about 30 µg/ml (Kim et al., 2014) and *Undaria pinnatifida* with an IC_{50} of 137 µg/ml (Koh et al., 2020).

Furthermore, literature has shown that most fucoidan extracts are more active in suppressing the activity of α-glucosidase compared to that of α-amylase (Kim et al., 2014; Koh et al., 2020; Shan et al., 2016). These observations agree with the findings of this study, which found that all the fucoidan extracts were inactive against α-amylase, but were potent inhibitors of α-glucosidase. In addition, natural product research contributing to diabetes treatment and prevention has focused more on α-glucosidase inhibition. The enzyme is directly responsible for releasing glucose from maltose and sucrose (Kim et al., 2014). Notably, the complete inhibition of α-amylase is not desirable as the gut microbiota may utilise the undigested starch to release gases which may provoke intestinal complications (Cho et al., 2011). Therefore, the perfect inhibitor should inhibit α-glucosidase to a greater extent than α- amylase. Hence the extracted fucoidans in this study could be fit for purpose.

The chosen water extracted fucoidans which were the most potent of all within the extracts, displayed a mixed type mode of inhibition. The kinetic parameters of α-glucosidase determined from Michaelis-Menten modelling (using GraphPad Prism) illustrated an increase of K_M and decrease of V_{max} (which was represented as k_{cat}) with increasing inhibitor concentrations (Fig. 4.6). The Lineweaver-Burk plots could not be classified in the characteristic competitive, non-competitive, or uncompetitive inhibition models (Appendix B14). These findings concur with literature and enzyme kinetics

phenomena in enzyme inhibitions, where it is challenging to model mixed types of inhibition using Lineweaver-Burk plots (Lopina, 2017). Also, some minimal studies have been performed in which the mode of inhibition of the most characterised fucoidans have been identified. Shan et al. (2016) reported fucoidans isolated from *Sargassum* spp. seaweeds to be competitive inhibitors like acarbose. In our study, acarbose was confirmed to be a competitive inhibitor (Fig. 4.6); this agrees with the literature (Kim et al., 1999; Osonoi et al., 2010). However, acarbose has also been reported to behave as a mixed type non-competitive inhibitor (Son & Lee, 2013). These inconsistencies and limited studies on the mode of fucoidan inhibition highlight how challenging it is to characterise this aspect of enzyme inhibition.

The pre-incubation of the enzyme with the inhibitors improved their potency, as the fucoidans and acarbose seemed to deactivate the enzyme (Fig. 4.7). This observation agreed with several studies that reported that pre-incubation of inhibitors with enzymes or transporter molecules increased the strength of the inhibition (Barrett et al., 2011; Baumhardt et al., 2015; Tatrai et al., 2019). It was also noted that pre-incubation had a more significant beneficial effect on the weaker inhibitors, i.e. *E. maxima* fucoidan and acarbose (Fig. 4.7A, E), compared to the more potent inhibitors. This could be explained by the slow equilibrium of association linked to slow binding inhibitors (Barrett et al., 2011). Pre-incubation had a minimal beneficial effect on fast binding inhibitors (Fig. 4.7). The concept of enzyme deactivation by pre-incubation becomes an important consideration in diabetic patients when the drugs have to be administered a few moments before taking major meals. Fucoidans were shown to interact with the enzyme independently of the formation of an enzyme-substrate complex.

Perturbations caused by the fucoidan inhibitors resulted in conformational changes in the tertiary structure shown by the dose-dependent shifts of relative tryptophan fluorescence with increased inhibitor concentration (Fig. 4.8). A similar pattern was observed within the secondary structure conformation, where the presence of fucoidan shifted the de-convoluted spectrum towards the positive horizontal axis with the addition of fucoidan (Fig. 4.9). These experiments both suggested direct interaction between the fucoidans and α-glucosidase. Although limited studies are available on the interaction of fucoidans with α-glucosidase, several other inhibitors directly interact with the enzyme. Our findings agree with reports which have stated that slight shifts in

the secondary and tertiary structure of α-glucosidase have been observed in the presence of inhibitors (Liu et al., 2011; Ma et al., 2015).

The compound combination studies suggest that the extracted fucoidans combined with acarbose acted synergistically, which may help in the combination therapy of Type 2 diabetes mellitus. The major carbohydrate digesting enzymes, namely α-amylase and α-glucosidase, play a significant role in controlling blood sugar levels (via absorption of glucose into the bloodstream). It has recently been shown in a review by Mabate and colleagues (2021) that most fucoidans lack efficacy towards α-amylase but are excellent inhibitors of α-glucosidase. Conversely, acarbose is a good inhibitor of α-amylase but a less potent inhibitor of α-glucosidase. Therefore, their combination may have an additive or potentially synergistic interaction, as illustrated by the findings of this study (Table 4.3) - or combinations may be used to inhibit both α-amylase and α-glucosidase. The synergistic potential of fucoidans has been investigated using this approach before, suppressing measles virus proliferation (Morán-Santibañez et al., 2016). Moreover, the Chou-Talay method of quantifying synergy was selected for this (our) study, as it is the most widely used model to date (Roell et al., 2017).

The fucoidan-acarbose combination may also help to reduce the side effects of acarbose in the human alimentary canal. In addition, a reduction in toxicity and side effects of this drug is one of the key rationales of using drug combinations (Greco et al., 1996). Combining compounds with non-overlapping side effects, such as fucoidan and acarbose, allows total efficacy with limited expected side effects. Considering the viscosity of fucoidans, the drug dose may be available for longer before excretion as high viscosity of the digesta slows down gastric emptying.

In conclusion, this chapter sought to show the feasibility and relevance of fucoidans extracted from seaweeds (endemic to South African coastlines) as inhibitors of amylolytic enzymes. The study revealed that the selected seaweed fucoidans inhibited α-glucosidase more potently than the commercial acarbose standard. Fucoidan extracts were found to be mixed-type inhibitors of this enzyme. Fucoidans perturbed the secondary and tertiary structures of α-glucosidase, as they interacted directly with the enzyme. The extracted fucoidans and commercial acarbose synergistically inhibited the activity of α-glucosidase. Finally, this chapter also highlighted the fact that

acarbose and fucoidans may be applied in a combined compound approach to regulate the activities of the amylolytic enzymes in a search to manage T2DM.

Fucoidans are plausible anti-T2DM compounds and can be used either on their own or combined with existing therapeutic agents. The progression of diabetes has been linked with tumour proliferation; thus, fucoidans may have a dual therapeutic effect. These seaweed polysaccharides are deemed to have several beneficial biological activities, including anti-cancer properties. Fucoidans were therefore explored for their anti-cancer activities in the next chapter.

CHAPTER 5: EXPLORATION OF THE ANTITUMOR ACTIVITY OF FUCOIDANS ON HUMAN COLON CANCER CELLS

5.1 Introduction

Cancer describes a diverse group of diseases characterised by the uncontrolled growth of abnormal cells. Cancers can invade surrounding tissues and spread to invade other tissues and organs through metastasis using the circulatory or the lymphatic system (Marudhupandia et al., 2015). According to the World Health Organisation (WHO), cancer is one of the diseases with the highest mortality rates (WHO, 2021). It is a significant barrier to increasing life expectancy globally (WHO, 2021). The global cancer burden is expected to rise by about 47% (28.4 million) of the current incidences by 2040. However, the increase is expected to be varied as the socioeconomic status of countries may aggravate it. Also, the rise may be linked with increased risk factors associated with globalisation and the growing economy, around the globe (Sung et al., 2021). It is, therefore, critical to tap into novel cancer therapeutic approaches to contribute to global cancer control efforts. There are many types of cancers, and the most common worldwide include lung cancer, breast cancer, colorectal cancer, and stomach cancer. Breast cancer has overtaken lung cancer in incidence with 11.7% and 11.4%, respectively. Moreover, colorectal cancers have an incidence of 10% but have an estimated mortality of 9.4% second to lung cancer with 18% mortality (Sung et al., 2021). The significance of these numbers justified the selection of the cell line employed in our study.

There are several strategies used currently to combat cancer. One of the standard methods is chemotherapeutic drugs, which may be used alone or in combination (Mokhtari et al., 2017). These drugs have a range of modes of action, which ultimately result in cellular toxicity or senescence. Some chemotherapeutics are alkylating agents and prevent the proliferation of cancer cells by damaging DNA. Other agents are mitotic and topoisomerase inhibitors, encompassing several plant alkaloids (Ogawa, 1997). Another major group of chemotherapeutics is antimetabolites, which interfere with DNA and RNA replication. Antimetabolites mimic the free nucleotides required to build DNA and RNA, thereby inhibiting proliferation (Lansiaux, 2011). A typical example of such a drug is 5-fluorouracil (5-FU), which was used as a positive

control in this study. The choice of 5-FU was also influenced by its wide range of use in treating breast cancers, leukaemias, and, significantly, intestinal tract cancers, including colorectal cancer.

During cancer progression, cancer cells tend to invade the surrounding tissue and vascular system as a mechanism of metastasis. For metastasis to occur, cancer cells need to migrate by the protrusive activity of the cell membrane and attachment to the extracellular matrix (ECM) (Yamaguchi et al., 2005). In some instances, cancer cells move collectively, ensuring the local expansion of tumour cells into the ECM. Tumour spheroids have become a popular system to model tumours in 3D. Spheroids are dense 3D cancer cell structures that form due to culture conditions that promote cell-cell adhesions over cell to matrix adhesions (Antoni et al., 2015).

The migration of tumour cells follows a sequence of coordinated steps that involve initiating the expression of a cascade of proteins, including surface adhesion molecules, to allow a more migratory phenotype (Huber et al., 2005). Cells develop pseudopods that protrude and make focal contacts with the ECM for migration to occur. The pseudopods contain filamentous actin and several structural and signalling proteins which facilitate the dynamic interactions with the ECM. Proteases expressed on the cell surface to degrade ECM locally to create tunnels for migration (Friedl & Wolf, 2003). Due to the plasticity of tumours, the integrin and protease isoforms, and signalling molecules in the migration process depend on the type of cancer cells and the homogeneity of individual cells (Friedl & Wolf, 2003). As tumour migration is a hallmark of cancers, it is plausible to target this process to alleviate the burden of tumour progression.

Furthermore, cancerous cells can reprogram glucose metabolism, which is essential for their survival and progression. Usually, pyruvate formed from the enzymatic breakdown of glucose during glycolysis is converted to acetyl-coenzyme A (acetyl-CoA), then fully oxidised in normoxic conditions to produce carbon dioxide and water via the Krebs cycle (Yu et al., 2017). However, cancer cells can switch from oxidative phosphorylation (OXID-P) to anaerobic glycolysis, which yields two pyruvate molecules from the degradation of a single molecule of glucose (Yu et al., 2017). The pyruvate is converted to lactate through an anaerobic glycolytic pathway (without or with limited oxygen). Most cancer cells rely on the latter process, characterised by high

glycolysis rates, even when there is oxygen (Gottschalk et al., 2004). This phenomenon is widely known as the Warburg effect (Warburg et al., 1924). As tumour cells prefer to switch to anaerobic glycolysis, they tend to increase glucose uptake to adapt to the high energy demands, as only 2 ATP molecules can be produced per glucose molecule. This aspect has been exploited in clinical cancer diagnosis where radiolabelled glucose analogues are used (Bomanji et al., 2001). We have also used a similar method in this study to track glucose uptake by the selected cancer cell line. The Warburg phenomenon by cancer cells produces lactate through the oxidation of pyruvate. This makes the regulation of glucose uptake important and may influence the glycolytic flux. This study attempted to investigate whether the extracted compounds could affect the glycolytic flux, which was deemed a plausible target for therapeutic compounds (Mabate et al., 2021). Therefore, this study sought to screen the (previously characterised) fucoidan extracts for anti-cancer activity.

5.1.1 Objectives

The objectives of this chapter were to:

- Determine the potential cytotoxic effects of fucoidan extracts on HCT116 colon cancer cells;
- Explore the potencies of the fucoidan extracts as inhibitors of HCT116 tumour migration; and
- Investigate the effect of the fucoidan extracts on the glucose uptake and glycolytic flux in the HCT116 cells.

5.2 Methods

5.2.1 Cell culture

The HCT116 human colon cancer cell line was purchased from the American Type Culture Collection (ATCC CCL-247). The cell line was cultured in Dulbecco's Modified Eagle's Medium (DMEM) with GlutaMAX™-I, supplemented with 10% (v/v) fetal bovine serum (FBS) and 1% (v/v) sodium pyruvate. The cell culture was maintained at 9% CO_2 in a humidified incubator at 37 °C. Cells were subcultured every three days.

5.2.2 Cytotoxicity screening of fucoidan and HCT116 cells

The susceptibility of the HCT116 cell line to the fucoidan extracts was determined using the resazurin assay (Mabate et al., 2021). Briefly, 50 µl cells were seeded in DMEM growth medium at a density of 1 x 10^5 cells/well into a 96 well plate. The cells were allowed to adhere overnight before treatment with compounds at varying amounts (0 - 2.5 mg/ml). Fluorouracil (5-FU) was included as a positive control. The experiment was incubated for 72 hours at 37 °C in a 9% CO_2 atmosphere. Thereafter, resazurin (~0.1 mM) was added to each well, and the experiment was incubated at 37 ^oC for 3 hours. Lastly, end-point fluorescence was measured at an excitation wavelength of 560 nm and emission at 590 nm. All experiments were performed in triplicate. The half-maximal inhibitory concentration (IC_{50}) of 5-FU was calculated by non-linear regression, using GraphPad Prism version 6.0.

5.2.3 Tumor migration assays

5.2.3.1 Wound healing assay

A volume of 500 µl/well of HCT116 cells were seeded at 7 x 10^5 cells/ml into 24 well plates. The cells were allowed to adhere and grow to 100% confluence overnight at 37 °C. A wound was made down the centre of the well with a white pipette tip. After wounding, the floating cells were removed by carefully pipetting down with the residual medium. The spent medium was removed, and fresh medium without or with varying doses of fucoidan (0.1 - 0.5 mg/ml) treatments were added to the wounds. Pre-migration images of the wounds were taken at 4x magnification. The experiment was incubated at 37 ^oC for 12 hours. The *in vitro* scratch wound-healing images were analysed on ImageJ using a wound healing plugin as described by Suarez-Arnedo et al. (2021). Images were taken after 12 hours from the same position as the premigration images. Wound closure was calculated using the formula below

$$Would\ closure = \%\ wound\ area\ (t = 0) - \%\ wound\ area\ (t = 12)$$

.

5.2.3.2 Sphere based tumour migration assays

Trypsinised HCT116 cells were resuspended in an appropriate volume of Dulbecco's Modified Eagle's Medium (DMEM) with GlutaMAX™-I, 10% (v/v) FBS and 1% (v/v) sodium pyruvate to a final concentration of 1 x 10^4 cells/10 µl of medium for the formation of spheres by the hanging drop method. About 5 ml of sterile PBS was poured into the bottom portion of the tissue culture plate (100 mm diameter) to create a humidified environment. After that, 10 µl multiple culture drops were deposited inside the lid of the culture dish. The lid with the hanging drops was placed back on top of the PBS containing dish carefully to avoid disturbing the droplets. The plate was incubated for 48 hours at 37 ^oC to allow the spheres to grow. After that, the spheres were transferred to a 24 well plate prefilled with 300 µl medium and respective treatments with various compounds ranging from 0.1 mg/ml to 0.5 mg/ml. In some experiments, the trypsinised HCT116 culture at density 10 000 cells/10 µl was pre-treated with 0.5 mg/ml and 0.1 mg/ml of the compounds during sphere formation. Untreated or pre-treated spheres (as relevant) transferred to the adherent plate were allowed to adhere by incubation at 37 ^oC for 4 hours. Images were taken at 4x magnification at t = 0 (which was 4 hours post seeding of spheres into adherent plates). The spheroids were monitored over time up to t=24 hours. The areas of migration were quantified using Fiji/ImageJ. The results presented were represented for 3 experimental biological replicates. The data were normalised to the initial size of each spheroid at time 0, to determine cell spread and migration from the spheroid. The spheres migration was calculated as:

$$\text{Distance migrated} = \text{area measured at time 24hrs} - \text{area at time 0 hours}$$

5.2.4 Cell adhesion assays

HCT116 cells were seeded at a density of 6 x 10^4 cells/well in a 96 well plate. The cultures were treated with varying concentrations of fucoidan (0.1 - 0.4 mg/ml) and the untreated culture was used as the control. The culture was incubated at 37 ^oC under 9% CO_2 for 8 hours. The spent medium was decanted from the plate and the adhered cells were washed thrice with 1 x sterile PBS (137 mM NaCl, 2.7 mM KCl, 10 mM Na_2HPO_4 and 2 mM KH_2PO_4, pH = 7), decanting the liquid after every wash. The cells were fixed by adding 100 µl/well of a 3:1 methanol: acetic acid solution and incubated

at room temperature for 15 minutes. The methanol-acetic acid mixture was washed off using ddH_2O and blotted dry on a paper towel. The cells were stained with 0.1% (w/v) crystal violet dye (40 µl/well) and incubated at room temperature for 20 minutes with gentle agitation at 30 rpm. The crystal violet dye was discarded, and the plate was washed four times with distilled water. A volume of 100 µl/well of 1% SDS was added, the cells were incubated overnight, and the optical density was then measured at wavelength 590 nm.

5.2.5 Clonogenic assay

HCT116 cells were seeded at a density of 1.5 x 10^3 cells/ml in a six-well plate and allowed to adhere overnight. The cells were treated with fucoidan extracts or 4-nitroquinoline 1-oxide (4NQO), which was used as a positive control. The cultures were incubated at 37 ºC for 48 hours, upon which half the volume of spent medium was removed and replaced with fresh medium lacking treatment. The cultures were incubated, and the medium changed every two days until individual colonies of approximately 50 cells/colony were visible. The medium was removed, and the cells were washed once with PBS. The cells were fixed for 10 minutes by a 3:1 methanol to acetic acid mixture. The fixative was removed, and the plate allowed to air dry for 2 minutes. The HCT116 cell colonies were stained with 5% crystal violet (w/v) in methanol for 4 – 6 hours. The wells were washed three times in PBS and rinsed in water. The plates were air dried, and the images were captured using a ChemiDoc™-XRS (BioRad, USA). The cells were solubilised completely using 1 M acetic acid, and the absorbance was read at a wavelength of 590 nm.

5.2.6 Fluorescent-based glucose uptake assays by HCT116 cells

The glucose uptake assay was carried out using the glucose analogue 2-(N-(nitrobenz-2-oxa-1,3-diazol-4-yl)-amino)-2-deoxyglucose (2-NBDG) (Thermo Scientific). HCT116 cells were seeded in a 96-well black-walled plate at a density of 5 X 10^5 cells/well in 100 µl culture and allowed to adhere overnight. After the overnight incubation, spent medium was removed, and cells were washed with glucose-free medium. Subsequently, cells were treated with 50 µl of each fucoidan extract and

controls suspended in glucose-free medium. The positive control for glucose uptake was a treatment with 10 µM of insulin, and the negative control experiment contained 300 µM phloretin. A volume of 50 µl glucose-free medium containing 100 µM of the 2-NBDG was added 'labelled cells' and incubated for 5 hours at 37 °C. The cells were washed with cold PBS. The fluorescence was measured in the FITC range (excitation= 465nm; emission= 540nm) using a SpectraMax M3 multimode plate reader (Separations). Cells were lysed with 5 x Triton X-100 for 20 min at 37 °C. The protein content of the cell lysates (25 µl) was determined by adding 230 µl BCA protein assay reagent (Thermo Scientific™, Pierce) in clear 96-well microtitre plates. The amount of protein was quantified colourimetrically (at a wavelength of 562 nm) after 30 min incubation at 37 °C. Protein concentration was extrapolated from the BSA calibration curve (Appendix B2). Glucose uptake was reported as fluorescence (AU)/protein (mg), accounting for seeding variations between wells.

5.2.7 Glycolytic flux assays

HCT116 cells were seeded at 4 x 10^5 cells/ml in T25 flasks. The cultures were treated with 0.1 mg/ml fucoidan extracts at seeding. One flask was left as the untreated control, and a second was treated with 300 µM phloretin (positive control). The cultures were incubated at 37 °C under 9% CO_2. Spent medium samples were collected at 0, 2, 4, 8, 24, 28, 32, 48 and 72 hours. The collected samples were stored at -20 °C until further required. After 72 hours, the cells were trypsinised and harvested for subsequent protein determination.

5.2.7.1 Glucose uptake quantification (enzymatic)

The collected samples from section 5.2.6 were analysed for the presence of glucose. Glucose quantification was performed using an enzymatic method, using a glucose standard curve with glucose standards ranging from 0 – 5 mM. Briefly, the glucose assay was performed in a 96-well microtitre plate and was constituted as follows: 10 µl of glucose standard was pipetted into each well, and 90 µl of assay cocktail (5 mM (w/v) Mg-ATP, 5 mM (w/v) NADP+, 10 mM (w/v) $MgCl_2$, 0.8 mg/mL (w/v) hexokinase, (0.1% (v/v) glucose-6-phosphate dehydrogenase in 1X PBS) was added to each well. The reaction was allowed to proceed for 90 minutes, and the absorbance (due to

NADPH production) was read at 340 nm. Fucoidan controls were also tested to establish whether they could inhibit the activity of the glycolytic enzymes in the assay.

5.2.7.2 Lactate production

Lactate produced within the medium collected in section 5.2.6 was quantified using a lactate standard curve constructed in the range of 0 - 5 mM lactic acid. The assay was performed in a 96-well microtiter plate as follows: A volume of 10 µl of lactate standard and 90 µl of assay cocktail (5 mM (w/v) NAD+, 1% (v/v) lactate dehydrogenase (LDH), 2.5% (v/v) hydrazine in 1X PBS) was added to each well. The reaction proceeded for 60 minutes, and the optical density at wavelength 340 nm was measured to quantify the amount of NADH produced. Fucoidan controls were also tested to establish whether they could inhibit the activities of the glycolytic enzymes in the assay.

The glucose import assay measures the disappearance of glucose and thus conversion into glycolytic intermediates over time. The lactate production assay measures extracellular lactic acid build-up level over time. The lactate and glucose concentrations were calculated as a function of time and protein concentration using the equation:

$$\frac{gradient\ (m)\ (mM..\min -1)x1000}{mg\ protein} = \frac{\mu mol.min}{mg}$$

5.2.8 Statistical analysis

The data presented in this section was obtained from three biological replicates with values represented as mean ± standard deviation. One-way ANOVA was used to test differences between the means of distinct data groups. The p values less than 0.05 were considered significant. Analyses were all performed using Microsoft Excel 2016 and GraphPad Prism v6.01 (GraphPad Inc).

5.3 Results

5.3.1 Fucoidan cytotoxicity to HCT116 cells

The potential cytotoxicity of all the fucoidan extracts towards the HCT116 colon cancer cell line was examined and compared to the chemotherapeutic drug 5-fluorouracil (5FU). The cell reducing capacities of the fucoidan extracts were expressed as the percentage of viable cells remaining after treatment compared to the vehicle treated control cells. None of the fucoidan extracts under investigation displayed any significant cytotoxic effect on the HCT116 cells (Fig. 5.1). However, higher concentrations of the EDTA extracts of all the seaweeds showed some activity against the HCT116 cells. As expected, the positive control 5FU showed a significant dose-dependent cytotoxic effect on the HCT116 cells with an IC_{50} value of 9.9 µM with an r^2= 0.98 (Appendix B16).

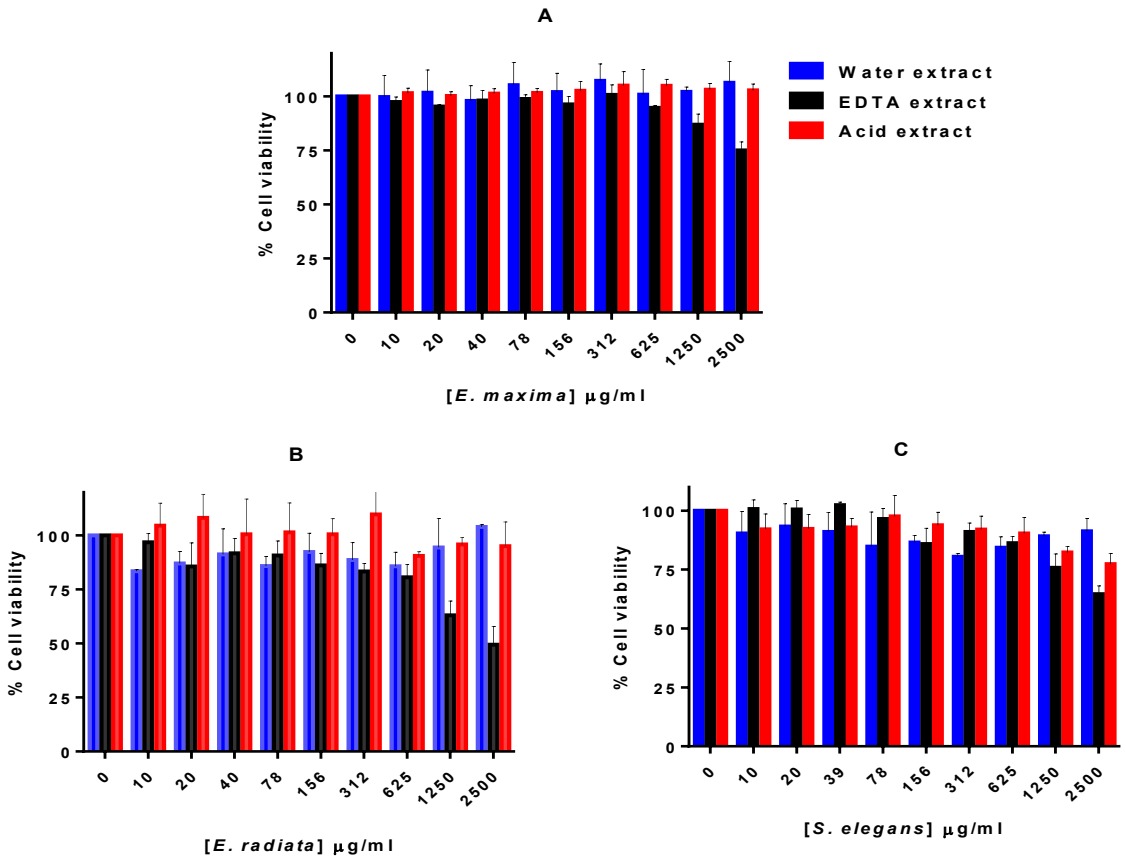

Figure 5.1: Cytotoxicity of fucoidan extracts on HCT116 cells.
Cell viability was assessed by the resazurin assay. The data represent values obtained from 3 biological replicates which are expressed as means ± SD (n=3).

5.3.2 The effect of fucoidans on wound healing by HCT116 cells

Most extracts showed some inhibitory effect on the wound healing migration of HCT116 cells, although these were not pronounced. However, one-way ANOVA ($p<0.05$) confirmed that the fucoidans of *S. elegans* and *F. vesiculosus* had statistically significant inhibitory effects compared to the untreated experiments (Fig. 5.2). *S. elegans* fucoidan extracts inhibited the relative migration of the HCT116 cells by about 20% compared to the untreated cells (Fig. 5.2D). However, the inhibition patterns did not show a clear dose-dependence (Fig. 5.2).

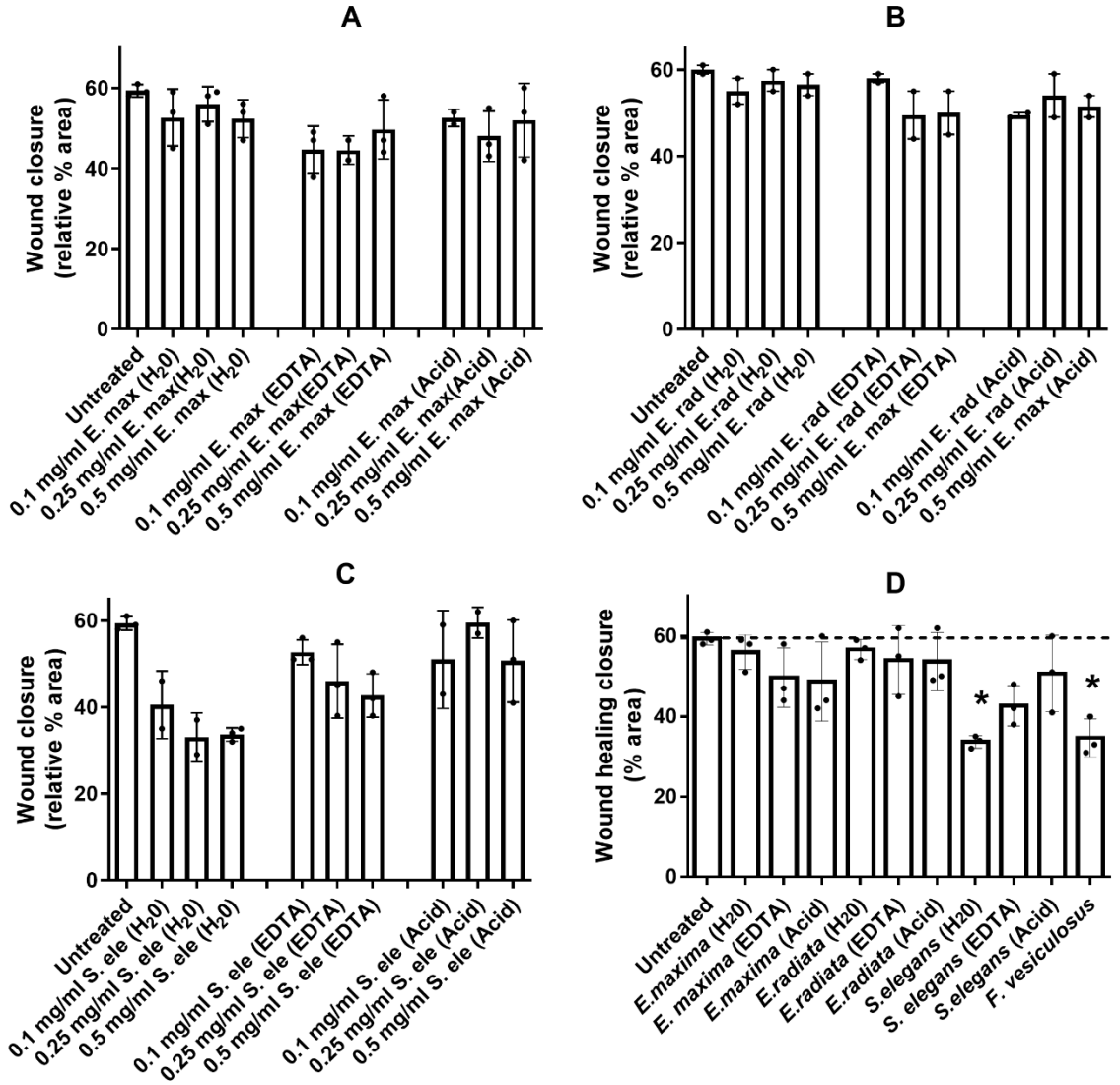

Figure 5.2:The effect of fucoidan extracts on HCT116 cell 2D migration.
A: represents the quantified migration profile of HCT116 cells treated with *E. maxima* fucoidan extracts, **B**: treatments with *E. radiata* fucoidan extracts, **C**: treatments by *S. elegans* fucoidan extracts **D**: Treatments with all the fucoidan extracts and commercial *F. vesiculosus* fucoidan at a constant concentration of 0.5 mg/ml. The data are represented as mean values ± SD (n=3).

5.3.3 Fucoidans inhibit HCT116 spheroid migration

The fucoidan extracts inhibited migration from HCT116 spheres on to the tissue culture plastic. The *E. maxima* water extract and EDTA extract displayed a similar effect on inhibiting the migration of the HCT116 spheroids after 24 hours. However, the EDTA extract displayed a higher inhibitory effect between 4 and 24 hours. The *E. maxima* acid extract displayed the lowest inhibitory effect. Similarly, the *E. radiata* water-extracted and EDTA-extracted fucoidans strongly inhibited the migration of cells from the spheres, while the acid-extracted fucoidan displayed the weakest inhibition. In general, the acid extracts were significantly the least potent inhibitors, as the cells migrated from spheres considerably more than those treated with water and EDTA extracts (Fig. 5.3; $p < 0.05$).

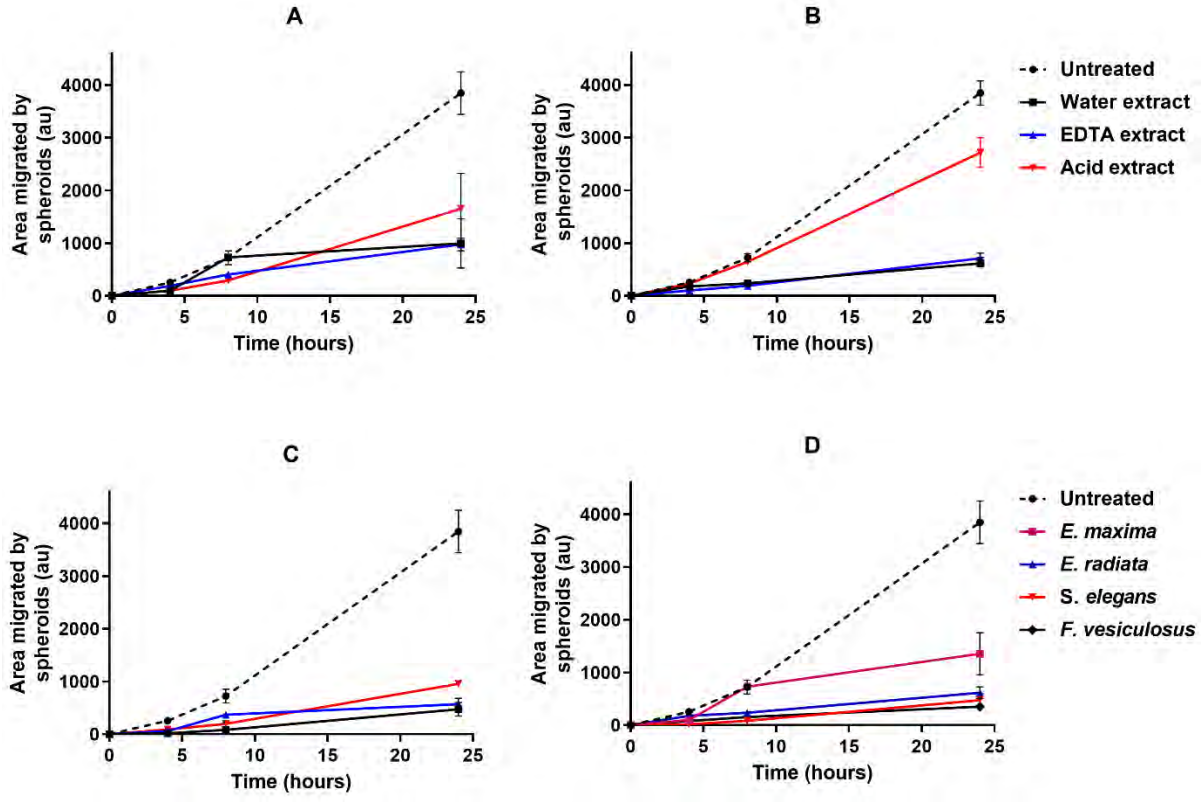

Figure 5.3:Quantification of HCT116 cell migration from spheres.
Inhibition of the migration properties of fucoidan extracts. The representative graphs show quantification of HCT116 migration in the presence of **A**: *E. maxima* fucoidan extracts, **B**: *E. radiata* fucoidan extracts, **C**: *S. elegans* fucoidan extracts and **D**: different water-extracted fucoidans and commercial *F. vesiculosus* fucoidan at time 0, 4, 8 and 24 hours. The figure key (legend) for A, B and C is in figure B, and figure 2D has its own figure key (legend). The data is represented as means ± SD of biological replicates of spheroids (n = 3).

The *E. radiata and S. elegans* water extracts and commercial *F. vesiculosus* displayed comparable spheroid migration inhibition potential (with the 0.1 mg/ml extracts showing more than 80%) (Fig. 5.4). Although the *E. maxima* water extract showed a slightly lower inhibition potential than the *E. radiata* and *S. elegans* extracts, it still significantly inhibited migration from HCT116 spheres. This trend is similar to what was observed in the time-dependent spheroid migration experiments at a constant compound or inhibitor concentration (Fig. 5.3).

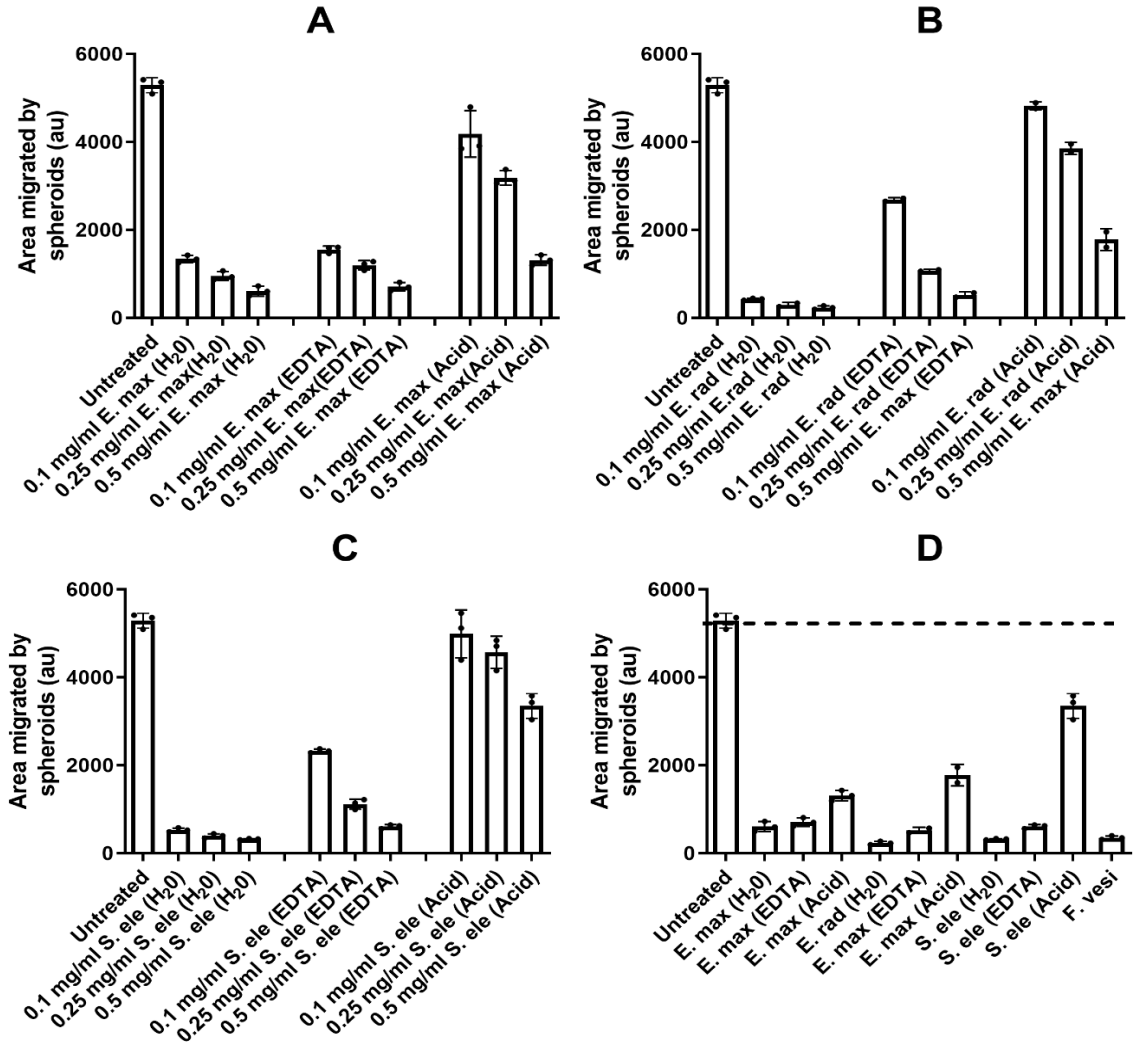

Figure 5.4: Quantification of the dose-dependent effect of fucoidan on HCT116 migration from spheres.

The migration inhibitory properties of fucoidan extracts: **A**: *E. maxima* extracts, **B**: *E. radiata* extracts, **C**: *S. elegans* extracts and **D**: single point concentrations (0.5 mg/ml) of all fucoidan extracts and the commercial *F. vesiculosus* fucoidan. The data are represented as means ± SD of biological replicates of spheroids (n = 3).

Once again, the water-extracted fucoidans generally displayed better bioactivity than the EDTA- and acid-extracted fucoidans (Fig. 5.4D; $p < 0.05$).

5.3.4 The effect of fucoidan treatments on HCT116 spheroid formation

The HCT116 cells were pre-treated with two final concentrations of compounds at 0.1 mg/ml and 0.5 mg/ml. The morphology of the spheres formed was different from the untreated samples. The spheroids pre-treated with EDTA extracts already started disintegrating before transfer into untreated medium (Fig. 5.5).

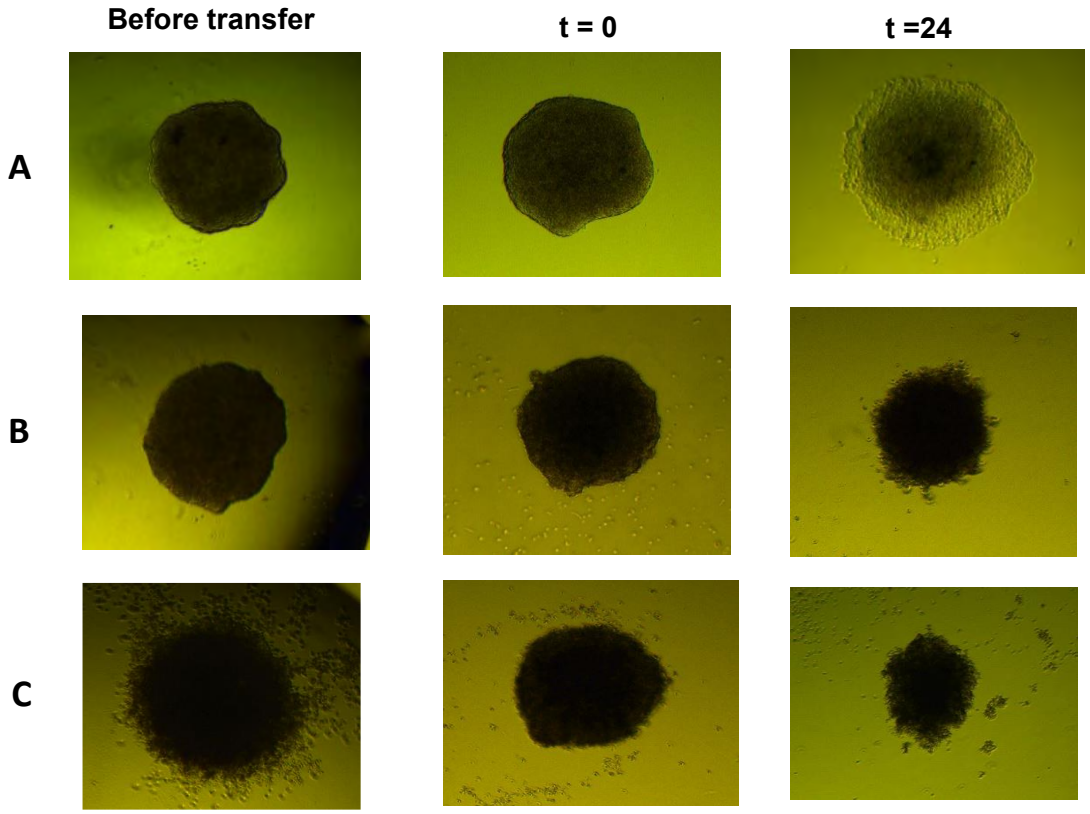

Figure 5.5: A visual illustration of the effect of pre-treatment of HCT116 cells on spheroid formation.
The images of spheroids before transfer to fresh medium, at t = 0, and after 24 hours (t = 24). **A:** representative sphere formed from untreated HCT116 culture, **B:** sphere formed from HCT116 cells pre-treated with *F. vesiculosus* fucoidan and **C:** sphere formed from HCT116 pre-treated with EDTA solution. All treatments were at 0.5 mg/ml (w/v) final concentration.

The sizes of the spheres formed after pre-treatment with the water-extracted fucoidans were quantified (Fig. 5.6A). All the fucoidan extracts hindered the size of spheroid formation significantly compared to the untreated sample (Fig. 5.6A; $p< 0.05$). The *S. elegans* fucoidan treated HCT116 culture yielded the smallest spheroids. However,

there was no significant difference in the size of spheroids formed between the *E. maxima* and *E. radiata* pre-treatment experiments (Fig. 5.6A; $p < 0.05$)

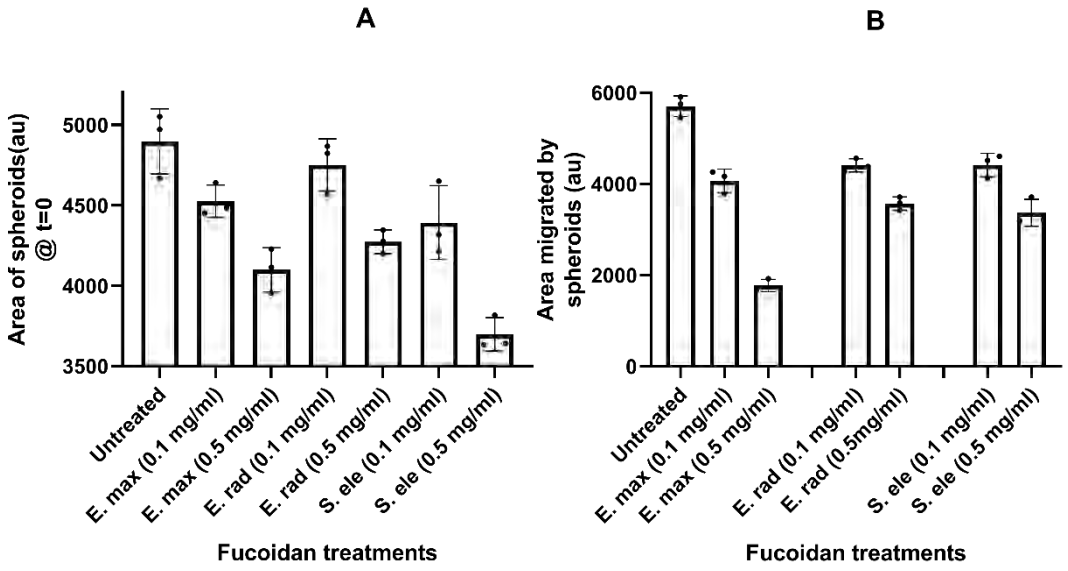

Figure 5.6:The effect of fucoidan pre-treatment on spheroid morphology and 3D migration.
A; Size of spheroids at t = 0 and **B;** migration profile of pre-treated spheroids in normal medium. The data are represented as means ± SD of biological experimental replicates (n = 3).

The pre-treated spheroids were transferred to the untreated medium to investigate the migration of cells to tissue culture plastic (Fig. 5.6B). The fucoidan pre-treated spheroids did not recover fully in normal culture conditions as all treatments migrated less than the untreated spheroids. There was a statistically significant difference between the migration profile of the untreated experiment and all treatments (Fig. 5.6B; $p<0.05$). Therefore, pre-treatment of the HCT116 cell culture indicated that water-extracted fucoidan hindered the spheroid formation process and subsequent migration of cells from spheres back to the tissue culture plastic.

5.3.5 Fucoidans disrupt HCT116 cell adhesion

The effect of fucoidans on the adhesion of HCT116 colorectal cancer cells was investigated using the standard tissue culture plates as the extracellular matrix (ECM). The cells were allowed to sit for 8 hours, and those that did not attach to the ECM

were washed off. The fucoidan extracts inhibited the adhesion of HCT116 cells, as shown visually in Figure 5.7.

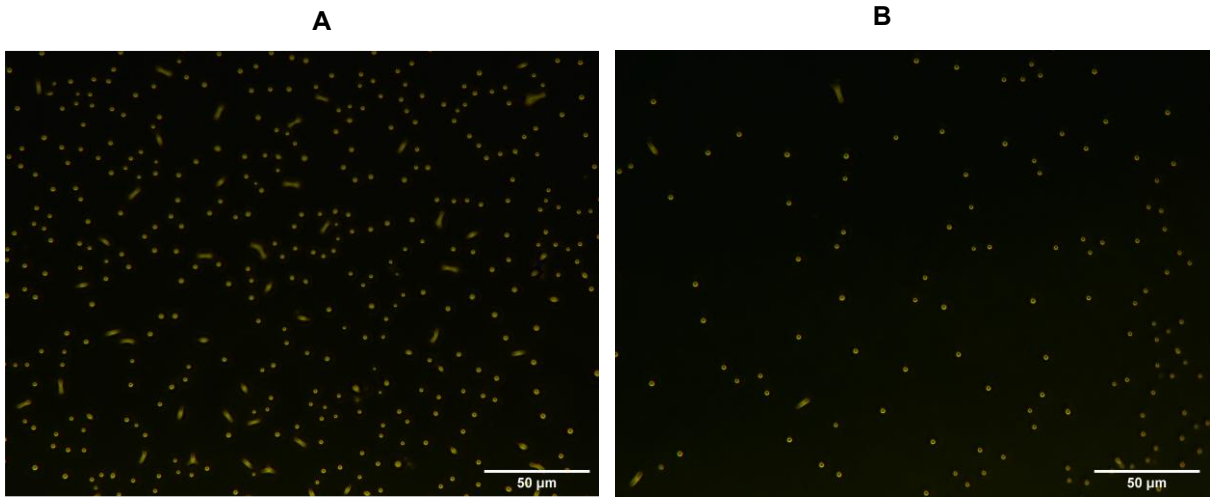

Figure 5.7: Representative visual illustration under light microscopy of HCT116 adhered cells after crystal violet staining.
A: untreated cells, **B:** cells treated with fucoidan.

The adhered cells were stained by crystal violet, and attached cells took up the dye. After washing off the residual dye, the cells were lysed using 1 % (w/v) SDS. The amount of crystal violet quantified was inferred from the amount of adhered HCT116 cells. Generally, all the fucoidan extracts significantly inhibited the adhesion of HCT116 cells to the plate surface (Fig. 5.8; $p < 0.05$) - compared to the untreated samples. Also, the adhesion inhibition showed a dose-dependence within all the extracts. While the extracts had a consistent effect on HCT116 adhesion, there were no significant differences in inhibition between the extracts themselves. EDTA was also included as a positive control, as it is a well-known chelator of divalent cations which are required for cell-matrix interactions. The EDTA control also showed a dose-dependent inhibition profile (Fig. 5.8D). We tested for the possible presence of EDTA in the EDTA extracted fucoidan. However, no detectable EDTA was found in the extracts (Table 3.2).

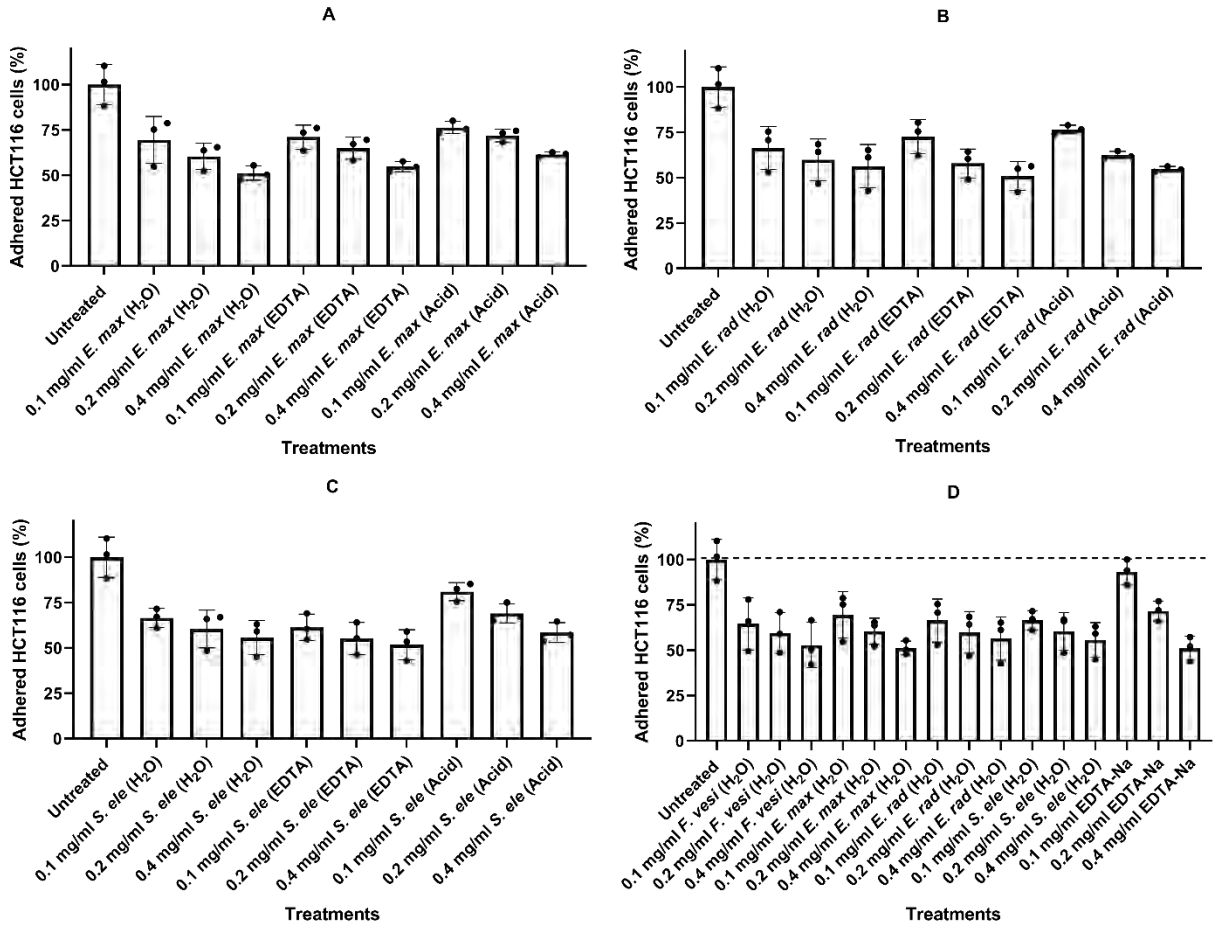

Figure 5.8:Crystal violet based HCT116 cell adhesion assays.
A: HCT116 cells treated with *E. maxima* fucoidan extracts, **B***: E. radiata* fucoidan extracts*,* **C***: S. elegans* fucoidan extracts *and* **D***:* all the screened fucoidan water-extracts and controls (EDTA –Na and commercial *F. vesiculosus*). The data are represented as means ± SD of three biological replicates (n = 3).

5.3.6 The effect of fucoidans on HCT116 colony formation

Clonogenic or colony formation assays are based on cell survival assay and the ability of a single cell to grow into a colony over time. This assay generally tests each cell's ability to undergo unlimited division. We used the clonogenic assay to determine the long-term survival of HCT116 cells after treatment with the fucoidan extracts. Figure 5.9 shows the visual illustration of the effect of the compounds on HCT116 cell colony formation. Some of the fucoidan extracts notably reduced HCT116 colony formation. Notably, our EDTA extracted fucoidans inhibited HCT116 colony formation better than the water and acid extracted fucoidans. Moreover, the commercial *F. vesiculosus* fucoidan showed the highest degree of inhibition of the HCT116 colony formation (Fig.5.9).

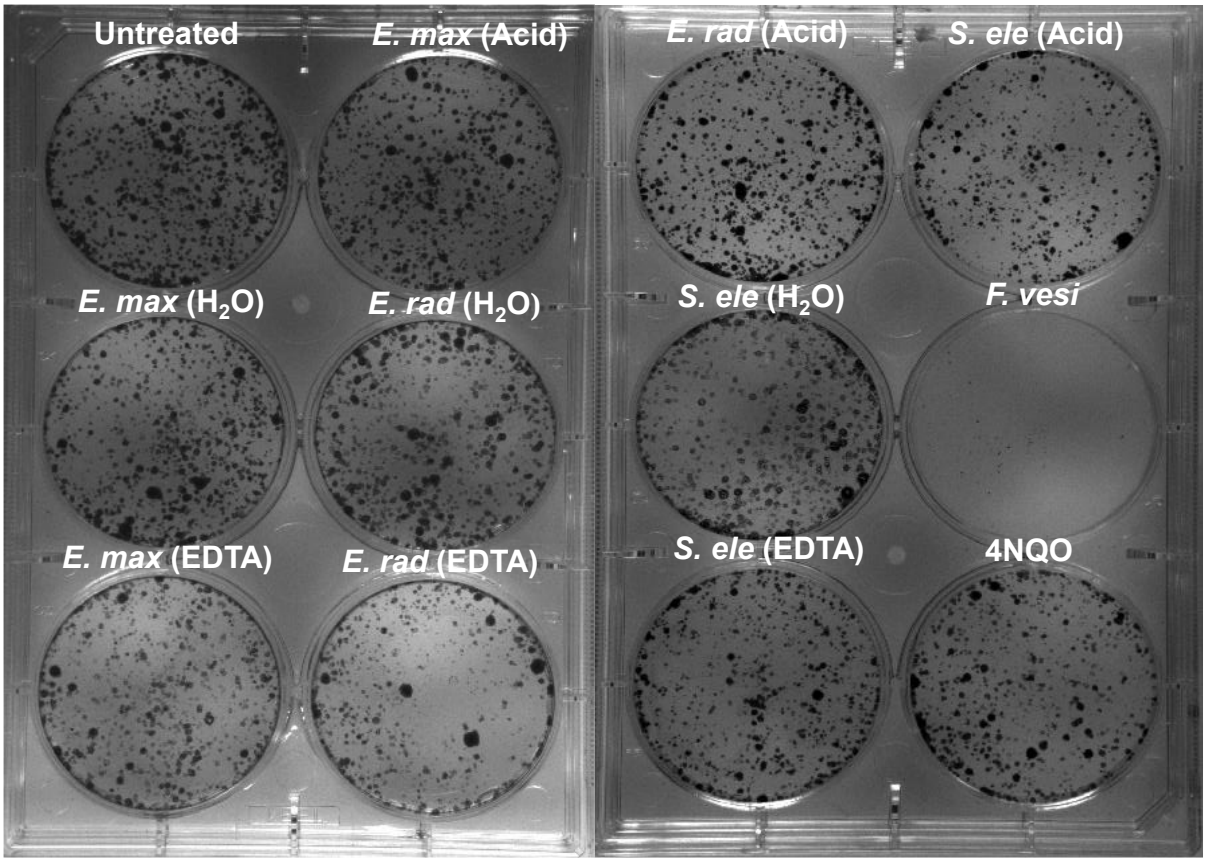

Figure 5.9: Visual representation of the effect of fucoidan extracts on HCT116 colony formation.

The fucoidan treatments were at 1 mg/ml concentration, while the 4NQO treatment was at 10 nM within the culture. Colony formation images were captured under an inverted light microscope.

HCT116 colony formation was quantified colourimetrically by the amount of crystal violet absorbed by cells. The EDTA extracted fucoidans, water extracted *S. elegans* fucoidan, and the *F. vesiculosus* fucoidan, significantly inhibited HCT116 colony formation ($p < 0.05$) (Fig. 5.10A). This observation reinforced the visual illustration of the experimental results (Fig. 5.9). Also, the dose-dependent effect of fucoidans was investigated, and the results are presented in Figure 5.10B-D. The more potent HCT116 cells colony formation inhibitors showed a dose-dependent response as the treatment concentrations increased (Fig. 5.10). Like the single concentration treatments (Fig. 5.9 & 5.10A), the dose-dependent experiments also showed the most potent HCT116 colony formation inhibitors to be the EDTA fucoidan extracts, *S. elegans* water and acid fucoidan extracts (Fig. 5.10B-D).

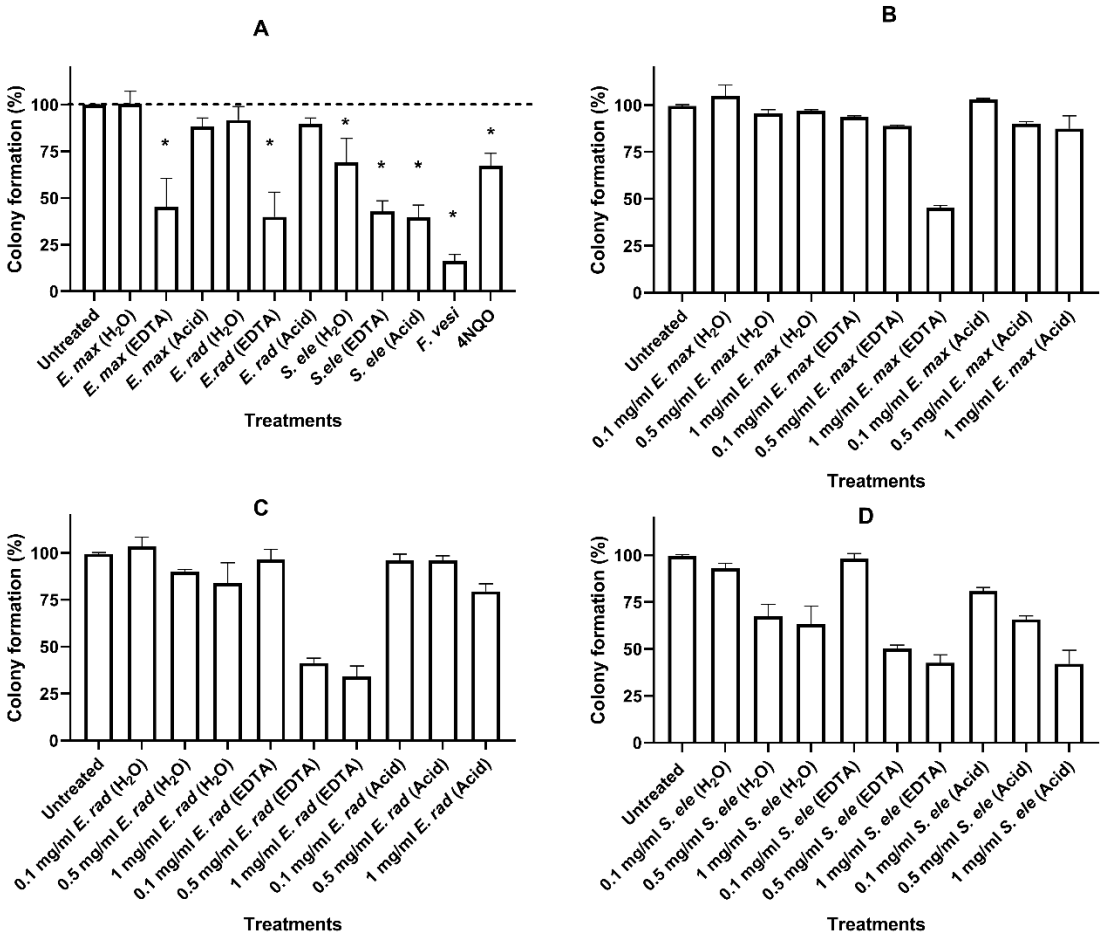

Figure 5.10: The dose-dependent clonogenic effect of fucoidan on HCT116 cancer cells. **A:** The effect of compounds at a fixed concentration (1 mg/ml for fucoidans and 10 nM for 4NQO). **B:** dose-dependent effect of *E. maxima* fucoidan extracts. **C:** concentration-dependent clonogenic effect of *E. radiata* fucoidan extracts on HCT116 cells and **D:** - dose effects of *S. elegans* extracts on the colony formation of HCT116 cells. The HCT116 colony cells were calculated and expressed as the means ± standard deviation percentages (n =3). The * shows a significant treatment difference versus the untreated control ($p < 0.05$).

5.3.7 Fluorescence-based glucose uptake by HCT116 cells

The ability of fucoidan extracts to influence glucose uptake by HCT116 cells was investigated using the fluorescently labelled glucose analogue 2-NBDG, where fluorescence quantified is proportional to glucose uptake by the cells. The fucoidan extracts either caused a slight decrease or increase in 2-NBDG uptake compared to the labelled untreated cells (cells + 2-NBDG) (Fig. 5.11).

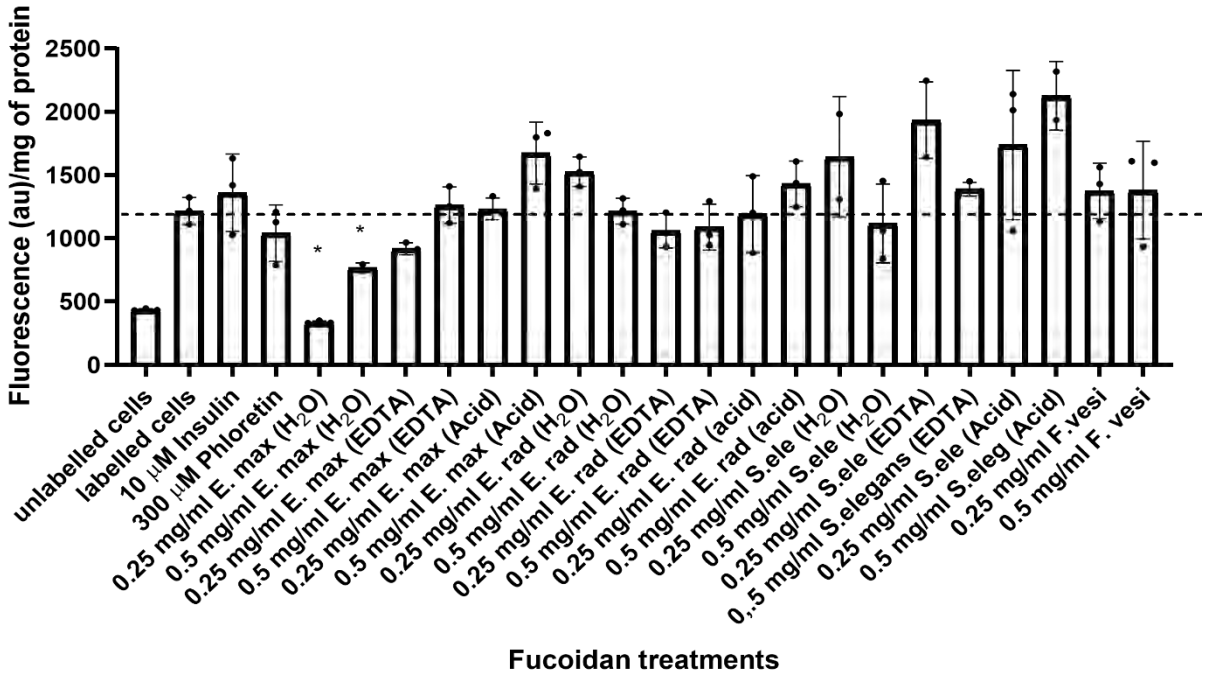

Figure 5.11: Effect of fucoidan extracts on the fluorescent-based glucose uptake by HCT 116 colon cancer cells.

Glucose uptake is represented as fluorescence intensity per mg protein of seeded HCT116 cells. The glucose uptake was investigated in the presence of fucoidan. Insulin and phloretin were employed as controls. The data are represented as mean values ± SD (n=3), and results were subjected to one-way ANOVA, $p < 0.05$. The * shows a significant treatment difference versus the untreated control ($p < 0.05$).

Most fucoidan extracts did not significantly stimulate or inhibit the 2-NBDG uptake by HCT116 cells. However, the *E. maxima* water and EDTA extract decreased glucose uptake, and *S. elegans* EDTA extract increased glucose uptake ($p< 0.05$). Furthermore, insulin was used as a glucose uptake activator control as it is known to stimulate glucose uptake. Phloretin was also used as another control as it is documented to inhibit some glucose transporters and hence glucose uptake. The fluorescent-based quantification of 2-NBDG uptake revealed HCT116 cell lines glucose uptake was not significantly stimulated by insulin ($p <0.05$). Nevertheless, phloretin decreased HCT116 cells 2-NBDG uptake, although the effect was not statistically significant (Fig. 5.11).

5.3.8 The effect of fucoidan on glycolytic flux

The effect of fucoidan treatment on the glycolysis flux of HCT116 cells was investigated by measuring glucose import and lactate accumulation periodically for 72 hours. The rates of glucose disappearance and lactate accumulation are represented in Figure 5.10A. The amounts of glucose taken up and lactate produced are illustrated in Figure 5.10B. Lastly, the residual glucose and lactate accumulated in the medium are illustrated in Figure 5.10C. The *E. maxima* water-extracted fucoidan was the most active with a significant decrease in glucose uptake by the HCT116 cells (Fig. 5.12B). Lactate accumulation seemed constant across all treatments, although it was reduced in the phloretin treatment (Fig. 5.12B).

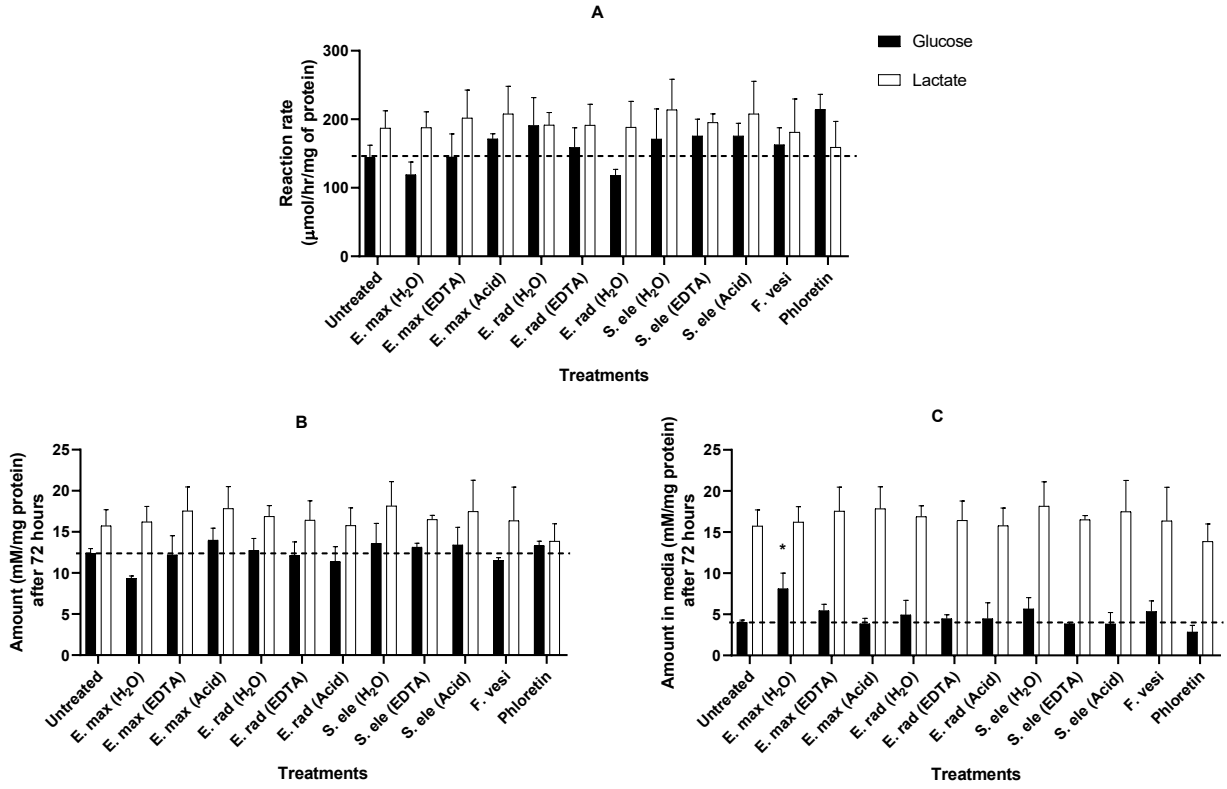

Figure 5.12:The glycolytic flux of HCT116 cells in the presence of various compounds. A: Rate of glucose disappearance and lactate export by HCT116 cells over 72 hours. **B:** Calculated amount of glucose uptake and lactate export over 72 hours. **C:** Amount of residual glucose in the medium and lactate exported by HCT116 cells over 72 hours. All the amounts of product/substrate were normalised per mg of protein from lysed harvested HCT 116 cells after 72 hours. The values and error bars represent the means ± SD of independent biological replicates (n=3). The * shows a significant treatment difference versus the untreated control ($p < 0.05$).

The ability of the fucoidan extracts to inhibit the glycolytic flux enzymes was also investigated. The fucoidan extracts did not affect the glucose enzyme cocktail hexokinase and glucose-6-phosphate dehydrogenase) (Fig. 5.13A). This finding suggests that the observation that *E. maxima* fucoidan inhibited glucose uptake (Fig. 5.12) was not due to inhibition of the enzymes used in the coupled assay.

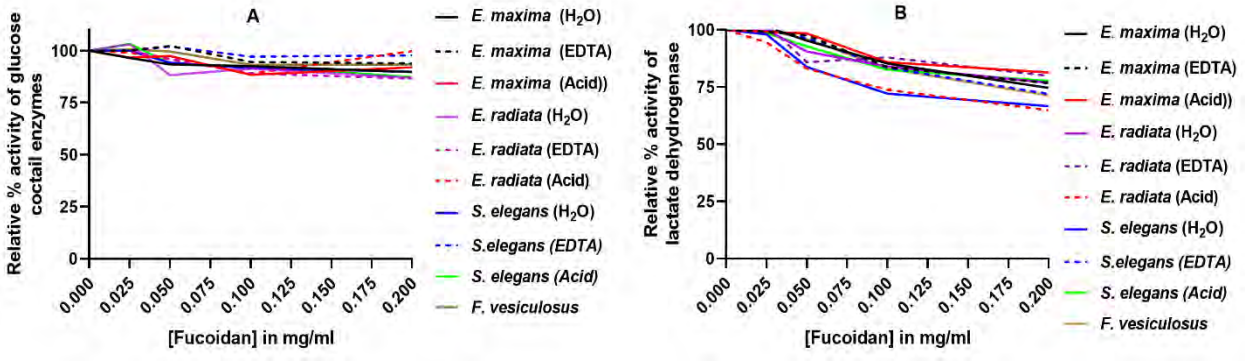

Figure 5.13:The activity of glycolytic enzymes in the presence of fucoidan.
A: Activity assay for the hexokinase and G6PDH (glucose-6-phosphate dehydrogenase) cocktail. **B:** Activity assay for LDHa.

However, the fucoidans slightly (but significantly) inhibited LDHA in a dose-dependent manner (Fig. 5.13B). This may be significant as LDHA converts pyruvate into lactate, a substrate for normoxic tumour cells. The switching between the hypoxic (glycolytic) phenotype and the normoxic phenotypes is a hallmark of tumour resistance to chemotherapeutics (Abdel-Wahab et al., 2019). Therefore, the inhibition of LDHA by fucoidans may be beneficial in regulating the glycolytic flux.

5.4 Discussion

The extracted fucoidans were investigated for their potential cytotoxicity to human colon cancer cells (HCT116 cell line). Our extracts did not show any significant cytotoxicity to the cancerous cells. The lack of cytotoxicity of our fucoidan extracts could be attributed to the large molecular sizes, which makes penetration into the cell difficult. Large molecular sizes of fucoidan have been reported to limit the bioaccessibility of these compounds, posing a challenge for their applications (Wang et al., 2019). In the study by Wang and colleagues (2019), the native *Undaria pinnatifida* fucoidan (5 100 kDa) had minimal anti-tumour activity compared to its

depolymerised counterpart (490 kDa). This observation indicates the need for depolymerising fucoidans to increase toxicity, while at the same time, maintaining their bioactivities.

Although extracted fucoidans were not significantly cytotoxic to the HCT116 cancerous cells, their potencies in inhibiting tumour migration were investigated. Our fucoidan extracts showed significant migration inhibition of the HCT116 cancerous cells from 3D spheres. There are limited reports in the literature that have investigated the effects of fucoidans on spheroid-based migration. However, a study by Han and colleagues showed that tumour migration of a human colon cancer cell line (HT-29) was inhibited by fucoidan (Han et al., 2015a). Our study also agreed with their findings that fucoidan prevented or distorted cancer cell sphere formation (Fig. 5.5). Thus, it can be suggested that fucoidan can prevent or slow down cancer cell sphere formation and its migration, reducing cancer cell invasion and making it easier to manage cancers.

The effect of fucoidan extracts on the cell adhesion of HCT116 cells was also investigated. Cell adhesion of cancer cells is vital for various biological processes, including cellular organisation, communication, differentiation, migration, and subsequently metastasis (Lazarovici et al., 2020). Inhibiting the adhesion process of cancerous cells is, therefore, a plausible approach to reduce cancer progression. Our fucoidan extracts showed significant ability to prevent the adhesion of HCT116 cancerous cells (Fig. 5.8). The cancer cell adhesion process is dependent on several adhesion molecules and receptors, including integrins, selectins, glycoprotein, immunoglobulins, and proteoglycans (Lazarovici et al., 2020). Our fucoidan extracts may be hindering the proper functioning of these molecules, thus impacting the proliferation of cancerous cells. The effect on cell adhesion may also in part explain the effect of these compounds in inhibiting migration from spheres.

A few characterised fucoidans have been reported to prevent the adhesion of cancer cells onto the extracellular matrix (ECM). Thus, our findings also were in agreement with the work performed by Li and colleagues from 2005. Fucoidan from *A. nodosum* was found to inhibit the MDA-MB-231 cancerous cells adhering to fibronectin ECM (Liu et al., 2005). Also, literature has reported that several fucoidans have anti-proliferative effects on some cancer cell lines (Han et al., 2015a; Wang et al., 2019). Potential fucoidan anti-proliferative mechanisms are poorly understood. With our cell

adhesion inhibition results (Fig. 5.7 & 5.8), it is reasonable to suggest that one of the mechanisms of fucoidan inhibition of cancer cell proliferation is through the inhibition of cell adhesion.

Fucoidans are negatively charged polysaccharides due to their sulphated nature, which may interfere with integrins that require Mg^{2+} as a cofactor for adhesion (Lazarovici et al., 2020). Fucoidans interacting with Mg^{2+} may negatively affect HCT116 cell adhesion. Commercial *F. vesiculosus* displayed a similar profile (Fig. 5.8D) to our extracted fucoidans. Furthermore, clonogenic assays were used to determine the HCT116 long term cell survival after treatment with fucoidans. Some of our fucoidan extracts showed potency by inhibiting HCT116 cells colony formation (Fig. 5.9 & 5.10). The commercial *F. vesiculosus* fucoidan showed superior colony formation inhibition compared to all our extracts. This may be attributed to the superior sulphate content within the commercial fucoidan (Table 3.2). Limited studies have reported the ability of fucoidans to decrease tumour cell survival using this assay. Nevertheless, our findings agree with Shin and colleagues who reported that manganese dioxide nanoparticles coated with fucoidan suppressed a pancreatic cancer cell line (Shin et al., 2018). Another independent study also reported fucoidan potency in inhibiting HepG2 liver cancer cells (Arumugam et al., 2019). This assay has been the method of choice to determine reproductive cell death after ionising radiation, although it is used to determine the effectiveness of other cytotoxic agents (Franken et al., 2006).

In addition, the ability of our fucoidan extracts to inhibit glucose uptake was investigated using a fluorescent-tagged glucose analogue (2-NBDG). Tumour cells have elevated glucose uptake rates compared to normal cells, to compensate for the high energy demands associated with their fast growth and proliferation. This labelled glucose analogue approach has been utilised to diagnose cancerous tissues (Raez et al., 2013). However, most of the extracted fucoidans did not inhibit or stimulate glucose uptake (Fig. 5.11). The glucose uptake within the HCT116 human colorectal carcinoma cell line was not significantly stimulated by insulin. The insensitivity of the HCT116 cancerous cells to insulin was expected as most cancer cell lines overexpress GLUT1, 3 and 5, which are not insulin-mediated like GLUT4 (Tanner et al., 2018).

Phloretin, a common GLUT inhibitor, was used as a positive control. Although phloretin seemed to reduce the glucose uptake by the HCT116 cells (Fig. 5.11), the effect was not statistically significant (One-way ANOVA, $p< 0.05$). However, phloretin could inhibit glucose transporters and aquaporin almost completely to achieve almost zero glucose 2NBDG uptake in MIN 6 cells which are models of pancreatic β-cells (Sasaki et al., 2016). The observed differences in these two cases may be explained by the GLUTs expressed. The MIN 6 cells are associated with GLUT4 as a glucose transporter, but this may differ from the HCT116 cells used in the present study. In another study, phloretin reduced glucose uptake by inhibiting GLUT2 transporters in colorectal cancer cells (HT-29) (Lin et al., 2016). Thus, the efficacies of inhibitors also depend on the types of tissues and cell lines.

Fucoidan extracts were also screened for their potential to alter the glycolytic flux of HCT116 cells. The glycolytic flux (Fig. 1.8) is a complex pathway. However, the critical steps identified in regulating this pathway are glucose import facilitated by glucose transporters and lactate export by lactate transporters. Enzymes within the glycolytic pathway are critical in the glycolytic flux process (Tanner et al., 2018). Therefore, the rate of glucose import and lactate production was investigated. In addition, the potential of fucoidans to inhibit the glucose enzyme mixture (hexokinase and glucose 6 phosphate dehydrogenase) and lactate dehydrogenase (LDHa) were investigated. The fucoidans did not affect the activity of the glucose enzyme mixture but slightly (and significantly) inhibited the LDHA activity. The ability of fucoidans to inhibit LDHA may be useful in regulating the glycolytic flux, like oxamate, a well-characterised inhibitor of LDHA (Abdel-Wahab et al., 2019), which has been implicated in increasing the radiosensitivity of cancer cells (Zhai et al., 2013). The inhibitory effect of fucoidans on LDHA may be important in disrupting the tumour hybrid metabolic states that characterise invasive and drug-resistant cancers. However, the effect of the fucoidans on LDHA needs to be considered when interpreting the effects of these compounds on lactate production when using the coupled assay.

The *E. maxima* water extracted fucoidan significantly inhibited glucose import into the HCT116 cells (Fig. 5.12 $p< 0.05$). Again, phloretin did not appear to inhibit glucose uptake by these cells (Fig. 5.12). This observation was not unexpected, as our previous labelled glucose uptake experiments did not show a significant phloretin

induced decreased glucose uptake (Fig. 5.11). These observations suggest that the HCT116 cell line does not express phloretin susceptible GLUTs, including types 2 and 4. In addition, Tanner and colleagues have suggested that most cancer cells predominantly express GLUT1, GLUT3 and GLUT5 (Tanner et al., 2018).

In conclusion, some of our fucoidan extracts exhibited anti-cancer activities on the HCT116 colorectal cancer cells. Although the extracted fucoidans lacked cytotoxicity possible due to their large size, they still influenced long term survival and growth of HCT116 cells in hanging drop spheres, as well as blocking migration of cells from 3D spheroids. These biological characteristics are implicated in chemotherapeutic resistance by cancerous cells. Some of our screened fucoidan extracts partially prevented the adhesion of HCT116 cells to the surface matrix, an essential process in cancer cell invasion. In addition, selected extracts also reduced glucose uptake by HCT116 cells, which may influence the glycolytic flux, a plausible target for controlling cancer cell proliferation and metastasis.

CHAPTER 6: GENERAL DISCUSSION, FUTURE PERSPECTIVES AND CONCLUDING REMARKS

6.1 General discussion and future perspectives

This study sought to link the structure of fucoidans to their biological activities, which have been reported in recent years in the literature. This chapter attempts to relate the structural and chemical profiles of the extracted fucoidans to their biological activities (i.e. anti-diabetic and anti-cancer activities). This section also attempts to elucidate the link between diabetes and cancer, and how the two diseases can be targeted via a central process. In addition, the limitations of this study are also highlighted, along with future perspectives and concluding remarks.

Fucoidans were extracted using three technologies: hot water, EDTA assisted, and acid extraction. The water-extracted fucoidans are known for their high biological activities; however, they are produced with a relatively low yield. The acid extraction method, widely used in industry, provides a better yield, but the bioactivity of fucoidan is usually compromised. Therefore, a fairly new protocol, the EDTA extraction method, was investigated. Fucoidan yield was significantly affected by the extraction method, where the new (EDTA) extraction technology produced significantly more fucoidan than the acid- and water-extraction methods (Fig.3 2). Therefore, the EDTA extraction technology has potential to improve fucoidan yields and may be considered by industry to produce fucoidans on a larger scale in the future. This method also uses fewer organic solvents, as EDTA helps with the depigmentation process. Moreover, this method would save time, as the regular depigmentation step may be omitted. This method could cut costs when scaling up the extraction of fucoidan. Although the EDTA extraction method produced higher yields, the biological activity of the fucoidans was somewhat reduced and the presence of possible EDTA impurities may be a significant drawback from a drug development perspective. Nevertheless, it is worth noting that seaweeds of different genera and species also exhibited different yields of fucoidan. This phenomenon was expected as literature has reported similar observations (Fletcher et al., 2017; Rani et al., 2017).

The biological activity of fucoidan has been linked to three main attributes: molecular size, sulphate content and monosaccharide composition (Kim et al., 2014). The

species of seaweed and different extraction technologies affect the structure and bioactivities of the resulting fucoidan. Despite the accelerated interest in brown seaweed as the primary source of fucoidans, there have been some knowledge gaps in linking the yield, composition, and structure of fucoidans to their biological function (Fitton et al., 2015; Skriptsova et al., 2010). Our study found that most extracted fucoidans have a high carbohydrate content, which is assumed to be the fucose content in most literature. However, the amount of carbohydrates did not seem to be linked to bioactivity. For example, our *S. elegans* extracts and commercial *F. vesiculosus* fucoidan had the lowest carbohydrate contents. However, these extracts showed relatively high bioactivity in inhibiting the carbohydrate digesting enzyme α-glucosidase (Fig. 4.4) and in their anti-cancer properties (Fig. 5.3D). Our EDTA extracted fucoidans had relatively low carbohydrate contents but still displayed excellent bioactivities. Thus, carbohydrate content may be a necessary but not essential determinant factor of fucoidan bioactivity. This deduction is further supported by the significant bioactivities of the commercial *F. vesiculosus* and *S. elegans* fucoidans, which had relatively low carbohydrate contents.

Molecular weight is another determinant feature linked with the biological activity of the fucoidan. Low molecular weight fucoidans have mostly been associated with high biological activity due to their improved bio-accessibility (Wang et al., 2019). Our fucoidans had relatively high molecular weights and did not display any cytotoxicity against HCT116 human colorectal cancer cells (Fig. 5.1). This observation could be caused by the fucoidan extracts failing to penetrate the cells. Although, the size of fucoidans could be a limitation, these compounds may still be applied in the prevention and slowing down of cancer progression. However, our extracts inhibited the carbohydrate digesting enzyme α-glucosidase activity *in vitro*, regardless of the relatively high molecular weight. It can be deduced that molecular weight indeed affects the bio-accessibility of fucoidan for cellular processes. Nevertheless, high molecular weight fucoidans are still relevant with exceptional bioactivities. In fact, the bioactivity may be limited by high molecular weight; however, this may be an opportunity to pursue research that will provide drug delivery technologies to improve the bio-accessibility of fucoidans.

Another well-documented link between the structures of fucoidans and their bioactivities is the degree of sulphation (Fletcher et al., 2017). In the present study, our extracts, especially the *Ecklonia* spp. fucoidans, had relatively lower sulphate content compared to the extracted *S. elegans* and commercial *F. vesiculosus* fucoidan. However, the *E. radiata* fucoidan showed good levels of bioactivity (Fig. 4.4; Fig. 5.6) compared to the highly sulphated fucoidan. The presence of sulphates was confirmed as a vital feature for the biological activity of fucoidans, as the acid extracted fucoidans had little to no activity in most experiments. This observation was linked to the low sulphation associated with our acid extracted fucoidans.

Besides the biological activities of fucoidan in this study, the research scope also included anti-diabetic and anti-cancer studies. The rationale for this was motivated by the epidemiological evidence that individuals with diabetes are at risk of developing several types of cancers (Tudzarova & Osman, 2015). In addition, events that lead to T2DM include pancreatic β-cell impairment, insulin resistance and altered hepatic glucose production (Giovannucci et al., 2010; Noto, 2017). The resulting hyperglycaemia, which is a direct cause of T2DM, may lead to metabolic reprogramming and increased glycolysis which is characteristic of cancer development (Tudzarova & Osman, 2015). Also, hyperglycaemia and hyperinsulinemia have been reported to stimulate growth factors (insulin growth factor & epidermal growth factor), which activate the mTOR and Wnt/β-catenin pathway and inhibit apoptosis, encouraging tumour proliferation (Noto, 2017). Therefore, our study attempted to use fucoidan to regulate glucose availability, a dual control point in controlling diabetes and cancer.

Glucose metabolism pathophysiology has been suggested to be a central process in the manifestation of hyperglycemia which increases the risk of T2DM and several cancers (Mabate et al., 2021). The current study showed that fucoidans extracted from selected South African brown seaweeds are potent inhibitors of the carbohydrate digesting enzyme, α-glucosidase (Fig. 4.4), contributing significantly to blood glucose availability. Additionally, the fucoidan extracts displayed some synergism with the commercial acarbose in the inhibition of α-glucosidase (Table 4.3). This characteristic was deemed particularly important in achieving a high total efficacy with therapeutic remedies. Our fucoidans may possibly limit the side effects, including abdominal

discomfort and flatulence associated with acarbose use. Essentially, this synergy work provides insight into a drug combination approach (using fucoidans and chemotherapeutics) to prevent hyperglycemia by inhibiting the carbohydrate digesting enzymes. Inhibiting these enzymes lowers the appearance of glucose in the bloodstream, thus controlling the degree of monosaccharides such as glucose within the circulatory system. Also, there could be a hybrid approach between traditional and modern medicine in rural areas or traditional societies. Usually, patients and caregivers have no idea which different combined remedies would be detrimental or beneficial. These types of synergism studies and platforms could provide a basis for rapidly checking for potential synergy or antagonism. These types of platforms could also limit the possible negative impacts of mixing medicines.

Hyperglycemia favours the progression of cancerous cells, mostly the glycolytic phenotype that conform to the Warburg effect. Therefore, manipulating the glucose uptake of cancer cells is another therapeutic target. This study investigated how our fucoidan extracts influence the insulin/non-insulin-dependent glucose uptake by HCT116 colorectal cancerous cells using a fluorescent labelled glucose analogue. Most of our extracts did not seem to significantly impact the HCT116 cells' fluorescent-based glucose uptake, including phloretin, which is a known inhibitor of glucose transporters (Fig. 5.11). However, the water extracted *E. maxima* fucoidan significantly inhibited glucose uptake by HCT116 cells (Fig. 5.11; $p < 0.05$).

Insulin did not enhance glucose uptake, suggesting that the primary glucose transport receptors on the HCT116 cell line are insulin insensitive. This deduction is supported by Tanner and colleagues (2018), who showed that GLUT1, GLUT3 and GLUT5 were overexpressed in cancer cells and that these transporters are insensitive to insulin. The current study also showed that fucoidans inhibit lactate dehydrogenase activity (Fig. 5.13), an enzyme in the lower glycolytic flux pathway. An obvious challenge lies in delivering the fucoidan into the cell due to its large size. However, the area of drug delivery is another avenue worth exploring, where technologies such as nanoparticles and drug delivery lysosomes can be designed. Also, the idea of targeting the glycolytic flux can also be applied to normal cells, including muscle and liver cell lines which would further elucidate how glucose appearance and disappearance can be regulated using fucoidans.

Although our fucoidan extracts did not display any cytotoxicity, they exhibited anti-tumour properties by inhibiting the migration of cells from three-dimensional (3D) spheroids of HCT116 cells. To the best of our knowledge, no studies have investigated the effect of fucoidans on the spheroid migration of the HCT116 human colorectal cells. However, very few chemotherapeutics on spheroid migration have been investigated using various cancer cell lines. The spheroid culture systems provide similar physicochemical environments to *in vivo* models, making them ideal for studying tumour migration. The spheroid culture system facilitates cell-to-cell and cell-to-matrix interactions, which overcomes the limitations of traditional monolayer cell cultures, which are two dimensional (2D) and do not consider tumour heterogeneity (Ryu et al., 2019; Vinci et al., 2013). Our fucoidan extracts are relevant as potential anti-cancer remedies, as they significantly inhibited the 3D spheroid migration of the HCT116 cancerous cells. As limited literature is available on this topic, future studies investigating the mechanisms associated with MMP2, mTOR and other pathways involved with antimigration are necessary.

Several studies have reported that fucoidans have antiproliferative properties, but only a few reports in the literature suggest mechanisms for how this happens. However, guided by the findings of this current study, it is reasonable to suggest that inhibition of cell adhesion may be one of the mechanisms involved. Indeed, a cell migration defect would be consistent with reductions in migration and long-term survival. Future studies could investigate the inhibition potential of fucoidans on extracellular matrices like fibronectin and use immunofluorescence to elucidate adhesion inhibition mechanisms. Investigating the mechanisms of fucoidans on the functions of integrins, selectins, and other adhesion molecules are required, as limited information is available on this niche. In addition, it would be interesting to expand the number of cell lines in the study and include matched metastatic and non-metastatic models such as the SW480/SW620 colon carcinomas (Slater et al., 2018). Considering the properties illustrated by the fucoidans, using these compounds as cancer preventive measures is reasonable.

6.2 Conclusion

This study has shown that South Africa has a diversity of brown seaweeds, which are a rich source of bioproducts, including fucoidans, and these compounds are pharmacologically relevant. Bioactive fucoidans were successfully extracted from South African brown seaweeds. The current study has suggested an alternative fucoidan extraction method (EDTA) that is more environmentally friendly, time-efficient, and possibly more economical. Extracted fucoidans were chemically and structurally characterised, and these were similar to those in the literature, although they exhibited unique characteristics. These fucoidans were biologically active as they showed anti-diabetic and anti-cancer activities. Some fucoidan extracts displayed impressive inhibitory effects on one of the amylolytic enzymes α-glucosidase. This inhibition is vital in controlling the appearance of glucose within the bloodstream, which is a major determinant of hyperglycaemia. Fucoidans in this study were established to be mainly mixed inhibitors of α-glucosidase.

Fucoidans were established to interact synergistically with acarbose (a commercial anti-diabetic drug). This synergistic interaction was implicated in lowering the amount of acarbose required, as it is associated with side effects that may limit the dosage used. However, with fucoidan, a higher total efficacy is possible.

The fucoidans showed remarkable anti-cancer activities by inhibiting HCT116 colorectal cancer cell adhesion, migration, long term survival (colony formation) and glucose uptake, which are essential processes in cancer cell proliferation and invasion.

Finally, the findings of this study confirmed the relevance of fucoidans and their effects on glucose metabolism to assist in the efforts to control diabetes and cancer.

References

Abdel-Wahab, A.F., Mahmoud, W. & Al-Harizyd, R.M., 2019. Targeting glucose metabolism to suppress cancer progression: prospective of anti-glycolytic cancer therapy. *Pharmacol. Res*, 150, pp.104511, https://doi.org/10.1016/j.phrs.2019.104511.

Ahmad, T.B.S., 2015. *Methods for quantification and extraction of fucoidan, and quantification of the release of total carbohydrate and fucoidan from the brown algae Laminaria hyperborea*. Norwegian University of Science and technology.

Akins, N.S., Nielson, T.C. & Le, H.V., 2018. Inhibition of glycolysis and glutaminolysis emerging drug discovery approach to combat cancer. *Cancer, Curr. Top. Med. Chem*, 6, pp.494–504, https://doi.org/10.2174/1568026618666180523111351.

Ale, M.T. & Meyer, A.S., 2013. Fucoidans from brown seaweeds: an update on structures, extraction techniques and use of enzymes as tools for structural elucidation. *RSC Adv*, 3, pp.8131-8141, https://doi.org/10.1039/C3RA23373A.

Ale, M.T., Mikkelsen, J.D. & Meyer, A.S., 2011. Important Determinants for Fucoidan Bioactivity: A Critical Review of Structure-Function Relations and Extraction Methods for Fucose-Containing Sulfated Polysaccharides from Brown Seaweeds. *Mar. Drugs*, 9, pp.2106–30, https://doi.org/10.3390/md9102106.

Alwarsamy, M., Gooneratne, R. & Ravichandran, R., 2016. Effect of fucoidan from *Turbinaria conoides* on human lung adenocarcinoma epithelial (A549) cells. *Carbohydr Polym*, 152, pp.207–213, https://doi.org/10.1016/j.carbpol.2016.06.112.

Anastyuk, S.D. et al., 2017. Structural features and anticancer activity *in vitro* of fucoidan derivatives from brown alga *Saccharina cichorioides*. *Carbohydr Polym*, 157, pp.1503–1510, https://doi.org/10.1016/j.carbpol.2016.11.031.

Annunziata, A.. & Vecchio, R., 2011. Functional foods development in the European market. A consumer perspective. *J. Funct. Foods*, 3, pp.223-228, https://doi.org/10.1016/j.jff.2011.03.011.

Antoni, D., Josset, H.B.E. & Noel, G., 2015. Three-dimensional cell culture: A breakthrough *in vivo*. *Int J Mol Sci*, 16, pp.5517–5527, https://doi.org/10.3390/ijms16035517.

Aronoff, M.D. et al., 2004. Glucose metabolism and regulation: beyond insulin and glucagon. *Diabetes Spectr*, 17, pp.183-190, https://doi.org/10.2337/diaspect.17.3.183.

Aronson, P.S., Boron, W.F. & Boulpaep, E.L., 2003. Physiology of membranes. In B.W. F, ed. *Medical Physiology: a Cellular and Molecular Approach*. Philadelphia: Saunders. pp.66–67.

Arumugam, P. et al., 2019. Anticancer effect of fucoidan on cell proliferation, cell cycle progression, genetic damage and apoptotic cell death in HepG2 cancer cells. *Toxicol Rep*, 6, pp.556-563, https://doi.org/10.1016/j.toxrep.2019.06.005.

Atashrazm, F. et al., 2015. Fucoidan and Cancer: A Multifunctional Molecule with Anti-Tumor Potential. *Mar. Drugs*, 13, pp.234-240, https://doi.org/10.3390/md13042327.

Attjioui, M. et al., 2021. Comparison of edible brown algae extracts for the inhibition of intestinal carbohydrate digestive enzymes involved in glucose release from the diet. *J Nutr Sci*, 10, pp.e5, https://doi.org/10.1017/jns.2020.56.

Badrinathan, S. et al., 2012. Purification and Structural Characterization of Sulfated Polysaccharide from *Sargassum myriocystum* and its Efficacy in Scavenging Free Radicals. *Indian J Pharm Sci.*, 74(6), pp.549–55, https://doi.org/10.4103/0250-474x.110600.

Baron, A.D., Brechtel, G., Wallace, P. & Edelman, S.V., 1988. Rates and Tissue Sites of Non-Insulin- and Insulin-Mediated Glucose Uptake in Humans. *Am. J. Physiol. Metab.*, 255, pp.E769–E774, https://doi.org/10.1152/ajpendo.1988.255.6.e769.

Barrett, S., Mohr, P.G., Schmidt, P.M. & McKimm-Breschkin, J.L., 2011. Real Time Enzyme Inhibition Assays Provide Insights into Differences in Binding of Neuraminidase Inhibitors to Wild Type and Mutant Influenza Viruses. *PLoS ONE*, 6(8), pp.e23627, https://doi.org/10.1371/journal.pone.0023627.

Baumhardt, J.M., Dorsey, B.M., McLauchlan, C.C. & Jones, M.A., 2015. An Additional Method for Analyzing the Reversible Inhibition of an Enzyme Using Acid Phosphatase as a Model. *Curr Enzym Inhib*, 11(2), pp.140-46, https://doi.org/10.2174/1573408011666150605223952

Black, W., 1954. The seasonal variation in the combined L-fucose content of the common British Laminariaceae and Fucaceae. *J. Sci. Food Agric*, 5, pp.445-448, https://doi.org/10.1002/jsfa.2740050909.

Bolton, J.J. & Stegenga, H., 2002. Seaweed species and diversity in South Africa. *Afr. J. Mar. Sci*, 24, pp.9 -18, https://doi.org/10.2989/025776102784528402

Bomanji, J.B., Costa, D.C. & Ell, P.J., 2001. Clinical Role of Positron Emission Tomography in Oncology. *Lancet Oncol*, 2(3), pp.157–164, https://doi.org/10.1016/s1470-2045(00)00257-6.

Boo, H.J. et al., 2013. The anticancer effect of fucoidan in PC-3 prostate cancer cells. *Mar. Drugs*, 11, pp.2982–2999, https://doi.org/10.3390/md11082982.

Boo, H.-J. et al., 2011. Fucoidan from *Undaria pinnatifida* Induces apoptosis in A549 human lung carcinoma cells. *Phytother Res*, 25, pp.1082–1086, https://doi.org/10.1002/ptr.3489.

Bradford, M.M., 1976. A rapid and sensitive for the quantitation of microgram quantities of protein utilizing the principle of protein–dye binding. *Anal. Biochem*, 72, pp.248-252, https://doi.org/10.1006/abio.1976.9999.

Buck, M.D., Sowell, R.T., Kaech, S.M. & Pearce, E.L., 2017. Metabolic instruction of immunity. *Cell*, 169, pp.570–586, https://dx.doi.org/10.1016%2Fj.cell.2017.04.004.

Burz, C., Berindan-Neagoe, I., Balacescu, O. & Irimie, A., 2009. Apoptosis in cancer: Key molecular signaling pathways and therapy targets. *Acta Oncol*, 48, pp.811–821, https://doi.org/10.1080/02841860902974175.

Carpio, R.B. et al., 2019. Characterization and thermal decomposition of demineralized wastewater algae biomass. *Algal Res*, 38, pp.1-12, https://doi.org/10.1016/j.algal.2018.101399.

Castro, L.S.E.P.W. et al., 2015. Potential anti-angiogenic, antiproliferative, antioxidant, and anticoagulant activity of anionic polysaccharides, fucans, extracted from brown algae *Lobophora variegata*. *J. Appl. Phycol*, 27(3), pp.1315–1325, http://dx.doi.org/10.1007%2Fs10811-014-0424-1.

Catarino, M.D., M., A., Silva, S. & Cardoso, S.M., 2018. Phytochemical Constituents and Biological Activities of *Fucus* spp. *Mar. Drugs*, 16, pp.249, https://doi.org/10.3390/md16080249.

Chapman, V.J. & Chapman, D.J., 1980. *Seaweeds and Their Uses*. London: Chapman and Hall.

Chen, M.C., Hsu, W.L., Hwang, P.A. & Chou, T.C., 2015. Low molecular weight fucoidan inhibits tumor angiogenesis through downregulation of HIF-1/VEGFsignaling under hypoxia. *Mar. Drugs*, 13, pp.4436–4451, https://doi.org/10.3390/md13074436.

Chen, Z. et al., 2015. Characteristics and kinetic study on pyrolysis of five lignocellulosic biomass via thermogravimetric analysis. *Bioresour. Technol.*, 192, pp.441-450, https://doi.org/10.1016/j.biortech.2015.05.062.

Chen, L., Tuo, B. & Dong, a.H., 2016. Regulation of Intestinal Glucose Absorption by Ion Channels and Transporters. *Nutrients*, 8, pp.1-11, https://doi.org/10.3390/nu8010043.

Cho, M., Han, J.H. & You, S., 2011. Inhibitory effects of fucan sulfates on enzymatic hydrolysis of starch. *Lwt-Food Sci. Technol*, 44, pp.1164–71, https://doi.org/10.1016/j.lwt.2010.09.019

Choi, J.-S. et al., 2014. Characteristics and in vitro anti-diabetic properties of the Korean rice wine, makgeolli fermented with *Laminaria japonica*. *Prev Nutr Food Sci*, 19, pp.98-104, https://doi.org/10.3746/pnf.2014.19.2.098.

Chou, T., 2010. Drug combination studies and their synergy quantification using the Chou-Talalay method. *Cancer Res.*, 70, pp.440-46, https://doi.org/10.1158/0008-5472.can-09-1947.

Chou, T., 2020. *Functional Dynamics of the Mass-Action Law (MAL) in Biology (BD), Pharmacology (PD) and Bioinformatics (BI): "Doctrine of the Median" Algorithm for Single Drug and Drug Combinations by Computer Simulation.* [Online] Available at: http://www.Combosyn.com [Accessed 10 January 2021].

Chung, H.-J. et al., 2010. Toxicological evaluation of fucoidan from *Undaria pinnatifida in vitro* and *in vivo*. *Phytother Res.*, 24, pp.1078-83, https://doi.org/10.1002/ptr.3138.

Colombo, S.L. et al., 2010. Anaphase-promoting complex/cyclosome-Cdh1 coordinates glycolysis and glutaminolysis with transition to S phase in human T lymphocytes. *Proc. Natl. Acad. Sci. U.S.A.*, 107, pp.18868–18873, https://doi.org/10.1073/pnas.1012362107.

Cortés-Cros, M. et al., 2013. M2 isoform of pyruvate kinase is dispensable for tumor maintenance and growth. *PNAS*, 110(2), pp.489-494,https://doi.org/10.1073/pnas.1212780110.

Dalva-Aydemir, S. et al., 2015. Targeting the metabolic plasticity of multiple myeloma with FDA approved ritonavir and metformin. *Clin. Cancer Res*, 21, pp.1161–1171, https://doi.org/10.1158/1078-0432.ccr-14-1088.

Daub, C.D., Mabate, B., Malgas, S. & Pletschke, B.I., 2020. Fucoidan from *Ecklonia maxima* is a powerful inhibitor of the diabetes-related enzyme, α-glucosidase. *Int. J. Biol*, 151, pp.412-420, https://doi.org/10.1016/j.ijbiomac.2020.02.161.

Davidson, N.O.. et al., 1992. Human intestinal glucose transporter expression and localization of GLUT5. *Am J Physiol*, 262, pp.795–800, https://doi.org/10.1152/ajpcell.1992.262.3.c795.

De Saedeleer, C.J. et al., 2012. Lactate activates HIF-1 in oxidative but not in Warburg-phenotype human tumor cells. *PLoS One*, 7, pp.e46571, https://dx.doi.org/10.1371%2Fjournal.pone.0046571.

Deberardinis, R.J., Sayed, N., Ditsworth, D. & Thompson, C.B., 2008. Brick by brick: metabolism and tumor cell growth. *Curr. Opin. Genet. Dev.*, 18(1), pp.54–61, https://doi.org/10.1016/j.gde.2008.02.00.

Devlin, T.M., 2006. *Textbook of Biochemistry with Clinical Correlations*. Hoboken: Wiley-Liss.

DiNicolantonio, J.J., Bhutani, J. & H, O.J., 2015. Acarbose: safe and effective for lowering postprandial hyperglycaemia and improving cardiovascular outcomes. *Open Heart*, 2, pp.e000327, https://doi.org/10.1136/openhrt-2015-000327.

Dodgson, K.S. & Price, R.G., 1962. A note on determination of ester sulphate content of sulphated polysaccharides. *Biochem. J*, 84(1), pp.106–110, https://doi.org/10.1042/bj0840106.

Dubois, M. et al., 1956. Colorimetric method for determination of sugars and related substances. *Anal. Chem*, 28(3), pp.350–356, https://doi.org/10.1021/ac60111a017.

Dunbar, E.M., Coats, B.S. & Shroads, A.L., 2014. Phase 1 trial of dichloroacetate (DCA) in adults with recurrent malignant brain tumors. *Invest. New Drugs*, 32, pp.452–464, https://dx.doi.org/10.1007%2Fs10637-013-0047-4.

Eluvakkal, T., Sivakumar, S.R. & Arunkumar, K., 2010. Fucoidan in Some Indian Brown Seaweeds Found along the Coast Gulf of Mannar. *Int. J. Botany*, 6, pp.176-81.

Ermakova, S.P. et al., 2016. Structure, chemical and enzymatic modification, and anticancer activity of polysaccharides from the brown alga *Turbinaria ornata*. *J. Appl. Phycol*, 28, pp.2495–2505, http://dx.doi.org/10.1007%2Fs10811-015-0742-y.

FDA , 2020. *U.S Food & Drug Administration*. [Online] Available at: https://www.fda.gov/news-events/press-announcements/fda-alerts-patients-and-health-care-professionals-nitrosamine-impurity-findings-certain-metformin [Accessed 9 January 2022].

Felman, A., 2020. *Medical News Today*. [Online] Available at: https://www.medicalnewstoday.com/articles/323716 [Accessed 9 January 2022].

Ferlay, J. et al., 2015. Cancer incidence and mortality worldwide: Sources, methods and major patterns in GLOBOCAN 2012. *Int J Cancer*, 136, pp.359 386, https://doi.org/10.1002/ijc.29210.

Ferrara, N., Gerber, H.P. & Le-Couter, J., 2003. The biology of VEGF and its receptors. *Nat Med*, 9, pp.669–676, https://doi.org/10.1038/nm0603-669.

Fitton, J.H., Stringer, D.N. & Karpiniec, S.S., 2015. Therapies from fucoidan: An update. *Mar. Drugs*, 19(9), pp.5920–5946, https://dx.doi.org/10.3390%2Fmd13095920.

Fitzgerald, C.P., 2014. *Development of peptide bioactive bread fraction enriched with a seaweed with potential heart health effects*. PhD Thesis. London: University College London.

Fletcher, H.R., Biller, P., Ross, A.B. & Adams, J.M.M., 2017. The seasonal variation of fucoidan within three species of brown macroalgae. *Algal Res*, 22, pp.79-86, https://doi.org/10.1016/j.algal.2016.10.015.

Foley, S.A. et al., 2011. An Unfractionated Fucoidan from *Ascophyllum nodosum*: Extraction Characterization, and Apoptotic Effects *in vitro*. *J. Nat. Prod*, 74, pp.1851–1861, https://doi.org/10.1021/np200124m.

Franken, N.A.P. et al., 2006. Clonogenic assay of cells *in vitro*. *Nat Protoc*, 1, pp.2315-2319, https://doi.org/10.1038/nprot.2006.339.

Friedl, P. & Wolf, K., 2003. Tumour-cell invasion and migration: Diversity and escape mechanisms. *Nat Rev Cancer*, 3, pp.362–374, https://doi.org/10.1038/nrc1075.

Gabbia, D. et al., 2017. The Phytocomplex from *Fucus vesiculosus* and *Ascophyllum nodosum* Controls Postprandial Plasma Glucose Levels: An *In Vitro* and *In Vivo* Study in a Mouse Model of NASH. *Mar. Drugs*, 15(2), pp.41, https://dx.doi.org/10.3390%2Fmd15020041.

Galicia-Garcia, U. et al., 2020. Pathophysiology of Type 2 Diabetes Mellitus. *Int. J. Mol. Sci.*, 21, pp.6275, http://dx.doi.org/10.3390/ijms21176275.

Ganapathy-Kanniappan, S., 2018. Targets Evolution of GAPDH as a druggable target of tumor glycolysis?. *Expert Opin. Ther.*, 22(4), pp. 295–298, https://doi.org/10. 1080/14728222.2018.1449834.

Gao, K. & McKinley, K.R., 1994. Use of macroalgae for marine biomass production and CO_2 remediation: a review. *J. Appl. Phycol*, 60, pp.45-60, https://doi.org/10.1007/BF02185904.

Garcimartín, A., Benedí, J., Bastida, S. & Sánchez-Muniz, F.J., 2015. Aqueous extracts and suspensions of restructured pork formulated with *Undaria pinnatifida*, *Himanthali aelongata* and *Porphyra umbilicalis* distinctly affect the in vitro α-glucosidase activity and glucose diffusion. *LWT*, 64(2), pp.720-726, http://dx.doi.org/10.1016%2Fj.lwt.2015.06.050.

Gatenby, R.A. & Gillies, R.J., 2004. Why do cancers have high aerobic glycolysis? *Nat. Rev. Cancer*, 4, pp.891–899, https://doi.org/10.1038/nrc1478.

Giovannucci, E. et al., 2010. Diabetes and Cancer: a consensus report. *Diabetes Care*, 33, pp.1674-1685, https://doi.org/10.2337/dc10-0666.

Goodman, B.E., 2010. Insights into digestion and absorption of major nutrients in humans. *Adv Physiol Educ*, 34, pp.44–53, https://doi.org/10.1152/advan.00094.2009.

Gottschalk, S. et al., 2004. Imatinib (STI571)-Mediated Changes in Glucose Metabolism in Human Leukemia BCR-ABL-Positive Cells. *Clin Cancer Res*, 10, pp.6661–6668, https://doi.org/10.1158/1078-0432.ccr-04-0039.

Gouda, H.N. et al., 2019. Burden of non-communicable diseases in sub-Saharan Africa, 1990–2017: results from the Global Burden of Disease Study 2017. *Lancet Glob Health*, 7, pp.e1375–87, https://doi.org/10.1016/s2214-109x(19)30374-2.

Gould, G.W., Thomas, H.M., Jess, T.J. & Bell, G.I., 1991. Expression of human glucose transporters in Xenopus oocytes: kinetic characterization and substrate specificities of the erythrocyte, liver, and brain isoforms. *Biochem.*, 30, pp.5139–5145, https://doi.org/10.1021/bi00235a004.

Greco, W.R., Faessel, H. & Levasseur, L., 1996. The search for cytotoxic synergy between anticancer agents: a case of Dorothy and the ruby slippers? *J Natl Cancer Inst*, 88(11), pp.699-700, https://doi.org/10.1093/jnci/88.11.699.

Hahn, T., Lang, S., Ulber, R. & Muffler, K., 2012. Novel procedures for the extraction of fucoidan from brown algae. *Process Biochem*, 47, pp.1691–1698, https://doi.org/10.1016/j.procbio.2012.06.016.

Hakayawa, K. & Nagamine, T., 2009. Effect of Fucoidan on the Biotinidase Kinetics in Human Hepatocellular Carcinoma. *Anticancer Res.*, 29, pp.1211–17.

Halestrap, A.P., 2012. The monocarboxylate transporter family– structure and functional characterization. *IUBMB Life*, 64, pp. 1–9, https://doi.org/10.1002/iub.573.

Hall, A.C., Fairclough, A.C., Mahadevan, K. & Paxman, J.R., 2012. *Ascophyllum nodosum* enriched bread reduces subsequent energy intake with no effect on post-prandial glucose and cholesterol in healthy, overweight males. A pilot study. *Appetite*, 58, pp.379–386, https://doi.org/10.1016/j.appet.2011.11.002.

Haneji, K. et al., 2005. Fucoidan extracted from *Cladosiphon okamuranus* Tokida induces apoptosis of human T-cell leukemia virus type1-infected T-Cell lines and primary adult T-cell leukemia cells. *Nutr Cancer*, 52, pp.189–201, https://doi.org/10.1207/s15327914nc5202_9.

Han, Y.-S., Lee, J.H. & Lee, S.H., 2015a. Fucoidan inhibits the migration and proliferation of HT-29 human colon cancer cells via the phosphoinositide-3 kinase/Akt/mechanistic target of rapamycin pathways. *Mol Med Rep*, 2, pp.3446-3452, https://doi.org/10.3892/mmr.2015.3804.

Han, Y.S., Lee, J.H. & Lee, S.H., 2015b. Antitumor effects of fucoidan on human colon cancer cells via activation of Akt signaling. *Biomol Ther (Seoul)*, 23, pp.225–232, https://doi.org/10.4062/biomolther.2014.136.

Heiden, M.G.V., Cantley, L.C. & Thompson, C.B., 2009. Understanding the Warburg effect: the metabolic requirements of cell proliferation. *Science*, 324, pp.1029–1033, https://doi.org/10.1126/science.1160809.

Heo, S.J., Park, E.J., Lee, K.W. & Jeon, Y.J., 2005. Antioxidant activities of enzymatic extracts from brown seaweeds. *Bioresour. Technol.*, 96, pp.1613–1623, https://doi.org/10.1016/j.biortech.2004.07.013.

He, K., Shi, J.-C. & Mao, X.-M., 2014. Safety and Efficacy of Acarbose in the Treatment of Diabetes in Chinese Patients. *Ther. Clin. Risk.Manag.*, 10, pp.505–511, https://doi.org/10.2147/tcrm.s50362.

Hifney, A.F., Fawzy, M.A., Abdel-Gawad, K.M. & Gomaa, M., 2016. Industrial optimization of fucoidan extraction from *Sargassum* sp. and its potential antioxidant and emulsifying activities. *Food Hydrocoll*, 54, pp.77-88, https://doi.org/10.1016/j.foodhyd.2015.09.022.

Honya, M. et al., 1999. Monthly changes in the content of fucans, their constituent sugars and sulphate in cultured Laminaria japonica. *Hydrobiologia*, 398, pp.411-416, https://doi.org/10.1023/A:1017007623005.

Hsu, H. & Hwang, P., 2019. Clinical applications of fucoidan. *Clin Transl Med*, 8, pp.15, https://doi.org/10.1186/s40169-019-0234-9.

Huang, D., Ou, B. & & Prior, R.L., 2005. The chemistry behind antioxidant capacity assay. *J Agric Food Chem*, 53(6), pp.1841–1856, https://doi.org/10.1021/jf030723c.

Huber, M.A., Kraut, N. & Beug, H., 2005. Molecular requirements for epithelial-mesenchymal transition during tumor progression. *Curr Opin Cell Biol*, 17, pp.548–558, https://doi.org/10.1016/j.ceb.2005.08.001.

Hu, X., Chao, M. & Wu, H., 2017. Central role of lactate and proton in cancer cell resistance to glucose deprivation and its clinical translation. *Signal Transduct Target Ther*, 2, pp.16047, https://dx.doi.org/10.1038%2Fsigtrans.2016.47.

Hu, S., Xia, G., Wang, J. & Wang, Y., 2014. Fucoidan from sea cucumber protects against high-fat high-sucrose diet-induced hyperglycaemia and insulin resistance in mice. *J. Funct. Foods*, 10, pp.128-138, https://doi.org/10.1016/j.jff.2014.05.012.

Imbs, T.I., Skriptsova, A.V. & Zvyagintseva, T.N., 2015. Antioxidant activity of fucose containing sulfated polysaccharides obtained from *Fucus evanescens* by different extraction methods. *J. Appl. Phycol*, 27, pp.545–53.

Indergaard, M. & Minsaas, J., 1991. Animal and human nutrition. In B. Guiry, ed. *In Seaweed Resources in Europe: Uses and Potential*. New York: John Wiley & Sons.

International Diabetes Federation, 2018. [Online] Available at: https://www.idf.org/our-network/regions-members/africa/members/25-south-africa.html [Accessed 28 May 2018].

Isnansetyo, A. et al., 2017. Cytotoxicity of Fucoidan from Three Tropical Brown Algae Against Breast and Colon Cancer lines. *Pharmacogn. J*, 9, pp.14-20, http://dx.doi.org/10.5530/pj.2017.1.3.

James, D.E., Strube, M. & Mueckler, M., 1989. Molecular cloning and characterization of an insulin-regulatable glucose transporter. *Nature*, 338, pp.83–87, https://doi.org/10.1038/338083a0.

January, G.G., Naidoo, R.K., Kirby-McCullough, B. & Bauerd, R., 2019. Assessing methodologies for fucoidan extraction from South African brown algae. *Algal Res.*, 40, pp.101517, http://doi.org/10.1016/j.algal.2019.101517.

Jeong, Y.T. et al., 2013. Low molecular weight fucoidan improves endoplasmic reticulum stress-reduced insulin sensitivity through AMP-activated protein kinase activation in L6 myotubes and restores lipid homeostasis in a mouse model of type 2 diabetes. *Mol. Pharmacol*, 84, pp.147-157, https://doi.org/10.1124/mol.113.085100.

Jiang, B., 2017. Aerobic glycolysis and high level of lactate in cancer metabolism and microenvironment. *Genes Dis*, 4, pp.25-27, http://dx.doi.org/10.1016/j.gendis.2017.02.003.

Jiang, G. & Zhang, B.B., 2003. Glucagon and regulation of glucose metabolism. *Am J Physiol Endocrinol Metab*, 284(4), pp.E671–680, https://doi.org/10.1152/ajpendo.00492.2002.

Jia, D. et al., 2018. Elucidating the metabolic plasticity of Cancer: mitochondrial reprogramming and hybrid metabolic states. *Cells*, 21, pp.21, https://doi.org/10.3390/cells7030021.

Jiménez-Escrig, A. & Sánchez-Muniz, F.J., 2000. Dietary fibre from edible seaweeds Chemical structure, physicochemical properties and effects on cholesterol metabolism. *Nutr. Res*, 20, pp.585-598, https://doi.org/10.1016/S0271-5317(00)00149-4.

Jin, J.-O. et al., 2021. The Therapeutic Potential of the Anticancer Activity of Fucoidan: Current Advances and Hurdles. *Mar. Drugs*, 19, pp.265, https://doi.org/10.3390/md19050265.

Kalekar, S.A., Munshi, R.P., Bhalerao, S.S. & Thatte, U.M., 2013. Insulin sensitizing effect of 3 Indian medicinal plants: an *in vitro* study. *Indian J Pharmacol*, 45, pp.30–33, https://doi.org/10.4103/0253-7613.106431.

Karleskint, G., Turner, G. & and Small, J., 2010. *Introduction to Marine Biology*. 3rd ed. Belmont: CA: Brooks/Cole.

Kelley, D. et al., 1988. Skeletal Muscle Glycolysis, Oxidation, and Storage of an Oral Glucose Load. *J. Clin. Investig*, 81, pp.1563–1571, http://doi.org/10.1172/JCI113489.

Khan, S.J. & Satam, S.B., 2003. Seaweed Mariculture. Scope and Potential in India. *Aquaculture Asia*, 8(4), pp.26-29.

Kim, M.J. et al., 1999. Comparative study of the inhibition of alpha-glucosidase, alpha-amylase, and cyclomaltodextrin glucanosyltransferase by acarbose, isoacarbose, and acarviosine-glucose. *Arch Biochem Biophys*, 371, pp.277–83, https://doi.org/10.1006/abbi.1999.1423.

Kim, K.T., Rioux, L.-E. & & Turgeon, S.L., 2014. Alpha-amylase and alpha-glucosidase inhibition is differentially modulated by fucoidan obtained from *Fucus vesiculosus* and *Ascophyllum nodosum*. *Phytochem*, 98, pp.27-33, https://doi.org/10.1016/j.phytochem.2013.12.003.

Koh, H.S.A., Lu, J. & Zhou, W., 2020. Structural Dependence of Sulfated Polysaccharide for Diabetes Management: Fucoidan From *Undaria pinnatifida* Inhibiting α-Glucosidase More Strongly Than α-Amylase and Amyloglucosidase. *Front. Pharmacol.*, 11(831), pp.https://doi.org/10.3389/fphar.2020.00831.

Kopplin, G. et al., 2018. Structural Characterization of Fucoidan from *Laminaria hyperborea*: Assessment of Coagulation and Inflammatory Properties and Their Structure−Function Relationship. *ACS Appl. Bio Mater*, 1, pp.1880−1892, https://doi.org/10.1021/acsabm.8b00436.

Kotowaroo, M.I., Mahomoodally, M.F., Gurib-Fakim, A. & Subratty, A.H., 2006. Screening of Traditional Antidiabetic Medicinal Plants of Mauritius for Possible Alpha-Amylase Inhibitory Effects *in Vitro*. *Phytother.Res*, 20, pp.228–231, https://doi.org/10.1002/ptr.1839.

Kushwaha, K., Sharma, S. & Gupta, J., 2013. Review on diabetes, synthetic drugs and glycaemic effects of medicinal plants. *Biochimie*, 7(36), pp.2628–2637, https://doi.org/10.1016/j.biochi.2020.01.007.

Kwak, J., 2014. Fucoidan as a Marine Anticancer Agent in Preclinical Development. *Mar. Drugs*, 12, pp. 851-870, https://doi.org/10.3390/md12020851.

Lakshmanasenthil, S., VinothKumar, T., Geetharamani, D. & Maruthupandi, T., 2013. Screening of seaweeds collected from south east coastal area of India for alpha amylase inhibitory activity, antioxidant activity and biocompatibility. *Int.J. Phar.Phar.Sci*, 5, pp.240-44.

Lansiaux, A., 2011. Antimetabolites. *Bull Cancer*, 98(11), pp.1263-1274, https://doi.org/10.1684/bdc.2011.1476.

Lazarovici, P., Marcinkiewicz, C. & Lelkes, P.I., 2020. Cell-Based Adhesion Assays for Isolation of Snake Venom's Integrin Antagonists. In A. Priel, ed. *Snake and Spider Toxins: Methods and Protocols, Methods in Molecular Biology*. Springer Science+Business Media, LLC. pp.205-20.

Le, A. et al., 2010. Inhibition of lactate dehydrogenase A induces oxidative stress and inhibits tumor progression. *Proc. Natl. Acad. Sci. USA.*, 107(5), pp.2037–2042, https://doi.org/10.1073/pnas.091443310.

Lee, S.H. et al., 2012. Molecular characteristics and anti-inflammatory activity of the fucoidan extracted from *Ecklonia cava*. *Carbohydr Polym*, 89, pp.599–606, https://doi.org/10.1016/j.carbpol.2012.03.056.

Liao, D.-W., Wang, L., Zhang, X.-G. & Liu, M.-Q., 2006. [Expression and significance of PTEN/PI3K signal transduction-related proteins in non-small cell lung cancer]. *Ai Zheng*, 10, pp.1238-42.

Li, J. et al., 2016. Protective effect of fucoidan from *Fucus vesiculosus* on liver fibrosis via the TGF-β1/Smad pathway-mediated inhibition of extracellular matrix and autophagy. *Drug Des Devel Ther*, 10, pp.619-630, https://doi.org/10.2147/dddt.s98740.

Li, C. et al., 2011. Fucoidan, a sulfated polysaccharide from brown algae, against myocardial ischemia-reperfusion injury in rats via regulating the inflammation

response. *Food Chem Toxicol*, 49, pp.2090-2095, https://doi.org/10.1016/j.fct.2011.05.022.

Li, B., Lu, F., Wei, X. & Zhao, R., 2008. Fucoidan: Structure and Bioactivity. *Molecules*, 13, pp.1671-1695, https://doi.org/10.3390/molecules13081671.

Lin, Y., Qi, X. & Liu, H., 2020. The anti-cancer effects of fucoidan: a review of both *in vivo* and *in vitro* investigations. *Cancer Cell Int*, 20, pp.154, https://doi.org/10.1186/s12935-020-01233-8.

Lin, S.T. et al., 2016. Apple Polyphenol Phloretin Inhibits Colorectal Cancer Cell Growth via Inhibition of the Type 2 Glucose Transporter and Activation of p53-Mediated Signaling. *J Agric Food Chem*, 64, pp.6826-6837, https://doi.org/10.1021/acs.jafc.6b02861.

Liu, J.M. et al., 2005. Inhibitory Effect of Fucoidan on the Adhesion of Adenocarcinoma Cells to Fibronectin. *Anticancer Res*, 25, pp.2129-34.

Liu, L. et al., 2012. Towards a better understanding of medicinal uses of the brown seaweed *Sargassum* in Traditional Chinese Medicine: A phytochemical and pharmacological review. *J Ethnopharmacol*, 142, pp.591-619, https://doi.org/10.1016/j.jep.2012.05.046.

Liu, X. & Yu, W., 2006. Evaluating the Thermal Stability of High Performance Fibers by TGA. *J. Appl. Polym. Sci.*, 99(3), pp.937–944, https://doi.org/10.1002%2Fapp.22305.

Liu, M., Zhang, W., Wei, J. & Lin, X., 2011. Synthesis and α-glucosidase inhibitory mechanisms of bis(2,3-dibromo-4,5-dihydroxybenzyl) ether, a potential marine bromophenol α-glucosidase inhibitor. *Mar. Drugs*, 9, pp.1554–1565, https://doi.org/10.3390/md9091554.

Locasale, J.W. & Cantley, L.C., 2010. Altered metabolism in cancer. *BMC Biol.*, 8, pp.88, http://www.biomedcentral.com/1752-0509/4/58/.

Longpré, J.P. & Lapointe, J.Y., 2011. Determination of the Na(+)/glucose cotransporter (SGLT1) turnover rate using the ion-trap technique. *Biophys. J.*, 100, pp.52–59, https://doi.org/10.1016/j.bpj.2010.11.012.

Lopina, O.D., 2017. Enzyme inhibitors and activators. In S. M, ed. *Enzyme Inhibitors and Activators*. IntechOpen. p.247.

Løvdal, T. et al., 2021. Microbiological Food Safety of Seaweeds. *Foods*, 10, pp.2719, https://doi.org/10.3390/foods10112719.

Lu, W. et al., 2012. Novel role of NOX in supporting aerobic glycolysis in cancer cells with mitochondrial dysfunction and as a potential target for cancer therapy. *PLoS Biol*, 10(5), pp.e1001326, https://doi.org/10.1371/journal.pbio.1001326.

Lunt, S.J., Chaudary, N. & Hill, R.P., 2009. The tumor microenvironment and metastatic disease. *Clin Exp Metastasis*, 26, pp.19–34, https://doi.org/10.1007/s10585-008-9182-2.

Lu, C.L. et al., 2015. Tumor cells switch to mitochondrial oxidative phosphorylation under radiation via mTOR-Mediated hexokinase II; inhibition-A Warburg-reversing effect. *PLoS One* , 10(3), pp.e0121046, https://doi.org/10.1371/journal.pone.0121046.

Luthuli, S. et al., 2019. Therapeutic Effects of Fucoidan: A review of recent studies. *Mar. Drugs*, 17, pp.487, http://dx.doi.org/10.3390/md17090487.

Mabate, B. et al., 2021. A Combination Approach in Inhibiting Type 2 Diabetes-Related Enzymes Using *Ecklonia radiata* Fucoidan and Acarbose. *Pharmaceutics*, 13, pp.1979, https://doi.org/10.3390/pharmaceutics13111979.

Mabate, B. et al., 2021. Fucoidan Structure and Its Impact on Glucose Metabolism: Implications for Diabetes and Cancer Therapy. *Mar. Drugs*, 19, pp.30, https://doi.org/10.3390/md19010030.

Maina, M.H., 2014. *Structural investigation of the natural product composition of selected South African seaweeds*. Capetown: University of Western Cape.

Maiuri, M.C. & Kroemer, G., 2015. Essential role for oxidative phosphorylation in Cancer progression. *Cell Metab*, 21, pp.11–12, https://doi.org/10.1016/j.cmet.2014.12.013.

Mak, W. et al., 2013. Fucoidan from New Zealand *Undaria pinnatifida*: monthly variations and determination of antioxidant activities. *Carbohydr Polym.*, 95, pp.606-614, https://doi.org/10.1016/j.carbpol.2013.02.047.

Marchiq, I. & Pouyssegur, J., 2016. Hypoxia, cancer metabolism and the therapeutic benefit of targeting lactate/H(+) symporters. *J. Mol. Med.*, 94(7), pp.155–171, https://doi.org/10.1007/s00109015-130.

Marini, C. et al., 2013. Direct inhibition of hexokinase activity by metformin at least partially impairs glucose metabolism and tumor growth in experimental breast cancer. *Cell Cycle*, 12(22), pp.3490-3499, https://doi.org/10.4161/cc.26461.

Marudhupandia, T. et al., 2015. *In vitro* anticancer activity of fucoidan from Turbinaria conoides against A549 cell lines. *Int J Biol Macromol*, 72, pp.919–923, https://doi.org/10.1016/j.ijbiomac.2014.10.005.

Mathupala, S.P., Ko, Y.H. & Pedersen, P.L., 2009. Hexokinase-2 bound to mitochondria: cancer's stygian link to the "Warburg Effect" and a pivotal target for effective therapy. *Semin. Cancer Biol*, 19(1), pp.17–24, https://doi.org/10.1016/j.semcancer.2008.11.006.

Ma, H. et al., 2015. Structure Activity Related, Mechanistic, and Modeling Studies of Gallotannins containing a Glucitol-Core and α-Glucosidase. *RSC Adv*, 5(130), pp.107904- 107915, https://doi.org/10.1039/c5ra19014b.

McHugh, D.J., 1987. Production and utilization of products from commercial seaweeds. *FAO Fish. Tech. Pap*, 288, pp.189-202.

Melkonian, E.A., Asuka, E. & Schury, M.P., 2020. *Physiology, Gluconeogenesis.In:* . [Online] StatPearls Publishing Available at: www.ncbi.nlm.nih.gov/books/NBK541119 [Accessed 15 September 2020].

Michanek, G., 2013. Seaweed resources for pharmaceutical uses. Boston: De Gruyter. pp.203-236, https://doi.org/10.1515/9783110882049.203.

Miller, G.L., 1959. Use of Dinitrosalicylic Acid Reagent for Determination of Reducing Sugar. *Anal. Chem*, 31(3), pp.426–428, https://doi.org/10.1021/ac60147a030.

Moini, J., 2019. The Epidemic and Prevalence of Diabetes in the United States. In *Epidemiology of Diabetes*. Elsevier. pp.45-55.

Mokhtari, R.B. et al., 2017. Combination therapy in combating cancer. *Oncotarget*, 8, pp.38022-38043, https://doi.org/10.18632/oncotarget.16723.

Molnar, C. & Gair, J., 2019. Digestive System Processes. In *Concepts of Biology – 1st Canadian Edition*. 1st ed. Pressbooks.

Monico, A., Martinez-Senra, E, Canada, F.J., Zorrilla, S & Perez-Sala, D, 2017.Proton NMR spectra of EDTA and its Ca2+ complexed forms at different pH. PLOS ONE, g001, http://doi.org/10.1371/journal.pone.0169843.

Morán-Santibañez, K. et al., 2016. Synergistic Effects of Sulfated Polysaccharides from Mexican Seaweeds against Measles Virus. *Biomed Res Int*, pp.https://doi.org/10.1155/2016/8502123.

Morimoto, M. et al., 2014. Depolymerization of sulfated polysaccharides under hydrothermal conditions. *Carbohydr Res*, 384, pp.56–60, https://doi.org/10.1016/j.carres.2013.11.017.

Nagaoka, M., Shibata, H. & Gao, H., 2000. Anti-ulcer effects and biological activities of polysaccharides from marine algae. *BioFactors*, 12, pp.267-274, https://doi.org/10.1002/biof.5520120140.

National Cancer Registry, 2017. *Cancer statistics*. [Online] Available at: www.cansa.org.za/south-african-cancer-statistics [Accessed 28 May 2018].

Nauck, M.A. & Meier, J.J., 2016. The Incretin Effect in Healthy Individuals and Those with Type 2 Diabetes: Physiology, Pathophysiology and Response to Therapeutic Interventions. *Lancet Diabetes Endocrinol.* , 4, pp.525–536, http://doi.org/10.1016/S2213-8587(15)00482-9.

Nauck, M.A. & Meier, J.J., 2019. GIP and GLP-1: Stepsiblings Rather Than Monozygotic Twins Within the Incretin Family. *Diabetes*, 68, pp.897–900, http://doi.org/10.2337/dbi19-0005.

Nelson, N.J., 1998. Inhibitors of angiogenesis enter phase III testing. *J Natl Cancer Inst*, 90, pp.960–963, https://doi.org/10.1093/jnci/90.13.960a.

Nelson, D.M. et al., 2002. Coupling of DNA synthesis and histone synthesis in S phase independent of cyclin/cdk2 activity. *Mol. Cell. Biol*, 22, pp.7459–7472, https://doi.org/10.1128/mcb.22.21.7459-7472.2002.

Nguyen, T.T. et al., 2020. Enzyme-Assisted Fucoidan Extraction from Brown Macroalgae *Fucus distichus* subsp. *evanescens* and *Saccharina latissima*. *Mar. Drugs*, 18, pp.1-18, https://doi.org/10.3390/md18060296.

NIH, 2021. *Understanding cancer*. [Online] US Department of Health & Human services Available at: https://www.cancer.gov/about-cancer/understanding/what-is-cancer [Accessed 22 August 2021].

Nolop, K.B. et al., 1987. Glucose utilization in vivo by human pulmonary neoplasms. *Cancer*, 60, pp.2682-9, https://doi.org/10.1002/1097-0142(19871201)60:11%3C2682:aid-cncr2820601118%3E3.0.co;2-h.

Noto, H., 2017. Unfolding link between diabetes and cancer. *Diabetes Investig*, 9, pp.473–474, http://doi.org/10.1111/jdi.12725.

Oben, J. et al., 2007. The effects of ProAlgaZyme novel algae infusion on metabolic syndrome and markers of cardiovascular health. *Lipids Health Dis*, 6, pp.45-53, https://doi.org/10.1186/1476-511x-6-20.

Ogawa, M., 1997. Anticancer drugs and pharmacologic actions. *Nihon Rinsho*, 55, pp.1017-23.

Oliveira, R.M. et al., 2018. Commercial Fucoidans from *Fucus vesiculosu*s Can Be Grouped into Antiadipogenic and Adipogenic Agents. *Mar. Drugs*, 16(6), pp.193, https://doi.org/10.3390/md16060193.

Osonoi, T. et al., 2010. The α-glucosidase inhibitor miglitol decreases glucose fluctuations and inflammatory cytokine gene expression in peripheral leukocytes of Japanese patients with type 2 diabetes mellitus. *Metabolism*, 59, pp.1816–1822, https://doi.org/10.1016/j.metabol.2010.06.006.

Park, H. E., Choi, W., Kim, G, Kim, B. W., Choi, Y. H., 2015. Fucoidan induces G1 arrest of the cell cycle in EJ human bladder cancer cells through down-regulation of pRB phosphorylation. *Rev. bras. Farmacogn*, 25, 246-251, https://doi.org/10.1016/j.bjp.2015.03.011

Park, M.H. & Han, S.J., 2012. Hypoglycemic effect of *Padina arborescens* extract in streptozotocin-induced diabetic mice. *Prev. Nutr. Food Sci*, 17, pp.239–44, https://doi.org/10.3746/pnf.2012.17.4.239

Park, H.Y. et al., 2014. Fucoidan inhibits the proliferation of human urinary bladder cancer T24 cells by blocking cell cycle progression and inducing apoptosis. *Molecules*, 19, pp.5981–5998, https://doi.org/10.3390/molecules19055981.

Park, H.S. et al., 2011. Antiproliferative activity of fucoidan was associated with the induction of apoptosis and autophagy in AGS human gastric cancer cells. *J Food Sci*, 76, pp.77–183, https://doi.org/10.1111/j.1750-3841.2011.02099.x.

Peasura, N., Laohakunjit, N., Kerdchoechuen, O. & Wanlapa, S., 2015. Characteristics and antioxidant of *Ulva intestinalis* sulphated polysaccharides extracted with different solvents. *Int J Biol Macromol*, 81, pp.912–919, https://doi.org/10.1016/j.ijbiomac.2015.09.030.

Peng, Y. et al., 2019. *In vitro* and *in vivo* immunomodulatory effects of fucoidan compound agents. *Int J Biol Macromol*, 127, pp.48-56, https://doi.org/10.1016/j.ijbiomac.2018.12.197.

Pereira, L., Gheda, S.F. & & Ribeiro-Claro, P.J.A., 2013. Analysis by Vibrational Spectroscopy of Seaweed Polysaccharides with Potential Use in Food, Pharmaceutical, and Cosmetic Industries. *Int. J. Carbohydr. Chem.*, pp.7, https://doi.org/10.1155/2013/537202.

Tatrai et al., 2019. A systematic in vitro investigation of the inhibitor preincubation effect on multiple classes of clinically relevant transporters. *Drug Metab Dispos*, 48(7), pp.541-550, https://doi.org/10.1124/dmd.118.085993.

Picot, C., Subratty, A.H. & Mahomoodally, M.F., 2014. Inhibitory potential of five traditionally used native antidiabetic medicinal plants on α-amylase, α-glucosidase, glucose entrapment, and amylolysis kinetics *in vitro*. *Adv Pharmacol Sci*, 2, pp.1-7, https://doi.org/10.1155/2014/739834.

Pinheiro, C. et al., 2012. Role of monocarboxylate transporters in human cancers: state of the art. *J. Bioenerg. Biomembr.*, 44(1), pp.127–139, https://doi.org/10.1007/s10863-012-9428-1.

Ponce, N.M.A. & Stortz, C.A., 2020. A Comprehensive and Comparative Analysis of the Fucoidan Compositional Data Across the Phaeophyceae. *Front Plant Sci.*, 3, p.103389, https://doi.org/10.3389/fpls.2020.556312

Rabanal, M. et al., 2014. The system of fucoidans from the brown seaweed *Dictyota dichotoma*: chemical analysis and antiviral activity. *Carbohydr Polym*, 101, pp.804-811, https://doi.org/10.1016/j.carbpol.2013.10.019.

Raez, L.E., Papadopoulos, K. & Ricart, A.D., 2013. A phase I dose-escalation trial of 2- deoxy-D-glucose alone or combined with docetaxel in patients with advanced solid tumors. *Cancer Chemother. Pharmacol*, 71, pp.523–530, https://doi.org/10.1007/s00280-012-2045-1.

Rahier, N.J. et al., 2015. Anticancer activity of koningic acid and semisynthetic derivatives. *Bioorg. Med. Chem.*, 23, pp.3712–3721, https://doi.org/10.1016/j.bmc.2015.04.004.

Rani, V., Shakila, R.J., Jawahar, P. & Srinivasan, A., 2017. Influence of Species, Geographic Location, Seasonal Variation and Extraction Method on the Fucoidan Yield of the Brown Seaweeds of Gulf of Mannar, India. *Indian J Pharm Sci*, 79(1), pp.65-71, https://doi.org/10.4172/pharmaceutical-sciences.1000202.

Rena, G., Hardie, D.G. & Pearson, E.R., 2017. The Mechanisms of Action of Metformin. *Diabetologia*, 60, pp.1577–1585, http://doi.org/10.1007/s00125-017-4342-z.

Rioux, E.L.., Turgeon, S.L. & Beaulieu, M., 2007. Characterization of polysaccharides extracted from brown seaweeds. *Carbohydr. Polym*, 69, pp.530–37.

Röder, P.V. et al., 2014. The role of SGLT1 and GLUT2 in intestinal glucose transportand sensing. *PLoS ONE*, 26, pp.e89977,https://doi.org/10.1371/journal.pone.0089977.

Roell, K.R., Reif, D.M. & Motsinger-Reif, A.A., 2017. An Introduction to Terminology and Methodology of Chemical Synergy-Perspectives from Across Disciplines. *Front Pharmacol*, 8, pp.158: https://doi.org/10.3389/fphar.2017.00158.

Roesch, A. et al., 2013. Overcoming intrinsic multidrug resistance in melanoma by blocking the mitochondrial respiratory chain of slow-cycling JARID1B high cells. *Cancer Cell*, 23, pp.811–825, https://doi.org/10.1016/j.ccr.2013.05.003.

Roohinejad, S. et al., 2017. Application of seaweeds to develop new food products with enhanced shelf-life, quality and health-related beneficial properties. *Int. Food Res. J.*, 99, pp.1066–1083, https://doi.org/10.1016/j.foodres.2016.08.016.

Rothman, M., Anderson, R., Kandjengo, L. & Bolton, J., 2020. Trends in seaweed resource use and aquaculture in South Africa and Namibia over the last 30 years. *Botanica Marina*, 63, pp.315-325, https://doi.org/10.1515/bot-2019-0074.

Ryu, N.-E., Lee, S.-H. & Park, H., 2019. Spheroid Culture System Methods and Applications for Mesenchymal Stem Cells. *Cells*, 8, pp.1620, https://doi.org/10.3390/cells8121620.

Saeedi, P. et al., 2019. Global and regional diabetes prevalence estimates for 2019 and projections for 2030 and 2045: Results from the International Diabetes Federation Diabetes Atlas, 9th edition. *Diabetes Res Clin Pract*, 157, pp.107843, https://doi.org/10.1016/j.diabres.2019.107843.

Sanjeewa, I.P.S.F.K.K.A. et al., 2017. FTIR characterization and antioxidant activity of water soluble crude polysaccharides of Sri Lankan marine algae. *Algae*, 32(1), pp.75-86, https://doi.org/10.4490/algae.2017.32.12.1.

Saravanaa, P.S. et al., 2018. Hydrothermal degradation of seaweed polysaccharide: Characterization and biological activities. *Food Chem*, 268, pp.179-187, https://doi.org/10.1016/j.foodchem.2018.06.077.

Sasaki, A. et al., 2016. Uptake of a fluorescent L-glucose derivative 2-NBDLG into three-dimensionally accumulating insulinoma cells in a phloretin-sensitive manner. *Hum Cell*, 29, pp.37–45, https://doi.org/10.1007/s13577-016-0135-9.

Schneider, T., Ehriq, K.L.I. & Alban, S., 2015. Interference with the CXCL12/CXCR4 axis as potential antitumor strategy: Superiority of a sulfated galactofucan from the brown alga *Saccharina latissima* and fucoidan over heparins. *Glycobiology*, 25, pp.812-2, https://doi.org/10.3390/md13074436.

Senthilkumar, K., Manivasagana, P. & Venkatesana, J., 2013. Brown seaweed fucoidan: Biological activity and apoptosis, growth signalling mechanism in cancer. *Int J Biol Macromol*, 60, pp.366 – 374, https://doi.org/10.1016/j.ijbiomac.2013.06.030.

Shan, X. et al., 2016. *In vitro* and *in vivo* hypoglycemic effects of brown algal fucoidans. *Int J Biol Macromol*, 82, pp.249-255, https://doi.org/10.1016/j.ijbiomac.2015.11.036.

Sharabi, K., Tavares, C.D.J., Rines, A.K. & Puigserver, P., 2015. Molecular pathophysiology of hepatic glucose production. *Mol. Asp. Med.*, 46, pp.21–33, https://doi.org/10.1016/j.mam.2015.09.003.

Sherr, C.J., 1996. Cancer cell cycles. *Science*, 274, pp.1672–1677, https://doi.org/10.1126/science.274.5293.1672.

Shin, S.-W. et al., 2018. Fucoidan-Manganese Dioxide Nanoparticles Potentiate Radiation Therapy by Co-Targeting Tumor Hypoxia and Angiogenesis. *Mar. Drugs*, 16, pp.510, https://doi.org/10.3390/md16120510.

Sim, S.Y., Shin, Y.E. & Kim, H.K., 2019. Fucoidan from *Undaria pinnatifida* has anti-diabetic effects by stimulation of glucose uptake and reduction of basal lipolysis in 3T3-L1 adipocytes. *Nutr Res*, 65, pp.54-62, https://doi.org/10.1016/j.nutres.2019.02.002.

Singla, R.K., Singh, R. & Dubey, A.K., 2016. Important Aspects of Post-Prandial Antidiabetic Drug, Acarbose. *Curr Top Med Chem*, 16, pp.1-9, https://doi.org/10.2174/1568026616666160414123500.

Skriptsova, A.V., Shevchenko, N.M., Zvyagintseva, T.N. & Imbs, T.I., 2010. Monthly changes in the content and monosaccharide composition of fucoidan from *Undaria pinnatifida* (Laminariales, Phaeophyta). *J Appl Phycol*, 22, pp.79–86, http://dx.doi.org/10.1007/s10811-009-9438-5.

Slater, C., De La Mare, J. A., Edkins, A.L., 2018. *In vitr*o analysis of putative cancer stem cell populations and chemosensitivity in the SW480 and SW620 colon cancer metastasis model. *Oncol Lett*, 15, 8516-8526, https://doi.org/10.3892/ol.2018.8431.

Smit, A.J., 2004. Medicinal and pharmaceutical uses of seaweed natural products. *A review. J. Appl. Phycol*, 16, pp.245-262, http://dx.doi.org/10.1023%2FB%3AJAPH.0000047783.36600.ef.

Smith, U., 2002. Impaired ('diabetic') insulin signaling and action occur in fat cells long before glucose intolerance--is insulin resistance initiated in the adipose tissue? *Int J Obes Relat Metab Disord*, 26, pp.897-904, https://doi.org/10.1038/sj.ijo.0802028.

Son, H.U. & Lee, S.H., 2013. Comparison of α-glucosidase inhibition by *Cudrania tricuspidata* according to harvesting time. *Biomed Rep.*, 1, pp.624–628, https://doi.org/10.3892/br.2013.111.

Sung, H. et al., 2021. Global Cancer Statistics 2020: GLOBOCAN Estimates of Incidence and Mortality Worldwide for 36 Cancers in 185. *CA Cancer J Clin*, 71, pp.209–249, https://doi.org/10.3322/caac.21660.

Suprunchuk, V.E., 2019. Low-molecular-weight fucoidan: Chemical modification, synthesis of its oligomeric fragments and mimetics. *Carbohydr Res*, 485, pp.107806, https://doi.org/10.1016/j.carres.2019.107806.

Suresh, V. et al., 2013. Separation, purification and preliminary characterization of sulfated polysaccharides from *Sargassum plagiophyllum* and its *in vitro* anticancer and antioxidant activity. *Process Biochem*, 48(2), pp.364 - 373, https://doi.org/10.1016/j.procbio.2012.12.014

Takahashi, H. et al., 2018. An Exploratory Study on the Anti-inflammatory Effects of Fucoidan in Relation to Quality of Life in Advanced Cancer Patients. *Integr Cancer Ther*, 17, pp.282-291, https://doi.org/10.1177/1534735417692097.

Tanner, L.B. et al., 2018. Four Key Steps Control Glycolytic Flux in Mammalian Cells. *Cell Syst*, 7, pp.49–62,https://doi.org/10.1016/j.cels.2018.06.003.

Thanh, T.T.T. et al., 2013. Structure of Fucoidan from Brown Seaweed *Turbinaria ornata* as Studied by Electrospray Ionization Mass Spectrometry (ESIMS) and Small Angle X-ray Scattering (SAXS) Techniques. *Mar. Drugs*, 11, pp.2431-2443, https://doi.org/10.3390/md11072431.

Thompson, K.D. & Dragar, C., 2004. Antiviral activity of *Undaria pinnatifida* against herpes simplex virus. *Phytother Res*, 18, pp.551-555, https://doi.org/10.1002/ptr.1487.

Torre, L.A. et al., 2015. Global cancer statistics, 2012. *CA Cancer J Clin*, 65, pp.87-108, https://doi.org/10.3322/caac.21262.

Tudzarova, S. & Osman, M.A., 2015. The double trouble of metabolic diseases: the diabetes-cancer link. *Mol Biol Cell*, 26, pp.3129–3139, https://doi.org/10.1091/mbc.e14-11-1550.

Ustyuzhanina, N.E. et al., 2014. Fucoidans: Pro- or antiangiogenic agents? *Glycobiology*, 24, pp.1265–1274, https://doi.org/10.1093/glycob/cwu063.

Ventola, C.L., 2015. The antibiotic resistance crisis. *Medline*, 40, pp. 277–283.

Vinci, M., Box, C., Zimmermann, M. & Eccles, S.A., 2013. Tumor Spheroid-Based Migration Assays for Evaluation of Therapeutic Agents. In J. Moll & R. Colombo, eds. *Target Identification and Validation in Drug Discovery: Methods and Protocols, Methods in Molecular Biology*. New York: Springer Science & Business Media. pp.253-66.

Vinoth Kumar, T. et al., 2015. Fucoidan- a α-D-glucosidase inhibitor from *Sargassum wightii* with relevance to type 2 diabetes mellitus therapy. *Int. J. Biol. Macromol*, 72, pp.1044–1047, https://doi.org/10.1016/j.ijbiomac.2014.10.013.

Wada, T. & Penninger, J.M., 2004. Mitogen-activated protein kinases in apoptosis regulation. *Oncogene*, 23, pp.2838-2843, https://doi.org/10.1038/sj.onc.1207556.

Wang, J.L. et al., 2010. Sulfated modification, characterization and structure-antioxidant relationships of *Artemisia sphaerocephala*. *Carbohydr. Polym*, 81, pp.897–905,https://doi.org/10.1016/j.carbpol.2010.04.002.

Wang, Y. et al., 2016. Fucoidan from sea cucumber *Cucumaria frondosa* exhibits anti-hyperglycemic effects in insulin resistant mice via activating the PI3K/PKB pathway and GLUT4. *J Biosci Bioeng.*, 121(1), pp.36-42, https://doi.org/10.1016/j.jbiosc.2015.05.012.

Wang, Y. et al., 2019. Biological Activities of Fucoidan and the Factors Mediating Its Therapeutic Effects: A Review of Recent Studies. *Mar. Drugs*, 17, pp.183, https://doi.org/10.3390/md17030183.

Wang, J., Yu, J., Kong, X.Z. & Hou, L., 2013. Spectrophotometric determination of EDTA in aqueous solution through ferroin formation using sodium sulfite as the reducer. *Chemosphere*, 91, pp.351-357, https://doi.org/10.1016/j.chemosphere.2012.11.060.

Warburg, O., Posener, K. & Negelein, E., 1924. Über Den Stoffwechsel Der Carcinomzelle. *Biochem. Zeitschr.*, 152, pp.309–344, http://doi.org/10.1007/BF01726151.

Wasserman, D.H. et al., 2011. The physiological regulation of glucose flux into muscle in vivo. *J. Exp. Biol.*, 214, pp.254-262, https://doi.org/10.1242/jeb.048041.

Wei, H., Gao, Z. & Zou, X., 2017. Protective Effects of Fucoidan on Aβ25–35 and d-Gal-Induced Neurotoxicity in PC12 Cells and d-Gal-Induced Cognitive Dysfunction in Mice. *Mar.Drugs*, 15, pp.77, https://dx.doi.org/10.3390%2Fmd15030077.

Weiler-Sagie, M. et al., 2010. 18FFDG avidity in lymphoma readdressed: a study of 766 patients. *J. Nucl. Med*, 51, pp.25-30, https://doi.org/10.2967/jnumed.109.067892.

White, J.E., Catallo, W.J. & Legendre, B.L., 2011. Biomass pyrolysis kinetics: A comparative critical review with relevant agricultural residue case studies. *J Anal Appl Pyrolysis*, 91, pp.1-33, https://doi.org/10.1016/j.jaap.2011.01.004.

Whitmore, L. & Wallace, B.A., 2008. Protein secondary structure analyses from circular dichroism spectroscopy: Methods and reference databases. *Biopolymers*, 89, pp.392-400, https://doi.org/10.1002/bip.20853.

WHO, 2020. *Diabetes*. [Online] Available at: https://www.who.int/health-topics/diabetes#tab=tab_1 [Accessed 11 June 2020].

WHO, 2020. *World Health Organization*. [Online] Available at: https://www.who.int/news-room/fact-sheets/detail/diabetes [Accessed 18 March 2021].

WHO, 2021. *Cancer*. [Online] Available at: https://www.who.int/news-room/fact-sheets/detail/cancer [Accessed 5 January 2022].

WHO, 2021. *Noncommunicable diseases*. [Online] Available at: https://www.who.int/news-room/fact-sheets/detail/noncommunicable-diseases [Accessed 7 September 2021].

WHO, 2021. *World Health Organisation*. [Online] Available at: https://www.who.int/health-topics/cancer#tab=tab_1 [Accessed 24 July 2021].

Wilcox, G., 2005. Insulin and Insulin Resistance. *Clin Biochem Rev*, 26, pp.19-39, https://www.ncbi.nlm.nih.gov/pubmed/16278749.

Wu, L. et al., 2016. A review about the development of fucoidan in antitumor activity: Progress and challenges. *Carbohydr Polym*, 154, pp.96–111, https://doi.org/10.1016/j.carbpol.2016.08.005.

Wu, W.S., Wu, J.R. & Hu, C.T., 2008. Signal cross talks for sustained MAPK activation and cell migration: the potential role of reactive oxygen species. *Cancer Metastasis Rev*, 27, pp.303-314, https://doi.org/10.1007/s10555-008-9112-4.

Xing, R. et al., 2013. Extraction and Separation of Fucoidan from *Laminaria japonica* with Chitosan as Extractant. *Biomed Research International*, 4, pp.193689, https://doi.org/10.1155/2013/193689.

Xue, M. et al., 2012. Anticancer properties and mechanisms of fucoidan on mouse breast cancer *in vitro* and *in vivo*. *PLoS One*, 7, pp.e43483, https://doi.org/10.1371/journal.pone.0043483.

Yamaguchi, H., Wyckoff, J. & Condeelis, J., 2005. Cell migration in tumors. *Curr Opin Cell Biol*, 17, pp.559-564, https://doi.org/10.1016/j.ceb.2005.08.002.

Yang, C., Chung, D. & You, S.G., 2008. Determination of physicochemical properties of sulphated fucans from sporophyll *Undaria pinnatifida* using light scattering technique. *Food Chem*, 111, pp.503-507, https://doi.org/10.1016/j.foodchem.2008.03.085.

Yan, M.-D. et al., 2015. Fucoidan elevates microRNA-29b to regulate DNMT3B-MTSS1 axis and inhibit EMT in human hepatocellular carcinoma cells. *Mar. Drugs*, 13, pp.6099–6116, https://doi.org/10.3390/md13106099.

Yuan, Y. & Macquarrie, D., 2015. Microwave assisted extraction of sulfated polysaccharides (fucoidan) from *Ascophyllum nodosum* and its antioxidant activity. *Carbohydrate Polymers*, 129, pp.101–07.

Yuan, H., Ma, Q., Ye, L. & Piao, G., 2016. The Traditional Medicine and Modern Medicine from Natural Product. *Molecules*, 21, pp.559, https://doi.org/10.3390/molecules21050559.

Yu, L. et al., 2017. The Glycolytic Switch in Tumors: How Many Players Are Involved? *J. Cancer*, 8, pp.3430–3440, https://doi.org/10.7150/jca.21125.

Zayed, A. et al., 2016. Physicochemical and biological characterization of fucoidan from *Fucus vesiculosus* purified by dye affinity chromatography. *Mar. Drugs*, 14, pp.79, http//www/doi: 10.3390/md14040079..

Zhai, X. et al., 2013. Inhibition of LDH-A by oxamate induces G2/M arrest, apoptosis and increases radiosensitivity in nasopharyngeal carcinoma cells. *Oncol Rep*, 19, pp.2983-2991, https://doi.org/10.3892/or.2013.2735.

Zhang, Z. et al., 2013. Fucoidan extract enhances the anti-cancer activity of chemotherapeutic agents in MDA-MB-231and MCF-7 breast cancer cells. *Mar. Drugs*, 11, pp.81–98, https://doi.org/10.3390/md11010081.

Zhang, Y. & Yang, J.-M., 2013. Altered energy metabolism in cancer; A unique opportunity for therapeutic intervention. *Cancer Biol Ther*, 14(2), pp.81–89, https://dx.doi.org/10.4161%2Fcbt.22958.

Zhao, D., Xu, J. & Xu, X., 2018. Bioactivity of fucoidan extracted from *Laminaria japonica* using a novel procedure with high yield. *Food Chem*, 245, pp.911-918, https://doi.org/10.1016/j.foodchem.2017.11.083.

Zhao, Y. et al., 2018. Fucoidan Extracted from *Undaria pinnatifida*: Source for Nutraceuticals/Functional Foods. *Mar. Drugs*, 16(9), pp.321, https://dx.doi.org/10.3390%2Fmd16090321.

Zhou, H. et al., 2014. The inhibition of migration and invasion of cancer cells by graphene via the impairment of mitochondrial respiration. *Biomaterials*, 35, pp.1597–1607, https://doi.org/10.1016/j.biomaterials.2013.11.020.

Zhu, Z. et al., 2018. Glutathione reductase mediates drug resistance in glioblastoma cells by regulating redox homeostasis. *JNC*, 144, pp.93-104, https://doi.org/10.1111/jnc.14250.

Zhu, W. et al., 2016. PFK15, a Small Molecule Inhibitor of PFKFB3, Induces Cell Cycle Arrest, Apoptosis and Inhibits Invasion in Gastric Cancer. *PloS One*, 11(9), pp.e0163768. https://doi.org/10.1371/journal.

Zininga, T. et al., 2015. Overexpression, Purification and Characterization of the *Plasmodium falciparum* Hsp70-z (PfHsp70-z) Protein. *PLOS ONE*, 10, p.e0129445. 10.1371/journal.pone.0129445.

Zininga, T. et al., 2016. *Plasmodium falciparum* Hsp70-z, an Hsp110 homologue, exhibits independent chaperone activity and interacts with Hsp70-1 in a nucleotide-dependent fashion. *Cell Stress Chaperones*, 21, pp.499-513, https://doi.org/10.1007/s12192-016-0678-4.

APPENDIX A: LIST OF REAGENTS

Table A1: Name of the reagents utilised and their suppliers.

Reagent name	Supplier
α-Amylase porcine pancreatic	Megazyme™ (E-PANAA-9G)
Acarbose	Sigma-Aldrich (LRAA9057)
Acetone	MERCK (8.22251.2500)
Barium chloride dihydrate	Sigma-Aldrich (217565)
Bovine serum albumin (BSA)	Sigma (A7906)
Bradford reagent	Sigma (B6916)
Calcium chloride	Saarchem (1524920EM)
D-(+)-Cellobiose	Sigma (C7252)
3,5-Dinitrosalicylic acid	Sigma (D0550)
2-Deoxy-2-[(7-nitro-2,1,3-benzoxadiazol-4-yl)amino]-D-glucose (2-NBDG)	Sigma-Aldrich (72987)
D_2O	Sigma-Aldrich (151882)
Ethanol	MERCK (8.18700)
5-Fluorouracil	Sigma-Aldrich (04541)
Formaldehyde	Sigma-Aldrich (47670)
Folin-Ciocalteu reagent	Sigma-Aldrich (F9252)
Formic acid	MERCK (1038392)
Fucoidan from *F. vesiculosus*	Sigma-Aldrich (F5631)
L-Fucose	Sigma (F2252)
L-Fucose kit	Megazyme™ (K-FUCOSE)
Gelatine	Fluka (48723)
α-Glucosidase from *Saccharomyces cerevisiae*	Sigma-Aldrich (029M4179V)
D-Glucuronic acid kit	Megazyme™ (K-URONIC)
GOPOD	Megazyme™ (K-GLUC)
Hydrochloric acid	MERCK (1047705)
Lactose and D-Galactose kit	Megazyme™ (K-LACGAR)
Methanol	Sigma-Aldrich (34860)
D-Mannose, D-Fructose & D-Glucose kit	Megazyme™ (K-MANGL)
Phloretin	Sigma-Aldrich (P7912)
p-nitrophenol	Sigma (42,575-3)
p-nitrophenyl-α-D-glucopyranoside	Sigma (N1377)

Phosphate buffered saline	Sigma-Aldrich (P4417)
Phenol	Sigma-Aldrich (P1037)
Potato starch	Sigma (54501)
Sodium azide	MERCK (8.22335)
Sodium carbonate	Sigma-Aldrich (223484)
Sodium hydroxide	MERCK (1.06469.1000)
Sodium metabisulfite	Sigma-Aldrich (255556)
Sodium phosphate dibasic	Sigma-Aldrich (71640)
Sodium sulphate	Saarchem (8525200EM)
Sulfuric acid	Sigma-Aldrich (30743)
Trichloroacetic acid	Sigma-Aldrich (T9159)
Trifluoroacetic acid	Sigma-Aldrich (T6508)
D-Xylose kit	Megazyme™ (K-XYLOSE)

Table A2: HPLC instrument parts and models

Instruments	Model
Shimadzu Solvent Delivery Unit, with Tandem Plunger Mechanism	LC-20AT
Shimadzu Differential Refractive Index Detector	RID-10A
Shimadzu autosampler, Injection range: 0.1 to 1000 µl	Sil-20A
Shimadzu Column Oven, temperature range: ambient -15ºC to 80ºC	CTO-10ASVP
Shimadzu system controller	CBM-20Alite
Shimadzu 5-channel degasser,	DGU-20A5
Shimadzu LC solutions software	Version 1.24 single

APPENDIX B: SUPPLEMENTARY RESULTS

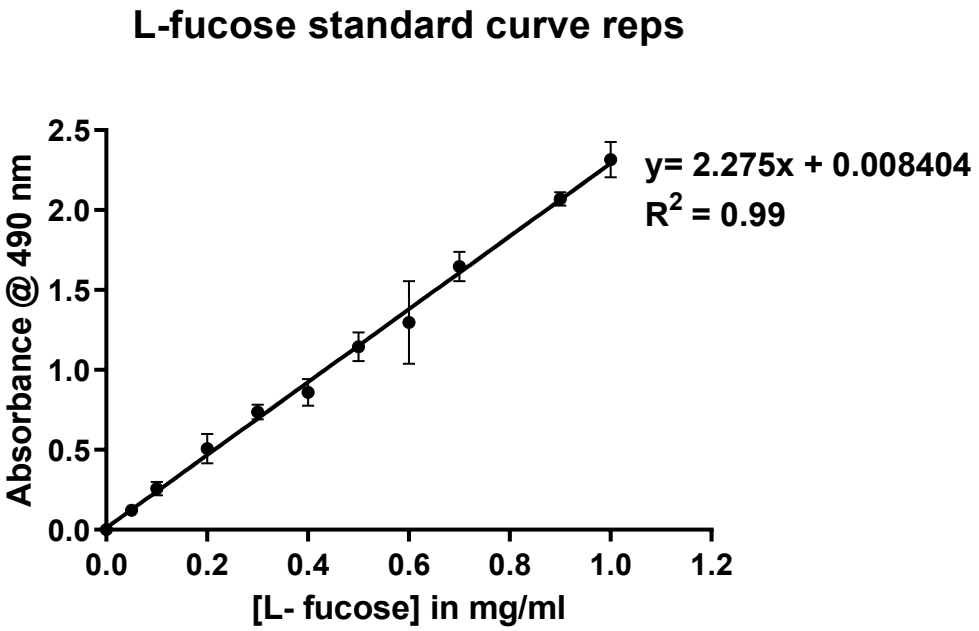

Figure B1: Total sugar assay L-fucose standard curve
The data are represented as means ± SD of at least 3 independent experiments.

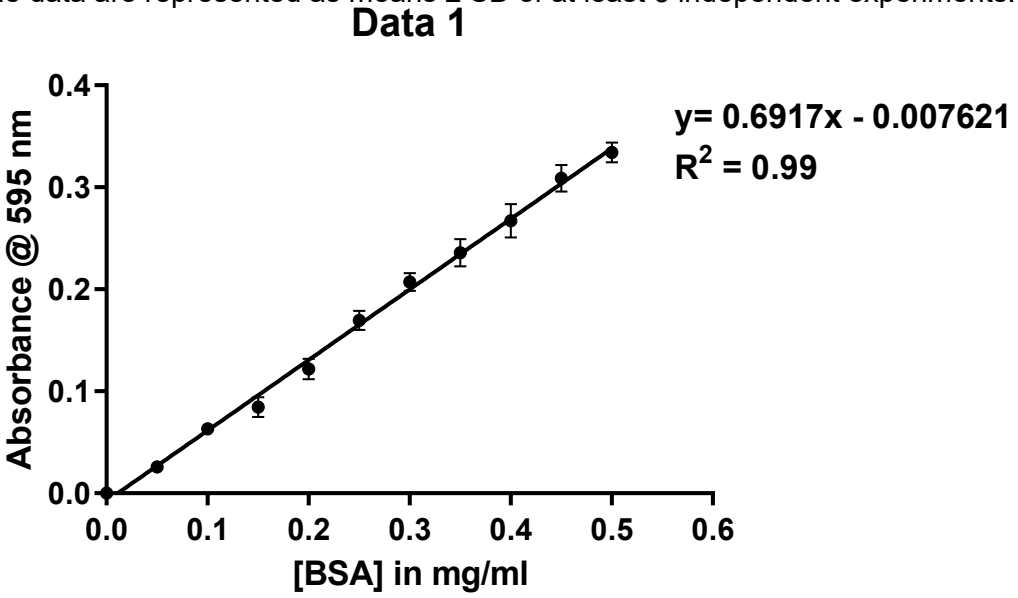

Figure B2: BSA standard curve obtained by Bradford's assay
The data are represented as means ± SD of at least 3 independent experiments.

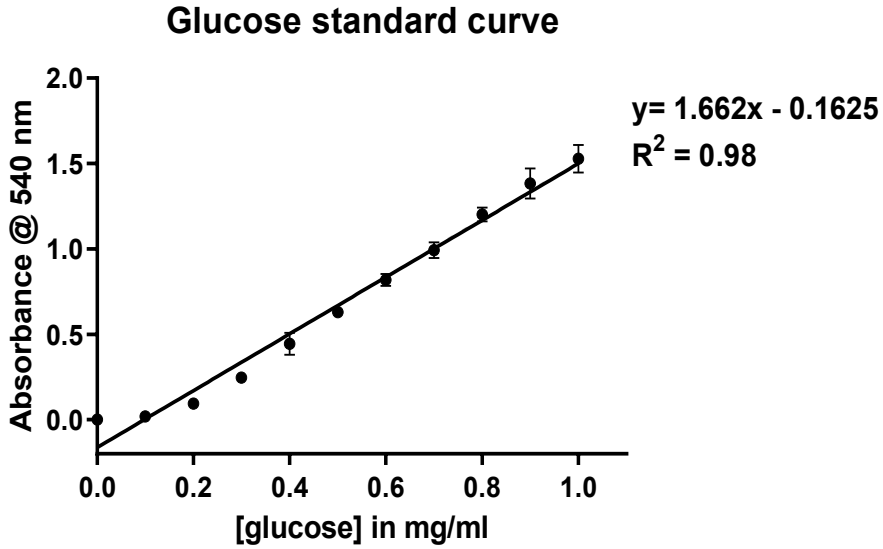

Figure B3:Total reducing sugars assay glucose standard curve
The data are represented as means ± SD of at least 3 independent experiments.

Table B1: Linearity of sugar standards in the HPLC (RID) method

Sugar Monomer	Linearity range mg/ml	Linear regression	Coefficient of correlation (r^2)
Fucose	0.05 - 1	Y = 338671x - 2568	0.98
Arabinose	0.05 - 1	Y = 128270x - 2699	0.99
Fructose	0.05 - 1	Y = 240649x - 3721	0.99
Mannose	0.05 - 1	Y = 130199x - 2501	0.99
Glucose	0.05 - 1	Y = 224704x - 2429	0.99
Galactose	0.05-1	Y = 191621x - 7787	0.99

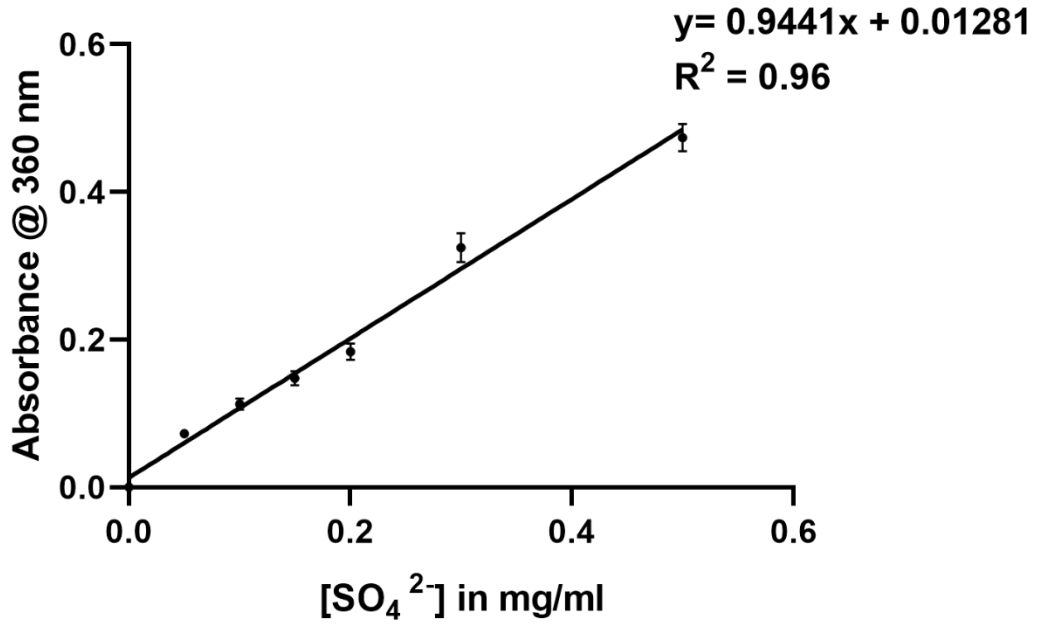

Figure B4:Sulphate standard curve
The data are represented as means ± SD of at least 3 independent experiments.

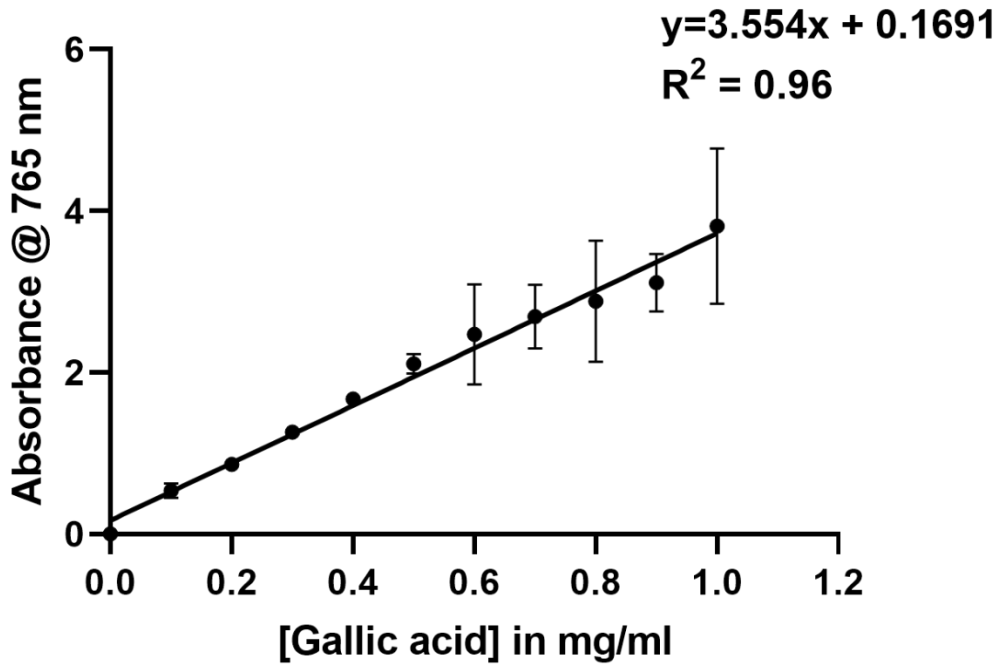

Figure B5: Gallic acid standard curve
The data are represented as means ± SD of at least 3 independent experiments.

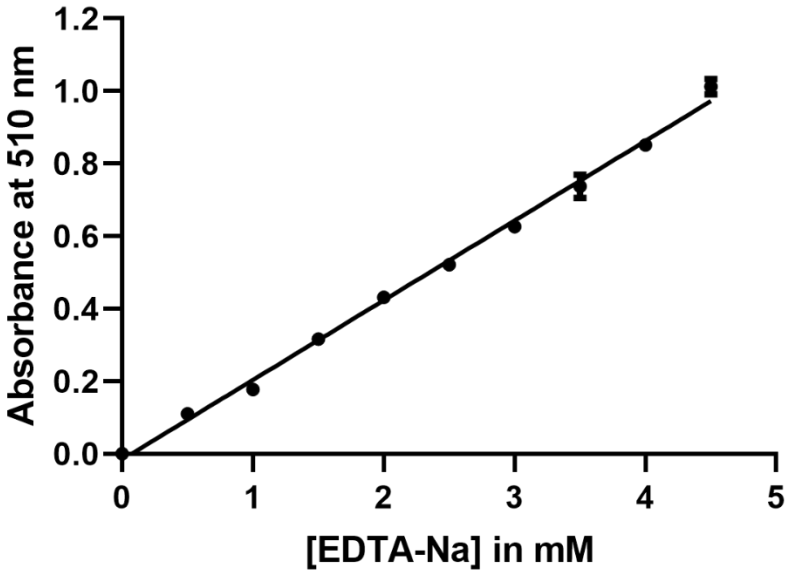

Figure B6: EDTA-Na standard curve
The data are represented as means ± SD of at least 3 independent experiments.

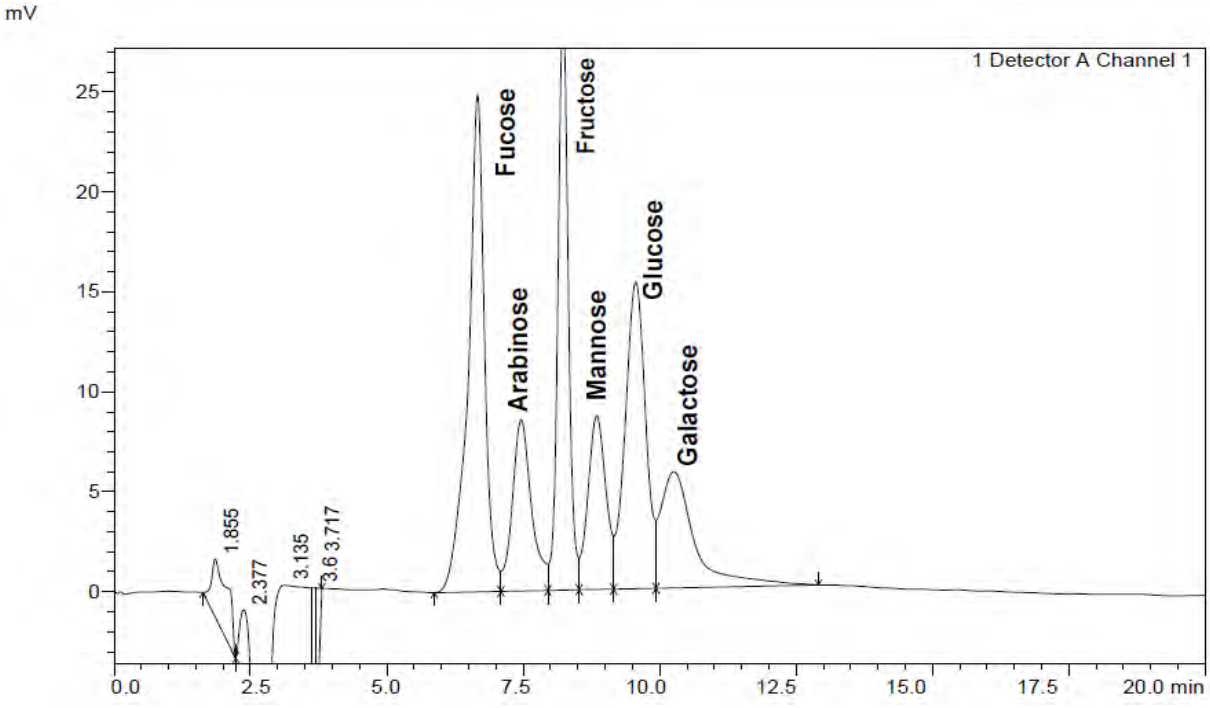

Figure B7: Chromatogram of the simultaneous detection of monosaccharides

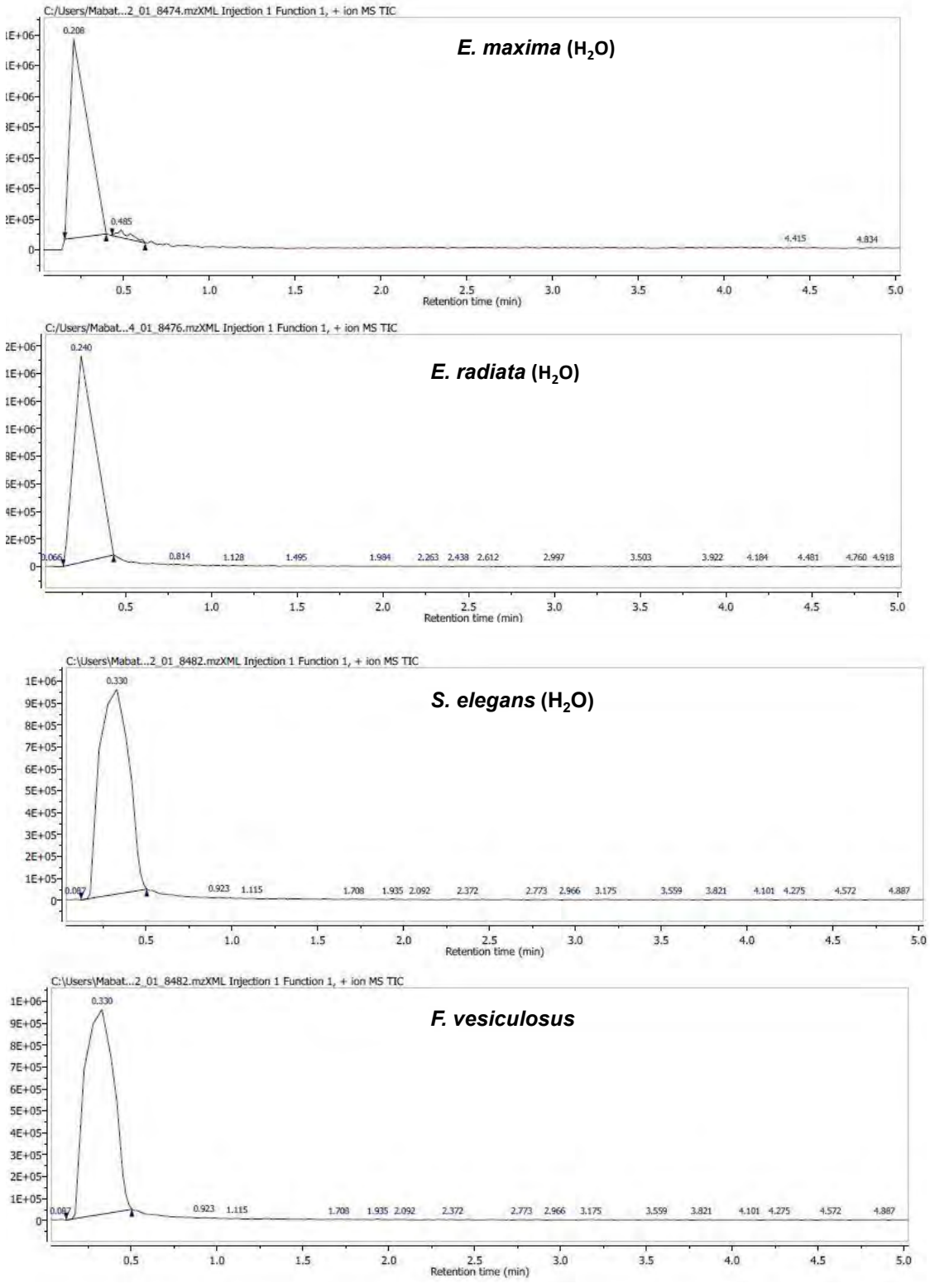

Figure B8: Elution profiles of fucoidan using reverse phase HPLC

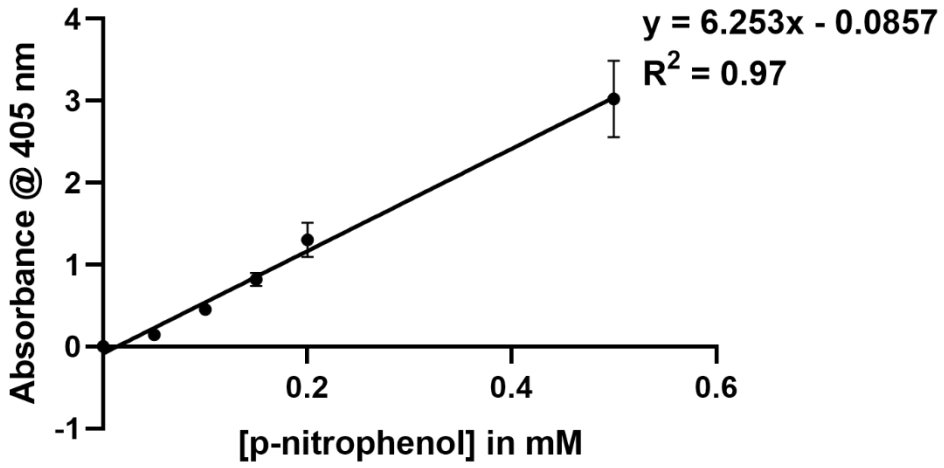

Figure B9: *p*-nitrophenol standard curve
The data are represented as means ± SD of at least 3 independent experiments.

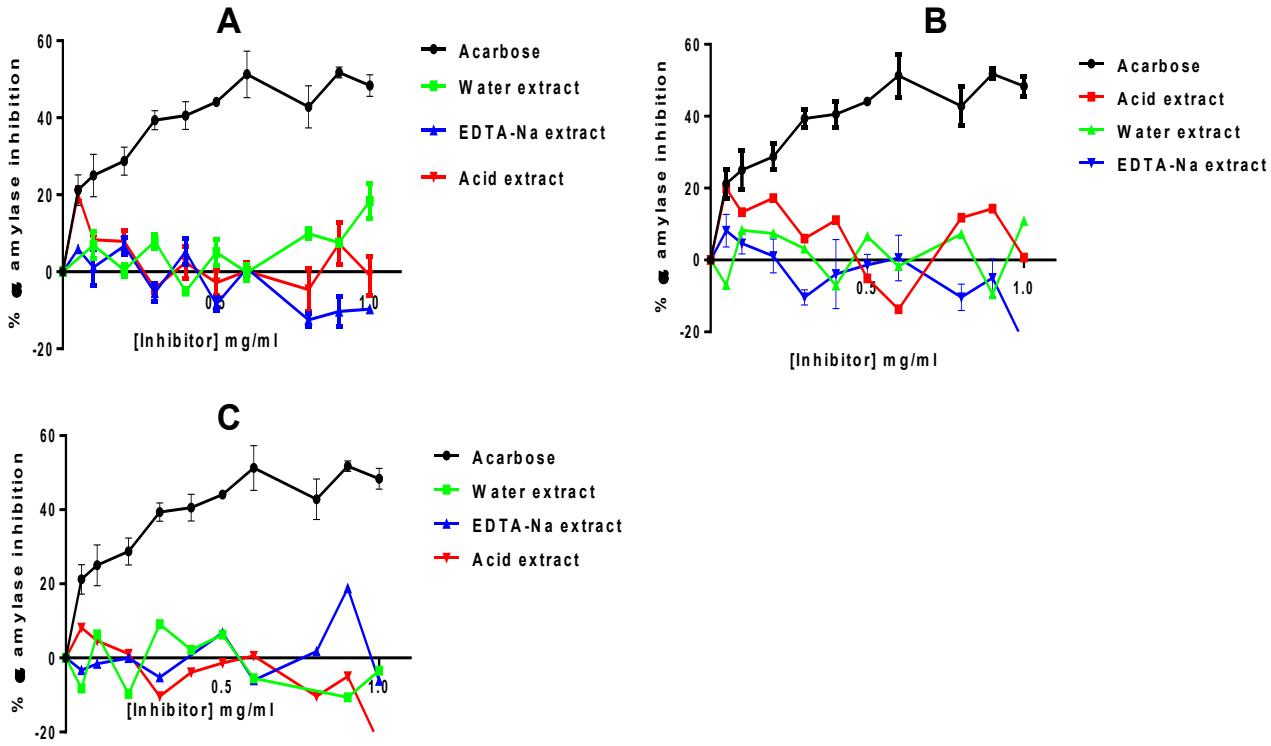

Figure B10: Fucoidan extracts inhibition potential with porcine α-amylase.
A- Inhibition of α-amylase by *E. maxima* fucoidan extracts. **B**- inhibition of α-amylase by *E. radiata* fucoidan extracts and **C**- inhibition of α-amylase by *S. elegans* fucoidan extracts. Fucoidan extracts did not inhibit the activity of α-amylase except, while the acarbose positive control inhibited the enzyme. The data are represented as means ± SD of at least 3 independent experiments.

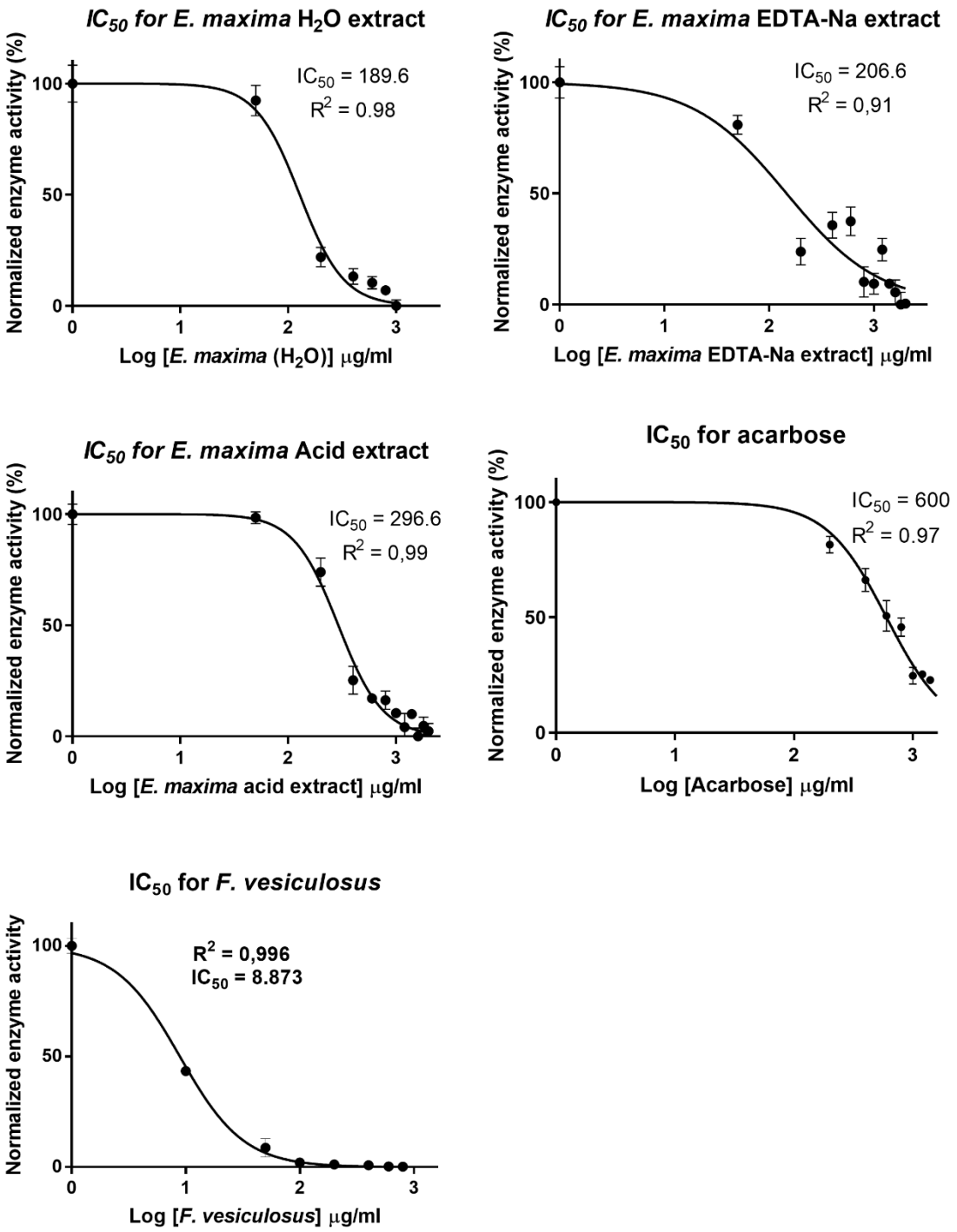

Figure B11: IC_{50} values for the different *E. maxima* fucoidan extracts, *F. vesiculosus* fucoidan and the acarbose control

The data are represented as means ± SD of at least 3 independent experiments.

Table B2: Tukey's multiple comparisons test for *E. maxima* fucoidan extracts and acarbose

Tukey's multiple comparisons test	Mean Diff,	95% CI of diff	Significant?	Summary
Acarbose vs *F. vesiculosus*	614.8	486.1 to 743.5	Yes	****
Acarbose vs water extract	505.6	377.0 to 634.3	Yes	****
Acarbose vs. EDTA-Na extract	432.2	303.5 to 560.9	Yes	****
Acarbose vs. acid extract	342.3	213.7 to 471.0	Yes	****
F. vesiculosus vs. water extract	-109.2	-237.8 to 19.51	No	ns
F. vesiculosus vs. acid extract	-272.5	-401.1 to -143.8	Yes	****
Water vs. EDTA-Na extract	-73.43	-202.1 to 55.23	No	ns
Water vs. acid extract	-163.3	-292.0 to -34.64	Yes	*
EDTA-Na vs. acid extract	-89.87	-218.5 to 38.80	No	ns

The results are presented as means ± standard deviation from triplicates of three independent experiments. The statistical significance of the IC_{50} values of *E. maxima* fucoidan extracts was tested using One-way Analysis of Variance (ANOVA) employing the Tukey-Kramer's test between the control and different groups. The results were considered significant at (*) a p value in the range 0.001 <p < 0.05, (****) represents a p value < 0.001 <0.05 and "ns" represents non-significant differences at 95 % confidence interval.

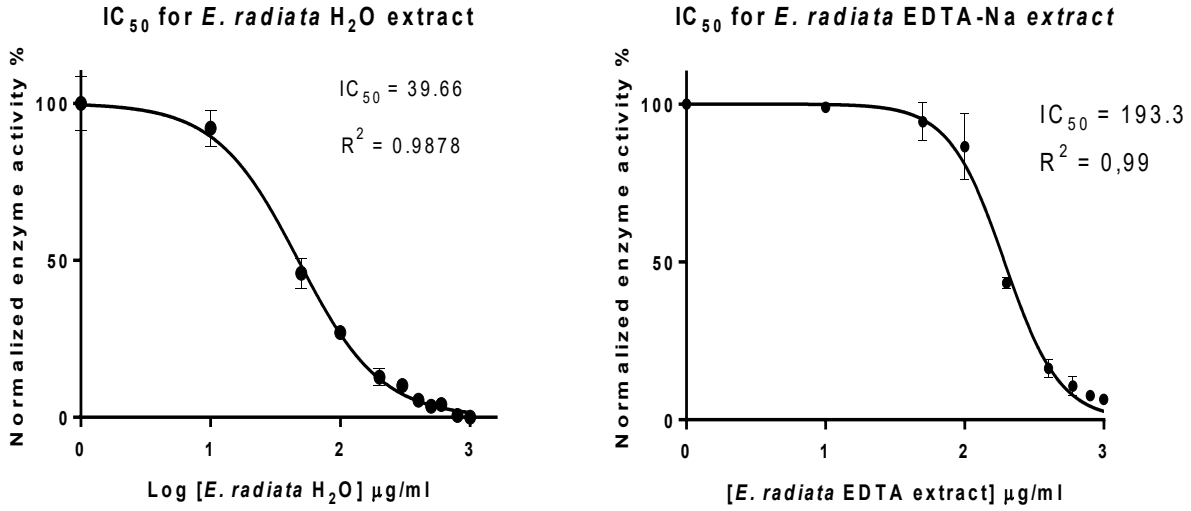

Figure B12: IC_{50} values of *E. radiata* fucoidan extracts
The data are represented as means ± SD of at least 3 independent experiments.

Table B3: Tukey's multiple comparisons test for *E. radiata* fucoidan extracts and acarbose

Tukey's multiple comparisons test	Mean Diff,	95% CI of diff,	Significant?	Summary
Acarbose vs. *F. vesiculosus*	519.7	404.9 to 634.6	Yes	****
Acarbose vs. Water extract	491.7	376.8 to 606.5	Yes	****
Acarbose vs. EDTA-Na extract	340.2	225.3 to 455.0	Yes	****
F. vesiculosus vs. Water extract	-28.04	-142.9 to 86.80	No	ns
F. vesiculosus vs. EDTA-Na extract	-179.6	-294.4 to -64.73	Yes	**
Water extract vs. EDTA-Na extract	-151.5	-266.4 to -36.69	Yes	*

The results are presented as ± standard deviation from triplicates of three independent experiments. The statistical significance of the IC_{50} values of *E. radiata* fucoidan extracts were tested using One-way Analysis of Variance (ANOVA) employing the Tukey-Kramer's test between the control and different groups. The results were considered significant at (*) a p value in the range 0.001 <p < 0.05, (****) represents a p value < 0.001 and "ns" represents non-significant differences.

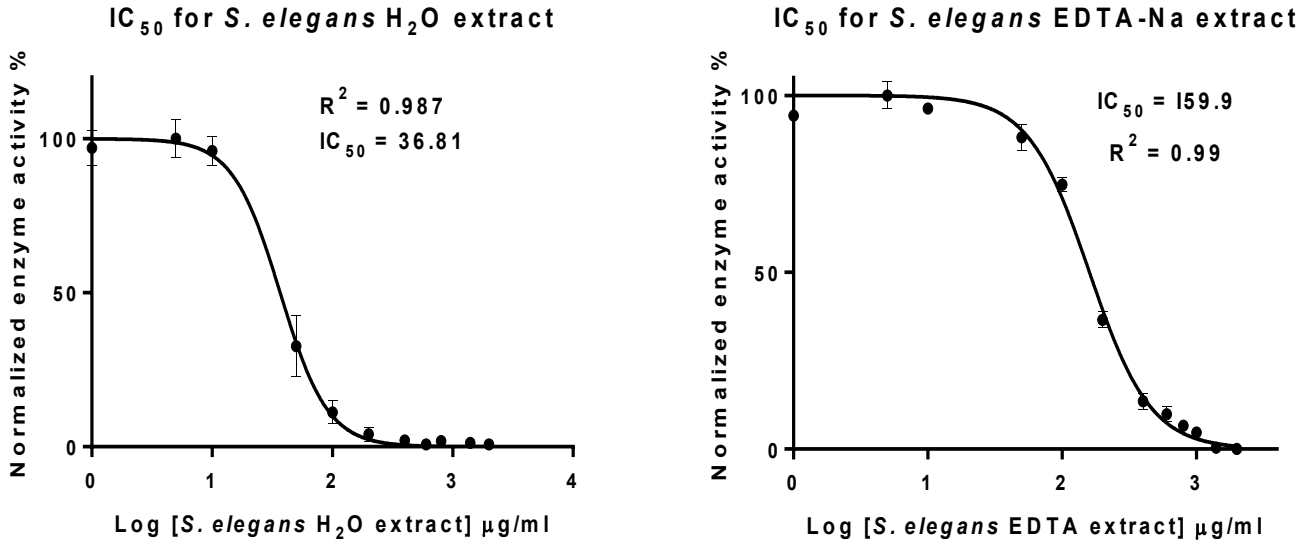

Figure B13: IC_{50} of *S. elegans* fucoidan extracts
The data are represented as means ± SD of at least 3 independent experiments.

Table B4: Tukey's multiple comparisons test for S. elegans fucoidan extracts & acarbose

Tukey's multiple comparisons test	Mean Diff,	95% CI of diff,	Significant?	Summary
Acarbose vs. *F. vesiculosus*	519.7	403.8 to 635.7	Yes	****
Acarbose vs. Water extract	495.9	379.9 to 611.8	Yes	****
Acarbose vs. EDTA-Na extract	371.4	255.5 to 487.4	Yes	****
F. vesiculosus vs. Water extract	-23.86	-139.8 to 92.11	No	ns
F. vesiculosus vs. EDTA-Na extract	-148.3	-264.3 to -32.32	Yes	*
Water extract vs. EDTA-Na extract	-124.4	-240.4 to -8.459	Yes	*

The results are presented as means ± standard deviation from triplicates of three independent experiments. The statistical significance of the IC_{50} values of *S. elegans* fucoidan extracts were tested using One-way Analysis of Variance (ANOVA) employing the Tukey-Kramer's test between the control and different groups. The differences were considered significant at (*) a p value in the range 0.001 <p < 0.05, (****) represents a p value < 0.001 and "ns" represents non-significant differences.

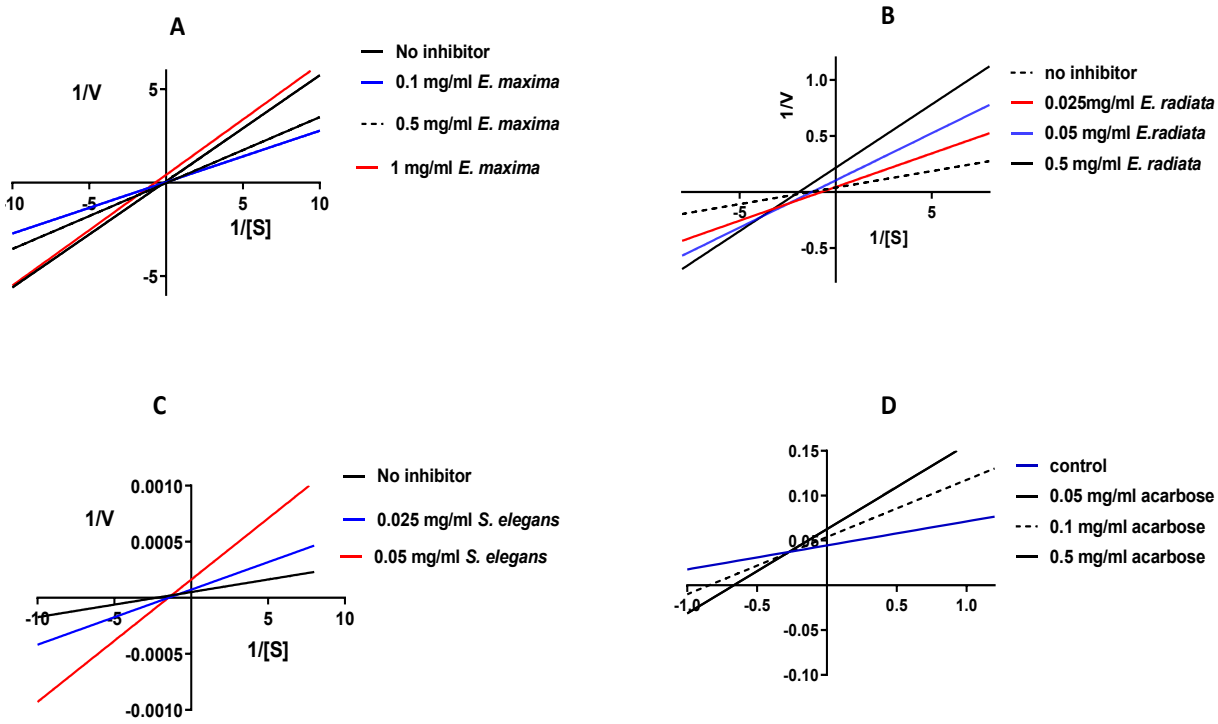

Figure B14: Lineweaver-Burk plots for identifying the type of enzyme inhibition

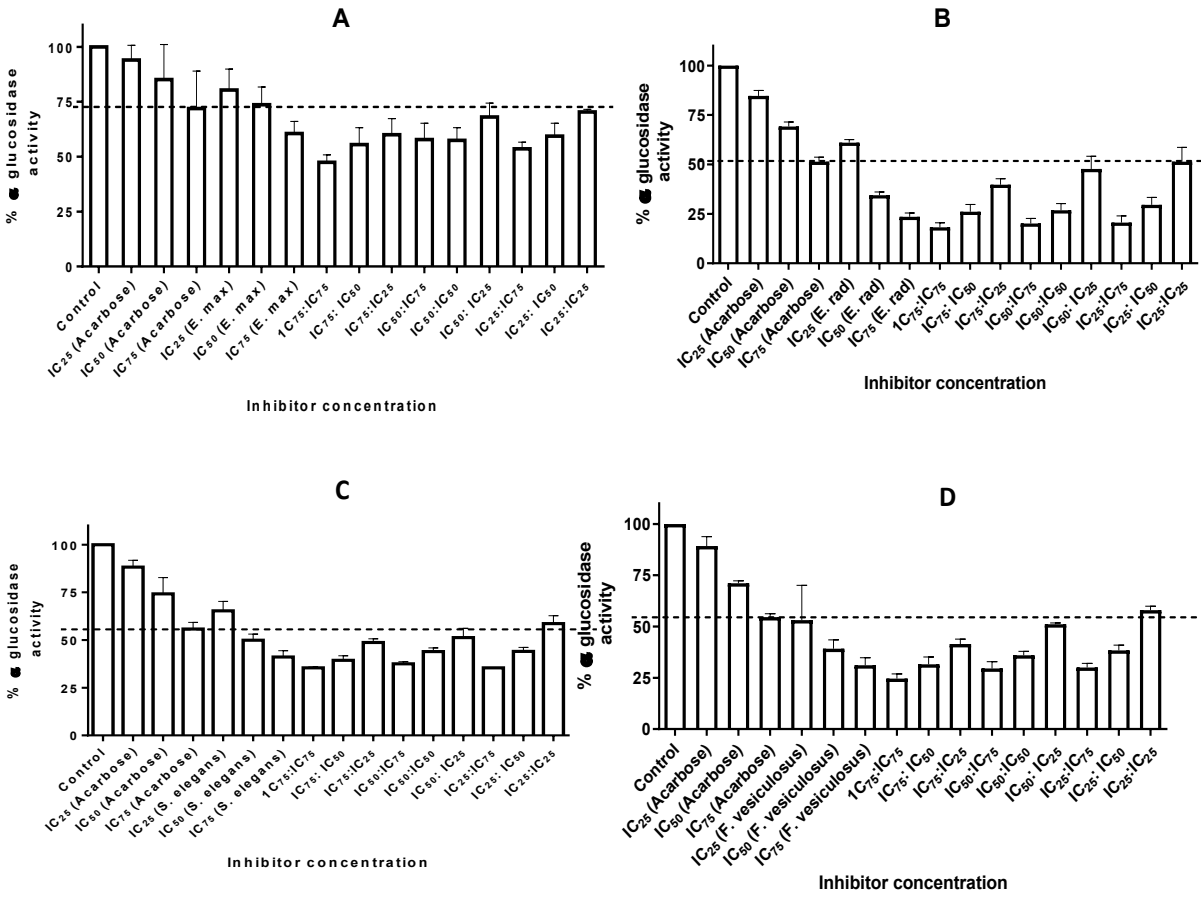

Figure B15: Synergistic effects of non-constant ratio of compounds on the inhibition of α-glucosidase.

A: Combinations of acarbose and *E. maxima* fucoidan**, B:** Combinations of acarbose and *E. radiata* fucoidan**, C:** Combinations of acarbose and *S. elegans* fucoidan and **D:** Combinations of acarbose and *F. vesiculosus* fucoidan. The data are represented as means ± SD of at least 3 independent experiments.

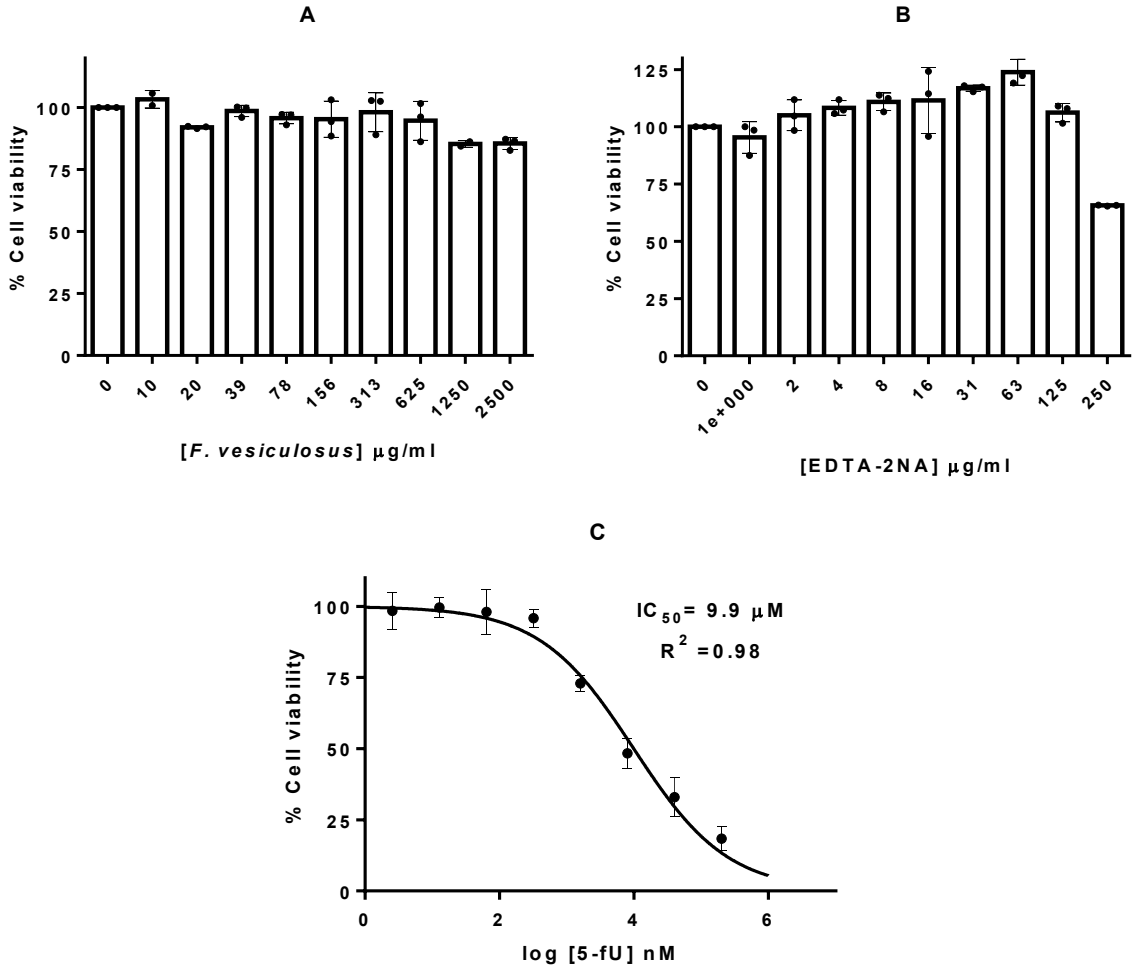

Figure B16: Cytotoxicity of commercial *F. vesiculosus* fucoidan and EDTA to HCT116 cells.

A. The commercial *F. vesiculosus* fucoidan was not cytotoxic to HCT116 cells. **B**. EDTA did not show any cytotoxic effect, although higher concentrations seemingly lowered the viability of the cells. **C**. The positive control (5-FU) lowered the viability of the HCT116 in a dose-dependent manner. The data are represented as means ± SD of at least 3 independent experiments.

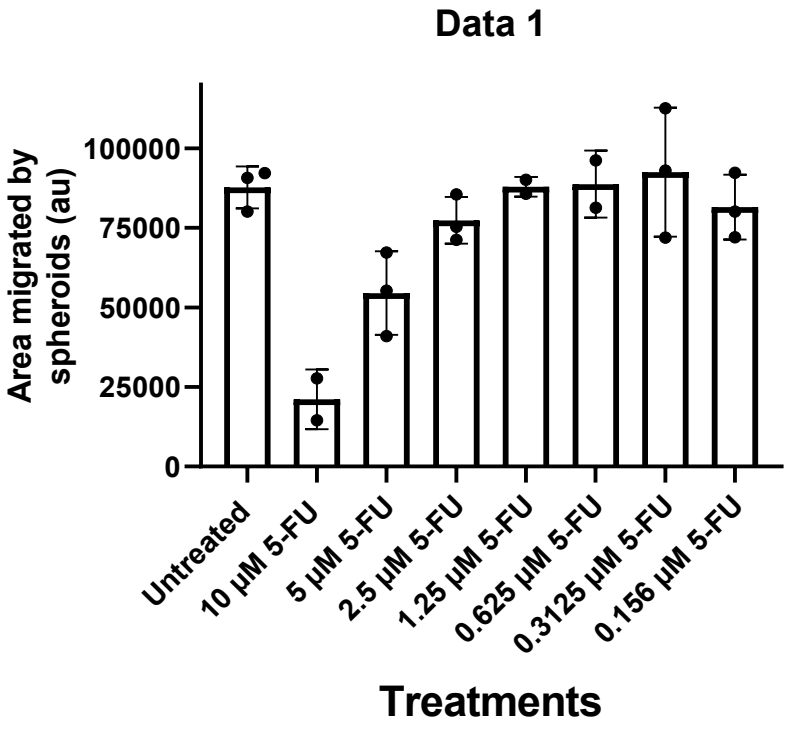

Figure B17: Dose dependent response of HCT116 spheroid migration to 5-FU
The data are represented as means ± SD of at least 3 independent experiments.